Dipl.-Ing. Birgit Wilding

Synthese von Strukturanaloga von 7-Cyano-7-deazaguanin zur Untersuchung der Substratbindung im aktiven Zentrum und des Substratspektrums von Nitrilreduktase queF

DISSERTATION

zur Erlangung des akademischen Grades
Doktor der technischen Wissenschaften (Dr. techn.)

erreicht an der

Technischen Universität Graz

Ao. Univ.-Prof. Dr. phil. Norbert Klempier
Institut für Organische Chemie
Technische Universität Graz

2013

Birgit Wilding, MSc

Synthesis of structural analogues of 7-cyano-7-deazaguanine to investigate the active site binding and substrate scope of nitrile reductase queF

PhD thesis

submitted in partial fullfilment of the requirements for the degree of
Doctor of Technical Sciences (Dr. techn.)

at

Graz University of Technology

Ao. Univ.-Prof. Dr. phil. Norbert Klempier
Institute of Organic Chemistry
Graz University of Technology

2013

Eidesstattliche Erklärung

Ich erkläre an Eides statt, dass ich die vorliegende Arbeit selbstständig verfasst, andere als die angegebenen Quellen/Hilfsmittel nicht benutzt, und die den benutzten Quellen wörtlich und inhaltlich entnommenen Stellen als solche kenntlich gemacht habe.

_____ _____

Unterschrift

Statutory Declaration

I declare that I have authored this thesis independently, that I have not used other than the declared sources / resources, and that I have explicitly marked all material which has been quoted either literally or by content from the used sources.

_____ _____

Signature

Almost all aspects of life are engineered at the molecular level,
and without understanding molecules we can only have a very sketchy understanding of life itself.

Francis Crick
What Mad Pursuit: A Personal View of Scientific Discovery

KURZFASSUNG

Nitrilreduktase queF katalysiert die Reduktion von 2-Amino-5-cyanopyrrol[2,3-*d*]pyrimidin-4-on ($preQ_0$) zu 2-Amino-5-aminomethylpyrrol[2,3-*d*]pyrimidin-4-on ($preQ_1$) im Biosyntheseweg zum hypermodifizierten Nukleosid Queuosin. Dieses bisher einzige für die Reduktion eines Nitrils zum entsprechenden primären Amin bekannte Enzym könnte die Möglichkeiten biokatalytischer Reaktionen von Nitrilen erweitern. Um diese neue Oxidoreduktase für eine Anwendung in biokatalytischen Reaktionen zu evaluieren, sind Charakterisierung des Enzyms und Untersuchung seines Substratspektrums Voraussetzung.

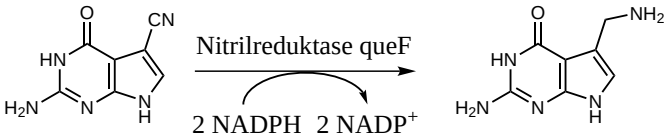

7-Cyano-7-deazaguanin ($preQ_0$) → 7-Aminomethyl-7-deazaguanin ($preQ_1$)

Abbildung 1 Reduktion von 7-Cyano-7-deazaguanin ($preQ_0$) zu 7-Aminomethyl-7-deazaguanin ($preQ_1$), katalysiert von Nitrilredukase queF.

In dieser Dissertation wurden Substratbindung im aktiven Zentrum und Substratspektrum von Typ I und Typ II Nitrilreduktase, von *G. kaustophilus* bzw. *E. coli*, untersucht. Die Nitrilreduktase von *G. kaustophilus*, eine neue, moderat thermophile Nitrilreduktase, wurde charakterisiert. Screenings mit einfachen Substratstrukturen zeigten hohe Substratspezifität der Enzyme. Bindungen zwischen Substrat und dem aktiven Zentrum wurden mit Hilfe von Homologiemodellen identifiziert. Verschiedene Strukturanaloga des natürlichen Substrats $preQ_0$ wurden synthetisiert, in diesem Fall verschieden substituierte Pyrrol[2,3-*d*]pyrimidine, Pyrrol[3,2-*c*]pyridine, Pyrrol[2,3-*b*]pyridine, Thieno[2,3-*d*]pyrimidine, Cyclopenta[*d*]pyrimidine und Pyrazol[3,4-*d*]pyrimidine. Diese Analoga des natürlichen Substrats wurden mit Wildtyp queF und Mutanten des aktiven Zentrums gescreent. Die essentielle Rolle zweier Aminosäurereste in *E. coli* queF, Cys190 und Asp197, wurde bewiesen. Drei nicht-natürliche Substrate wurden identifiziert und mit dem natürlichen Substrat mit Wildtyp-Enzym und mutierter Nitrilreduktase hinsichtlich ihrer spezifischen Aktivitäten verglichen. Vorversuche bezüglich der Aktivität von Nitrilreduktase für die Reduktion von C-N- und C-O-Doppelbindungen wurden durchgeführt, im Speziellen für die Reduktion von Iminen, Oximen und Aldehyden.

ABSTRACT

Nitrile reductase queF catalyzes the reduction of 2-amino-5-cyanopyrrolo[2,3-*d*]pyrimidin-4-one ($preQ_0$) to 2-amino-5-aminomethylpyrrolo[2,3-*d*]pyrimidin-4-one ($preQ_1$) in the biosynthetic pathway to the hypermodified nucleoside queuosine. It is the only enzyme known to catalyze a reduction of a nitrile to its corresponding primary amine and could therefore expand the toolbox of biocatalytic reactions of nitriles. In order to evaluate this new oxidoreductase for application in biocatalytic reactions, enzyme characterization and investigation of its substrate scope are prerequisite.

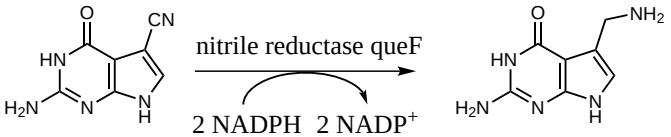

7-cyano-7-deazaguanine ($preQ_0$) → 7-aminomethyl-7-deazaguanine ($preQ_1$)

Scheme 1 Reduction of 7-cyano-7-deazaguanine ($preQ_0$) to 7-aminomethyl-7-deazaguanine ($preQ_1$) catalyzed by nitrile reductase queF.

In this thesis, the active site binding and substrate scope of type I and type II nitrile reductase, from *G. kaustophilus*, and *E. coli* respectively, was investigated. Nitrile reductase from *G. kaustophilus*, a novel, moderately thermophilic queF, was characterized. Screenings with simple nitrile structures revealed high substrate specificity of the enzymes. Binding interactions of the substrate to the active site were identified based on homology models. Various structural analogues of the natural substrate $preQ_0$ were synthesized, namely differently substituted pyrrolo[2,3-*d*]pyrimidines, pyrrolo[3,2-*c*]pyridines, pyrrolo[2,3-*b*]pyridines, thieno[2,3-*d*]pyrimidines, cyclopenta[*d*]pyrimidines, and pyrazolo[3,4-*d*]pyrimidines. These natural substate analogues were screened with wild-type queF and several active site mutants. Two amino acid residues of *E. coli* queF, Cys190 and Asp197, were shown to play an essential role in the catalytic mechanism. Three non-natural substrates were identified and compared to the natural substrate regarding their specific activities by using wild-type and mutant nitrile reductase. Nitrile reductase queF was preliminarily investigated towards its activity for the reduction of C-N and C-O double bonds, specifically imines, oximes, and aldehydes.

Acknowledgements

First and foremost, I would like to express my gratitude to my supervisor Ao.Univ.-Prof. Dr.phil Norbert Klempier for his continuous support and enthusiasm throughout my PhD research. He gave me freedom in my research and provided guidance, expertise, and encouragement whenever needed.
I am grateful to Ao.Univ.-Prof. Dr.phil. Norbert Klempier and Assoc. Prof. Dipl.-Ing. Dr.techn. Tanja Wrodnigg for giving me the opportunity to gain teaching experience at the Institute of Organic Chemistry.

I would like to thank Univ.-Prof. Dipl.-Ing. Dr.techn. Helmut Schwab for acting as second examiner of my thesis and Univ.-Prof. Dipl.-Ing. Dr.rer.nat. Rolf Breinbauer for chairing my PhD defense.

I wish to express my appreciation to Dipl.-Ing. Dr.techn. Margit Winkler and Dipl.-Ing. Dr.techn. Barbara Petschacher for excellent project management and uncomplicated, inspiring collaboration. I am especially grateful to Dipl.-Ing. Dr.techn. Margit Winkler for supportive advice throughout my thesis and to Dipl.-Ing. Dr.techn. Barbara Petschacher for helpful discussions particularly on enzyme cloning and expression.

I would like to thank Univ.-Prof. Dipl.-Ing. Dr.techn. Bernd Nidetzky, for helpful comments on this work and use of the equipment at the Institute of Biotechnology and Biochemical Engineering. I am grateful Dipl.-Ing. Dr.techn. Regina Kratzer and Dipl.-Ing. Dr.techn. Sigrid Egger for a valuable collaboration, insightful discussions and suggestions improving my knowledge of biotechnology.

I would like to acknowledge the rewarding cooperations with Alicja Vesela of the group of Dr. Ludmila Martínková at the Laboratory of Biotransformations, Institute of Microbiology, Academy of Sciences of the Czech Republic and Xinrui Zhou of the group of Prof. Dr. Peter Neubauer at the TU Berlin.

I would like to thank MSc Dr.rer.nat. Jana Rentner, Dipl.-Chem. Dr.rer.nat Martin Peters, Dipl.-Ing. Dr.techn. Harald Stecher, MSc Jihye Jung and Mag.rer.nat Christiane Wünsch for helpful discussions.

I acknowledge my gratitude to Ao.Univ.-Prof. Dipl.-Ing. Dr.techn. Jörg Weber, Carina Illaszewicz-Trattner, Mag.rer.nat. Dr.rer.nat. Gernot Strohmeier, and Dipl.-Ing. Dr.techn. Mandana Gruber-Khadjawi for assistance in NMR spectroscopy and advice on HPLC-MS respectively. I would like to thank Gerlinde Offenmüller for excellent technical support, especially for flexible time-management when purifying nitrile reductase from *E. coli*, Margaretha Schiller for technical support and assistance at the Institute of Biotechnology and Biochemical Engineering, Peter

Plachota, Peter Urdl, and Mag.rer.soc.oec. Astrid Nauta for IT, HPLC-MS and GC support, general technical support and administrative support.

I acknowledge the effort of the students I had the pleasure to work with. MSc. Cornelia Hojnik, Wilfried Sailer-Kronlachner and Stefan Faschauner worked on the synthesis of substituted 5- and 7-azaindoles, pyrrazolo[3,4-*d*]pyrimidines, thieno[2,3-*d*]pyrimidines and cyclopenta[*d*]pyrimidines during their master thesis. Martin Gollowitzer and Wolfgang Binder contributed to the syntheses of pyrrolo[2,3-*d*]pyrimdines, Christoph Staudinger and Melanie Zechner to thieno[2,3-*d*]pyrimidines and Carina Vidovic to pyrrolo[2,3-*b*]pyridines in their bachelor theses. Indira Zahirovic and Melanie Zechner were also supporting substrate synthesis for nitrile reductase queF as summer students. Jasmin Resch contributed to substrate synthesis and screening of a taxol sidechain precursor during her master thesis. Carina Hasenöhrl and Maria Koshanskaya worked on the taxol sidechain precusor project during their bachelor theses. Carina Hasenöhrl is especially thanked for her support in both projects over seven months, and Carina Vidovic for her diligence in the synthesis of 3-cyano-4-hydroxypyrrolo[2,3-*b*]pyridine.

Special thanks go to my friends and family. I am grateful to Andi for his patience, being supportive of my work and contributing to the layout of this thesis. I am indebted to my parents and my sisters for unwavering support and encouragement throughout the years.

Contents

List of Figures

List of Schemes

List of Tables

List of Abbreviations

ADME	absorption, distribution, metabolism, and excretion (of a pharmaceutical compound within an organism)
Akt	Protein Kinase B
APT	Attached Proton Test
ATCC	American Type Culture Collection
ATP	adenosine triphosphate
B.	*Bacillus*
BINAP	2,2'-Bis(diphenlphosphino)-1,1'-binaphthyl
BLAST	Basic Local Alignment Search Tool
boc	di-*tert*-butyl dicarbonate
BSA	bis(trimethylsilyl)acetamide
Bu	butyl
CDK	cyclin-dependent kinases
cGMP	cyclic guanosine monophosphate
CLEA	cross linked enzyme aggregate
cod	2,5-cyclooctadiene
COG	conserved oligomeric Golgi
DABCO	1,4-diazabicyclo[2.2.2]octane
DAD	diode array detector
dba	dibenzylideneacetone
DCM	dichloromethane
dGTP	deoxyguanosine triphosphate
DHFR	dihydrofolate reductase
DIBAL-H	diisobutylaluminium hydride
DMF	dimethylformamide
DMSO	dimethyl sulfoxide
DNA	deoxyribonucleic acid
dNTPs	deoxyribonucleotide phosphates
dppe	1,2-Bis(diphenylphosphino)ethane
dppf	Bis(diphenylphosphino)ferrocene
dppp	1,3-Bis(diphenylphosphino)propane
DSMZ	Deutsche Sammlung von Mikroorganismen und Zellkulturen, German Collection of Microorganisms and Cell Cultures

DTT	dithiothreitol
E.	*Escherichia*
EC	Enzyme Commission number
EDTA	ethylenediaminetetraacetic acid
EGFRs	epidermal growth factor receptor
Et	ethyl
eq	equivalents
FAD	flavin adenine dinucleotide
FDA	US food and drug administration
G.	*Geobacillus*
G^+	archaeosine
FGFR	fibroblast growth factor receptor
GCH	guanosine triphosphate cyclohydrolase
GDP	guanosine diphosphate
GSK	glycogen synthase kinase
GMP	guanosine monophosphate
GTP	guanosine triphosphate
HMBC	heteronuclear multiple bond correlation
HMDS	hexamethyldisiloxane
HMPA	hexamethylphosphoramide
HMTA	hexamethylenetetramine
HNL	hydroxynitrile lyase (oxynitrilase)
HPLC	high performance liquid chromatography, high pressure liquid chromatography
HSP	heat shock proteins
HSQC	heteronuclear single quantum coherence
IC50	half maximal inhibitory concentration
IMI	Innovative Medicines Initiative
IPTG	isopropyl β-*D*-1-thiogalactopyranoside
JAK	Janus kinase
JCM	Japan Collection of Microorganisms
LAH	lithium aluminium hydride, $LiAlH_4$
LB	Luria Broth
lck	lymphocyte-specific protein tyrosine kinase
Me	methyl
MS	mass spectrometry
mTOR	mammalian target of rapamycin
MWD	multi wavelength detector
NADH	nicotinamide adenine dinucleotide
NADPH	nicotinamide adenine dinucleotide phosphate
NBS	*N*-bromosuccinimide
NCIMB	National Collections of Industrial, Marine and Food Bacteria
NCS	*N*-chlorosuccinimide

NHase	nitrile hydratase
NHB	Nematophagous Fungi Helper Bacteria
NMO	*N*-methylmorpholine *N*-oxide
NMR	nuclear magnetic resonance
NSAID	non-steroidal and anti-inflammatory drugs
PCR	polymerase chain reaction
PMHS	polymethylhydrosiloxane
PI3K	phosphatidylinositol-3-kinase
PI4K	phosphatidylinositol 4-kinase
PIM kinase	proto-oncogene serine/threonine-protein kinase
Q	queuosine
R.	*Rhodococcus*
rNTPs	ribonucleotide triphosphates
RTK	receptor tyrosine kinase
SAM	*S*-adenosyl-*L*-methionine
SDS-PAGE	sodium dodecyl sulfate polyacrylamide gel electrophoresis
TBDMS	*tert*-butyldimethylsilyl
TBDPS	*tert*-butyldiphenylsilyl
TCEP	tris(2-carboxyethyl)phosphine hydrochloride
TEMPO	(2,2,6,6-tetramethylpiperidin-1-yl)oxyl
THF	tetrahydrofuran
TIPS	triisopropylsilyl
TGT	transfer ribonucleic acid guanine transglycosylase
TLC	thin layer chromatography
trityl	triphenylmethyl
tRNA	transfer ribonucleic acid
UDP	uridine diphosphate
UV	ultraviolet light
VIS	visible light

amino acid residues

arginine	Arg	R
histidine	His	H
lysine	Lys	K
aspartic acid	Asp	D
glutamic acid	Glu	E
serine	Ser	S
threonine	Thr	T
asparagine	Asn	N
glutamine	Gln	Q
cysteine	Cys	C

glycine	Gly	G
proline	Pro	P
alanine	Ala	A
isoleucine	Ile	I
leucine	Leu	L
methionine	Met	M
phenylalanine	Phe	F
tryptophan	Trp	W
tyrosine	Tyr	Y
valine	Val	V

1

Introduction

In recent years, the design of greener, more sustainable products and processes has become a priority in many research institutions, chemical and pharmaceutical companies [1]. Green chemistry aspires to efficiently use raw materials and reduce waste and reduce or eliminate the use or generation of substances hazardous to humans, animals, plants and the environment [1, 2]. A number of green chemistry performance metrics, such as atom economy, raw material efficiency, and E-factor, have been developed to guide the development of new, green reactions and technologies [2].

The three key areas of research in green chemistry are catalysis, alternative reaction media, and the use of renewable raw materials as alternatives to fossil resources [3]. Catalysis is a key discipline to enable clean and cost-efficient processes [1, 4]. A number of Noble Prizes were awarded for catalysis, most recently to Richard F. Heck, Ei-ichi Negeshi, and Akira Suzuki for palladium-catalyzed cross couplings in organic synthesis in 2010. However, homogeneous and heterogeneous metal catalysis is mostly carried out in organic solvents [4]. Organic solvents are considered a major source of waste in the fine and speciality chemical industries, and are associated with health hazards and/or environmental problems [5]. In contrast to metal catalyzed reactions, biocatalytic reactions are mostly performed at ambient temperature and pressure, often in water as solvent [3, 5]. Biocatalysts themselves are biocompatible, have low ecotoxicity and are produced from natural, renewable raw materials [5]. Therefore, biocatalysis is considered one of the greenest technologies for chemical synthesis [1, 3–5].

Enzymes and whole cells are used as biocatalysts in organic synthesis and industrial synthetic chemistry [2]. Over 3,000 enzymes have so far been identified [5]. Both natural and engineered enzymes can be produced on a large scale in convenient host organisms using recombinant DNA technologies [5, 6]. Genetic engineering can alter enzyme stability, broaden substrate specificity or increase specific activities of enzymes. Whole cells are often used for reactions that require cofactors which are regenerated in metabolically active cells [2, 5–7]. The development of efficient cofactor regeneration systems makes biocatalytic reactions that require cofactors suitable for large scale processes [5, 6]. Biocatalytic processes can be carried out in organic solvents as well as in aqueous environments, so that apolar organic compounds as well as water-soluble compounds can be modified selectively and efficiently [2, 5–7].

Biocatalysts display chemo-, regio-, and enantioselectivity and show remarkable rate accelera-

tion of typically 10^5 to 10^8 [5]. Biocatalysis is therefore uniquely suited to the development of green chemistry routes for complex molecules, which are often labile and densely functionalized [2]. Synthetic pathways can often be shortened by avoiding protecting and deprotecting steps by replacement of a synthetic step by a biocatalytic reaction. The high selectivity of enzymatic synthesis affords efficient reactions with few by-products. [2, 5, 6, 8]

Enzyme catalyzed transformations of nitriles are of considerable interest for synthetic chemistry. Nitrile groups are often used as synthon for homologation of the carbon framework [9, 10]. Subsequently, nitriles may be hydrolyzed to carboxylic acids or carboxamides, or reduced to amines. Nitrile and amine containing compounds are used as feedstock, solvents, extractants, pesticides (e.g. dichlobenil, bromoxynil, ioxynil, buctril) and are ubiquitous intermediates in the pharmaceutical, specialty, and commodity chemical industries [10]. Chemical hydrolysis and reduction of nitriles requires harsh reaction conditions [10]. Hydrolysis uses strong acid or bases while reductions require metal catalysts in combination with molecular hydrogen or complex hydrides. A biocatalytic transformation of nitriles proceeds at near physiological conditions, often chemo-, regio-, and/or stereoselectively [10]. A biocatalytic transformation of nitriles consequently represents a very attractive and valuable alternative to the corresponding chemical reactions [10, 11]. Nitrile hydrolysing enzymes were employed for the preparation of carboxylic acids and amides, and for optically pure amino acids, hydroxy acids, and keto acids and several other commercially important organic compounds [10–12]. A nitrile reductase has so far not been exploited for biocatalysis.

1.1 Nitrile transforming enzymes

Nitrile degrading activity is known from a number of plants (*Gramineae, Cruciferae, Musaceae*), and fungi (*Fusarium, Aspergillus, Penicillium*), and more frequently from bacteria [10]. A number of bacteria (*Acinetobacter, Corynebacterium, Arthrobacter, Pseudomonas, Klebsiella, Nocardia, Rhodococcus*) are known to metabolize nitriles as sole source of carbon and nitrogen [10]. In plants, the physiological role of nitrile degrading organisms is implicated in nutrient metabolism, particularly in the degradation of glucosinolates and the synthesis of indole acetic acid [10]. In higher plants, nitrile degrading activity is also required for cyanide detoxification [10]. In microbes, different enzymes are responsible for the metabolism of nitriles: nitrile hydratase, amidase and nitrilase catalyze hydrolysis to carboxamides and carboxylic acids, oxygenase catalyzes oxidation to cyanohydrins, and nitrogenase reduction to alkanes and ammonia [9, 10, 13]

Nitrogenase is a nitrogen-fixing enzyme. Nitrogenase is a complex of two protein fractions, a molybdenum-iron protein and an iron protein [14]. In addition to fixation of nitrogen, nitrogenase can catalyze the reduction of compounds structurally similar to nitrogen, such as cyanide, azide, acetylene or nitro-groups [14, 15]. The nitrogenase catalyzed reductions have the same requirements as nitrogen fixation: ATP as energy source, a low potential electron donor, a divalent ion and an electron acceptor [14, 15].

Oxygenases are oxidoreductases, used in some plants and insects to oxidize nitrile substrates to cyanohydrins (α-hydroxynitriles) [10]. In plants, usually enzymes with monooxygenase activity, such as P450 (CYPs), catalyze the synthesis of *(R)*-hydroxynitrile through nitrile formation by dehydration and hydroxylation [16]. Cyanohydrins are then further converted to an aldehyde

and hydrogen cyanide by hydroxynitrile lyases (oxynitrilases) [10]. Hydrogen cyanide is used as a defense system and as nitrogen source [16]. This enzymatic system is almost unknown in microorganisms [10].

Oxynitrilases (hydroxynitrile lyases, HNLs) belong to the class of aldehyde lyases. Oxynitrilases are widespread in nature, over three thousand plant species are known to produce the enzyme. Oxynitrilases cleave the cyanohydrins present in plants as cyanogenic glycosides or cyanolipids. In cyanogenic glycosides or cyanolipids the cyanohydrin is stabilized and hydrogen cyanide cannot be released. Hydrogen cyanide is liberated by the oxynitrilase catalyzed reaction and can in turn be used either in plant defense or in the biosynthesis of amino acids. Two classes of oxynitrilases are known, differing in the presence, or absence, of FAD. FAD is however, not involved in a redox reaction, but appears to have a structure stabilizing effect. FAD-independent oxynitrilases show different substrate specificity than the FAD-dependent enzymes. Oxygenases from the plant family *Rosaceae* (e.g. *Prunus amygdalus* - almond) contain FAD. FAD-independent oxynitrilases have been isolated from a large variety of plant sources. The HNL from *Sorgum biocolor* uses aromatic cyanonitriles, whereas HNLs form *Linum usitatissimum*, *Manihot esculenta*, and *Hevea brasiliensis* use aliphatic cyanohydrins. The crystal structure of *Hevea brasiliensis* oxynitrilase was solved in 1999 and revealed this HNL to be a member of the α/β-hydrolase fold family. The active site is buried deeply inside the structure and is connected by a narrow channel to the surface [16–18].

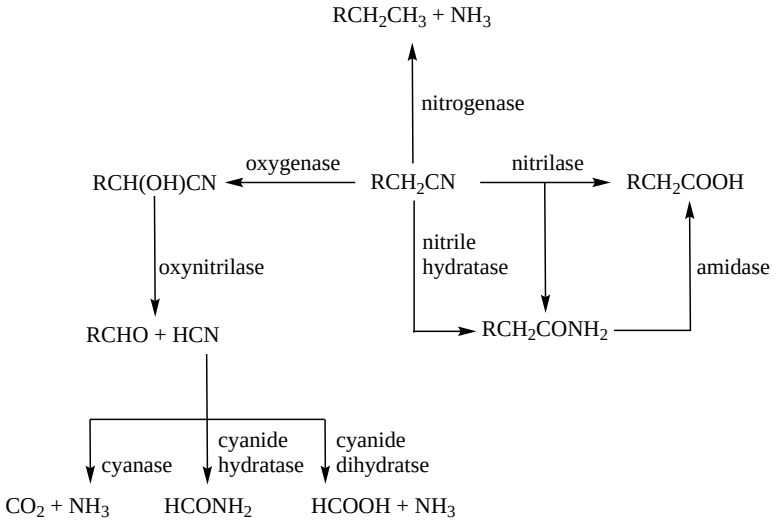

Scheme 1.1 Pathways of nitrile degrading enzymes.

In biocatalysis, hydroxynitrile lyases are valuable enzymes for the asymmetric synthesis of cyanohydrins. A tremendous variety of pharmaceuticals, agrochemicals, and biologically active compounds have been prepared from enzymatically synthesized cyanohydrins. HNLs from *Hevea brasiliensis* and *Manihot esculenta* provide *(S)*-cyanohydrins, while HNLs from *L. usitatissimum* and *P. amygdalus* yield *(R)*-cyanohydrins. HNLs from *Hevea brasiliensis*, *Manihot esculenta*, and *P. amygdalus* accept a wide variety of aldehydes and ketones of synthetic interest, including aromatic, heteroaromatic, aliphatic and alicyclic compounds [16, 17, 19].

Hydrogen cyanide can be converted by different enzymes. Cyanase, found in bacteria and plants, produces carbon dioxide and ammonia from hydrogen cyanide. Cyanase requires bicarbonate as cofactor. The bicarbonate attacks the cyanate, with elimination of carbon dioxide, thus

catalysing hydration of the cyanate to carbamate. The carbamate spontaneously hydrolyzes to ammonia and carbon dioxide. Cyanide hydratase produces formamide from hydrogen cyanide [10]. Cyanide hydratase was first identified in the fungus *Stemphylium loti*, a pathogen of the cyanogenic plant birdsfoot trefoil (*Lotus corniculatus*). Cyanide hydratases from *Fusarium oxysporum* N-10 and *Fusarium lateritium* show low activity (0.02-0.05% of HCN activity) with a number of nitriles. Cyanide dihydratase catalyzes the hydrolysis of hydrogen cyanide to formate without forming formamide as a free intermediate. Cyanide dihydratases occur mostly in bacteria, while the cyanide hydratases occur in filamentous fungi.[10, 20]

1.1.1 Nitrilase

Nitrilase (EC 3.5.5.1) catalyzes the cleavage of nitriles to the corresponding acids and ammonia. However, several nitrilases were reported to convert nitriles to both, acid and amide products [12, 21–23]. Nitrilases, along with cyanide hydratases and cyanide dihydratases, constitute branch 1 of the nitrilase superfamily [24, 25]. The majority of nitrilases known were obtained from bacteria, fungi, and plants by a variety of selection methods on media, containing nitriles as nitrogen source, or through direct cloning and expression [20, 21].

The enzyme nitrilase was first described by Thimann and Mahadevan in 1964 [26]. This nitrilase was found to hydrolyze indoleacetonitrile to indoleacetic acid. The conversion of indoleacetonitrile to indoleacetic acid was identified by a colour reaction of indoleacetic acid with Salkowski reagent, measured by calorimetry, or alternatively, by TLC analysis with staining with Salkowski and Ehrlich's reagent [26, 27]. Nitrilase activity was found in a number of plant species, including *Hordeum vulgare* (barley leaves, stem, leaf sheath, and roots), several members of the *Cruciferae*, including *Brassica oleracea var. capitata* (cabbage leaves), *Brassica oleracea var. botyytis* (cauliflower inflorescence), *Brassica oleracea var. gemmifera* (brussel sprouts), *Brassica oleracea var. gongylodes L.* (kohlrabi leaves), members of the *Musaceae* (banana, leaves), and *Strelitzia reginae* (bird of paradise leaves). The enzyme was partially purified from barley leaves. In addition, the hydrolysis of indoleacetonitrile was shown in seedlings of *Avena* (oats), *Triticum* (wheat) and *Raphanus* (radish). Among 29 plants species from 21 families were tested, 19 showed no activity, indicating nitrilase is not common in the plant kingdom [26].

Both, indoleacetonitrile and indoleacetic acid, are inhibitory to the mycelial growth of the fungus *Fusarium oxysporum* f. sp. *cubense* suggesting the nitrile might be converted to the acid by this fungus. The hydrolysis of indoleacetonitrile and indoleacetic acid could be verified by TLC. Several other fungi, including *Fusarium oxysporum* f. sp. *dianthi*, *F. solani*, *Fusarium* isolates from carrot and Easter lily, *Gibberella fujikuroi*, *Aspergillus niger* and *Penicillium chrysogenum*, are capable of this hydrolysis, however do not excrete the enzyme into the culture medium [26].

The first bacterial nitrilase, ricinine nitrilase, was isolated from a soil bacterium by Hook and Robinson in 1964. The enzyme was isolated by selection for growth on the naturally occuring nitrile ricinine (*N*-methyl-3-cyano-4-methoxy-2-pyridone) as sole carbon source. Ricinine nitrilase catalyzes the hydrolysis of ricinine to *N*-methyl-3-carboxy-4-methoxy-2-pyridone and ammonia, and a small amount of *N*-methyl-3-carboxamide-4-methoxy-2-pyridone. Similar amounts of amide were found in reactions with crude extract and purified enzyme. *N*-methyl-3-carboxamide-4-methoxy-2-pyridone was not enzymatically hydrolyzed to the carboxylic acid. A common

intermediate for amide and acid formation was therefore proposed [28].

The physiological role of nitrilases is still not clear. Bacteria, such as *Bacillus subtilis*, constitutively express nitrilases. The majority of the nitrilases characterized are inducible by the presence of nitriles in the growth media, indicating a role in detoxification or utilization. The role in detoxification was shown for cyanide in plants, glucosinolates, and the aldoxime degrading pathway. Nitrilases are also considered to be involved in the production of metabolites, as exemplified by the synthesis of indoleacetic acid [21].

Structure and catalytic mechanism

Most nitrilases consist of a single polypeptide chain with a molecular mass of approximately 40kDa. All the superfamily enzymes demonstrate significant structural homology. Microbial nitrilases, cyanide dihydratases and cyanide hydratases form left-handed spiral quaternary structures [21]. The superfamily is characterized by having a homodimeric building block with an eight layered αββα-αββα sandwich fold. Crystal structures show dimers, tetramers, hexamers or octamers. The dimer is the building block for oligomerization. Microbial nitrilases form larger homo-oligomeric spirals with varying numbers of 6-26 subunits. Plant nitrilases possess two or three nitrilase isoforms in their tissues. These enzymes could either have a dual biological function or broaden their substrate spectrum through the formation of higher heteromeric complexes. The functional significance of the oligomerization is, however, not yet fully understood [20, 21]. The nitrilase active site contains three positionally conserved amino acid residues: cysteine, glutamic acid, and lysine. All microbial nitrilases possess an extended C-terminal sequence of about 40-100 amino acids [21]. Deletion of 55 or 64 amino acids from the C-terminus from *Rhodococcus rhodochrous* led to inactive enzyme. An analogous deletion of 47-67 C-terminal amino acids reduced enzymatic activity of *Pseudomonas fluorescens*, increased amide formation, and changed enantioselectivity. No significant differences in enzymatic properties were observed when about 50-80 amino acid residues in the C-terminus were swapped with those from other superfamily enzymes, namely *Rhodococcus rhodochrous* and *Alcaligenes faecalis* [21, 25]. The C-terminal region in microbial nitrilases might therefore facilitate spiral formation by positioning residues located at the interfaces in close proximity with each other and thereby strengthening the interfaces. This C-terminal region probably interacts with another part of the subunit which is located near the actives site influencing activity and stability of the nitrilase [21] .

The first crystal structures of nitrilase superfamily members were of *N*-carbamyl-*D*-amino acid amidohydrolase from *Agrobacterium* and a NitFhit protein from *C. elegans* [29, 30] Recently, the first crystal structure of an enzyme of the nitrilase family exhibiting nitrilase activity, the nitrilase from *Pyrococcus abyssi*, was solved [31]. This nitrilase is a thermophilic enzyme, exhibiting maximum activity at 80°C. Small, aliphatic dinitriles, like fumaro- and malononitrile, are converted to the corresponding monoacid mononitriles [32]. The enzyme crystallized as a dimer, possessing twofold symmetry in the asymmetric unit. Each subunit contains 262 residues and has an αββα sandwich fold forming a αββα-αββα structure when the two subunits associate. The C-terminal part of each subunit extends away from the core and interacts with other subunits. The dimer interface contains hydrophobic as well as charged residues. Salt bridges between arginine and glutamate residues constitute a considerable part of the interaction responsible for dimer formation.

The binding pocket, located near the inter-subunit interface, is lined with hydrophobic residues, mostly phenylalanine [31].

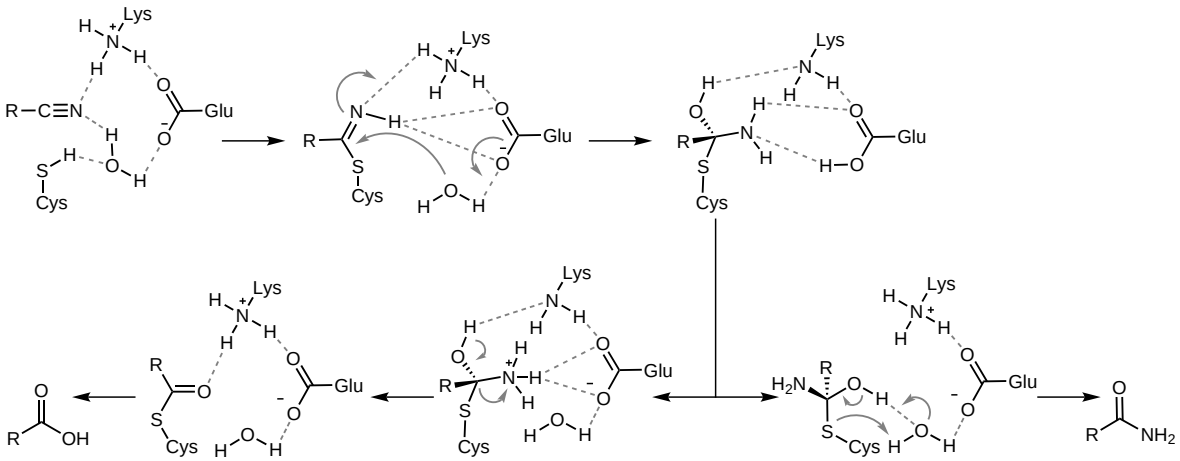

Scheme 1.2 Proposed mechanism for the hydrolysis of nitriles to carboxylic acids and carboxamides catalyzed by nitrilase.

Nitrilases conserve the catalytic residues, namely a cysteine, a glutamate, and a lysine in the active site. These residues were identified as essential for catalysis by mutation experiments yielding inactive enzyme [24]. The catalytic residues in *Pyrococcus abyssi* nitrilase were identified as Glu42, Lys113 and Cys146 by sequence and structure comparison with other proteins from the nitrilase superfamily. The catalytic mechanism proceeds via a thioimidate intermediate, as depicted in Scheme 1.2. In the first step, the active site cysteine initiates nucleophilic attack on the carbon of the nitrile with concomitant protonation of the nitrogen to form a thiomidate intermediate stabilized by lysine. Attack by water, accompanied by further protonation on the nitrogen leads to an tetrahedral intermediate. The glutamate increases the nucleophilicity of the cysteine and participates in proton transfer, resulting in elimination of ammonia and an acyl-enzyme. In *Pyrococcus abyssi* nitrilase, Glu42 and the thiol-sulfur of Cys146 are in close contact of 2.6Å, supporting the role of Glu42 as a catalytic base responsible for activation of the nucleophile Cys146. The acyl-enzyme then reacts with water to form the acid product [21, 31, 33]. The tetrahedral intermediate can also release the amide product. In absence of the assistance of other amino acids, the cysteine is expected to leave preferentially, as the C-S bond is much weaker than the C-N bond. However, a π-electron withdrawing group switches the amide formation to that of acid, possibly because the sulphur offers a greater mesomeric stabilization of the transition state [20, 22]. Elimination of ammonia from the tetrahedral intermediate, to subsequently yield the acid product, requires a positive charge on the nitrogen atom of the substrate, stabilized by the glutamate residue. A positive charge on the nitrogen atom of the substrate can be destabilized demanding residues R or by steric interactions forcing the nitrogen atom away from the stabilizing glutamate residue. The charge distribution in the tetrahedral intermediate, therefore depends on the stereochemistry and electronic properties of the residue R and acts as a mechanistic switch [23]. The rate determining step was identified as rate of the breakdown of the covalent intermediate, for both good and poor substrates. It was considered possible that the enzyme could bind and react with many different nitriles in the first step and good substrates are only distinguished in later steps of the reaction [33].

Substrate specificity

Nitrilases are commonly classified in three subgroups according to their substrate specificity for aromatic, aliphatic or arylaliphatic nitriles [25]. Aromatic nitrilases are abundantly found in the *Rhodococcus* genus and are highly specific for aromatic and heterocyclic nitriles. However, there is a degree of flexibility in the nitrilases substrate range. The enzymes from *R. rhodochrous* J1 and *Rhodococcus* NCIMB 11216 can hydrolyze acrylonitrile and propionitrile, respectively. Aromatic nitrilases are also found in filamentous fungi, e.g. in *Fusarium solani* IMI196849, *Fusarium oxysporum f. sp. melonis*, *Aspergillus niger K10* and *Fusarium solani O1*. These enzymes share high specificity for aromatic substrates and good thermostability. Aliphatic nitrilases were reported from *Acidovorax*, *Comamonas*, *Pseudomonas*, and *Acinetobacter*. Arylacetonitrilases were typically reported in *Alcaligenes*, *Pseudomonas* or *Halomonas*. Arylacetonitrilases are generally enantioselective enzymes, displaying activity with benzonitrile and sometimes aliphatic nitriles. The natural substrates for the majority of nitrilases are not known [21, 25].

The substrate specifictiy of different nitrilases was investigated in literature. Nitrilase from *P. putida* was identified as arylacetonitrilase, accepting phenylacetonitrile derivatives, including indole 3-acetonitrile and 2-thiopheneacetonitrile as substrate. Substitution in *para*-position on the phenyl ring dramatically increased enzyme activity, while *ortho*-substitution decreased it, probably due to steric hinderance. The incorporation of under 5% of organic solvent (DMSO, DMF, *i*-propanol, ethanol, methanol, THF, dioxane, acetone) generally increased activity for the hydrolysis of mandelonitrile by increasing the availability of substrate. Higher concentrations of cosolvent led to denaturation of the enzyme [34].

Nitrilases are used for the enantioselective synthesis of amino acids from aminonitriles. In this enzymatic method, the nitrile is required to rapidly racemize, so the preferred enantiomer is availabe for the enzyme. Racemization is achieved either at higher pH values, typically above pH 10, or by preparing *N*-acylated aromatic aminonitriles, which racemize easily at pH 8 [25]. Nitrilases generally discrimiate between *cis*- and *trans*-configuration [25, 35]. Several *trans*- and *cis*-configured, carbocyclic and nonaromatic heterocyclic, nitriles were used as substrates for commercially available nitrilases from Codexis, Inc. and fungal nitrilases from *F. solani* and *A. niger* [35–38]. For α- and γ-aminonitriles, the *cis*-isomer was preferentially hydrolyzed [25, 35]. Pyrrolidine-3-carbonitriles were more easily converted than piperidine 3- and 4-carbonitriles, suggesting a preference of five-membered rings over those of six-membered rings as substrates [38]. The amino-group was protected with different protecting groups. *N*-Toluenesulfonyl protected acids were formed in superior enantioselecivities compared to the *N*-carbobenzyloxy protected analogues [38]. Similar conversions and similar tendencies in terms of substrate specificity were observed for the commercially available nitrilases and the fungal nitrilases [25, 35].

Amide formation has been observed in nitrilase catalyzed reactions since the first investigations of nitrilases in the 1960s. However, amide formation was often neglected, and ascribed to the presence of contaminating nitrile hydratases [23]. Amide was also found in reactions with purified ricinine nitrilase of *Pseudomonas sp.* [28] and purified nitrilases from *F. oxysporum f. sp. melonis*, *R. rhodochrous* ATCC39484, and *Pseudomonas* DSM7155. In these cases, the amide is usually less than 5% of the total reaction products [20]. Amide, however, was also found as major product in nitrilase catalyzed reactions. AtNIT4 nitrilase from *Arabidopsis thaliana* was

found to produce 1.5 times more asparagine than aspartic acid from the β-cyano-*L*-alanine. The AtNIT1 enzyme from *Arabidopsis thaliana* was shown to produce the amide from fumaronitrile in a ration of 93/7 of amide to acid, while acid was the predominant product in a ratio of 1/99 of amide to acid from crotononitrile as substrate [20, 23], Amide formation has also been reported for the arylacetonitrilase from *Pseudomonas fluorescens* EBC191, in a range of 8% to 89%, depending on the substrate. The time course of the hydrolysis of 2-phenylactonitrile in the presence of *Pseudomonas fluorescens* EBC191 was monitored, showing that amide and acid are formed concurrently in the reaction. Measurements of the initial rates of amide and acid formation showed that acid formation is more temperature dependent, indicating a higher activation barrier for the formation of acid. Similarily a shift towards acid product was observed at pH values below pH 3. Elevated temperature and low pH therefore favour the acid product, while low temperature and increased pH bend the selectivity towards the amide. A correlation between the electron-deficiency of the α-substituent and the amount of amide produced was suggested. The influence of the electronegativity of the α-substituent on amide formation was further investigated for *Arabidopsis* nitrilases, indicating the extend of amide increases with increasing electronegativity of the α-substituent in the order methyl<H<Cl [23]. *N*-Toluenesulfonyl- and *N*-carbobenzyloxy protected pyrrolidine-3-carbonitriles yielded up to 31% of carboxamide, while in the case of *N*-toluenesulfonyl pipecolic carbonitrile the amide was observed as predominately formed product in reactions catalyzed by commercially available nitrilases from Codexis, Inc [38]. When the α-activated nitrile *trans*-oxazoline-nitrile was used as substrate, 93% of amide were found as product, however, approximately 20% of which were attributed to chemical nitrile hydrolysis by DTT. In spin-concentrated nitrilases in buffers without DTT, conversions of up to 75% of amide were observed. For the correpsonding *cis*-substrate up to 56% of amide formation was found with similar amounts of amide formed by DTT [39]. The hydration of nitriles into amides may complicate the use of nitrilases for the production of carboxylic acids. However, nitrilases producing a high ratio of amide to acid may be useful for the synthesis of amides. Nitrilases exceed nitrile hydratases in terms of stability and enantioselectivity [23, 25].

Industrial applications

Nitrilases are attractive biocatalysts in the fine chemicals and pharamceutical industries. Nitrilases are versatile biocatalysts and exhibit high specificity, chemo-, regio, and enantioselectivity and operate in aqueous solutions at moderate temperature and pH, minimizing the costs of chemical processes and the negative impact of industry on the environment [10, 21, 40]. Many reactions catalyzed by nitrilases are already operated in large scale. Nicotinic acid is a vitamin used, amongst others, in animal feed supplementation and medicine. Nicotinic acid can be produced by enzymatic hydrolysis of 3-cyanopyridine with *R. rhodochrous J1* resting cells, a process commercially used by Lonza [12, 41]. *(R)*-Mandelic acid and *(R)*-3-chloromandelic acid are also produced by nitrilase biocatalysts by Mitsubishi Rayon Co and BASF [40, 41].

An attractive feature of nitrilases is their ability to selectively convert one cyano group of a polynitrile. 5-Cyanovaleric acid, an intermediate in the synthesis of nylon-6, can be prepared from adiponitrile by *R. rhodochrous* K22. Tranexamic acid, a drug used to treat or prevent excessive blood loss, is obtained by selective mono-hydrolysis of *trans*-1,4-dicyano cyclohexane by *Acremonium*

sp [10]. The application of nitrilases for selective hydrolysis of nitriles in the presence of labile functional groups is another topic currently investigated [40, 42].

Nitrilases are applied for herbicide degradation. Prolonged exposure to nitrile herbicides, including dichlobenil (2,6-dichlorobenzonitrile), and bromoxynil (3,5-dibromo-4-hydroxybenzonitrile), results in weight loss, fever, vomiting, headache, and urinary problems. Nitrile metabolizing enzymes efficiently degrade these cyano-group containing herbicides. The nitrilase of *Klebsiella pneumoniae subsp. ozaenae* is highly specific for bromoxynil. The bacterial gene was spliced to plant-promoters and the genes expressing the bromoxynil-specific nitrilase were introduced into cotton varieties of bromoxynil-resistant cotton (BXN^{TM}). Similarly, other bromoxynil resistant plants could be achieved or other nitrile-degrading enzymes could be candidates for molecular manipulation of biodegradative systems in plants [10, 21, 43]

Synthetic nitrile compounds are widespread in industrial waste water. Many of these nitriles are toxic, carcinogenic and mutagenic in nature. Biodegradation of nitriles using a mixed culture of bacteria containing different nitrile hydrolyzing enzymes are used as batch and continuous cultures for the treatment of waste. However, microbial treatment of toxic industrial waste is often hindered by varying levels of pH and temperature inhibiting microbial growth. Engineered organisms or enzymes tolerating harsh reaction conditions might be a valuable alternative [10, 21].

Screening of metagenomic libraries and gene site saturation mutagenisis, a high throughput screening technique in which possible point mutations are explored, led to a nitrilase suitable for the efficient, scalable mono-hydrolysis of 3-hydroxyglutaryl nitrile to *(R)*-4-cyano-3-hydroxybutyric acid. This compound is an important pharmaceutical intermediate for the synthesis of the cholesterol-lowering drug Atorvastatin (Lipitor®) [21, 25, 44].

Immobilization

On an industrial scale, heterogeneous catalysts are preferably used, as they may be separated easily and thus allow reuse and recycling of the catalyst, as well as application in continuous processes. Consequently, immobilized enzmyes are expected to reduce costs by enabling the efficient separation, recycling, and reuse of costly enzymes. Immobilization strategies are categorized into four main groups: heterogenization by adsorption onto a support material, heterogenization by electrostatic interaction, heterogenisation by encapsulation, and heterogenization by covalent bonding, including covalent immobilization on polymeric resins, colvent immobilization by copolymerization, and covalent immobilzation on an inorganic support [45–47]. A variety of methods for the immobilization of microbial cells are known, including encapsulation, adsorption, and covalent bonding. Immobilization simplifies catalyst recovery and reuse, improves the resistance of cells to lysis, and improves enzyme performance, such as activity, stability and selectivity [41, 47, 48]. In some cases, immobilized cells were found to hydrolyze a wider range of substrates than free cells, e.g. immobilized *Candida guilliermondii* CCT7207 cells degraded nitriles that could not be utilized by the corresponding free cells [41]. Whole cells of *E. coli* expressing the nitrilase from *A. facilis* were immobilized in carrageenan beads cross-linked with glutaraldehyde and polyethylenimine. The resulting biocatalyst was found stable for approximately 50 cycles. Analogous encapsulation methods using alginate as matrix were used for the preparation of reusable catalysts for the production of 3-hydroxyvaleric acid, *p*-methoxyphenylic acid, and *(R)*-

mandelic acid [25, 49]. Co-immobilization of a nitrilase from *Aspergillus niger* and an amidase from *Rhodococcus erythropolis* allowed highly selective continuous biotransformation of 4-cyanopyridine to isonicotinic acid. Nitrilase converted the nitrile substrate into an acid-amide mixture in a ratio of 3/1, while the amidase hydrolyzed the amide by-product to the acid [50].

Immobilization of subcellular samples is challenging, as most nitrilases are rather unstable in solution and harsh reaction conditions during the immobilization procedures may impair their activities [25]. Cross-linked enzyme aggregates (CLEAs®) are a simple method involving precipitation of the enzyme from aqueous buffer by changing the hydration state of enzyme molecules or by altering the electrostatic constant of the solution by adding appropriate aggregation agents. Originally highly solvated enzyme molecules associate together under these conditions to the extent that they precipitate as insoluble aggregates with native enzyme conformation. These insoluble physical aggregates can subsequently be cross-linked by the addition of bifunctional cross-linkers. The method is applicable to a wide variety of enzymes, and affords stable, recyclable catalysts with high retention of activity. The enzyme does not need to be of high purity, as this methodology combines purification and immobilization in one step [47, 51]. Low or no retention of activity was observed when glutaraldehyde was used as cross-linker for nitrilases. Glutaraldehyde might react with amino acids that are crucial for the activity of the enzyme. Bulky polyaldehydes were used as alternative cross-linkers, resulting in high retention of enzymatic activity [52]. CLEAs® of nitrilase from *E. coli* harbouring a gene of *Pseudomonas putida* were recently applied for the hydrolysis of mandelonitrile to *(R)*-mandelic acid [53]. CLEAs® increased the stability of the nitrilase from *A. faecalis* expressed in *E. coli*. Another immobilization method is encapsulation, as applied for NIT-102 from Codexis encapsulated in silica nanoparticles. These encapsulabted enzymes were recyclable without significant loss of activity. In a few studies, immobilized nitrilases were already used in continuous mode in continuous stirred tank reactors or columns filled with enzymes absorbed by hydrophobic or exchange interactions [25].

1.1.2 Nitrile hydratase

Nitrile hydratases (EC 4.2.1.84) are metalloenzymes that catalyze the hydration of nitriles to their corresponding amides. Nitrile hydratases can be classified into ferric nitrile hydratases and cobalt nitrile hydratases. Nitrile hydratase activity was found in many microbes, including various genera of Proteobacteria, Actinonobacteria, Cyanobacteria, and Firmicutes. The majority of nitrile hydratases investigated in literature are from various species of *Rhodococcus* [12, 54, 55]. Nitrile hydratase is, unlike nitrilase, exclusively a bacterial enzyme. Microbes usually contain either a nitrilase or a nitrile hydratase - amidase system for the hydrolysis of nitriles. However, some microorganisms, such as *Rhodococcus rhodochrous* J1, *Rhodococcus rhodochrous* LL 100-21, *Rhodococcus rhodochrous* PA-34, *Nocardia globerula* NHB-2, contain both, nitrilase and nitrile hydratase-amidase systems. These three enzymes can be induced selectively [54].

Nitrile hydratase activity in the wild type organism is inducible by its substrates, products or their analogues [10, 54]. In general, only one type of nitrile hydratase is produced by one organism. However, *Rhodococcus rhodochrous* J1 produces two types of nitrile hydratases. Their expression is regulated by supplementing the specific inducer for each in the culture media. Addition of cyclohexanecarboxamide resulted in induction of a low-molecular weight nitrile hydratase

(L-NHase), which showed higher activity with aromatic and heterocyclic nitriles, while urea induced a high-molecular weight nitrile hydratase (H-NHase), which exhibited higher specificity for aliphatic nitriles, particularly acrylonitrile [10, 54, 56]. The inducers are considered to act at the transcriptional level to induce the expression of nitrile hydratase genes and to regulate the assembly of α- and β- subunits of nitrile hydratase. Cobalt or iron are constitutional components of functional nitrile hydratases. The metal ion in the active site is either acting as catalyst for nitrile hydration, or required for folding or stabilizing the enzyme. Addition of cobalt- or iron-salts in the culture media is essential for active expression of nitrile hydratase. Nitrile hydratase is expressed intracellularly, therefore recovery of the whole cells from the production media is required [10, 54, 56].

Structure

Structural analysis of nitrile hydratases revealed a region of the α-subunit VC(T/S)LCSC(Y/T) highly conserved in both types of nitrile hydratases. This region was identified as metal binding domain. The cobalt-containing nitrile hydratase contains threonine and tyrosine as third and eighth amino acid residue in the metal binding domain, while in iron-containing nitrile hydratase these amino acids are replaced by serine and threonine respectively [54, 56]. Incorporation of cobalt into the iron-type nitrile hydratase from *Rhodococcus* sp. N-771 was achieved by expressing the nitrile hydratase in *E. coli* in cobalt supplemented medium. The metal substitution resulted in reduced nitrile hydratase activity. The enzymatic activity gradually increased by incubation with an oxidizing agent, potassium hexacyanoferrate. The oxidising agent is likely to activate the cobalt-substituent by oxidizing the cobalt atom to a low-spin Co^{3+}-state and/or modification of Cys-112 to a cysteine sulfinic acid [57]. Three cysteine residues are considered to be the ligands of the metal ion in the catalytic centre of nitrile hydratase. These cysteine residues (αC-102, αC-105, and αC-107) in the high molecular mass nitrile hydratase of *Rhodococcus rhodochrous* J1 were replaced with alanine by site directed mutagenesis. These cysteine residues were found necessary for the incorporation of a metal ion and active expression of nitrile hydratase [58]. The cobalt-containing nitrile hydratase from *Pseudonocardia thermophila* JCM 3095 was used to investigate the role of the threonine/serine (T/S) and tyrosine/threonine (Y/T) amino acid residues in the metal binding region. The T109S mutant exhibited similar characteristics to the wild type enzyme, however, the Y114T mutant showed very low cobalt content and decreased catalytic activity, as compared with the wild type enzyme. Oxidative modifications of Cys111 and Cys113 were not observed [59].

The nitrile hydratases from *Rhodococcus* R312 and *Pseudomonas chloraphis* B23 are the first examples of non-heme iron-containing enzymes with a low spin Fe(III) ion [60]. *Rhodococcus* N774 and *Rhodococcus* N771 contain nitrile hydratases with identical amino acid sequences as *Rhodococcus* R312. These nitrile hydratases are composed of α- and β-subunits, each with a molecular mass around 23kDa. One iron is found in each αβ-unit. These nitrile hydratases show unique reactivity to light. The inactive form of the nitrile hydratase exists in the dark. The inactive form is activated by light irradiation, whereas the active form is inactivated by aerobic incubation of the cells in the dark. The chromophore responsible for the photoactivation is an iron complex. In the inactive form of the nitrile hydratase, an endogeneous NO is bound to the non-heme iron. Photodissociation of the NO activates the enzyme [10, 55, 56].

Depending on the species of origin, different quaternary structures, αβ-dimers, or $\alpha_2\beta_2$-tetramers, have been observed for nitrile hydratase. The crystal structure of the photoactivated nitrile hydratase from *Rhodococcus* sp. 312 was solved at 2.65Å. The α-subunit consists of a long N-terminal arm and a C-terminal domain with a four layered αββα-structure. The β-subunit also contains a long N-terminal extension, a helical domain, and a C-terminal domain that folds into a β-roll. The two subunits form a tight heterodimer that is the functional unit of the enzyme. The active site is located in a cavity at the subunit-subunit interface. The iron centre is formed by three cysteine thiolates and two mainchain amide nitrogen atoms from residues of the α-subunit [55].

The crystal structure of the cobalt-containing nitrile hydratase from *Pseudonocardia thermophila* JCM 3095 at 1.8Å revealed the structure of the non-corrin cobalt at the catalytic centre. Two cysteine-residues coordinate to the cobalt and were post-translationally modified to cysteine sulfinic acid and to cysteine sulfenic acid, like in iron-containing nitrile hydratases. In cobalt-containing nitrile hydratases, a tryptophan residue replaces the tyrosine residue of iron-containing nitrile hydratase. This tryptophan residue in the active site is considered responsible for the different substrate preference of cobalt- and iron-containing nitrile hydratases. Cobalt-containing nitrile hydratases prefer aromatic nitrile substrates, whereas iron-containing nitrile hydratases convert aliphatic nitriles [61].

Catalytic mechanism

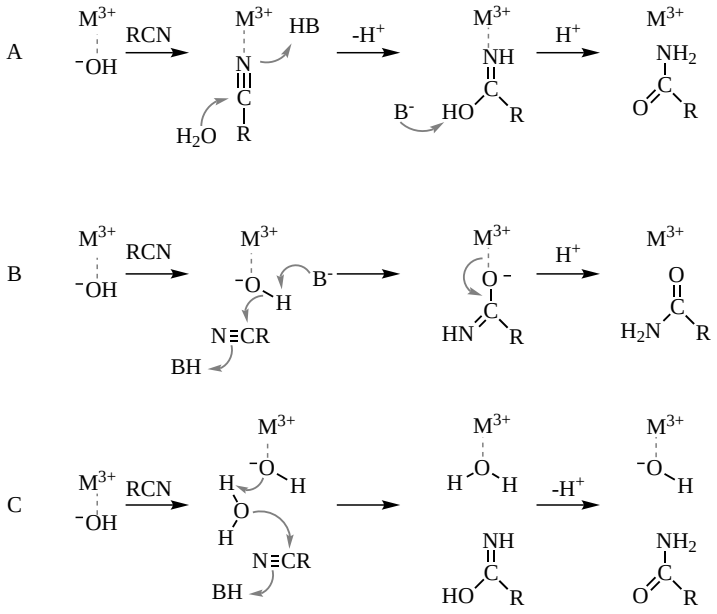

Scheme 1.3 Proposed mechanisms for the nitrile hydratase catalyzed hydration of nitriles.

Based on the crystal structure of nitrile hydratases, different mechanisms for the hydrolysis of the nitrile were proposed. In all mechanisms, the metal ions serve as Lewis acid. The first possible reaction model, depicted in Scheme 1.3, assumes direct coordination of the nitrogen of the substrate to the metal ion. The nitrile substrate approaches a metal bound hydroxide ion, which in turn attacks the nitrile carbon atom. This mechanism is supported by the presence of an iodoacetonitrile molecule in close proximity of the Fe(III) centre in the crystal structure of *Rhodococcus* sp. R312.

In the second mechanism proposed, nucleophilic attack of the metal bound hydroxide on the nitrile substrate occurs in the active site. The resulting transient iminolate is *O*-bonded to the metal and rearranges to the amide product. The third mechanism assumes catalysis without direct coordination of the substrate to the metal ion. A metal-bound hydroxide ion acts either as base activating a water molecule in the active site, which then attacks on the nitrile carbon. A imidate intermediate is formed and tautomerizes to the amide product. The coordination structures of the M(III) sites of the iron- and cobalt nitrile hydratase are very similar and thus, it is assumed that the metal ions function similarly [10, 54–56].

The active site of nitrile hydratase, the metal ion centre, is deeply buried in the protein scaffold. The distance of the channel from the nitrile hydratase surface to the active site is about 15Å. X-ray crystallographic analysis and enhanced sampling molecular dynamics simulations indicate that this channel plays a major role in nitrile hydratase functioning. The architecture and interior of the channel are considered responsible for the tuning of catalytic efficiency, stereospecificity and substrate affinity of nitrile hydratases [54, 62].

Enzyme characterization

Nitrile hydratases exhibit broad physiological pH optima, varying between pH 6.5 and pH 8.5. A rapid loss of activity was reported by decreasing or increasing the pH value. The loss of activity below pH 6.5 is either due to denaturation and subunit dissociation or due to change in the ionization of a critical active side residue, such as the cysteine thiol residues. Most nitrile hydratases are thermolabile, exhibiting maximum activity in a temperature range from 20°C to 35°C. However, thermophilic nitrile hydratases are available with maximum activity at temperatures of up to 60°C. Nitrile hydratases and amidases are often co-expressed. Amidases can hydrolyze the amide product of the nitrile hydratase catalyzed reaction. Applying reaction temperatures below 25°C drastically lowers amidase activity to negligible levels [54, 63].

Substrate specificity and selectivity

Nitrile hydratases catalyze the hydration of nitriles chemo-, regio-, and enantioselectively [64]. Aromatic, heterocyclic nitriles, aliphatic nitriles bearing ether or ester groups were chemoselctively hydrolyzed by nitrile hydratase from *Rhodococcus rhodochrous* NCIMB 11216 [65]. Monomethyl *(R,S)*-3-benzoyloxyglutarate and monomethyl *(R,S)*-3-benzyl-oxyglutarate were successfully prepared from their corresponding nitriles. However, in whole cell biotransformations product purity was impaired by cleavage of the ester groups by esterases. Esterase attack was found to be influenced by the polarity of the substrate. Cyanobenzoates were hydrolyzed by an esterase of *Rhodococcus equi* A4, while the corresponding aminobenoates were not hydrolyzed. The nitrile hydratase from this strain was therefore applied as purified enzyme to ensure chemoselectivity [64, 66]. A chemoselective biocatalyst, *R. rhodochrous*, is suitable for the treatment of polyacrylic fibre. Nitrile groups are converted into amide groups without undesirable hydrolysis of the ester moieties in the copolymer vinyl acetate. The efficiency of fibre dying is therefore enhanced by interaction of the dye with the amide groups [64].

Regioselective, biocatalytic hydrolysis of α,ω-dinitriles is a unique route to cyanocarboxylic acids or their amides, and to the correspnding lactams. Acid- or base catalyzed regioselective

hydrolysis of dinitriles requires stopping the reaction at an incomplete conversion of typcially less than 20%. Enzymatic hydrolysis affords cyanocarboxylates from dinitriles in nearly quantitative yields. 5-Cyanovaleramide, an intermediate in herbicide synthesis, can be produced from 2-ethylsuccinonitrile in a regioselective hydrolysis catalyzed by *Comamonas testosteroni*. The industrial manufacture of 5-cyanovaleramide uses immobilized *Pseudomonas chlororaphis* [64].

Stereoselectivity of some nitrile hydratases towards arylaliphatic nitriles was observed in whole-cell experiments and confirmed with purified enzymes. Stereoselective nitrile hydratases were isolated from *Pseudomonas putita*, *Agrobacterium tumefaciensis* d3 and *Rhodococcus equi* A4. These enzymes are *(S)*-selective and show preference for *(S)*-2-arylpropionitriles or *(S)*-2-arylbutyronitriles. *(R)*-Selective nitrile hydratases were also observed in whole cells. Substitution on the aromatic ring of the substrate decreases the stereoselectivity of the nitrile hydratase from *Agrobacterium tumefaciensis* d3, however, 4- or 6- substitution increases stereoselectivity for the nitrile hydratase from *Rhodococcus equi* A4 [63, 64, 67, 68].

Industrial Applications

Nitrile hydratases are used in several industrial processes. Acrylamide is prepared by hydrolysis of acrylonitrile in a 30,000 to 95,000 tons per year scale. The reaction was established with nitrile hydratase from *Rhodococcus sp.* N77 and *Pseudomonas chloroaphis* B23, currently nitrile hydratase from *Rhodococcus rhodochrous* J1 is used in the industrial process run by Mitsubishi Chemical Corporation and Mitsubishi Rayon Co., Ltd. [10, 12, 54, 56, 69]. Nicotinamide is prepared in a chemoselective enzymatic hydrolysis of 3-cyanopyridine and affords nicotinamide without contaminations of nicotinic acid. This process uses *R. rhodochrous* immobilized on poylacrylamide and is performed by Lonza AG, CH, under a license from Mitsubishi Rayon on a scale of 4,000 tons/year [64]. Nitrile hydratases have also been shown effective in the removal of nitriles from contaminated waste streams. Nitrile hydratases were successfully used for the biodegradation of organonitriles in pharmaceutical waste-water and nitrile contaminated soil [54, 55].

Amidases

Amidase and nitrile hydratase genes are often adjacent in the same operon and co-expressed. Amidases hydrolyze the amide product of the nitrile hydratase catalyzed reaction to the carboxylic acid and ammonia. In prokaryotes, amidases are involved in the carbon/nitrogen metabolism, in eukaryotes they transfer ammonia from glutamine to tRNAGlu, and in mammals they are responsible for the degradation of neuromodulatory fatty acid amides. Different amidases are known to be specific for aliphatic or aromatic amides or amides of α- or ω-amino acids. *Rhodococcus* sp. R312 was reported to have a wide spectrum of amidases, including an α-amio acid amidase specific for *L*-α-aminoamides, an aliphatic amidase, and an enantioselective amidase hydrolyzing aryloxypropioamides [10, 24, 70, 71].

1.2 Nitrile reductase queF

Nitrile reductase queF (EC 1.7.1.13) is the first enzyme known to catalyze the reduction of a nitrile to the corresponding primary amine. The enzyme queF was recently discovered in the biosynthetic

pathway of the 7-deazaguanine modified tRNA nucleoside queuosine, depicted in Scheme 1.4. QueF shows high sequence homology to GTP cyclohydrolase I (FolE) and was first described as a GTP cyclohydrolase like enzyme, proposed to be responsible for the initial step in queuosine biosynthesis [9, 72]. However, cyclohydrolase activity was not observed with GTP nor with the related metabolites GMP, GDP, and guanosine as substrates. The biosynthetic pathways of queuosine (in bacteria) and arachaeosine (in archea) diverge from the common intermediate $preQ_0$, as depicted in Scheme 1.6. The enzyme queF was proven to play an essential role in queuosine biosynthesis, whereas arachea lack a queF homologue. Therefore, queF catalyzes an enzymatic step exclusive to the biosynthesis of queuosine, after the formation of $preQ_0$. QueF was identified as an oxidoreductase, catalyzing the cofactor dependent reduction of 7-cyano-7-deazaguanine ($preQ_0$) to 7-aminomethyl-7-deazaguanine ($preQ_1$), a reduction of a nitrile group into its corresponding primary amine, a reaction unprecedented in biology [9, 13, 73].

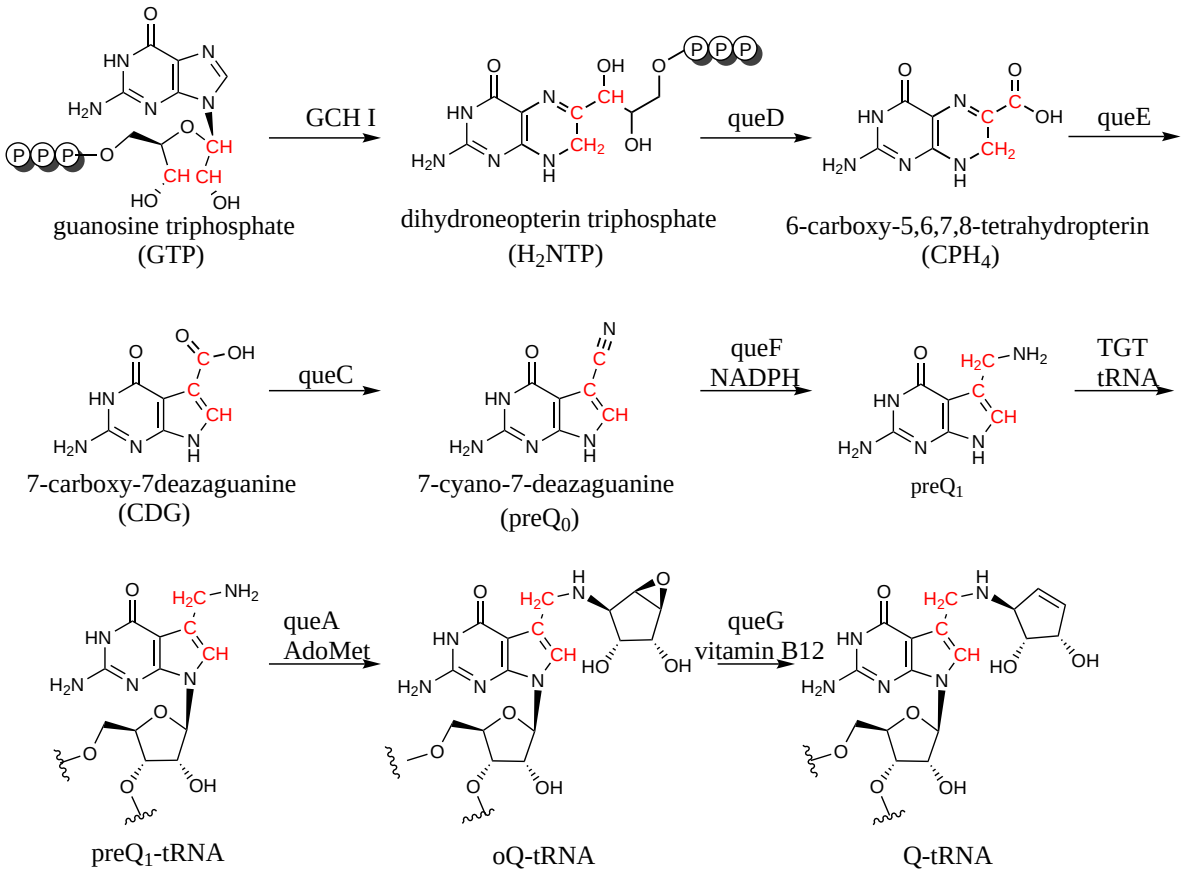

Scheme 1.4 Biosynthetic pathway of the hypermodified nucleoside queuosine (Q), including the enzymatic reduction of 7-cyano-7-deazaguanine ($preQ_0$) to 7-aminomethyl-7-deazaguanine ($preQ_1$) catalyzed by nitrile reductase queF.

Nitrile reductase activity was tested with different redox cofactors, activity was observed in presence of NADPH [9]. Therefore, queF is classified as $NAD(P)^+$-dependent four electron transfer dehydrogenase. $NAD(P)^+$-dependent four electron transfer dehydrogenases include UDP glucose dehydrogenase [74–78] and its homologues, histidinol dehydrogenase [79, 80], and 3-hydroxy-3-methylglutaryl-coenzyme A (HMG-CoA) reductase [13], all showing activities equivalent to alcohol and aldehyde dehydrogenase [13, 81–85]. These enzymes are similar in the overall

reactions catalyzed, however, were found to employ distinctly different mechanisms. UDP glucose dehydrogenase I catalyzes the NAD^+-dependent two-fold oxidation of UDP-glucose to UDP-glucuronic acid. A mechanism involving an active site cysteine and a thiohemiacetal intermediate, which is further oxidized to the thioester, was suggested [74, 75]. Histidinol dehydrogenase is a Zn^{2+}-dependent metalloenzyme and the reaction mechanism is facilitated by acid-base catalysis. HMG-CoA reductase does neither employ covalent catalysis nor is it metal-dependent [13].

Structure and catalytic mechanism

Structural and sequence analysis indicate that queF belongs to the tunnel-fold (T-fold) superfamily, a superfamily of functionally distant proteins that bind planar pterin or purine substrates. T-fold proteins consist of small monomeric units composed of a pair of two stranded antiparallel β-sheets and two antiparallel α-helices. They assemble into homo-oligomers that form a $\beta_{2n}\alpha_n$-barrel. The active sites of all T-fold proteins are located at the subunit interface, with amino acid residues from seperate monomers contributing to the active site architecture. Sequence identity between FolE and *B. subtilis* queF, belonging to the same structural superfamily, is approximately 25% , while sequence similarity is 40% in a 100 amino acid stretch. The sequence homology between these enzyme families allowed a preliminary understanding of the active site. However, queF shows a strictly conserved pattern E(S/L)K(S/A)hK(L/Y)(Y/F/W) (h is a hydrophobic amino acid) named the queF motif, which is not present in FolE. This motif is flanked by the strictly conserved residues Cys55 and Glu97 (*B. subtilis* numbering). In a homology model of queF with the substrate $preQ_0$ docked in the active site, the Cys55 residue was located in close proximity to the nitrile functionality of the substrate and was consequently suggested to play an important role in catalysis [9, 13].

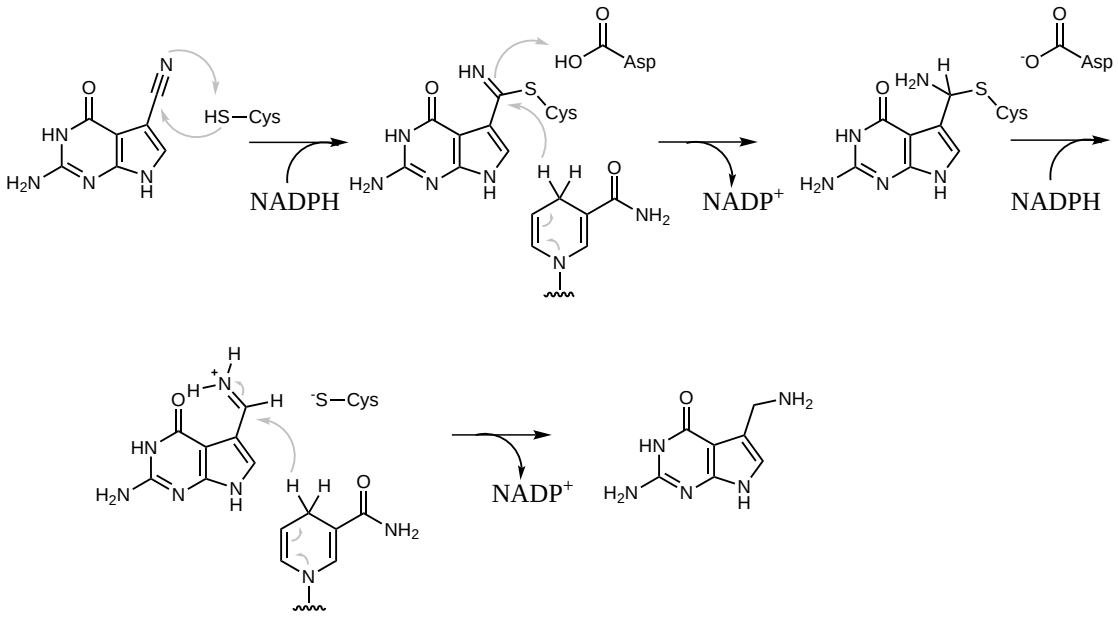

Scheme 1.5 Proposed mechanism for the reduction of $preQ_0$ to $preQ_1$ catalyzed by nitrile reductase queF.

QueF proteins are classified in two structural subfamilies: homodecameric enzymes of unimodular subunits, exemplified by *B. subtilis* YkvM, and larger, bimodular enzymes of two tandem GTP cyclohydrolase I like domains, exemplified by *E. coli* YqcD. The YkvM subfamily shows the queF motif on the N- and C-terminal sides, bracketed by an invariant Cys and Glu respectively,

while in the YqcD subfamily the queF motif and the invariant Cys and Glu residues are located separately in the weakly homologous N- and C-terminal domains respectively of the polypeptide chain. Similar structural subfamilies are also found in FolE: homodecameric, unimodular enzymes exemplified by bacterial and mammalian GTP cyclohydrolase I and bimodular proteins of two domains, found in plant GTP cyclohydrolase I. The homology of queF and FolE families clearly suggested that queF belongs to the tunneling fold structural superfamily [9, 73].

A covalent mechanism has been proposed for the nitrile reductase queF catalyzed reduction of $preQ_0$ to $preQ_1$. First, the substrate $preQ_0$ is bound to the enzyme, followed by nucleophilic attack of the thiol group of the cysteine residue on the nitrile group of the substrate, to form a thioimide intermediate. The first molecule of NADPH then binds to the enzyme and reduces the thioimide intermediate, giving a new covalent adduct, a thiohemiaminal. After releasing the oxidized cofactor, the second molecule of NADPH is bound. The imine is formed from the thiohemiaminal and is further reduced to yield the amine $preQ_1$ (Scheme 1.5) [13]. The reduction of a nitrile to an amine requires four electrons and thus two equivalents of the two-electron reductant NADPH. Consequently, the reaction must be performed stepwise, and involves an imine as two-electron reduction product. However, imines are vulnerable to nucleophilc attack by water, leading to hydrolysis, either in the active site or after dissociation from the enzyme, and formation of aldehyde. In case of nitrogenase catalyzed reduction of hydrogen cyanide, formaldehyde and methylamine are in fact both significant products of the reaction. However, the imine intermediate in the queF catalyzed reaction appears to be temporarily masked as covalent thiohemiaminal adduct, preventing hydrolysis. Presumably, the imine is only formed after binding of the second equivalent of NADPH [13, 86].

1.2.1 Type I nitrile reductase queF (YkvM)

Type I nitrile reductase queF, the YkvM subfamily, is a homodecameric enzyme, first found in *B. subtilis*. *B. subtilis* queF and GTP cyclohydrolase I exhibit 26% sequence similarity and 14% sequence identity, respectively. This homology was used to build a three-dimensional working model of two adjacent queF monomers of *B. subtilis* queF with $preQ_0$ docked in the putative active site. The model suggests catalysis at the intersubunit interface. In one monomer, the substrate interacts with the two invariant side chains Glu97 and Cys55, the conserved Phe95 and the main chain of His96. In the second monomer, the side chain of Ser97 and the mainchain of Val77 coordinate to the substrate. The queF motif is found in a nearby α-helix. According to this model, $preQ_0$ plays an important role in stabilization of the functional multimeric enzyme structure by bridging the two parts of the active site, namely the invariant Glu and Cys residues from one monomer and the queF motif from the other. These findings suggested an influence of $preQ_0$ on the crystallization properties of queF [9, 73].

Enzyme characterization

The pH profile and metal dependence of *B. subtilis* queF was determined. Enzymatic activity was investigated over a pH range from pH 5.4 to pH 9.4 in a tribuffer system to maintain constant ionic strength. The pH profile exhibits a bell curve with maximum activity at pH 7.5. The enzyme was

neither stimulated nor inhibited at KCl concentrations below 10mM, however showed inhibition when the concentration was above 100mM. The activity of queF was assayed with the chloride salts of Ca^{2+}, Mg^{2+}, Mn^{2+}, Co^{2+}, Ni^{2+}, Zn^{2+}, Fe^{2+}, and Fe^{3+}; Cu^{2+} was investigated as the sulfate salt. Most metals induced neither activation nor inhibition. Cu^{2+} and Fe^{3+}, however, led to irreversible inhibition of queF. Maximum activity was observed in the absence of added metal, or in the presence of EDTA, indicating queF is not metal dependent [13].

Steady state kinetic analysis provided kinetic constants that are typical for the enzymes of the queuosine pathway and NAD(P)H dependent dehydrogenases. Initial velocity data were fit to the equations describing a bi-uni-uni-bi ping-pong ter ter kinetic mechanism, with $preQ_0$ as the main substrate and both NADPH molecules binding with equal affinity [13]. A bi-uni-uni-bi ping-pong kinetic mechanism has been shown for other $NAD(P)^+$ dependent four electron transfer dehydrogenases [13, 75, 79, 80, 87]. Initial velocity analysis provided a k_{cat}=0.66±0.04min^{-1}, $K_m(preQ_0)$=0.237±0.045μM and a K_m(NADPH)=19.2±1.07μM. The k_{cat}-value is rather low compared to other dehydrogenases, most likely due to the relatively low flux through the biosynthetic pathway of queuosine which in turn did not induce selective pressure to evolve more efficient enzymes. The k_{cat}-value is not considered a consequence of the reactivity of the nitrile group, as nitrilases and nitrile hydratases exhibit significantly higher values as observed for queF [13].

Sequence analysis of queF revealed that Cys55, found in proximity to the nitrile functionality of the substrate, is strictly conserved over all members in this family.[13] This Cys residue aligns with a universially conserved Cys residue in GTP cyclohydrolase I where it is responsible for zinc binding.[88] As queF was identified not to be a metal-dependent enzyme, Cys55 was proposed as catalytic nucleophile, reacting with the nitrile to form a covalent thioimide intermediate [13]. A thioimide intermediate is analogous to the thioester intermediate found in the catalytic mechanism of UDP glucose dehydrogenase, another nicotinamide-dependent oxidoreductase catalyzing a four electron redox reaction [76]. Titrations of queF with $preQ_0$ in the absence of NADPH resulted in formation of a new peak at 376nm. UV/VIS absorption at 376nm is consistant with that of an α,β-unsaturated thioimide group. The adduct was isolated by dialysis. Three hours after dialysis, 89% of the enzyme existed as queF-$preQ_0$ adduct, indicating remarkable stability of the intermediate. Exposure to NADPH rapidly decreased the absorption at 376nm, supporting the existence of a thioimide intermediate [13].

The importance of Cys55 was further assessed by examining the iodoacetamide-induced inactivation of wild type enzyme, as well as by investigating Cys55 mutants. Iodoacetamide was found to inactivate the enzyme. However, when the substrate $preQ_0$ is included at saturating concentration, an attenuation of the protein inactivation is observed. These results support a catalytically important Cys residue in the active site, which reacts with iodoacetamide, while in the presence of substrate, it is protected from reaction. C55A and C55S mutants exhibited no activity. Titrations of C55A and C55S mutants with $preQ_0$ did not result in a new peak at 376nm. No significant changes, in neither secondary structure nor quaternary structure, were associated with the mutations. The loss of activity in the C55A and C55S mutants is consistent with the loss of essential catalytic functionality, not structural changes in the enzyme [13].

Structure

Crystal structures of wild type queF from *B. subtilis*, as well as from the inactive mutant C55A were determined at 2.5Å[89, 90]. Attempts to crystallize the apoenzyme led to single or clustered hexagonal crystal plates or highly mosaic crystals, diffracting poorly. The use of substrate or substrate analogues is known to improve crystal quality. Furthermore, the homology model suggested substrate binding at the intersubunit interface and therefore stabilisation of the quaternary structure by substrate binding [73]. Wild type queF from *B. subtilis*, as well as the mutant C55A were crystallized in presence of the substrate $preQ_0$. In wild type queF $preQ_0$ was covalently bound in the thioimide intermediate, while in the mutant, lacking the Cys residue responsible for thioimide formation, $preQ_0$ was bound non-covalently. A covalent thioimide adduct has been proposed in the nitrilase-catalyzed hydrolysis of nitriles to carboxylic acids, however this thioimide intermediate was first observed in a crystal structure of nitrile reductase queF [89]. The queF enzyme forms an asymmetric tunnel-fold homodecamer of two head-to-head facing pentamers, each composed of a cyclic arrangement of monomeric $\beta_4\alpha_2$-barrels. A large surface area in each pentamer is buried in the interpentamer interface, consistent with a stable decamer being the biologically active enzyme form. The two pentamers are further pinned together at the C-termini from opposing subunits, which form salt bridges at the interpentamer interface via the conserved residues Asp131 and Arg164. Residues Arg162 and Arg164 form pairs of high affinity metal sites, which are occupied by either Mg^{2+}, as in wild type queF, or Ca^{2+}, as in the C55A mutant. The similarity of both structures suggests, that either metal should result in a functional enzyme. Preliminary biochemical investigations showed that both metals, as well as Mn^{2+} are capable of supporting catalysis. Comparison of approximately 100 unimodular queF sequences for conservation of the metal binding site and the salt bridge pair, show that 80% of the sequences contain the residues for either the metal binding site, the salt bridge, or both. However, the salt bridge is more prevalent than the metal binding site. These sequence conservation patterns suggest that stabilization of the decamer at the interpentamer interface is important for the biological function of unimodular queF. Of the ten subunits in the decamer, two opposing subunits exhibit disordered C-termini, hence the corresponding salt bridges and metal binding sites are not formed [89].

In the queF crystal structure, ten active sites are found at the intersubunit interfaces. However, in the structures of both, the wild type queF and C55A mutant, $preQ_0$ was bound at eight sites. The substrate $preQ_0$ was included in 5-10 fold excess of the enzyme in the crystallization sample. However, it is unclear whether the asymmetric, partially occupied enzyme complex represents the true biological state of queF or is an outcome of the crystallization conditions and crystal lattice contacts. The $preQ_0$ binding pocket is defined by a cleft between the two subunits from the same pentamer. Several residues interact with $preQ_0$. From one subunit, the invariant Glu97 sidechain forms hydrogen bonds with the pyrimidine nitrogen atoms of $preQ_0$, His96 coordinates to the keto group in position 4. From the other subunit, Glu78, the first residue in the conserved queF motif, interacts with the pyrrole nitrogen from $preQ_0$. Additionally Ser79 and Val77 coordinate to the amino group in position 2 and the pyrimidine nitrogen in position 3, respectively. Furthermore, the hydrophobic residues Phe33, Phe95, and Ile130 make Van-der-Waals-interactions with $preQ_0$. The unoccupied active sites provide insight into the structure of the apoenzyme. Compared to an

occupied site, the empty site is widened by 13Å and does not form divalent metal bridges or salt bridges between the two pentamers. These observations suggest that $preQ_0$ binding induces closure of the active site and subsequent tightening of the pentamer as well as stabilization of the functional decamer. This observation is supported by ultracentrifugation experiments, where in presence of $preQ_0$ a sharper peak, indicating a tighter decamer, is found. Furthermore, while a pentamer and a decamer are assumed to exist in equilibrium, in presence of $preQ_0$ the equilibrium shifts towards the decamer [89].

Catalytic mechanism

The reduction of a nitrile substrate to an amine requires four electrons and four protons. According to the crystal structures of wild type *B. subtilis* queF and the C55A mutant, only two residues, Cys55 and Asp62, both conserved, appear to be positioned appropriately to serve as proton donors. In the minimal catalytic mechanism, a proton is transferred from Cys55 to $preQ_0$, followed by nucleophilic attack of the thiolate on the nitrile, forming the covalent thioimide intermediate. This intermediate is then reduced by NADPH to the thiohemiaminal, with Asp62 delivering the necessary proton. Binding of a second equivalent of NADPH is followed by breakdown of the thiohemiaminal to the protonated imine. Hydride transfer from NADPH gives the amine. An additional conserved residue, His96 in *B. subtilis* queF, appears to be not in an appropriate geometry or in close enough proximity to the thioimide to serve effectively as proton donor. However, His96 is within contact distance to Asp62 and was considered of being capable of proton transfer to Asp62, therby indirectly serving as source of the proton delivered by Asp62 [89].

1.2.2 Type II nitrile reductase queF (YqcD)

Type II nitrile reductase queF, the YqcD subfamily, is a bimodular enzyme highly conserved across species [91]. Characterization of type II nitrile reductase from *E. coli* and crystal structures of type II nitrile reductase from *V. cholerae* are available in literature [9, 91, 92]. BLAST analsyis of the protein sequence identified several hundred homologues [91, 93].

Type II nitrile reductase queF (YqcD) has notable sequence differences compared to type I queF (YkvM) [9]. Type II nitrile reductase queF, the YqcD subfamily, is composed of two conserved domains. The N-terminal sequence is a member of the COG2904 superfamily, a superfamily of uncharacterized proteins of unknown function, conserved in bacteria. The C-terminal sequence is classified as tunneling fold (T-fold) superfamily and encompasses the catalytic residues. The amino acid sequence of the YkvM subfamily (queF type I) maps into the T-fold C-terminal region of the YqcD superfamily [91].

Enzyme characterization

Nitrile reductase queF from *E. coli* was experimentally characterized. Temperature dependence studies showed a trend of increased enzyme activity with increasing temperature. However, half life times decreased rapidly with increasing temperature. At 37°C half life time is 28.2 hours, dropping to only 12.8 hours and six minutes at 40°C and 50°C respectively. Initial rates increase linearly with increasing temperature when the exponential increase of activity and enzyme deactivation at

elevated temperatures are superimposed. Nitrile reductase queF from *E. coli* showed the highest activity at pH 7. No decrease in activity was observed for four hours, whereas, at pH 9, less than 20% of the initial activity was retained. Determination of kinetic parameters provided a k_{cat}=7.61min^{-1}, K_m(preQ$_0$)<1.5μM and a K_m(NADPH)<0.2μM. The K_m(NADPH) is 90-fold higher than the one determined for *B. subtilis* queF, while the k_{cat} is ten-fold higher [92].

Structure

The reported structure of bimodular (type II) nitrile reductase queF is quite distinct from that of bimodular GTP-CH-I. Bimodular queF lacks the canonical T-fold quaternary structure of head-to-head association of two $\beta_{2n}\alpha_n$-barrels formed from oligomerization of subunits. Catalysis in bimodular queF therefore occurs at the intrasubunit interface between the N- and C-terminal T-fold modules, not at the intersubunit interface, as in bimolduar GTP-CH-I and other biomodular T-fold enzymes. Although preQ$_0$ does not bind in the interpentamer interface, ultracentrifugation data indicate that preQ$_0$ affects the pentamer-decamer equilibrium in solution [89]. The C-terminal domain of bimodular queF contains the region of homology to the bacterial and mammalian GTP-CH-I subfamily. The N-terminal domain contains the queF motif. The invariant cysteine and glutamate residues (Cys190 and Glu230 in *E. coli* queF) are only present in the C-terminal domain. A similar splitting of active site residues between two domains is seen in bimodular FolE. In both enzymes, a conserved central sequence is located on one domain, split from two flanking sequences, approximately 40 residues apart. This splitting of the YqcD active site suggests a gene duplication occurred, with each domain retaining some of the residues of the putative active site [9].

The structure of queF from *V. cholerae* was determined at 1.52Å. This protein shares 60% sequence identity with the experimentally characterized queF from *E. coli*. *V. cholerae* queF crystallizes as a tetramer, a dimer of dimers. Solution data suggest that the protein is a dimer and exists in equilibrium with its monomer. The queF monomer is made up of two ferredoxin like domains aligned together with their β-sheets that have additional embellishments. Each monomer consists of a seven-stranded, antiparallel β-sheet, eight α-helices, and several loops. These loops contribute to the dimer interface as well as to the formation of the tetramer in the crystal. Each loop is in contact with the loops from the other three monomers. Each monomer contains two units, the first is part of the COG2904 superfamily and consists of a three-stranded β-sheet and two α-helices, the second unit is similar to a T-fold and is composed of a four-stranded β-sheet with two α-helices [91].

Nitrile reductase queF from *V. cholerae* was co-crystallized with guanosine triphosphate, but only guanine, phosphate and pyrophosphate molecules were observed in the crystal structure. The enzyme might therefore retain residual nucleosidase activity [91]. However, nitrile reductase queF from *B. subtilis* (type I) and *E. coli* (type II) do not show cyclohydrolase activity [9]. GTP cyclohydrolase I utilizes a zinc-ion to facilitate the reaction. In the crystal structure of *V. cholerae* queF evidence of ordered metal ion binding was not found. The conserved residue His233 is in appropriate position to donate a proton to the N7 nitrogen of the guanine moiety of GTP [91]. Protonation of the nucleotide results in cleavage of the N9-C1' bond [94]. Another explanation for the presence of guanine, not guanine triphosphate in the crystal structure is either contaminations in the queF preparation or the GTP preparation [91].

In the crystal structure, one guanine molecule is bound to each of the four monomers in the tetrameric asymmetric crystal unit. Guanine is bound in the cavity near the dimer interface between the two sub-domains of a monomer. The two pyrophosphates bind on the interface between two monomers in the dimer, at equal distance from two guanines. These two pyrophosphates are presumable positioned close to where the diphosphate moiety of NADPH binds. All four sites in a tetramer can therefore be occupied by substrate, however only one molecule of NADPH can bind to a dimer and can serve only one of the two sites occupied by substrate. Consistent with solution studies, the dimer is the minimal biological unit and queF exhibits half-site reactivity [91].

NADPH binding was investigated in molecular dynamics simulations. The active site cannot accommodate the adenine moiety of NADPH at the same time as $preQ_0$. NADPH possibly displaces one of the $preQ_0$ molecules from its binding site, that the adenine moiety of NADPH occupies the same pocket as $preQ_0$. The recently solved structure of queF with adenosine triphosphate confirms that adenine can bind to the active site. The diphosphate moiety of NADPH occupies a position that is comparable to that of pyrophosphate. The nicotinamide is coordinated in a conformation where the nicotinamide ring is transverse to the $preQ_0$ ring plane [91]. The specificity of the queF motif to the queF family suggests that these residues are involved in NADPH binding. The binding of a modified base to queF, instead of the nucleoside to the highly homologous FolE, leaves the binding site occupied by the ribosyl part of GTP vacant in queF. This vacant ribosyl binding pocket might also contribute to NADPH binding [9].

The guanine in the *V. cholerae* queF crystal structure is precisely oriented by hydrogen bonds and ring stacking interactions. The N1 nitrogen atoms of guanine and the amino-substituent in position 2 are coordinated by the carboxyl moiety of Glu234. The amino-substituent is additionally interacting with the backbone carbonyl oxygen of Ile93. The N3 and N9 nitrogen atoms are coordinated by the amide and hydroxyl groups, respectively, of Ser95. The guanine N9 is also interacting with the carboxylate moiety of Glu94, and the keto-substituent on C6 of guanine with the backbone amide nitrogen of His233 [91]. Glu230 and Glu89 in *E. coli* queF, corresponding to Glu234 and Glu94 in *V. cholerae* queF, respectively, were identified from a homology model as residues which accommodate $preQ_0$ in the active site [92].

The catalytic Cys194 residue resides on the hairpin loop between strands β_7 and β_8 of the protein. This hairpin loop is disordered in all four monomers of the crystal structure. Numerical simulations demonstrated significant mobility of the hairpin loop. A large barrier between reactant and product states was observed. The relative barrier for a serine catalyzed reaction is, however, significantly higher than for the cysteine catalyzed reaction [91]. This is consistent with the loss of catalytic function of the C55A and C55S mutations of *B. subtilis* queF [13].

Catalytic mechanism

The proposed mechanism of $preQ_0$ reduction suggests covalent binding of the substrate to the enzyme, and hydride transfer of NADPH. The substrate remains covalently attached to the enzyme, assuring productive completion of the reaction and thereby resulting in high chemoselectivity [91, 92]. Asp62, corresponding to Asp201 in *V. cholerae* queF, was suggested to donate the last proton in *B. subtilis* queF [89]. In *V. cholerae* queF His233 was suggested to provide the last proton. His233

was found in close proximity to Asp201 in the crystal structure. Formation of the covalent adduct modifies the geometry of the cyanide carbon of $preQ_0$ from linear to planar, and was suggested to thereby push the cyanide nitrogen atom towards His233 [91]. In *B. subtilis* queF, the corresponding histidine residue, His96, is not in appropriate geometry or in close enough proximity to the thioimide to function as direct proton donor. His233 is similary positioned in *V. cholerae* queF as His96 in *B. subtilis* queF, but the significance is unclear, as *V. cholerae* queF has guanine, not $preQ_0$ bound in the active site and the loop containing the catalytic cysteine residue is disordered in the structure [89].

The structural change of the enzyme in presence of $preQ_0$ was investigated in transient kinetic studies of $preQ_0$ binding and thioimide formation. Kinetic studies were either based on monitoring the fluorescence of Trp119 or on directly monitoring the appearance of the thioimide absorbance band at 370nm. *V. cholerae* queF has a single tryptophan residue at position 119. When irradiated at 295nm, the protein fluoresces with an emission maximum at 224nm. A blue shift in the emission maximum (335-328nm) was found upon binding and/or reaction of $preQ_0$, coupled with quenching of the emission. Binding of $preQ_0$ was observed from quenching the fluorescence. The data found were monophasic, consistent with a one step binding mechanism. On the contrary, biphasic data were found when directly monitoring the appearance of the thioimide absorbance band. The biphasic data are consistent with a two step mechanism, comprising reversible binding of $preQ_0$ followed by reaction to give the thioimide. Structural changes in the protein, as monitored in the Trp environment, induce a conformational change in and closure of the active site. These structural changes are associated with $preQ_0$ binding, not thioimide formation. Formation of a covalent thioimide product is demonstrated by both kinetic and structural data. A global structural reorganization of the enzyme is induced upon $preQ_0$ binding, not with formation of the thioimide. The thioimide intermediate was stable over several hours. The rate constant for thioimide breakdown is disproportionally small, compared to all other rate constants. The fast rate of thioimide formation ($2.78 s^{-1}$) relative to k_{cat} indicates that steps later in the reaction, involving NADPH binding and subsequent hydride transfer, are rate-limiting in the reaction [89].

1.3 Biosynthesis of pyrrolo[2,3-*d*]pyrimidines

The biosynthetic pathway of 7-deazapurines was elucidated in independent studies focused on the biosynthesis of the hypermodified tRNA nucleosides queuosine and archaeosine as well as the nucleoside antibiotics toyocamycin and sangivamycin. The biosyntheses share the enzymatic steps to the intermediate 7-cyano-7-deazaguanine ($preQ_0$) as depicted in Scheme 1.6 [95].

Identification of the genes required for the biosynthesis of toyocamycin and sangivamycin in *S. rimus* provided insight into the biosynthesis of the 7-deazapurine intermediate found in the biosynthesis of nucleoside antibiotics, and in the the hypermodified nucleosides queuosine and archaeosine. GTP cyclohydrolase activity had been implicated in the biosynthesis of queuosine. Genes involved in a single biosynthetic pathway are sometimes co-localized in bacterial genomes. Accordingly, four open reading frames *ykvJ*, *ykvK*, *ykvL*, and *ykvM* were discovered in a search for genes in the proximity of GCH I homologues. These genes were renamed queC, queD, queE, and queF, respectively, for their role in queuosine biosynthesis. The set of genes involved in toyocamycin biosynthesis was designated toyA-L, where toyM, toyB, and toyC are homologous

to the genes queC, queD, and queE in the biosynthesis of queuosine [72, 95].

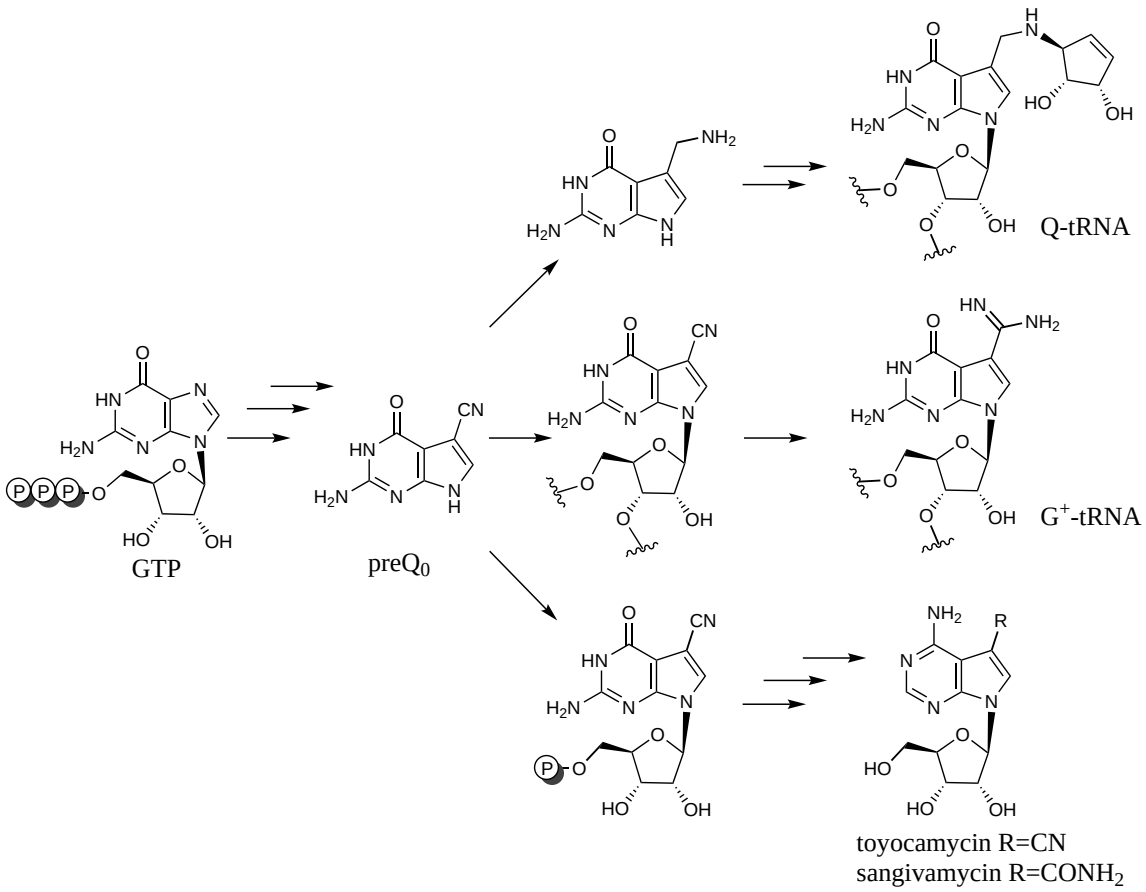

Scheme 1.6 Biosynthetic pathway of pyrrolo[2,3-*d*]pyrimidines.

Biosynthesis of 7-cyano-7-deazaguanine ($preQ_0$)

The first step in the biosynthesis of 7-deazapurines is the formation of dihydroneopterine phosphate (H_2NTP) from guanosine triphosphate catalyzed by guanosine triphosphate cyclohydrolase I (GCH I) [96]. The role of GCH I in the biosynthesis of deazapurines was first demonstrated in vivo with toyD from the toyocamycin biosynthesis of *S. rimosus* [95].

GCH I

Guanosine triphosphate (GTP) was established as starting material for the biosynthesis of 7-deazapurines in labelling experiments (Scheme 1.7). In feeding experiments the uptake of isotope labelled, potential precursors was monitored. The low incorporation of radioactivity into tubercidin from 1,4-^{14}C-succinate or 1-^{14}C-propionate demonstrated that deazapurines are not derived from C_3 or C_4 acids. Pyrimidine as well as a deazapurine were also eliminated as plausible precursors, as no radioactivity was incorporated into tubercidin in the presence of neither 4-^{14}C-1,2,3,6-tetrahydro-2,6-dioxo-4-pyrimidinecarboxylic acid nor 7-deazaadenine-U-^{3}H [97]. In the presence of 2-^{14}C-adenine and 8-^{14}C-adenine, respectively, only the 2-^{14}C-label was incorporated into the 7-deazaadenine base tubercidin [98]. Analogous results were found for the biosynthesis of queuosine when 2-^{14}C-, and 8-^{14}C-guanine were used in feeding experiments. Consequently,

the 7-deazapurine core is derived from a purine nucleoside precursor with incorporation of C-2, but loss of C-8 [99]. An analogous loss of C-8 is observed in the biosynthesis of pterins and folic acid. In these biosyntheses the C-8 is lost as formic acid, and the carbons of the ribosyl moiety are incorporated into the deazapurine and pterin rings in an Amadori rearrangement [100]. Radioactivity was found in the deazapurine base and the ribose moiety of toyocamycin when cells were grown in the presence of either 1-^{14}C-ribose or U-^{14}C-ribose. In the presence of 1-^{3}H-ribose or 3-^{3}H ribose, tritium was only incorporated into the deazapurine when the ribose was labelled at C-1. Radioactivity in toyocamycin was found in cells that were grown in the presence of either U-^{14}C-adenosine or adenosine in which a majority of the total ^{14}C-label was located in the ribose at C-1', C-2', and C-3'. It was therefore concluded, that 7-deazapurines are derived from a nucleoside precursor where the ribose is rearranged to form the pyrrole ring, as well as the cyano carbon in toyocamycin. A purine, likely GTP, is the precursor to all deazapurines. In course of the biosynthesis C-2 is retained, but C-8 is eliminated [98].

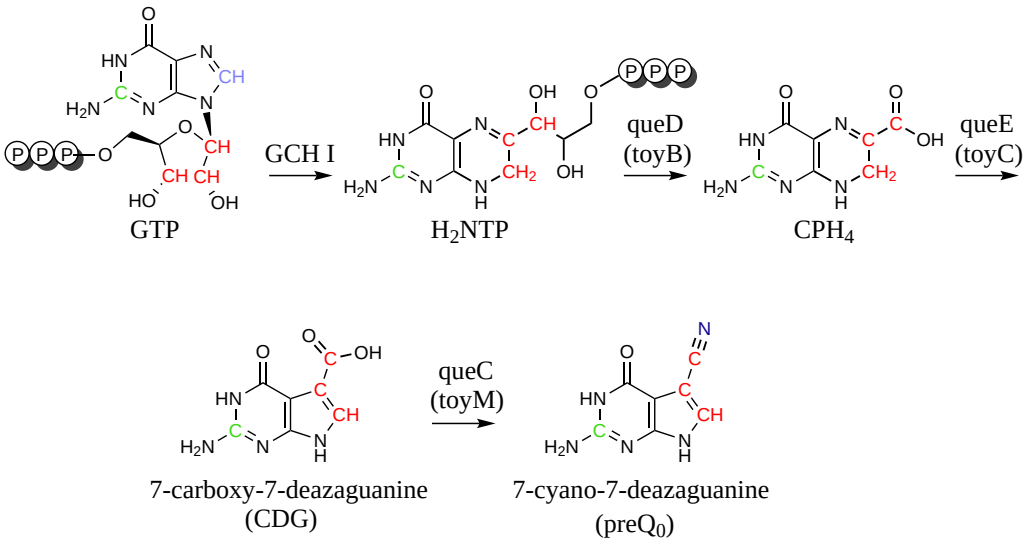

Scheme 1.7 Biosynthetic pathway of preQ$_0$.

queD

Dihydroneopterine phosphate is then transformed to 6-carboxy-5,6,7,8-tetrahydropterin (CPH$_4$) by the 6-pyruvoyltetrahydropterin synthase queD or toyB [101, 102]. This step entails cleavage of the side chain and loss of the carbon atoms C-4' and C-5' as acetaldehyde. The enzyme queD and toyB, respectively, is capable of utilizing dihydroneopterine phosphate (H$_2$NTP), 6-pyruvoyl-tetrahydropterin (PPH$_4$), and sepiapterin as substrates [101]. QueD and toyB, respectively, is homologous to the mammalian 6-pyruvoyltetrahydropterin synthase which catalyzes the second step, the conversion of dihydroneopterine to 6-pyruvoyltetrahydropterin, in the tetrahydrobiopterin biosynthesis in eukaryotes [72, 101].

queE

The next enzymatic step in the biosynthesis is catalyzed by queE and toyC, respectively. QueE was annotated as a member of the radical *S*-adenosyl-*L*-methionine (SAM) protein superfamily

and catalyzes the complex transformation of the tetrahydropterin (CPH_4) to the deazapurine 7-carboxy-7-deazaguanine (CDG) [102]. QueE was identified as part of the SAM superfamily of genes that encodes proteins that generate radical species of *S*-adenosylmethionine through unsusal Fe-S centres [72]. *S*-Adenosylmethionine is known as a source of methyl groups for DNA methylation, biosyntheses of hormones and neurotransmitters, and regulation of signal transduction. However, an increasing number of SAM-dependent enzymes involve free radicals as reaction intermediates. In these cases SAM serves as the free radical initiator by transient cleavage to the 5'-deoxyadenosyl radical which in turn abstracts hydrogen atoms from the substrates or glycosyl residues to activate them for radical-based reactions [102, 103].

The mechanism of the queE catalyzed reaction of CPH_4 to CDG was experimentally investigated. QueE was found active only in the presence of SAM and sodium dithionite. SAM is required as source of the 5'-deoxyadenosyl radical, and sodium dithionite is required to reduce the [4Fe-4S] cluster to the +1 oxidation state. In its +1 oxidation state, the cluster donates an electron to SAM, initiating the reductive cleavage of the C5'-S bond affording methionine and a 5'-deoxyadenosyl radical. The 5'-deoxyadenosyl radical abstracts a hydrogen atom from the substrate molecule. Abstraction of a hydrogen atom from CPH_4 can occur at either C-6 or C-7. The site of hydrogen atom abstraction was investigated with monodeuterated CPH_4 isomers containing deuterium atoms at C-6 or C-7. These deuterium labelling experiments support a radical-mediated rearrangement of CPH_4 to CDG, initiated by direct abstraction of a hydrogen atom from C-6 of the substrate by the 5'-deoxyadenosyl radical. Homolytic cleavage of the C-N bond of the substrate leads to an intermediate that rearranges to a nitrogen centred radical. This radical is subsequently quenched by the 5'-deoxyadenosyl radical, which in turn recombines with methionine to reform the cofactor. The 7-carboxy-7-amino intermediate is then transformed to CDG requiring the loss of the amino group and aromatization of the five-membered ring. QueE requires Mg^{2+} for activity. The role of the Mg^{2+} has not yet been clarified. Mg^{2+} may coordinate the substrate carboxylate group leading to activation of the C-6 proton by inductive effects. Alternatively, it may interact with N-5 of the substrate to facilitate the ring contraction [104].

queC

The last step in the biosynthesis of $preQ_0$ is the conversion of 7-carboxyl-7-deazaguanine to 7-cyano-7-deazaguanine ($preQ_0$) catalyzed by queC and toyM, respectively [72, 102]. The X-ray structure of queC from *B. subtilis* was reported before its enzymatic activity had been established [105]. QueC is a novel ATP-dependent enzyme catalysing the conversion of a carboxylic acid to a nitrile. Formation of enzymatically produced $preQ_0$ was ATP-dependent, but occurred in the absence of an exogenous nitrogen source. Incubation of 6-carboxy-5,6,7,8-tetrahydropterin with queE and queC and either $^{15}NH_4SO_4$ or $^{14}NH_4SO_4$ showed incorporation of ^{15}N into the product when a source of labelled ammonia was included. These results confirm ammonia as a nitrogen source for the nitrogen atom in the substituent in position 7 of deazapurines [102].

From this intermediate $preQ_0$ the biosynthetic pathways towards queuosine, archaeosine, toyocamycin, and sangivamycin, respectively, diverge.

Biosynthesis of queuosine (Q)

Queuosine and its derivatives are hypermodified versions of guanosine, found widely among eukaryotes and eubacteria. Queuosine occurs exclusively at position 34, the wobble position, in the anticodon of the tRNA sequence 5'-GUN-3' (N is any nucleotide) coding for the amino acids asparagine, aspartic acid, histidine, and tyrosine of eubacteria and of lower and higher eucaryotes, with the exception of yeasts. Eubacteria synthesize queuine *de novo*, whereas eucaryotes obtain queuine from their nutrition or the intestinal flora. The queuosine modification is connected to a variety of physiological phenomena. In Eukarya, the developmental stages of a cell are closely correlated with the extent of queuosine modification in tRNA. tRNAs of mature tissue exhibit full modification with queuosine while undermodification of tRNA is uniformly observed in developmental stages associated with cell proliferation and differentiation. Queuosine has recently been shown to be essential in the biosynthesis of tyrosine in animals. Queuosine is required for phenomena such as virulence in the pathogen *Shigella flexneri* and viability during stationary phase in *E. coli* [72, 73, 100, 106–110].

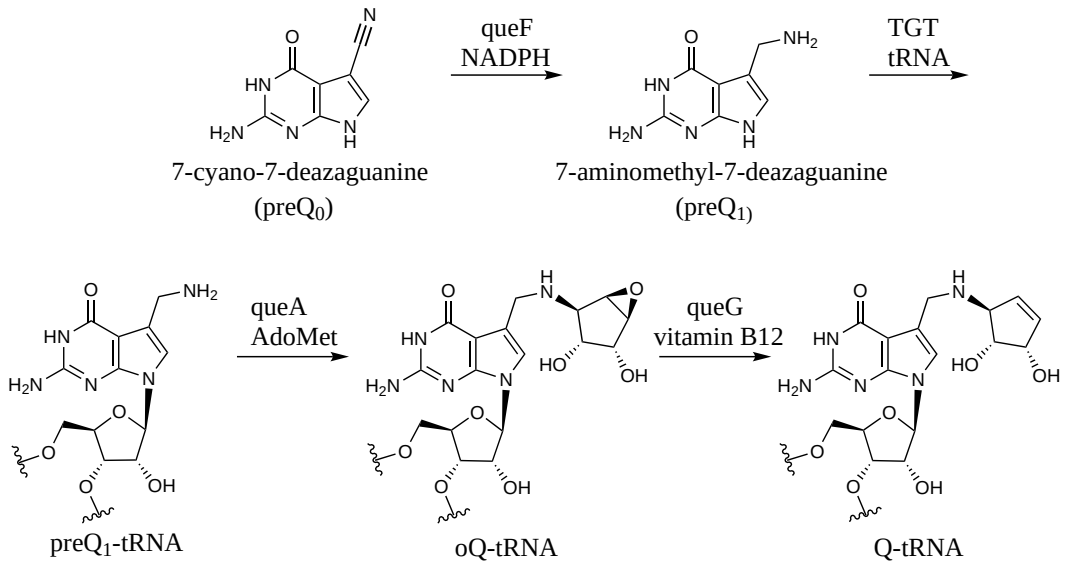

Scheme 1.8 Biosynthetic pathway of the hypermodified nucleoside queuosine, including the enzymatic step from $preQ_0$ to $preQ_1$ catalyzed by nitrile reductase queF.

The biosynthesis of queuosine follows three stages. First guanosine triphosphate is transformed to dihydroneopterin triphosphate, which is then further modified to yield 7-aminomethyl-7-deazaguanine in a series of enzymatic steps occuring at nucleotide level. In the last stage 7-aminomethyl-7-deazaguanine ($preQ_1$) is inserted into tRNA. Final derivatisations of the sidechain on C-7 occur at the tRNA bound nucleoside [100, 105].

queF

The intermediate 7-cyano-7-deazaguanine ($preQ_0$), common to all biosynthetic routes to 7-deazapurines, is reduced to the corresponding 7-aminomethyl-7-deazaguanine ($preQ_1$) by queF [9]. QueF exhibits significant homology to the type I guanosine triphosphate cyclohydrolase and was consequently first annotated as putative guanosine triphosphate cyclohydrolase like enzyme, responsible for the initial step in queuosine biosynthesis [72]. Biochemical studies established that

queF is not a guanosine triphosphate cyclohydrolase, but a previously uncharacterized class of oxidoreductase that catalyzes the unprecedented reduction of a nitrile group in $preQ_0$ to a primary amine in $preQ_1$ [9]. $PreQ_1$ is involved in the $preQ_1$ riboswitch, which regulates expression of the genes involved in the biosynthesis of queuosine [111–113].

TGT

7-Aminomethyl-7-deazaguanine ($preQ_1$) is subsequently inserted into tRNA by the enzyme tRNA-guanine transglycosylase (TGT), a reaction in which the genetically encoded base guanine is elimiated. The remaining steps of the biosynthesis occur at the level of the tRNA [100]. Bacterial tRNA-guanine transglycosylase catalyzes the post-transcriptional exchange of guanine in the wobble position of tRNA codons with the sequence 3'-GUN-5' (N = any base). The TGT enzyme from *E. coli* can utilize $preQ_1$, $preQ_0$, and guanine as substrates, with $preQ_1$ being the most efficient substrate. Other 7-deazaguanine analogues were found to be significantly poorer substrates, while queuine itself is not utilized at all. These results confirmed that the substrate for the enzyme in *E. coli* is not queuine, but a precursor of queuine involved in the biosynthesis of queuosine [100, 110, 114].

queA

In the next enzymatic step tRNA-bound $preQ_1$ is transformed to epoxyqueuosine (oQ) in a single *S*-adenosylmethionine requiring step. This enzymatic step is catalyzed by queA, a *S*-adenosylmethionine:tRNA ribosyltransferase-isomerase. Epoxyqueuosine was formed under both aerobic and anaerobic conditions, therefore it was concluded that molecular oxygen is not involved in its formation [107]. Various possible precursor molecules for the epoxycyclopentanediol ring were tested: dNTPs and rNTPs, NAD(H), NADP(H), FAD, adenosylcobalamin, riboflavin, ribose, ribitol, ribulose, and *S*-adenosylmethionine. Only *S*-adenosylmethionine was found to be utilized in the queA catalyzed reaction [108]. However, no radioactivity derived from 2-^{14}C-methionine or methyl-^{3}H- was incorporated into queuosine of the respective tRNAs of *E. coli* cells, indicating that neither the reactive methyl nor the equally activated 1-amino-1-carboxylpropyl moiety of *S*-adenosylmethionine are involved in the reaction. The ribose moiety of *S*-adenosylmethionine was therefore considered a likely precursor of the cyclopentanediol ring [107]. The utilization of the ribose moiety of *S*-adenosylmethionine was proven in labelling studies where a tritium label at C-5' of the ribose of SAM was incorporated into Q-specific tRNAs [115]. The C-4' of the ribosyl-moiety of SAM is transferred to the aminomethyl group of $preQ_1$ and isomerized to the epoxy cyclopentanediol [116]. This is the first example of the stoichiometric use of SAM as a ribosyldonor in an enzymatic reaction. The reaction itself is unprecedented in biological systems, and includes the elimination of methionine and adenine from SAM, the transfer of the ribosyl moiety to the tRNA and its rearrangement to form the epoxycyclopentanediol ring [100, 108]. All activated groups that can be transfered by SAM are used for tRNA modifications: methylation, e.g. in the formation of ribothymidine, 1-amino-1-carboxypropyl-moiety in a modification of uridine, and the ribosyl group emerges in queuosine. Queuosine biosynthesis is the first reaction known that utilizes the ribosyl group of SAM [108].

queG

In the last step of the biosynthesis of queuosine, epoxy-queuosine (oQ) is transformed to queuosine (Q) by reduction of the epoxy functionality to a double bond, catalyzed by queG. The reaction was believed to be vitamin B12 dependent, as minimal medium with vitamin B12 allowed to complete conversion of oQ to Q. A vitamin B12 dependent reduction of an epoxy group to a double bond is unprecedented in biochemistry [115]. It was further speculated, that the requirement for vitamin B12 implicates the involvement of radical chemistry [100]. QueG shows sequence similarities to reductive dehalogenases, which is intriguing as a vitamin B12 (cobalamin) cofactor is found in all reductive dehalogenases studied to date. However, purified queG catalyzed the reaction of oQ to Q under anerobic condition both in presence and in absence of vitamin B12. Vitamin B12 was found to stimulate the reaction approximately 1.3 fold. No conversion was observed when either the enzyme, dithionite, or methyl viologen were removed. This requirement for a reductant and a mediator, such as dithionite and methyl viologen, were also demonstrated for all reductive dehalogenases. The role of the vitamin B12 remains to be established [117].

Biosynthesis of archaeosine (G^+)

Archaeosine (G^+) is found specifically at position 15 in the dihydrouridine loop (D-loop) of the majority of archaeal tRNA and is believed to stabilize the overall tRNA structure [118, 119].

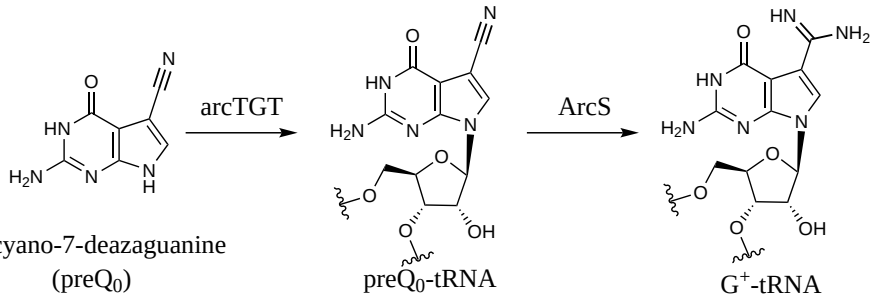

Scheme 1.9 Biosynthetic pathway of the hypermodified nucleoside arachaeosine.

arcTGT

In the biosynthesis of archaeosine, the intermediate $preQ_0$ is inserted into tRNA by replacing a guanine base at position 15 in a tRNA transgylcosylase (arcTGT) catalyzed reaction. ArcTGT is a modular enzyme comprised of an N-terminal catalytic domain with a characteristic zinc-binding site and a C-terminal extension of three domains C1, C2, and C3. C3 was found to be an oligonucleotide/oligosaccharide binding fold-like pseudouridine and archaeosine (PUA) domain [119]. The presence of guanine in position 15 was found to be the single most important determinant for ArcTGT activity. A G15A mutation in a $tRNA^{Val}$ transcript resulted in a >5000-fold loss of catalytic efficiency. In contrast to that, deletion of the C-terminal domains C1, C2, and C3 did not impair the reaction [118].

arcS

The last step in the biosynthetic pathway of archaeosine in Euryarcheota is catalyzed by an ATP-independent amidinotransferase, arachaeosine synthase (arcS). The absence of an ATP dependence suggests this conversion does not require initial hydrolysis of the nitrile to an amide, but instead involves the direct addition of NH_3, generated from glutamine or asparagine hydrolysis, to the nitrile of $preQ_0$. This enzymatic reaction constitutes a novel amidinotransferase reaction [119]. ArcTGT is found in all archaea sequenced to date, with the exception of the extreme halophile *Haloqadratum walsbyi*. Analysis of bulk tRNA extracted from *Haloqadratum walsbyi* showed that archeosine was not present in this organism. Many crenarchaeota known to contain archaeosine, lack arcS homologues. The amidino group of archaeosine must therefore be introduced by non-homologous enzyme families in these organisms. These crenarchaeota contain queC proteins with an additional N-terminal domain, homologous to proteins of the glutamine amidotransferase class II (GAT) or queF-like proteins, lacking the queF motif. The predicted queF-like structures were most similar to the C-terminal T-fold domain of bimodular queF (type II). These GAT-queC and queF-like proteins function as amidinotransferases, generating arachaeosine modified tRNA in *E. coli* [120].

Biosynthesis of toyocamycin and sangivamycin

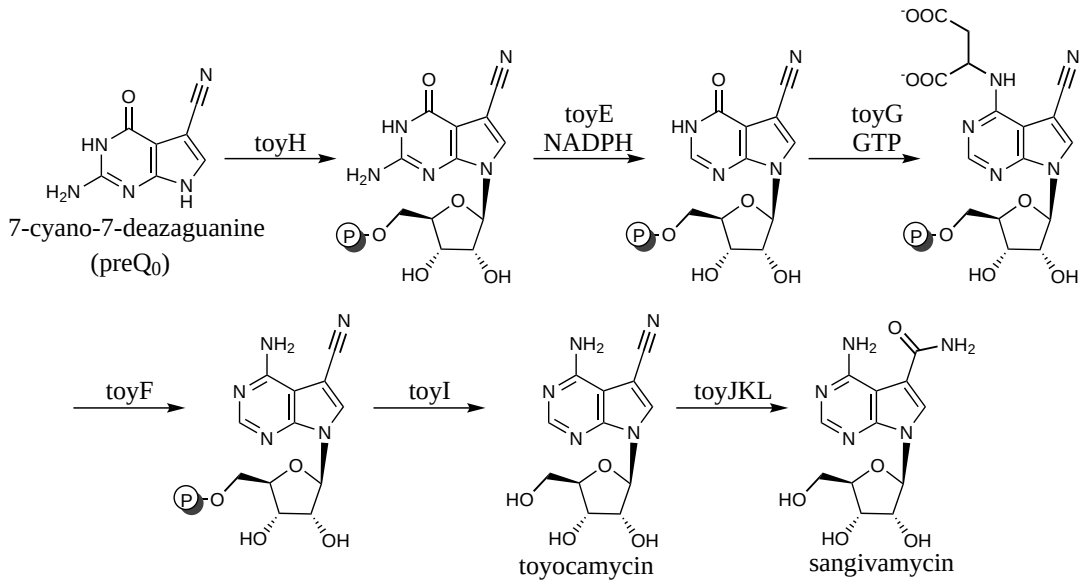

Scheme 1.10 Biosynthetic pathway of toyocamycin and sangivamycin.

The biosynthesis of toyocamycin and sangivamycin involes three stages. After formation of the common intermediate $preQ_0$ in the first stage, $preQ_0$ is converted to toyocymycin 5'-monophosphate by the successive action of toyH, toyE, toyG, and toyF. In the third and final stage the nitrile moiety of toyocamycin is hydrated by toyocamycin nitrile hydratase (TNHase, toyJKL)to yield sangivamycin [121].

In the biosynthesis of toycamycin and sangivamycin, a guanosine based purine is converted to an adenosine based deazapurine by a group of purine salvage proteins. The purine salvage enzymes were predicted, based on bioinformatics, to encode the homologues of phosphoribo-

sylpyrophosphate transferase (PRPTase, toyH), GMP reductase (toyE), adenosylsuccinate synthase (toyG), adenosylsuccinate lyase (toyF), and haloacid dehalogenase (toyI) [121].

Toyocamycin nitrile hydratase (TNHase) catalyzes the final step in the biosynthesis of sangivamycin, the hydration of the nitrile functionality of toyocamycin. The open reading frames encoding the TNHase protein were designated toyJKL and belong to a rare metal-dependent nitrile hydratase family [121].

1.4 Biological activity

1.4.1 Pyrrolo[2,3-*d*]pyrimidines

Pyrrolo[2,3-*d*]pyrimidines exhibit a wide variety of biological activities. Naturally occuring pyrrolo[2,3-*d*]pyrimidines include the nucleoside antitumor antibiotics tubercidin, toyocamycin, sangivamycin, and cadeguomycin, as well as selective and potent inhibitors of phosphatidylinositol 4-kinase (PI4K), such as echiguanines A and B, depicted in Figure 1.1. Over the past decade, fused pyrimidines have been among the pharmacologically most interesting chemical scaffolds in many natural products and several non-natural nucleoside and non-nucleoside compounds. Pyrimidine derivatives are associated with a variety of chemo-therapeutic effects, including antitumor, angiogenic effects, and enzyme inhibition. Pyrrolo[2,3-*d*]pyrimidines exhibit promising properties as antifolate inhibitors of dihydrofolate reductases (DHFR), tyrosine kinase inhibitors or adenosine receptor agonists [122].

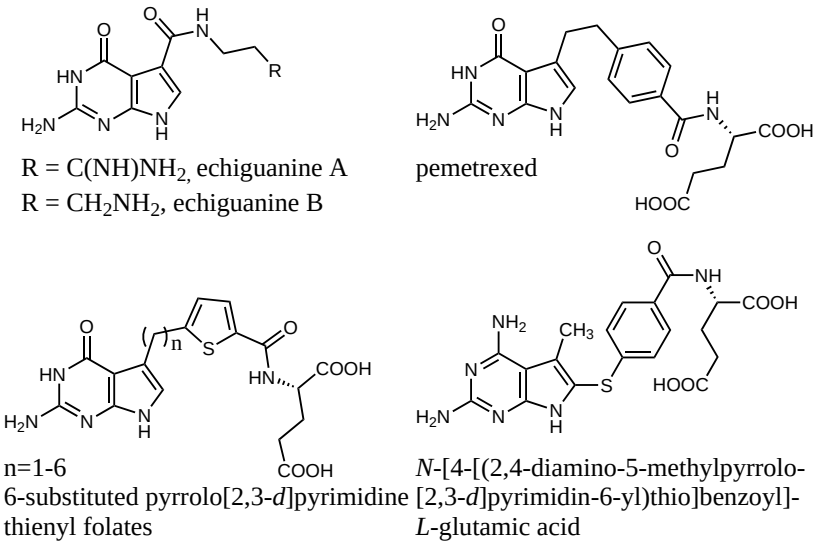

Figure 1.1 Examples of bioactive pyrrolo[2,3-*d*]pyrimidines as PI4K-inhibitors and inhibitors of folate dependent enzymes.

Folate metabolism has long been recognized as an effective target for chemotherapy, due to its crucial role in the biosynthesis of nucleic acid precursors. Inhibitors of folate-dependent enzymes have found clinical utility as antitumor, antimicrobial, and antiprotozoal agents. Pemetrexed (Figure 1.1) is a pyrrolo[2,3-*d*]pyrimidine-containing chemotherapy drug by Eli Lilly and Company. Pemetrexed inhibits thymidylate synthase (TS), dihydrofolate reductase (DHFR), and glycinamide ribonuceotide transferase (GARFT) in purine and pyrimidine synthesis. Pemetrexed is currently

marketed against pleural mesothelioma and non-small cell lung cancer. Studies to evaluate its potency against other cancers are ongoing [123]. Classic antifolates, such as pemetrexed, have minimal lipid solubility and therefore require transport mechanisms to enter mammalian cells [124–126]. There are three primary folate transporters in healthy tissue and tumors, the reduced folate carrier, the proton-coupled folate transporter, and the folate receptor. Levels and activities of reduced folate carrier are important determinants of drug efficiency. Loss of reduced folate carrier activity is a common mode of antifolate drug resistance. Reduced folate carrier exhibits a high level of activity at neutral pH. Healthy tissue is generally characterized by neutral pH. Transport of cytotoxic antifolates by reduced folate carrier could therefore easily preclude tumor selectivity and cause toxicity to healthy tissue [124–126]. 6-Substituted pyrrolo[2,3-*d*]pyrimidine thienyl folates with three or four bridge atoms present a new strategy. Many solid tumors show acidic microenvironments. 6-Substituted pyrrolo[2,3-*d*]pyrimidine thienyl folates can be transported into solid tumors by the proton-coupled folate transporter, functioning optimally at acidic pH values. These solid tumor targeted antifolates with proton coupled selective cellular uptake should have enhanced activities towards tumors lacking reduced folate carrier function [124–127]. Synergistic growth inhibition against *Lactobacillus casei*, and human lymphoma cells, was observed when a dihyrodofolate reductase inhibitor was used in combination with a thymidylate synthase inhibitor. Several compounds, including *N*-[4-[(2,4-diamino-5-methylpyrrolo[2,3-*d*]pyrimidin-6-yl)thio]benzoyl]-*L*-glutamic acid (Figure 1.1), were designed as dual inhibitors of dihydrofolate reductase and thymidylate synthase [128–131].

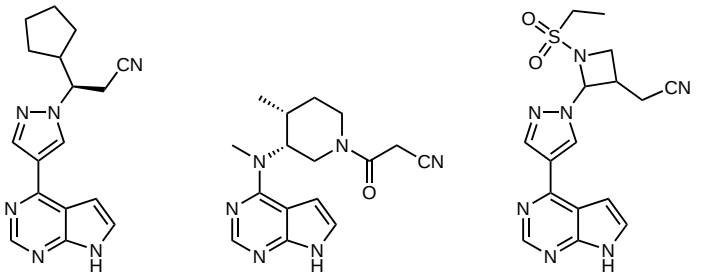

Figure 1.2 Pyrrolo[2,3-*d*]pyrimidines as JAK inhibitors.

A pyrrolo[2,3-*d*]pyrimidine, ruxolitinib (Jakafi, Figure 1.2) by Incyte/Novartis, was approved by the US Food and Drug Administration as Janus kinase (JAK) inhibitor. JAK inhibitors inhibit the activity of one or more of the Janus kinase family of enzymes, thereby interrupting signalling down-stream of a multiplicity of cytokines. JAK inhibitors have therapeutic application in the treatment of cancer, myelofibrosis, inflammatory and immune diseases. Xeljanz (tofacitinib, Figure 1.2) by Pfizer, another pyrrolo[2,3-*d*]pyrimidine JAK inhibitor, was FDA approved for the treatment of rheumatoid arthritis in November 2012. JAK inhibition is a completely novel mechanism in rheumatoid arthritis. Xeljanz was designed as a JAK3 inhibitor, however was shown to inhibit all three JAKs to some extent. Baricitinib (Figure 1.2) is a similiar JAK1 and JAK2 inhibitor by Eli Lilly and Company, which just entered phase 3 clinical trials [132–134]. Pyrrolo[2,3-*d*]pyrimidine compounds have recently been patented as JAK inhibiors by other companies, including Abbott laboratories and Novartis [135, 136].

7-Cyclopentyl-*N,N*-dimethyl-2-((5-(piperazin-1-yl)pyridin-2-yl)amino)-7*H*-pyrrolo[2,3-*d*]pyrim-

idine-6-carboxamide has recently been reported as combination of cyclin-dependent kinase CDK4/6 inhibitors and fibroblast growth factor receptor kinase inhibitors. Most human tumors display genetic alterations that activate CDK4 or CDK6 activity or that eliminate p16 or pRb tumor suppressor function. Molecular analysis of human tumors implicated cyclin D1 overexpression as driving force in various types of cancer, including mantle cell lymphoma, non-small cell lung cancer, and carcinomas of breast, head and neck, and esophagus. Overexpression of FGFRs occurs frequently in human breast tumors. Down-regulation of FGFR signalling causes a reduction in cyclin D1 protein levels. Therefore FGFR inhibitors are considered potent therapeutic agents to suppress angiogenesis and to inhibit growth of a subset of breast tumors. Novartis patented CDK kinase inhibitors this year, including a combination of cyclin-dependent kinase CDK4/6 inhibitors and fibroblast growth factor receptor kinase inhibitors and a combination of a CDK inhibitor and a phosphatidylinositol-3-kinase inhibitor. Both are considered for the treatment of solid tumors and haematological malignancies [137–140].

Pyrrolo[2,3-*d*]pyrimidines are relevant compounds for the inhibition of kinases and growth factors involved in tumor growth (Figure 1.3). Receptor tyrosine kinases (RTK) are a subfamily of protein tyrosine kinases, which play key roles in tumor growth, survival and dissemination. A variety of growth factors and their receptors are known to be overexpressed in several tumors, including vascular endothelial growth factor (VEGF), epithelial growth factor (EGF), and platelet derived growth factor (PDGF). These growth factors and their receptors are involved in cancer angiogenesis. The formation of new blood vessels from existing vasculature, in solid tumors is essential for both physiologic and pathologic processes. Several pyrrolo[2,3-*d*]pyrimidines were proven as inhibitors of receptor tyrosine kinase, protein tyrosine kinase 2 (PTK2, focal adhesion kinase), amongst others [141–143]. A general pharmacophore model was proposed for the binding of pyrrolo[2,3-*d*]pyrimidines to RTKs and EGFRs. A hinge region is formed out of three nitrogen atoms, which might be either amino-substituents in positions 2 and 4 and the N-3 heteroatom, or the N-1 and N-7 heteroatoms and the amino-substituent in position 2. Two hydrophobic sites bind to an aromatic substituent in position 4 or 6 and the residue on the amino-substituent on position 2. The sugar binding pocket and phosphate binding regions coordinate the aromatic substituents [141].

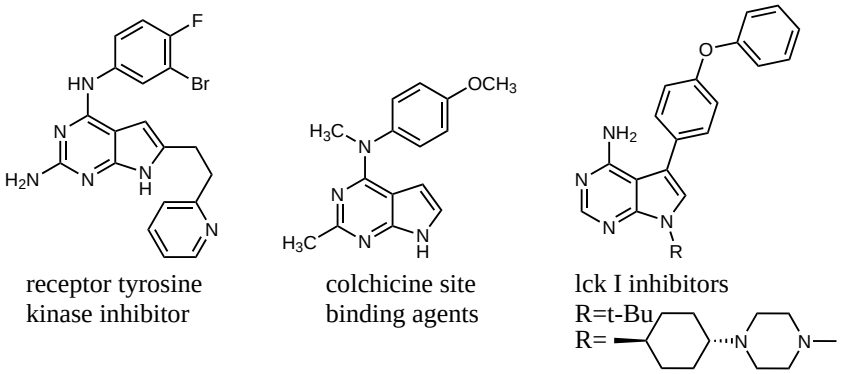

Figure 1.3 Examples of biologically active pyrrolo[2,3-*d*]pyrimidines for the treatment of cancers and autoimmune diseases.

Substituted pyrrolo[2,3-*d*]pyrimidines are colchicine site binding, microtubule depolymerizing agents. Microtubule active agents inhibit mitosis (cell division) by disrupting microtubles, the

structures that pull cells apart when they divide. Microtubule active agents are commonly used in cancer therapy, as cancer cells metastasise through continuous mitotic division and are more sensitive to inhibition of mitosis than other cells. Three major classes of microtubule active agents have been identified to date. Vinca alkaloids, including vincristine, vinblastine, bindesine, and vinorelbine are β-tubulin binding agents, important e.g. in the treatment of leukaemia, lymphomas, and non-small cell lung cancer. Taxoids, including paclitaxel (Taxol) and docetaxel (Taxotere), as well as epothilones are microtubule stabilizing agents stimulating tubulin polymermization useful in the treatment of breast, lung, ovarian, head and neck, and prostate carcinomas, amongst others. Colchicine site agents also inhibit tubulin polymerization. So far, there are no clinically approved antitumor agents that bind to the colchicine site. However, several compounds are currently in clinical trials. Colchicine site agents circumvent mechanisms of multidrug resistance, such as overexpression of P-gylcoprotein (Pgp) or expression of βIII-tubulin [144]. *N*-(4-Methoxyphenyl)-*N*,2-dimethyl-7*H*-pyrrolo[2,3-*d*]pyrimidin-4-amine hydrochloride, depicted in Figure 1.3 was identified as potent microtubule depolymerizer in cells and is considered a lead structure for the development of further compounds for *in vivo* evaulation and possible advancement into clinical trials [144]. The effects of a regioisomeric change on the biological activities of water soluble colchicine site binding, microtubule depolymerizing agents was investigated. The results indicated that pyrrolo[3,2-*d*]pyrimidines were even more potent than their pyrrolo[2,3-*d*]pyrimidine regioisomers [145].

Pyrrolo[2,3-*d*]pyrimidines with various substituents at C-5 and N-7 were shown to be potent inhibitors of lymphocyte-specific protein tyrosine kinase (Figure 1.3). Lymphocyte-specific protein tyrosine kinase (Lck) is an Src-family non-receptor tyrosine kinases expressed primarily in T lymphocytes relevant in immune response. A selective inhibitor of Lck inhibits specifically T-cell activation and can be used in the treatment of autoimmune and inflammatory diseases as well as in organ transplants [146, 147].

Pyrrolo[2,3-*d*]pyrimidines are also known for their cytotoxicity. 7-Benzyl-2-(4-chlorophenyl)-5,6-diphenyl-3,7-dihydro-4*H*-pyrrolo[2,3-*d*]pyrimidin-4-one analogues were identified as novel class of antiproliferative, cell growth inhibiting agents [148]. Pyrrolo[2,3-*d*]pyrimidines showed antimicrobial properties when screened against several pathogenic Gram-positive bacteria, namely *S. aureus* ATCC 29213, *B. subtilis* ATCC 6633, *Mycobacterium phlei* ATCC 10142, and Gram-negative bacteria, such as *Escherichia coli* ATCC 25922, *Pseudomonas aeruginosa* ATCC 278533 and *Candida albicans* ATCC 10231, as a representative for fungi. Anti-inflammatory activity was proven in the rat paw edema assay [149].

Pyrrolo[2,3-*d*]pyrimidines are capable of modulating the production of cyclic guanosine monophosphate (cGMP) and were patented as suitable compounds for the therapy and prophylaxis of diseases which are associated with a disturbed cGMP balance by Merck Sharp and Dohme Corporation [150].

1.4.2 Pyrrolo[2,3-*b*]pyridines and pyrrolo[3,2-*c*]pyridines

Various azaindoles, including pyrrolo[2,3-*b*]pyridines (7-azaindoles) and pyrrolo[3,2-*c*]pyridines (5-azaindoles), represent building blocks with potential applications in pharmaceutically important compounds. Azaindoles are considered as bioisosters of indoles and purines. Substitution of the

C-7 position of indole by an sp^2-hybridized nitrogen provides a skeleton containing a hydrogen bond donor and acceptor in a rigid three atom arrangement [151–153].

Protein kinases are responsible for the phosphorylation of proteins. The human genome encodes for 518 protein kinases. Protein kinases are one of the major mechanism for regulating cellular metabolism and function. Many of these kinases have been implicated in human disease and therefore present attractive therapeutic targets. Cyclin-dependent kinases (CDKs) regulate the cell division cycle, apoptosis, transcription, and differentiation, as well as control functions in the nervous system. Inhibitors for CDKs are currently being evaluated in a wide range of therapeutic areas. Variolins, 7-azaindole containing alkaloids isolated from the antarctic marine sponge *Kirkpatrickia varialosa*, are potent CDK inhibitors. Variolin B is an efficient activator of apoptosis, showing potent cytotoxic activity against a variety of human cancer cell lines, including those overexpressing p-glycoprotein, a cell efflux pump responsible for the resistance of cancerous cells to many chemotherapy agents. Variolin B and derivatives (Figure 1.4), e.g., meriolins and deoxyvariolin B, have been observed to affect cell cycle progression (Figure 1.4). The compounds inhibit CDKs and interrupt the normal progression of the cell cycle [142, 153–155]. A variety of azaindole structures has recently been patented as kinase inhibitors, potentially useful for the treatment of multiple diseases, including cancer, diabetes and asthma [156–160].

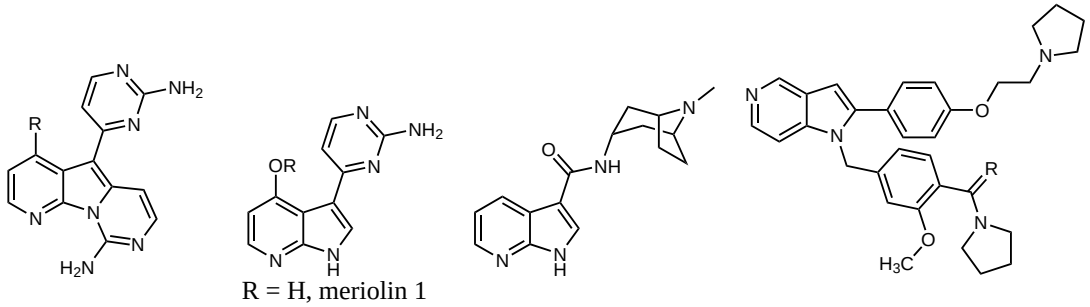

Figure 1.4 Examples of bioactive azaindoles.

A number of other biological activities are described for azaindoles. 7-Azaindolylcarboxy-*endo*-tropanamide (DF 1012, Figure 1.4) is the selected candidate drug in a new class of non-narcotic antitussive compounds, and is under investigation in phase II clinical trials [161]. 5-Azaindole derivatives show thrombin inhibitory activity. Thrombin, a trypsin-like serine protease, catalyzes fibrin formation and activates platelets, thereby playing a crucial role in the development of thrombotic diseases [162]. Leading pharmaceutical companies, such as Merck, GlaxoSmithKline, Sanofi Aventis, Hoffmann-La Roche, Schering, and others patented various azaindoles. Azaindoles are patented as selective inhibitors of 11-β-hydroxysteroid dehydrogenase type I for treatment and prevention of metabolic syndrome, diabetes, insulin resistance, obesity, anxiety, depression, immune disorders, and hypertension, against tumours, for the treatment of central nervous system disorders and asthma [163–166]. Azaindoles are also reported for treatment of HIV, inhibition of the enzyme renine, treating or preventing viral infections and nicotinic acetylcholine receptor agonism and dopamine re-uptake inhibition [167–171].

1.4.3 Thieno[2,3-*d*]pyrimidines

Thienopyrimidine derivatives show a wide variety of biological activities. Thienopyrimidines have been evaluated as analgesics, anti-inflammatory, antipyretic, antiviral, antidepressant, antidiabetic, antihistaminic, antibacterial and antihypertensive agents, as pesticides, herbicides, plant growth regulators. Thieno[2,3-*d*]pyrimidines were also reported as agents in prophylaxis and therapy of numerous diseases, including tuberculosis, Alzheimer's disease, Parkinson's disease, and the H5N1 influenza virus [172, 173]. Thieno[2,3-*d*]pyrimidines were reported to display immunosuppressive [174], trypanoside, anti-tuberculosis, leishmanicidal, and cytotoxic activities [175].

Protein kinase C isoenzymes are serine/threonine protein kinases involved in human disease pathologies such as cancer development and progression. Protein kinase C (PKC) exists as three isoenzymes, namely classical PKC (cPKC), novel PKC (nPKC), and atypical PKC (aPKC). Commercially available inhibitors of PKC show greater efficiency for cPKCs and nPKCs than for aPKCs. A thieno[2,3-*d*]pyrimidine, CRT0066854, depicted in Figure 1.5, is a highly selective inhibitor of aPKC. It acts as competitive ATP inhibitor, binding within the nucleotide binding pocket of aPKC. Overexpression of PKC has been linked to several types of cancer, including non-small lung cancer, and ovarian cancer. Further optimization of PKC inhibitors on the basis of CRT0066854 could yield more specific cancer therapeutics [176].

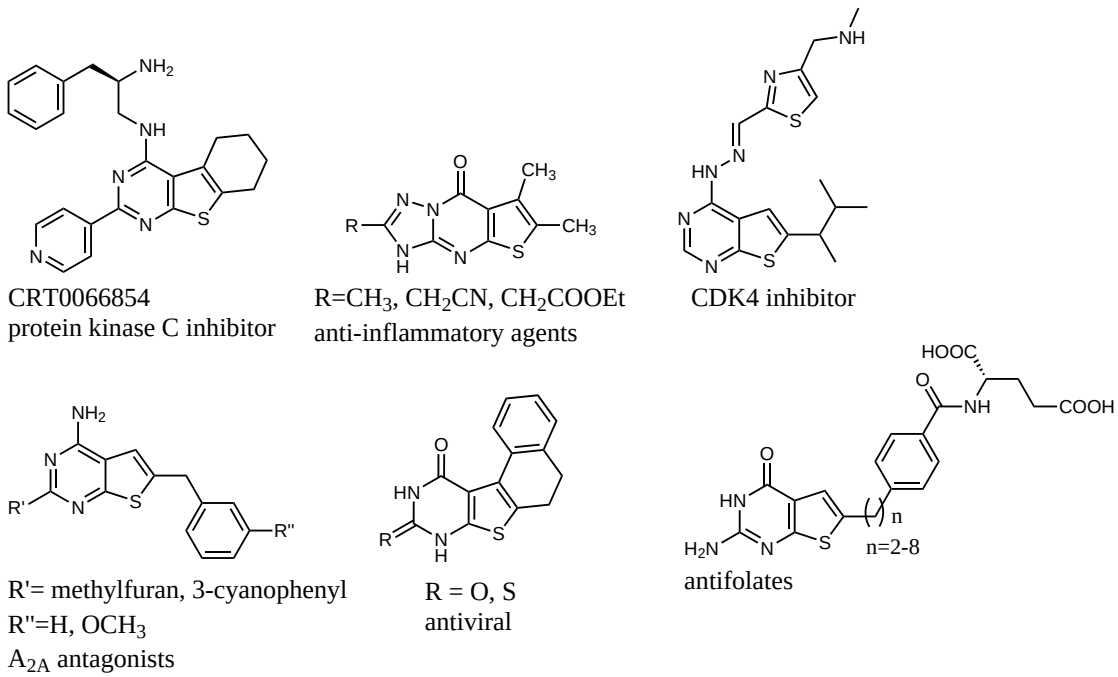

Figure 1.5 Examples of bioactive thieno[2,3-*d*]pyrimidines.

Cyclin-dependent kinase 4 (CDK4) is a family of serine/threonine kinases. Thieno[2,3-*d*]pyrimidine derivatives were identified as CDK4 inhibitors. CDK4 inhibitors are promising cancer therapeutics. Recently published CDK4 inhibitors, as depicted in Figure 1.5, are used as lead structures to further improve cytotoxic activity, CDK4 selectivity and water solubility of these inhibitors [177, 178].

Mnk genes are associated with the regulation of body weight or thermogenesis. Human Mnk genes, particularly Mnk2 variants, are investigated for their role in metabolic diseases including

obesity, eating disorders, cachexia, diabetes mellitus, hypertension, and coronary heart disease. Thieno[2,3-*d*]pyrimidines have recently been patented as inhibitors of Mnk kinase. Potent and selective Mnk1 and/or Mnk2 inhibitors may be valuable in the treatment of metabolic diseases and other diseases and disorders [179].

Thieno[2,3-*d*]pyrimidine derivatives exhibit biological activity as antifolate compounds. Antifolate compounds differ greatly in their inhibition of microbial and mammalian enzymes [180]. Inhibitors of *Pneumocystis carinii* and *Toxoplasma gondii* dihydrofolate reductase are considered for treatment of AIDS patients, immunosuppressed organ transplant recipients, and patients receiving cancer therapy [181].

Mammalian cells are unable to synthesize folates *de novo*, uptake of external folates is essential [182]. Dihydrofolate reductase catalyzes the reduction of dihydrofolate to its active cofactor form tetrahydrofolate. This cofactor is involved in amino acid and nucleic acid synthesis and is therefore an attractive target for chemotherapy [180, 183]. Dihydrofolate reductase, thymidylate synthase and serine hydroxymethyltransferase are enzymes involved in the synthesis of the essential metabolite thymidylate [184]. A number of inhibitors of DHFR as well as dual inhibitors of DHFR and TS have been reported. Folate analogues that inhibit DHFR generally contain 2,4-diaminopyrimidines, whereas inhibitors of TS contain 2-amino-4-oxo-or 2-methyl-4-oxo-pyrimidines [183–186].

Thieno[2,3-*d*]pyrimidine derivatives are investigated for their anti-inflammatory and analgesic activities. Non-steroidal and anti-inflammatory drugs (NSAIDs) are among the most widely used therapeutics. Their use is restricted by gastrointestinal side effects, therefore new therapeutic agents are intensively investigated. Thieno[2,3-*d*][1,2,4]triazolo[1,5-*a*]pyrimidine derivatives, as depicted in Figure 1.5 were found to display distincitve inflammatory activity [187]. Thieno[2,3-*d*]pyrimidines were patented as therapeutic agents for the diseases caused by activation of NF-κB, e.g., diseases caused by excessive production of various inflammatory mediators and viral propagation [188].

Aryl and benzyl substituted thieno[2,3-*d*]pyrimidines are potent adenosine A_{2A} antagonists (Figure 1.5). Selectivity against adenonsine A_1 receptors varies. Selective A_{2A} antagonists are a target for the symptomatic relief of Parkinson's disease. Thieno[2,3-*d*]pyrimidines showed good *in vitro* potency when substituted with methylfuran and 3-cyanophenyl, however suffer form a short half-life (Figure 1.5) [189].

Cyclopenta[*b*]thieno[2,3-*d*]pyrimidine and thieno[2,3-*c*]pyrimidine derivatives are novel 5-HT2A antagonists, showing antiserotonergic activities. These compounds are antagonists for one of the seven classes of serotonin receptors, namely 5-HT1 to 5-HT7. Mutations in the serotonin transporter protein are investigated in relation to anxiety-related personality, depression, and suicide [190].

Heat shock proteins (HSP) are a class of chaperones. They accumulate in the cell in response to various environmental stresses or play a role as chaperones for cellular proteins under stress free conditions. HSP-90 is unique with regard to other chaperones, as most of its known substrate proteins are signal transduction proteins. Inhibition of HSP-90 results in degradation of these signaling proteins involved in apoptosis, cell proliferation and cell cycle regulation. Thieno[2,3-*d*]pyrimidines were patented by Pfizer as modulators or inhibitors of HSP-90 for treating diseases

or conditions mediated by HSP-90, including cancer [191].

1.4.4 Cyclopenta[*d*]pyrimidines

Cyclopenta[*d*]pyrimidines have been investigated for their biological activities, especially as chemotherapeutic agents, and antimalarials since the 1940s [192–194].

More recently, cyclopenta[*d*]pyrimidines were identified as potent DHFR inhibitors with anticancer activity, along with other fused heterocyclic ring systems, such as pyrrolo[2,3-*d*]pyrimidines, furo[2,3-*d*]pyrimidines, and pyrrolo[3,2-*d*]pyrimidines. Several cyclopenta[*d*]pyrimidine based antifolates were designed analogously to *N*-[4-[3-(2,4-diamino-6,7-dihydrocyclopenta[*d*]pyrimidin-5-yl)propyl]benzoyl]-*L*-glutamic acid, depicted in Figure 1.6. The new analogues did not have the glutamate moiety and either the alkyl bridge or the benzene substituent were modified. The compounds were tested as inhibitors of *Pneumocystis carinii*, *Toxoplasma gondii*, and rat liver DHFR. The opportunistic microbes *Pneumocystis carinii* and *Toxoplasma gondii* cause life-threatening illnesses in persons with compromised immune systems, such as AIDS patients, immuno-suppressed organ transplant recipients, and patents receiving cancer chemo-therapy. Several new analogues were found highly potent as DHFR and cell growth inhibitors [195, 196].

Substituted cyclopenta[*d*]pyrimidines are microtuble active agents, binding to the colchicine site. *(RS)-N*-(4-Methoxyphenyl)-*N*,2,6-trimethyl-6,7-dihydrocyclopenta[*d*]pyrimidin-4-aminium are colchicine site agents and potent inhibitors of cancer cells in culture. The *(S)*-enantiomer is more active than the *(R)*-enantiomer against cellular microtubule loss and in the inhibition of tubulin assembly. Both enantiomers circumvent overexpression of P-gylcoprotein (Pgp) and expression of βIII-tubulin, thus overcoming two important mechanisms of multidrug resistance of many antibubulin agents [144, 197].

Several 6,7-dihydrocyclopenta[*d*]pyrimidine compounds are ATP-competitive, selective inhibitors of protein kinase B (Akt). Protein kinase B is a serine/threonine-specific protein kinase, a downstream target for phosphatidylinositol-3-kinase (PI3K), which comprises of three closely related isoforms (Akt1, Akt2, and Akt3). Akt functions as a pivotal node in the PI3K-Akt-mTOR pathway. Once activated, Akt can control key cellular processes by phosphorylating substrates. Akt is therefore involved in apoptosis, transcription, cell cycle progression, and translation. Akt activity is frequently elevated in cancer. Constitutive activation and overexpression of Akt isoforms has been identified in a wide variety of human tumors, including breast, prostate, and ovarian carcinoma, as well as melanoma. Strategies for targeting Akt in cancer therapy include ATP-competitive, active-site-directed inhibitors, and non-ATP-competetive allosteric compounds. Several Akt inhibitors, representing both classes of compounds, were or are being tested in clinical trials for the treatment of human cancers. GDC-0068 (Figure 1.6) is a novel, oral ATP-competitive inhibitor, and was identified as potent inhibitor of all three Akt isoforms, while showing poor inhibition of cAMP-dependent protein kinase/protein kinase G/protein kinase C. Biological studies of GDC-0068 demonstrate good oral exposure resulting in dose-dependent pharmacodynamic effects and a robust antitumor resonse. GDC-0068 is currently being evaluated in Phase I clinical trials for the treatment of solid tumors. GDC-0068 is developed by Genetech Research and Early Development (gRED), a member of Roche group, in collaboration with ArrayBioPharma [198–201].

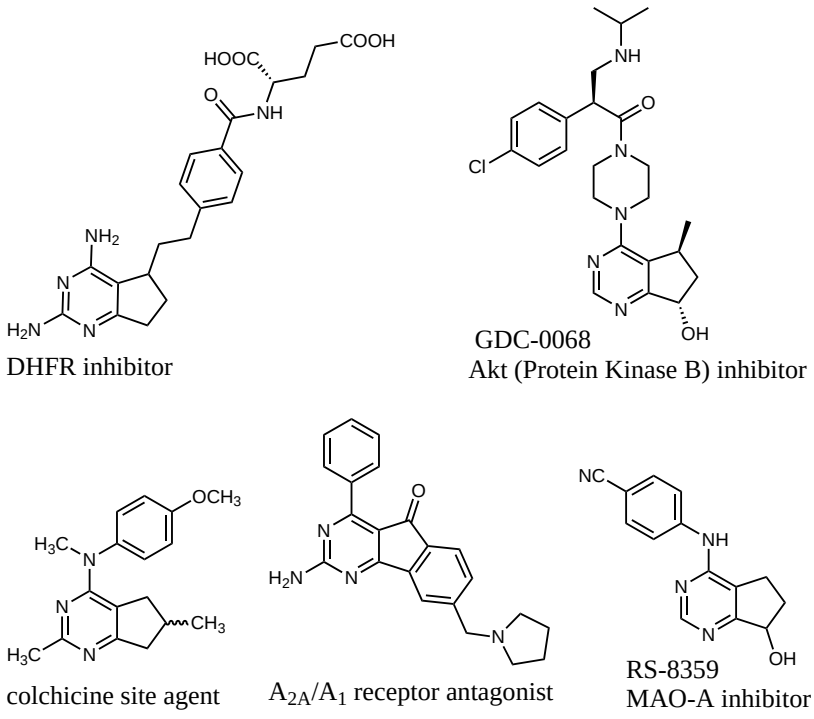

Figure 1.6 Examples of bioactive cyclopenta[*d*]pyrimidines.

Cyclopenta[*d*]pyrimidine containing compounds are reported in literature as adenosine A_{2A} receptor antagonists, as depicted in Figure 1.6. Adenosine receptors comprise four distinct receptor subtypes designated A_1, A_{2A}, A_{2B}, and A_3. A_1, and A_3 receptors are coupled to inhibitory G-proteins, while A_{2A}, and A_{2B} receptors are coupled to stimulatory G-proteins. A_{2A} and A_1 receptors are highly expressed in the brain, particularly striatum, whereas A_{2B}, and A_3 receptors are not [202, 203]. Pharmacological blockage of A_{2A} receptors has shown dramatic beneficial effects in preclinical animal models of Parkinson's disease, showing potentiation of dopamine-mediated responses in dopamine depleted animals and dramatic relief in parkinsonian symptoms in 1-methyl-4-phenyl-1,2,3,6-tetrahydropyridine (MPTP) treated non-human primates. A_{2A} antagonists facilitate dopamine receptor signalling and thereby normalize motor function in animal models of dopamine dysregulation. A_1 receptor antagonists facilitate dopamine release in the striatum and, like A_{2A} antagonists, potentiate dopamine mediated responses. Antagonism of both, the A_{2A} and A_1 are synergistic, inhibition of the A_1 receptor facilitates dopamine release, while inhibition of the A_{2A} receptor will enhance postsynaptic responses to dopamine. The major unmet medical needs of Parkinson's disease are improved symptomatic treatment without adverse effects like dyskinesia, associated with long-term L-DOPA or dopamine agonist therapy, opportunity to slow disease progression by protecting midbrain dopamine and other neurons from degeneration, and treatment of disease comorbidities, including cognitive dysfunction, anxiety, and depression. A dual A_{2A}/A_1 receptor antagonist may address many of these needs. The original adenosine receptor antagonists were xanthines, such as caffeine and theophylline, which show little or no selectivity for this receptor. A_{2A} receptor antagonists from Merck (Schering-Plough) have already completed phase II clinical trials for Parkinson's disease [203–205]. Recently, non purine antagonists, e.g. 4-aryl-5*H*-indeno[1,2-*d*]pyrimidin-2-ylamine derivatives were identified as a novel class of dual A_{2A}/A_1 receptor antagonists. These analogues demonstrated very potent activity for both A_{2A} and A_1 in

vitro and in an animal model of Parkinson's disease [202, 203, 206, 207].

4-(4-Cyanoanilino)-5,6-dihydro-7-hydroxy-7*H*-cyclopenta[*d*]pyrimidine (RS-8359, Figure 1.6) is a selective and reversible MAO-A inhibitor, which has been developed as antidepressant. MAO inhibitors show limited clinical use as they inhibit the catabolism of dietary amines. Consumption of tyramine may lead to hypertensive crisis, known as the "cheese-effect". RS-8359 shows a selectivity ratio of approximately 2200 for MAO-A as opposed to MAO-B, therefore showing little effect on blood pressure when administered together with tyramine. RS-8359 has two enantiomeric forms, derived from the secondary alcohol in position 7. The *(R)*-enantiomer was found pharmacologically active. After oral administration of RS-8359 to rats, mice, dogs, monkeys and humans, blood plasma concentrations of the *(S)*-enantiomer were markedly lower than those of the *(R)*-enantiomer. Analysis of the metabolites suggested that the *(S)*-enantiomer was rapidly excreted after being metabolized. The enzymes involved in the drug metabolism were different depending on the species. In humans and monkeys, the keto-derivative is formed by aldehyde oxidase, a reaction highly stereoselective for the *(S)*-enantiomer of R-8359. In rats and mice diol metabolits were formed, posibly by cyctochrome P450, while in dogs RS-8359 glucuronide was formed, presumably with UDP-glucurosyl transferase [208–210].

A number of cyclopenta[*d*]pyrimidines were patented by Squibb Bristol Meyers as inhibitors of amyloid β peptide production. Amyloid β is a peptide of 36 to 43 amino acids, constituting a component of amyloid plaques, known in association with Alzheimer's disease. A role of amyloid β in other diseases, including mild cognitive impairment, Down syndrom, cerebral amyloid angiopathy, dementia with Lewy bodies, amytrophic lateral sclerosis, and inclusion body myositis was suggested recently [211].

1.4.5 Pyrazolo[3,4-*d*]pyrimidines

Pyrazolo[3,4-*d*]pyrimidines are well-known for a number of biological activities. The most prominent example of a biologically active pyrazolo[3,4-*d*]pyrimidine is allopurinol (Zykloprim). Allopurinol, depicted in Figure 1.7, is an inhibitor of xanthine oxidase used primarily to treat hyperuricemia (excess uric acid in blood plasma) and chronic gout. This biological activity of allopurinol was found by Gertrude B. Elion and George H. Hitchings, who were awarded the 1988 Nobel Prize in Pysiology or Medicine for "discoveries of important principles for drug treatment", together with James W. Black. Allopurinol is not only a potent competitive inhibitor of xanthine oxidase, but also a substrate. Oxidation of allopurinol in vivo leads to oxypurinol, again an inhibitor of xanthine oxidase. Oxypurinol binds tightly to the reduced form of the enzyme, thereby inactivating it. Oxypurinol has a half-life of 18 to 30 hours, consequently, steady-state levels of oxypurinol are achieved in a few days, and uric acid concentrations can be maintained at the desired level by dose-adjustment. Allopurinol remains the ideal pro-drug for oxypurinol, as it is completely absorbed orally, whereas oxypurinol is not [212, 213]. Xanthine oxidase was also suggested to play a role in various forms of tissue and vascular injuries, inflammatory diseases, and cardiac indications, such as chronic heart failure. Allopurinol and oxypurinol showed beneficial effects in the treatment of these conditions in experimental animal models and small scale human clinical trials. Some of the beneficial effects of these compounds go beyond inhibition of xanthine oxidase. Novel xanthine oxidase inhibitors with pyrazolo[3,4-*d*]pyrimidine core strcutures were

published and patented in recent years [213–216].

PP1 and PP2, depicted in Figure 1.7, are selective inhibitors for the Src family of tyrosine kinases. Src family kinases interact with cellular cytosolic, nuclear and membrane proteins, modifying these proteins by phosphorylation of tyrosine residues. Receptor induced T-cell activation is a process dependent on the Src kinases Lck and FynT. PP1 inhibits Lck, FynT, anti-CD3-induced protein tyrosine phosphorylation, and subsequent IL-2 gene activation in T lymphocytes. A selective inhibitor of Lck should inhibit T-cell activation and has therefore broad applications for the treatment of autoimmune and inflammatory diseases, as well as organ transplant rejection. PP1 shows selectivity for the Src family over other families of tyrosine kinases. PP2 also shows high selectivity for Src family kinases. These compounds are therefore useful tools in cancer research [217]. Similar compounds were developed, that bind more strongly to the hydrophobic binding pocket of tyrosine receptor kinases than PP1. Several compounds were patented by Pfizer and Abbott laboratories for the treatment of a number of diseases, including abnormal cell growth, inflammatory conditions, and proliferative disorders [218–220]. Drug delivery systems of self-assembling peptide nanostructures with pharmaceutical compositions of PP1 and PP2 were recently patented [221].

Pyrazolo[3,4-*d*]pyrimidines and pyrrolo[2,3-*d*]pyrimidines are potent Lck inhibitors and exhibit comparable *in vitro* potency. Potency and selectivity were, however, found to be influenced by the nature of the Ph-X-Ph linker (Figure 1.7). Regarding pharmacological properties, pyrazolo[3,4-*d*]pyrimidines exhibit an enhanced pharmacokinetic profile and show prolonged activity in animal models of T-cell activation after oral administration [222].

Pyrazolo[3,4-*d*]pyrimidines were reported to block Src phosphorylaton, induce apoptosis, and reduce cell proliferation. The activation of Src is an important step in the progression of cancer. Inhibition of the Src phosphorylation process may halt uncontrolled tumor cell growth and may therefore be applied for therapeutic agents for the treatment of cancer. Pyrazolo[3,4-*d*]pyrimidine compounds bearing an N-1 chlorophenyl ethyl side chain in combination with a 6-methylthio group showed best antiproliferative activity. Substituents in position 4 were used to fine-tune the antiproliferative activity [223].

Chronic myeloid leukemia is a hematopoietic stem cell cancer that is caused by chromosomal abnormality resulting in the formation of a Philadelphia chromosome. This chromosome encodes for a constitutively activated fusion protein: the oncogenic tyrosine kinase BcrAbl. Imatinib, by Novartis, selectively inhibits this tyrosine kinase. The success of Imatinib is, however, limited by drug resistances. Consequently, compounds acting on multiple targets are favoured to overcome the drug resistance often connected to the activation of alternative signaling pathways. Several pyrazolo[3,4-*d*]pyrimidine were found to induce apoptosis and reduce cell proliferation in different solid tumor cell lines, inhibit the proliferation of three Bcr-Abl positive leukaemia cell lines, reduce Bcr-Abl tyrosine phosphorylation and to promote apoptosis of Bcr-Abl expressing cells. A lead structure was identified and is further optimized regarding in vitro ADME properties, especially regarding water solubility [224, 225].

4-Morpholino-6-arylpyrazolo[3,4-*d*]pyrimidines are highly potent and selective ATP-competitive inhibitors of mTOR (mammalian target of rapamycin). The mammalian target of rapamycin is a serine/threonine protein kinase, a member of the phosphoinositide-3-kinase related kinase family

and is a key mediator of signaling through the PI3K-Akt pathway. Deregulation of PI3K-Akt-mTOR signalling is one of the most common genetic alterations in proliferative diseases. mTOR exists in at least two functional complexes, namely mTORC1, which is inhibited by rapamycin analogues, and mTORC2, unaffected by rapamycin analogues, which activates Akt. An ATP-competitive inhibitor is expected to affect both mTOR complexes and thus lead to decreased Akt activity. Akt activation has anti-apotopic, pro-survival effects, therefore ATP-competitive mTOR inhibitors may have increased antitumor effects compared to rapamycin analogues. Replacement of the morpholino-group with fluoroethyl urea or 4-urea-phenyl groups provided potent inhibitors of mTOR with higher selectivity for mTOR compared to PI3K [226, 227].

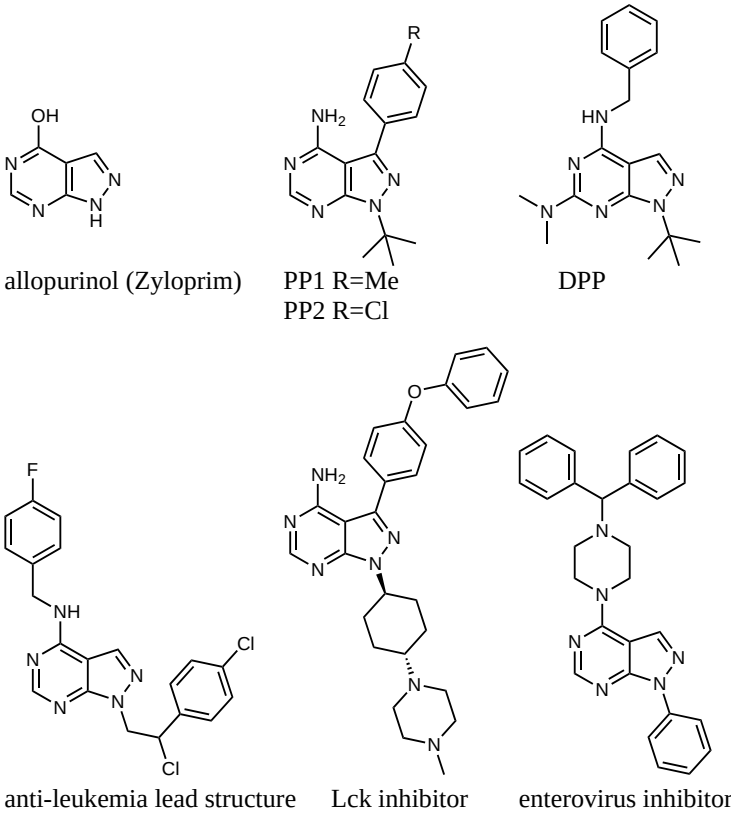

Figure 1.7 Examples of bioactive pyrazolo[3,4-*d*]pyrimidines.

6-Anilinopyrazolo[3,4-*d*]pyrimidin-4-ones are novel dGTP analogues that inhibit the replication-specific enzyme DNA polymerase III of *Staphylococcus aureus* and other Gram positive bacteria. 6-Anilino substituents with small hydrophobic groups in *meta*- or *para*-position enhance both, antipolymerase and antimicrobial activity. Substitution of the pyrazolo[3,4-*d*]pyrimidine ring in position 4 by oxygen gave optimum activity, whereas substitution at the pyrazolo NH was not tolerated. 2-Benzyl-substituted inhibitors were found to be substantially less active. A number of life-threatening infectious diseases are caused by multiply resistant Gram-positive bacteria. The development of chemotherapeutic agents, capable of selectively attacking new bacterial targets, is a possible approach for the treatment of such diseases. DNA polymerase III is essential for the replication of Gram-positive bacterial DNA and is therefore a sought after target [228, 229].

Pyrazolo[3,4-*d*]pyrimidines were shown to exhibit anti-inflammatory properties. Classical non-steroidal, anti-inflammatory drugs inhibit both cyclooxygenase isozymes. More recently,

highly selective inhibitors of cyclooxygenase-2 were developed that demonstrate anti-inflammatory and analgesic activities equivalent to those of dual cyclooxygenase inhibitors, however with lower gastrointestinal toxicity. 6-Dimethylaminopyrazolo[3,4-*d*]pyrimidine derivatives show acute anti-inflammatory, analgesic and anti-angiogenic effects [230, 231]. Bacterial infections often produce pain and inflammation. Usually, chemotherapuetic, analgesic, and anti-inflammatory drugs are prescribed simultaneously, which increases the risk of non steroidal anti-inflammatory drug complications. Drugs having both antimicrobial, and analgesic/anti-inflammatory activities would therefore decrease adverse effects. 1-(1,3-Benzothiazol-2-yl)-3-methyl-4-arylpyrazolo[3,4-*d*]pyrimidines, with different aryl groups in position 4, showed dual antimicrobial-anti-inflammatory agents with minimum ulcerogenic effects. Significant inhibitory activity against *Pseudomonas aeruginosa* and *Candida albicans* was observed [232].

Pyrazolo[3,4-*d*]pyrimidines are under investigation for their antimycobacterial and antiviral properties. *N,S*-Bis-alkylated thiopyrazolo[3,4-*d*]pyrimidines showed significant anti-mycobacterial activity and could therefore be new lead structures for drugs against *Mycobacerium tuberculosis*. Drugs for treating tuberculosis have been available for over half a century, however, new drugs to extent the treatment options, especially in regard to multi-drug resistant strains of tuberculosis, are necessary [233]. 1,4-Substituted pyrazolo[3,4-*d*]pyrimidines were shown to possess specific antiviral activity for human enteroviruses. Enteroviruses are the most common cause for viral infections in humans, along with rhinoviruses. Five billion enteroviral infections occur worldwide annually, and currently there is no effective antiviral drug for the treatment of enteroviral disease. Pyrazolo[3,4-*d*]pyrimidines substituted with a phenyl group at the N-1 and a hydrophobic diarylmethyl group at the piperazine-substituent in position 4, showed highest activities [234].

1.5 Chemical reduction of nitriles

The reduction of nitriles is a common method to obtain primary amines. A number of other methods for the synthesis of primary amines is available in literature [235]. Biocatalytic preparations of amines are known, however methods for the preparation of secondary and tertiary amines are more prevalent than those for primary amines [236–242].

Chemical reduction of nitriles is commonly achieved by catalytic hydrogenation or complex metal hydrides. In industrial applications, catalytic hydrogenations are favoured as versatile and efficient process [243, 244]. Various metal catalysts are suitable for the reduction of nitriles, including Raney nickel, Raney cobalt, platinum, palladium, ruthenium, rhenium [243–246]. Complex metal hydrides, especially sodium borohydride and lithium aluminium hydride variations, have been successfully used for nitrile reductions [245, 247, 248].

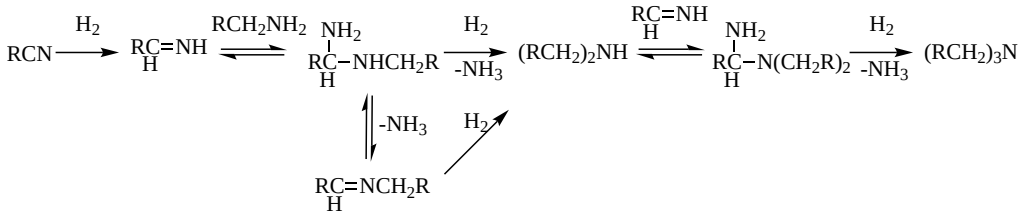

Scheme 1.11 Mechanism of the hydrogenation of nitriles and formation of secondary and tertiary amines.

A general problem in the catalytic hydrogenation of nitriles is the formation of secondary amines. This unwanted side reaction is caused by the nucleophilic attack of the initially formed primary amine on the imine intermediate, as depicted in Scheme 1.11. Subsequent elimination of ammonia and reduction of the secondary imine leads to the secondary amine [243, 247, 249]. Tertiary amines are formed by addition of the secondary amine to the imine and subsequent hydrogenolysis of the intermediate [244, 247]. In the hydrogenation of aromatic nitriles, the formation of Schiff bases was also observed [250].

The chemoselectivity of the hydrogenation reaction can be improved by a low concentration of imine to suppress secondary amine formation and by shifting the equilibrium towards the primary amine by addition of ammonia or an appropriate base [243]. In hydrogenations of nitriles with Raney nickel, the formation of secondary amines can be almost entirely prevented by carrying out the reaction in the presence of sufficient ammonia. Ammonia reacts with the imine intermediate to give amine substituted secondary amines, which yield two equivalents of primary amine upon hydrogenation, as depicted in Scheme 1.12. The importance of the use of ammonia was also demonstrated in nitrile reductions with cobalt, iron and ruthenium catalysts [244]. Primary amines are also obtained in the hydrogenation of nitriles in the absence of ammonia, when nickel is employed as catalyst and sodium hydroxide as an additive. The hydrogenation of nitriles to primary amines over Raney nickel or cobalt with a catalytic amount of lithium hydroxide and water or sodium carbonate was also reported. The hydroxide ions prevent catalyst deactivation by inhibiting polyamine formation on the catalyst surface and are also believed to block active sites responsible for by-product formation [244, 246]. The reaction rate and the product composition in the hydrogenation of nitriles are affected primarily by the type of catalyst used. The mechanisms that justify the addition of bases or water on the activity and selectivity of catalysts are not unambiguously identified yet. Individual catalysts differ in their responses to a change in reaction conditions and often contradictory results were obtained [244].

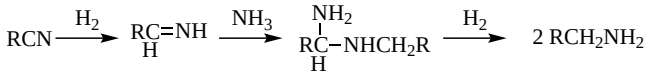

Scheme 1.12 Effect of ammonia on the selectivity of the hydrogenation of nitriles.

Raney nickel and Raney cobalt catalysts represent the most common catalyst choice for hydrogenation reactions of nitriles, based on patent literature [244]. However, Raney nickel has certain disadvantages, as it is fragile, difficult to handle and mostly requires elevated temperatures and pressures. Functional group tolerance is a common issue with Raney nickel catalyzed hydrogenations. The addition of ammonia or base to avoid formation of secondary and tertiary amines, as well as the presence of triethyl amine to retard the hydrogenation of an aromatic system are known [244, 251]. Cobalt was used under similar or even more severe conditions than nickel catalysts. Several other metal catalysts are found in literature for the reduction of nitriles to amines. However, platinum, palladium, iron and copper are considered to be less active than Raney nickel [244]. In recent years, Raney nickel catalyzed reductions of nitriles using mild hydrogenation conditions, replacing hydrogen with other hydrogen donors, were published. The conversion of aromatic and aliphatic nitriles to their corresponding primary amines by using a Raney nickel potassium borohydride system was described in ethanol at mild temperatures [247].

Hydrazinium monoformate was also described as hydrogen donor in Raney nickel catalyzed reductions of aromatic and aliphatic nitriles to yield primary amines. Ammonium formate is extensively used in the field of catalytic transfer hydrogenation, however it is sparingly soluble in methanol. Hydrazinium monoformate offers the advantage of being freely soluble in methanol, ethanol, tetrahydrofuran, dimethylformamide and glycols [252].

Hydrogenations of nitriles with homogeneous transition-metal catalysts are mainly based on ruthenium, rhodium, and iridium complexes. However, many of these catalysts display low selectivity towards primary amines and significant amounts of secondary amines were formed. Optimized catalyst complexes for certain substrates are described in literature. An *in situ* catalyst system composed of [Ru(cod)(methylallyl$_2$)] (cod = 2,5-cyclooctadiene) and 1,1'-bis(diphenylphosphino)-ferrocene (dppf), using optimized reaction conditions, was described for excellent chemoselectivities towards primary amines for aromatic, heterocyclic and aliphatic substrates [243, 253].

Lithium aluminium hydride is an exceedingly powerful reducing agent, while sodium borohydride is much milder. Except for a few examples, sodium borohydride cannot reduce nitriles to amines. The reducing ability of sodium borohydride can be enhanced by additives, such as $CoCl_2$, $ZrCl_4$, $NiCl_2$ and iodine [247]. Mostly water and alcohols are used as solvents, other solvents are found in literature for selective reductions of certain specific groups. Sodium cyanoborohydride, lithium cyanoborohydride and tetrabutylammonium cyanoborohydride are weaker reducing agents than their borohydride equivalents, due to the electron withdrawing effect of the cyano group. Sulphurated sodium borohydride is formed when sodium borohydride and sulphur are reacted at room temperature in tetrahydrofuran. Sulphurated sodium borohydride is a more powerful reducing agent than sodium borohydride and reduces aromatic nitriles to the corresponding amines, in the absence of more reactive nitro-groups [254]. Potassium borohydride is usually used to prepare metal borides that are used as catalysts in catalytic hydrogenations [247].

Borane dimethylsulfide, BH_3-THF, and borane-amine adducts are important reducing agents applied for the reduction of nitriles. Nitriles can be readily reduced in tetrahydrofuran or dioxane under reflux conditions. Reactions with *tert*-butyl-*N*-methyl-*N*-isopropylamineborane are faster than with borane dimethylsulfide in refluxing tetrahydrofuran [255].

2

Aim of this work

Biocatalytic reactions offer the advantage of mild reaction conditions and high chemo-, regio-, and enantioselectivity. The use of safe and environmentally friendly biocatalysts in non-flammable solvents is compelling from a process safety and environmental perspective [2]. Biocatalysis therefore aspires to replace traditional chemical reactions by a biocatalytic equivalent and has succeeded in various cases [71, 256]. Nitrile transforming enzymes, e.g., nitrilase and nitrile hydratase, have been applied successfully in industrial processes. Nitrile reductase is a novel enzyme discovered in 2005 [9]. It is the first enzyme capable of reducing a nitrile group to the corresponding primary amine [9].

This thesis aims to investigate the possible application of nitrile reductase queF in biocatalysis. In order to evaluate this new oxidoreductase for use in biocatalytic reactions, enzyme characterization and investigation of the substrate scope are prerequisite.

Two types of nitrile reductase are known, both types are investigated in this thesis. Type I and type II nitrile reductases were cloned, expressed and purified. The novel nitrile reductase from *G. kaustophilus* was characterized regarding its stability, pH, temperature and co-factor dependence. The substrate scope and substrate binding of nitrile reductase were investigated in detail. Several natural substrate analogues, differing from the natural substrate in the functional groups or heteroatoms, were designed and synthesized. These substrate analogues belong to the structural classes of pyrrolo[2,3-*d*]pyrimidines, pyrrolo[2,3-*b*]pyridines, pyrrolo[3,2-*c*]pyridines, thieno[2,3-*d*]pyrimidines, cyclopenta[*d*]pyrimidines and pyrazolo[3,4-*d*]pyrimidines. Homology models of type I and type II nitrile reductase were used to identify amino acid residues potentially involved in substrate binding. Screening reactions of substrate analogues with wild type and mutant queF can provide insight into the substrate scope and substrate binding of nitrile reductase queF.

Bioreduction of C-N double bonds is so far only known from reductive aminations in the synthesis of α-amino acids, catalyzed by transaminases [236–239] and very recently, from the enzymatic reduction of cyclic imines [241, 242]. Both reactions, however, are currently limited in their substrate scope. Nitrile reductase queF was therefore also preliminarily investigated towards its activity for two electron reductions, particularly the reduction of the C-N double bond in imines and oximes, and the C-O double bond in aldehydes. An aldehyde, imine and oxime, bearing the core-structure of the enzyme's natural substrate $preQ_0$, were prepared.

3

Results and Discussion I
Substrates

3.1 5-Cyanopyrrolo[2,3-*d*]pyrimidines

3.1.1 2-Amino-5-cyanopyrrolo[2,3-*d*]pyrimidin-4-one (preQ$_0$)

2-Amino-5-cyanopyrrolo[2,3-*d*]pyrimidin-4-one (preQ$_0$, **1**) is the natural substrate of nitrile reductase queF and was therefore synthesized for activity tests of nitrile reductase queF.

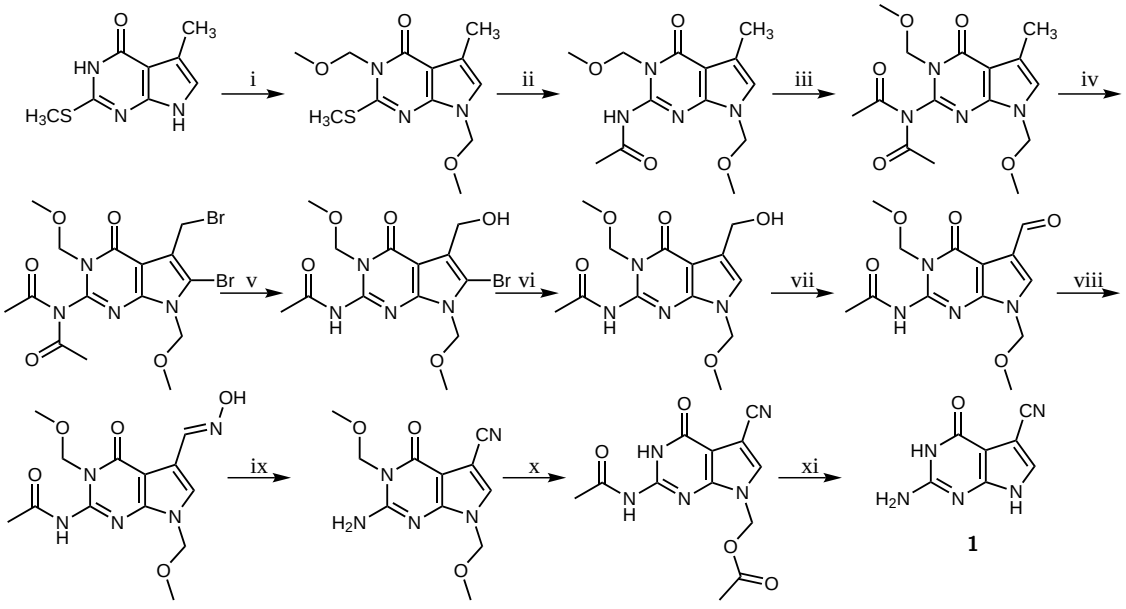

Scheme 3.1 First synthesis of 2-amino-5-cyanopyrrolo[2,3-*d*]pyrimidin-4-one (preQ$_0$). (i) NaH, chloromethyl methyl ether, dimethoxyethane, (ii) acetamide, sodium acetamide, 120°C, (iii) acetic anhydride, pyridine, 80°C, (iv) 1. NBS, CCl_4, benzoyl peroxide, reflux, 2. NBS, anhydrous K_2CO_3, benzoyl peroxide, reflux, (v) 1. Ag_2CO_3, water/dioxane, 2. water/dioxane, triethylamine, (vi) H_2, 10% Pd/C, methanol, potassium acetate, (vii) chromic anhydride-pyridine, dichloromethane, pyridine, (viii) NH_2OH, Ag_2CO_3, ethanol, (ix) 1. acetic anhydride, pyridine, 55°C, 2. ammonia in methanol, (x) acetic anhydride, CF_3COOH, 60°C, (xi) ammonia in dioxane, 60°C.

The first synthesis of preQ$_0$ was published in 1980 [257]. In this synthesis, depicted in Scheme 3.1, preQ$_0$ is prepared in several steps from 5-methyl-2-methylthiopyrrolo[2,3-*d*]pyrimidin-4-one. The

cyano-functionality is derived from a methyl group. The methyl-group is oxidized to an alcohol and further to the aldehyde, which is then transformed into an oxime and dehydrated to give the nitrile [257].

A significantly shorter synthetic pathway was published by Migawa *et al.* in 1996 [258]. In this synthetic pathway, depicted in (Scheme 3.2), $preQ_0$ is prepared in a condensation reaction of 2,4-diamino-6-hydroxypyrimidine with 2-chloro-3-oxopropanenitrile (**2**). Various modifications of this procedure are available in literature [258–263]. 2-Chloro-3-oxopropanenitrile is prepared from methyl formate and chloroacetonitrile, using sodium methoxide in THF or toluene [259, 260, 263]. In the next step, $preQ_0$ is formed from 2,4-diamino-6-hydroxypyrimidine and 2-chloro-3-oxopropanenitrile in an aqueous sodium acetate solution at temperatures between 50°C and reflux [259, 260, 263]. The hydroxylated reaction intermediate, depicted in (Scheme 3.2) was observed by Migawa *et al.*, when 2-chloro-3-oxopropanenitrile (**2**) was added to the reaction mixture at 0°C, and the reaction mixture was then stirred at room temperature for 12 hours. The loss of water is therefore considered to be the last step in the reaction mechanism [258].

$PreQ_0$ is purified by converting it into its potassium salt, by dissolving the crude product in aqueous KOH. When the resulting solution is neutralized by addition of aqueous HCl, $preQ_0$ precipitates from the solution [260, 263]. Alternatively, the crude product can be washed with water and acetone, to remove impurities [259].

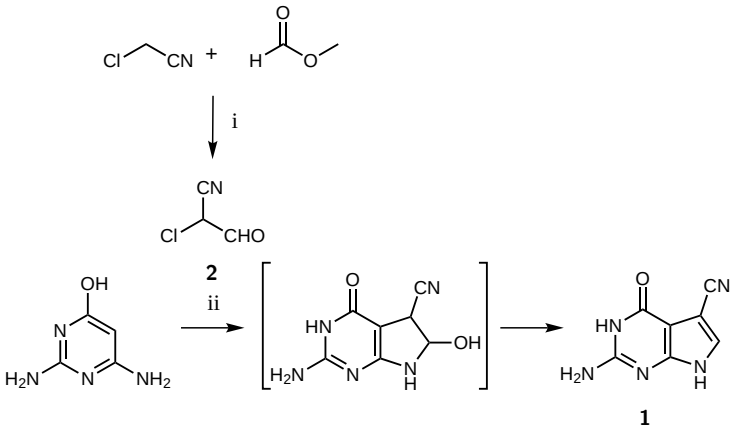

Scheme 3.2 Synthetic pathway to 2-amino-5-cyanopyrrolo[2,3-*d*]pyrimidin-4-one ($preQ_0$). (i) NaH, THF, 0°C or NaOMe, toluene, 0°C or NaOMe, THF, 0°C, (ii) sodium acetate, water, reflux.

In this thesis, reaction conditions for the preparation of $preQ_0$ were modified, improving the overall yield of the synthesis [264]. Different reaction conditions for the synthesis of 2-chloro-3-oxopropanenitrile (**2**), and subsequently $preQ_0$, are summarized in Table 3.1. The two major modifications involved firstly, changing the base from sodium methanolate to sodium hydride in the first synthetic step, and secondly, changing the solvents for extraction during work-up of 2-chloro-3-oxopropanenitrile. The product of the first synthetic step, 2-chloro-3-oxopropanenitrile, is unstable, especially upon heating. To avoid degradation of the product, the solvent for extraction was changed from ethyl acetate to the lower boiling diethyl ether, which can be easily removed in vacuum at room temperature. Purification of 2-chloro-3-oxopropanenitrile was achieved during work-up, by extracting the basic reaction mixture to remove remaining starting material. The aqueous layer is then acidified to pH 4, to protonate 2-chloro-3-oxopropanenitrile, which can then

be extracted into the organic layer. 2-Chloro-3-oxopropanenitrile (**2**) was then used directly for the next synthetic step.

Table 3.1 Comparison of the reaction conditions for the synthesis of $preQ_0$

method	base first step	solvent first step	yield $preQ_0$	reference
A	NaH	THF	51.43%	[264]
B	NaOMe	toluene	35.89%	[259, 263]
C	NaOMe	THF	18.51%	[260, 262]

In the next step, $preQ_0$ is formed in a condensation reaction of 2,4-diamino-6-hydroxypyrimidine and 2-chloro-3-oxopropanenitrile (**2**). Solubility of 2,4-diamino-6-hydroxypyrimidine in water improved upon heating above 85°C. 2-Chloro-3-oxopropanenitrile (**2**) was added dropwise to the hot reaction mixture. The product $preQ_0$ precipitated from the reaction mixture and was isolated by filtration. The crude product was washed with copious amounts of deionized water and acetone, yielding highly pure $preQ_0$.

3.1.2 2-Amino-5-aminomethylpyrrolo[2,3-*d*]pyrimidin-4-one ($preQ_1$)

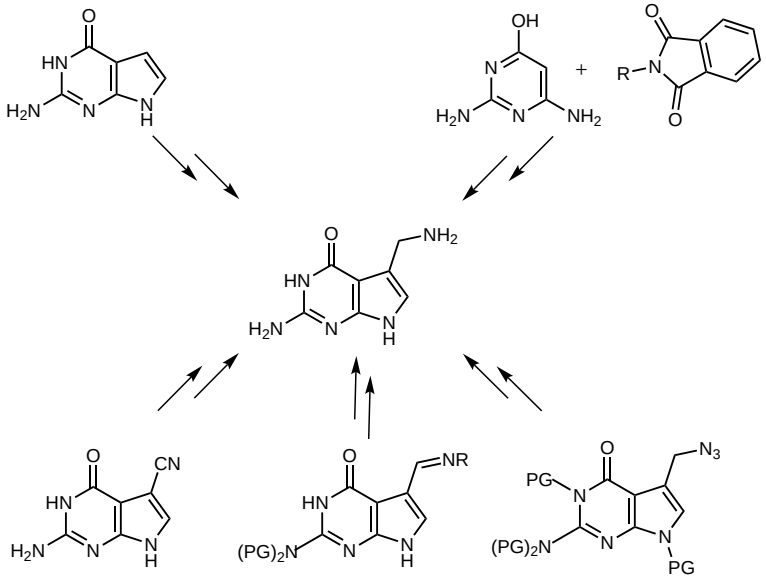

Scheme 3.3 Synthetic strategies for the synthesis of 2-amino-5-aminomethylpyrrolo[2,3-*d*]pyrimidin-4-one ($preQ_1$). PG = protecting group.

Various different synthetic pathways to 2-amino-5-aminomethylpyrrolo[2,3-*d*]pyrimidin-4-one (**3**, $preQ_1$) are available in literature [260, 265–268]. The synthetic pathways follow three general strategies: firstly, synthesis of an appropriate cyano-, imino-, or azido-precursor and subsequent reduction, secondly, reaction of an appropriate phthalimide with 2,4-diamino-6-hydroxypyrimidine, and thirdly, synthesis of 2-aminopyrrolo[2,3-*d*]pyrimidin-4-one and introduction of an aminomethyl substituent. These general strategies are depicted in Scheme 3.3.

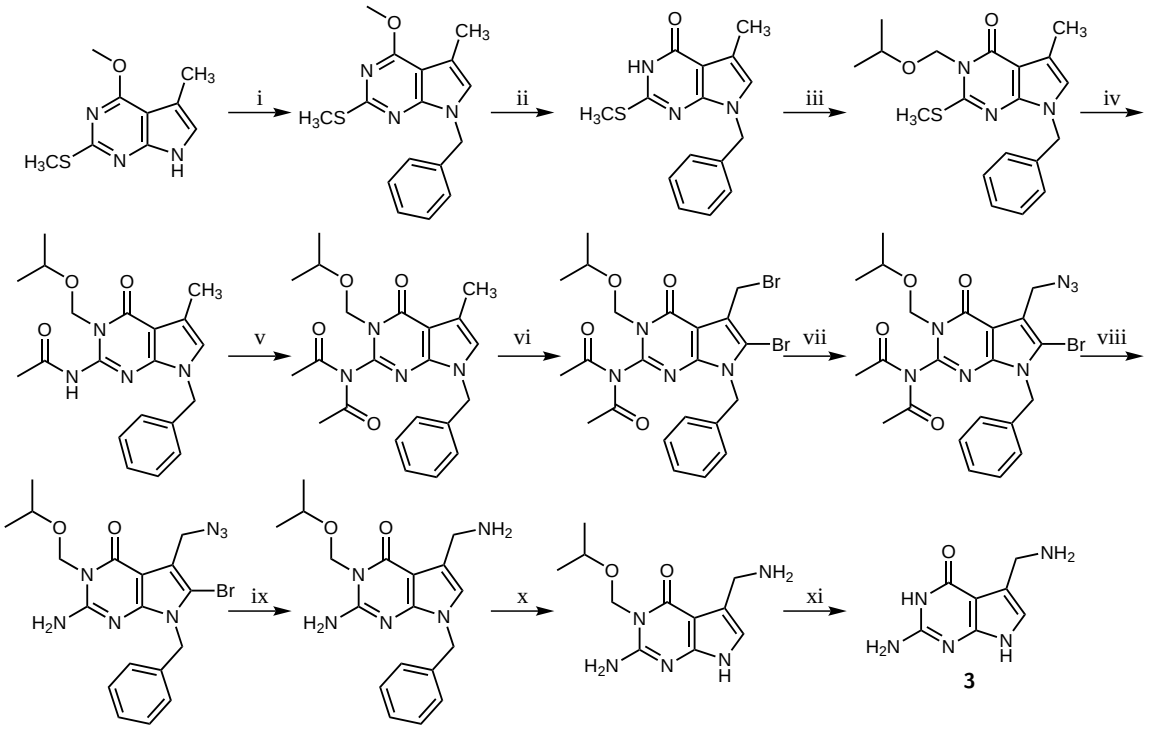

Scheme 3.4 First synthesis of 2-amino-5-aminomethylpyrrolo[2,3-*d*]pyrimidin-4-one (preQ$_1$). (i) NaH, benzyl bromide, DMF, (ii) 0.5N HCl, dioxane, 4,4'-thiobis-(6-*t*-butyl-3-methylphenol), (iii) NaH, isopropoxymethyl chloride, (iv) sodium acetamide, (v) acetic anhydride, pyridine, 60°C, (vi) 1. NBS, benzene, benzoyl peroxide, 2. NBS, anhydrous K_2CO_3, benzoyl peroxide, CCl_4, reflux, (vii) NaN_3, anhydrous DMF, room temperature, (viii) NH_3 in methanol, (ix) H_2, Pd/C, methanol, benzene, (x) sodium in liquid ammonia, NH_4Cl, (xi) 1. 2N HCl, 70°C, 2. neutralization with Amberlite IR-420.

2-Amino-5-aminomethylpyrrolo[2,3-*d*]pyrimidin-4-one (preQ$_1$) was first synthesized in 1979 by Ohgi *et al.* [265]. This synthesis, depicted in Scheme 3.4, starts from 4-methoxy-5-methyl-2-methylthiopyrrolo[2,3-*d*]pyrimidine. In the first step, a benzyl protecting group is introduced on the pyrrole nitrogen. Subsequently, the methoxy group in position 4 is cleaved, and the NH in position 3 is protected. Displacement of the thioether with sodium acetamide gives a 2-acetylamino substitutent in position 2. Bromination is then achieved with *N*-bromosuccinimide. The resulting compound was treated with sodium azide. In the subsequent hydrogenation reaction, the azide is reduced to the amine and concurrently, the bromine is removed by catalytic hydrogenation. After deprotection, preQ$_1$ is obtained as hydrochloride salt. The free base preQ$_1$ is available by neutralization with Amberlite IR-240 [265].

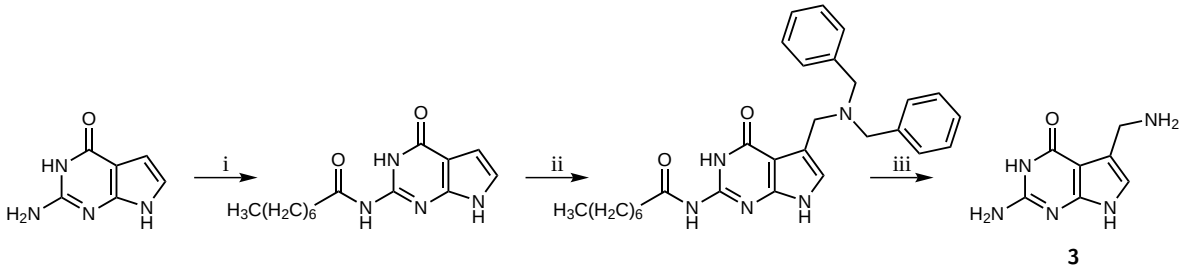

Scheme 3.5 Synthesis of preQ$_1$ by Mannich reaction. (i) 1. octanoylchloride, pyridine, 2. ethanolic ammonia, (ii) dibenzylamine, formaldehyde, (iii) 1. ammonia, methanol/THF, 2. KOH.

$PreQ_1$ was successfully prepared by Mannich reaction and subsequent amine exchange reaction by Akimoto *et al.* (Scheme 3.5) [266]. Mannich reaction was described for the synthesis of 5-((dimethylamino)methyl)pyrrolo[2,3-*d*]pyrimidin-4-one [269]. Substitution in 5-position is achieved in absence of a electron donating substituent in position 2. In absence of an electron donating substituent in position 2, the pyrrole-nitrogen stabilizes the cation. Aminomethylation of 2-methylthiopyrrolo[2,3-*d*]pyrimidin-4-one yielded the 5-substituted product. However, Mannich reaction of 2-aminopyrrolo[2,3-*d*]pyrimidin-4-one with an appropriate amine and formaldehyde gave the 6-substituted product [266, 270]. The substitution in position 6 was explained by the amino-substituent in position 2. This amino substituent stabilizes the cation which results from electrophilic attack at the carbon in position 6 [270]. The Mannich reaction of 2-acylaminopyrrolo[2,3-*d*]pyrimidin-4-one provided predominately the 5-substituted aminomethyl compounds [266].

The ratio of 5- and 6-substituted pyrrolo[2,3-*d*]pyrimidin-4-ones is not only influenced by the substitutent in position 2, but also by the amine used for the Mannich reaction. The structure of the amine used was found to influence the substitution pattern more than the structure of the acyl on the pyrrolo[2,3-*d*]pyrimidines. An amine with a bulky substitutent favoured the introduction of the Mannich reagent to position 5, regardless of the difference in size of the 2-acyl group. Thus, in the reaction of 2-acylaminopyrrolo[2,3-*d*]pyrimidines with a less hindered secondary amine, e.g. dimethylamine, the 6-substituted Mannich base is the major product. In contrast, the reaction using bulky secondary amines, e.g. dibenzylamine and diisobutylamine, mainly gave the desired 5-substituted pyrrolo[2,3-*d*]pyrimidine. The 2-acylamino group therefore appears to affect the electronic properties of the pyrrolo[2,3-*d*]pyrimidine ring, increasing the nucleophilicity of the β-carbon of the pyrrole ring compared to the 2-aminopyrrolo[2,3-*d*]pyrimidine. When a 2-acylaminopyrrolo[2,3-*d*]pyrimidine and a hindered amine are reacted, the first attack by the Mannich reagent appears to be on the pyrrole nitrogen. The second attack consequently occurs at the 5-position, which is less hindered, to give a 5,7-bis(substituted aminomethyl) compound. The N-7-substituent is very labile and is cleaved upon very mild acid hydrolysis[266].

The amine exchange reaction of 3-((dimethylamino)methyl)indole (gramine) and its related compounds has been shown to proceed by an elimination-addition mechanism to afford indoles with a variety of aminomethyl sidechains at position 3. A similar exchange reaction was applied for the preparation of $preQ_1$, as depicted in Scheme 3.5. The primary amine of $preQ_1$ was prepared by heating 5-((dibenzylamino)methyl)-2-octanoylaminopyrrolo[2,3-*d*]pyrimidin-4-one with an excess of ammonia, and subsequently deprotection of the 2-octanoyl moiety with alkali. The reaction was presumed to progress via formation of a conjugated unsaturated ring system by amine elimination from 5-((dibenzylamino)methyl)-2-octanoylaminopyrrolo[2,3-*d*]pyrimidin-4-one, followed by the addition of ammonia. The less active 6-substituted aminomethyl pyrrolo[2,3-*d*]pyrimidines failed to react under similar conditions [266].

$PreQ_1$ was prepared by Gabriel synthesis as depicted in Scheme 3.6 [260]. *N*-(3-hydroxypropyl)phthalimide was oxidized with Dess-Martin periodinane. The resulting aldehyde was α-brominated with trimethylsilyl bromide and subsequently reacted with 2,4-diamino-6-hydroxypyrimidine yielding the phthalimido-protected $preQ_1$. Deprotection was achieved with hydrazine according to the Ing-Manske procedure [271]. The crude product was boc-protected and purified

by column chromatography. $preQ_1$ was obtained after cleavage of the boc-group. This synthesis is limited by the poor yield of 10% in the Ing-Manske procedure and subsequent isolation of $preQ_1$ by boc-protection, column chromatography and boc-deprotection [260].

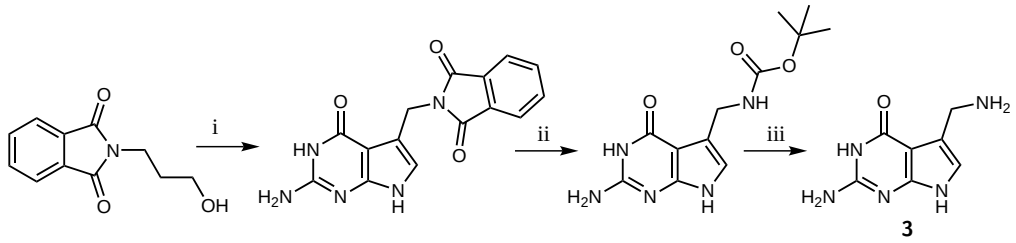

Scheme 3.6 Synthesis of $preQ_1$ by Gabriel synthesis. (i) 1. Dess-Martin periodinane, DCM, 2. TMSBr, DMSO, acetonitrile, (ii) 2,6-diamino-4-hydroxypyrimidine, sodium acetate, water/acetonitrile, (iii) 1. hydrazine, methanol, reflux, 2. Boc_2O, DMF, (iv) CF_3COOH.

A similar synthetic pathway for the preparation of $preQ_1$, depicted in Scheme 3.7, is described by Gerber *et al.* [267]. Commercially available phthalimidoacetaldehyde was converted to the corresponding nitroalcohol by Henry reaction. The nitroalcohol was then dehydrated by hydroxyl group activation and subsequent elimination. The resulting nitro-olefin was then reacted with 2,4-diamino-6-hydroxypyrimidine in a Michael addition. A Nef reaction gave the aldehyde intermediate, which directly underwent intramolecular cyclization. During this synthetic step, hydrolysis of the phthalimido moiety was observed. Deprotection could be achieved by acidic cleavage with hydrochloric acid. The Ing-Manske procedure, diminishing the yield of the Gabriel synthesis depicted in Scheme 3.6 could therefore be avoided and excellent overall yields were achieved [267].

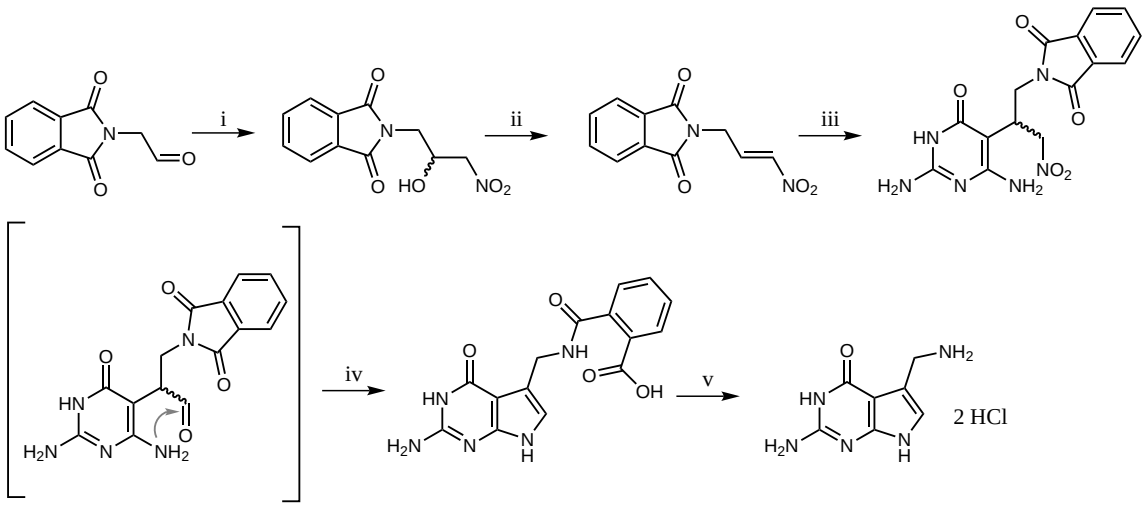

Scheme 3.7 Synthesis of $preQ_1$ by Nef reaction. (i) CH_3NO_2, *t*-BuOK, THF/methanol, 0°C to 20°C, (ii) 1. CF_3COOH, THF, -5°C, 2. triethyl amine, THF, -10°C, (iii) 2,4-diamino-6-hydroxypyrimidine, THF/ethyl acetate/deionized water, 60°C, (iv) 1. NaOH, water, 2. H_3O^+, water, -5°C to room temperature, (v) 6M HCl, reflux.

$PreQ_1$ can also be prepared by reduction of the corresponding imine, as depicted in Scheme 3.8. The trityl protected aldehyde is tranformed into the imine by reaction with trityl amine. Subsequent reduction with sodium borohydride yielded the secondary amine. After deprotection, $preQ_1$

was obtained as its hydrochloride [268]. All reaction steps were performed with high yields of over 79%. However, the starting material 5-formyl-2-tritylaminopyrrolo[2,3-*d*]pyrimidin-4-one is not commercially available and needs to be prepared in a number of synthetic steps, leading to a long overall synthetic pathway.

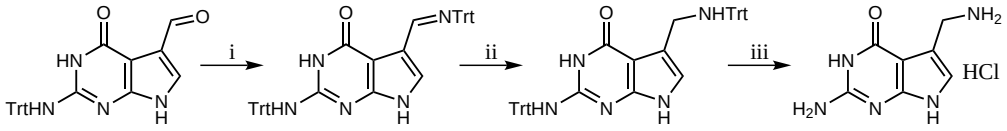

Scheme 3.8 Synthesis of $preQ_1$ by reduction of an imine. Trt = triphenylmethyl, (i) trityl amine, sodium sulphate, anhydrous THF, reflux, (ii) 2eq. $NaBH_4$, THF, 0°C to 25°C, (iii) 1.25M methanolic HCl, reflux.

Reduction of the cyano group in $preQ_0$ to the aminomethyl group in $preQ_1$ by hydrogenation under 3.5bar hydrogen pressure with palladium on charcoal was described by Klepper *et al.* The reaction afforded $preQ_1$, however, only as a crude reaction product, from which the isolation of $preQ_1$ was difficult. The crude reaction product was therefore reacted with di-*t*-butyl dicarbonate. The boc-protected $preQ_1$ was then purified by flash chromatography and subsequently deprotected with trifluoroacetic acid. The reaction yield of the protection and deprotection was only 10% [260].

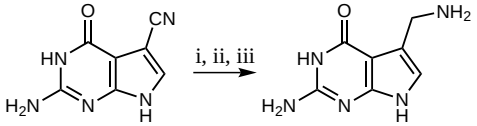

Scheme 3.9 Synthesis of $preQ_1$ by reduction of $preQ_0$. (i) H_2, Pd/C, DMF or (ii) nitrile reductase queF or (iii) H_2, Raney-Ni, triethyl amine, aqueous ammonia.

$PreQ_1$ was also isolated from an enzymatic reduction of $preQ_0$ with nitrile reductase queF from *E. coli*. The reaction was stopped after three hours and the protein was removed by ultrafiltration. $PreQ_1$ was purified by reverse phase HPLC [9].

Table 3.2 Comparison of the reaction conditions for the synthesis of $preQ_1$ applied in this thesis.

method	catalyst	reaction conditions	conversion
A	Pd/C	40bar H_2, DMF, 16h, 55°C	no product
B	Raney nickel	40bar H_2, DMF, 10eq. aqueous ammonia, 0.25eq. triethyl amine, 55°C, 24h	$preQ_1$, 60% conversion
C	Raney nickel	100bar H_2, DMF, 10eq. aqueous ammonia, 0.25eq. triethyl amine, 70°C, 54h	40% $preQ_1$, 15% 2-amino-5-methylpyrrolo[2,3-*d*]pyrimidin-4-one, 45% $preQ_0$

In this thesis, the cyano group in $preQ_0$ was reduced to the aminomethyl group in $preQ_1$ by hydrogenation in a steel autoclave with Raney-nickel as catalyst. Hydrogenation of a nitrile to the corresponding amine can lead to formation of secondary and tertiary amines, which can be

avoided by addition of ammonia. A minimum of 2.5 equivalents of ammonia is needed to avoid a competitive reaction between ammonia and imine and primary amine and imine [272]. Raney nickel is also known to catalyze the hydrogenation of an aromatic system. Hydrogenation of an aromatic ring can be delayed by the presence of triethylamine [251]. $PreQ_1$ was successfully prepared in a hydrogenation reaction in a steel autoclave with 40bar of hydrogen pressure at 55°C in the presence of ten equivalents aqueous ammonia and 0.25 equivalents of triethyl amine. Neither hydrogenation of the aromatic system, nor secondary or tertiary amines were observed as side product. When temperature and hydrogen pressure are increased to 70°C and 100bar, respectively, 2-amino-5-methylpyrrolo[2,3-*d*]pyrimidin-4-one (**4**) is observed as side product.

3.1.3 $preQ_0$ analogues

Various $preQ_0$ analogues were synthesized to investigate enzyme-substrate interactions in the active site of nitrile reductase queF. Two different synthetic routes for the preparation of $preQ_0$ analogues, depicted in Scheme 3.11 and Scheme 3.12, were developed in this thesis. In these pathways several $preQ_0$ analogues were prepared starting from either $preQ_0$ or a pyrrole precursor.

Syntheses starting from pyrimidine precursors

In this thesis, 2,4-diamino-5-cyanopyrrolo[2,3-*d*]pyrimidine was prepared analogously to $preQ_0$ using 2,4,6-trimethylpyrimidine as pyrimidine precursor, as depicted in Scheme 3.10. In literature, 2,4-diamino-5-cyanopyrrolo[2,3-*d*]pyrimidine was prepared from a pyrrole precursor. 2-Amino-5-bromo-3,4-dicyanopyrrole was prepared from tetracyanoethylene. The bromine was subsequently removed by hydrogenation. 2,4-diamino-5-cyanopyrrolo[2,3-*d*]pyrimidine was then prepared in a condensation reaction with formamidine hydrochloride [273, 274].

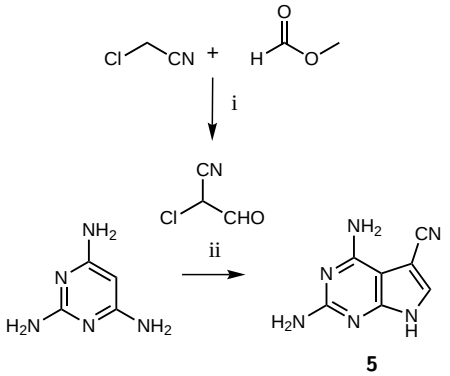

Scheme 3.10 Synthesis of 5-cyano-2,4-diaminopyrrolo[2,3-*d*]pyrimidine. (i) NaH, THF, 0°C, (ii) sodium acetate, water, reflux.

Four structural analogues of $preQ_0$, differing in their substituents on the pyrimidine ring, were prepared according to the pathway depicted in Scheme 3.11. Derivatisation of the 4-oxo functionality in pyrimidines is reported to be a versatile method of influencing the reactivity of pyrrolo[2,3-*d*]pyrimidines [275]. In this thesis, 2-amino-4-chloro-5-cyanopyrrolo[2,3-*d*]pyrimidine (**6**) was prepared in excellent yields of 96% by heating a suspension of $preQ_0$ in acetonitrile, triethylamine and phosphorous oxychloride to reflux. Similar procedures for the preparation of compound **6** are

found in literature, using phosphorous oxychloride and *N,N*-diisopropylamine, or phosphorous oxychloride and diethanolamine achieving yields between 27% and 60% [275–277].

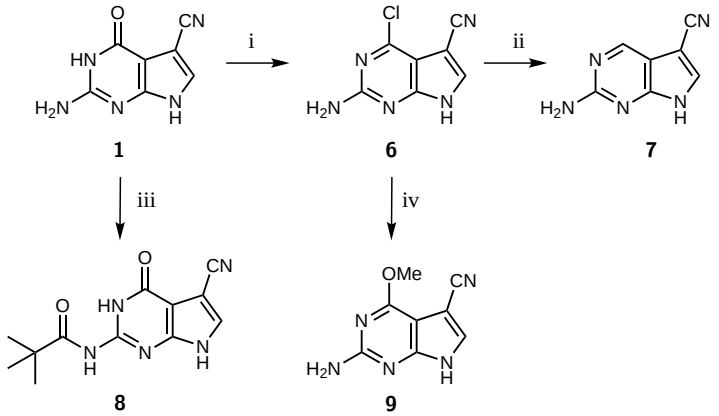

Scheme 3.11 Synthesis of preQ$_0$ analogues starting from preQ$_0$. (i) $POCl_3$, triethylamine, acetonitrile, reflux, (ii) Pd/C, 80bar H_2, $NaHCO_3$, ethanol, (iii) trimethylacetyl chloride, pyridine, triethylamine, 90°C, (iv) $NaOCH_3$, methanol, reflux.

2-Amino-5-cyanopyrrolo[2,3-*d*]pyrimidine (**7**) was first synthesized in this thesis. Compound **7** was achieved in good yields of 82% by dehalogenation of 2-amino-4-chloro-5-cyanopyrrolo[2,3-*d*]pyrimidine (**6**) by hydrogenation with a palladium on charcoal catalyst in ethanol and sodium bicarbonate, as depicted in Scheme 3.11. Various similar procedures for the dehalogenation of pyrrolo[2,3-*d*]pyrimidines are available in literature. The preparation of pyrrolo[2,3-*d*]pyrimidine from 4-chloropyrrolo[2,3-*d*]pyrimdine is described with palladium on charcoal in methanol or ethanol [278–280]. In similar procedures base, e.g., aqeuous ammonia, or sodium bicarbonate, is added to the reaction mixture [281, 282]. When sodium hydroxide is used as base, nucleophilic substitution of an ethoxy group, instead of removal of the halogen group, was observed [281]. Dehalogenation is also described by using palladium hydroxide as catalyst in combination with ammonium formate as hydrogen source [283].

5-Cyano-2-pivaloylaminopyrrolo[2,3-*d*]pyrimidin-4-one (**8**) was prepared according to a modified literature procedure [262]. In literature, the pyrrolo[2,3-*d*]pyrimidine is dissolved in pyridine and trimethylacetyl chloride is added to the reaction mixture [262, 266, 284–286]. This procedure is described to yield a mixture of N-2-monoacylated, and N-2-, N-7-bisacylated product. Addition of aqueous ammonia during work up selectively cleaves the N-7-pivaloyl protecting group [285, 286]. Yield of pivaloyl-proteced product (**8**) was improved by adding 2.5eq. triethylamine to the reaction mixture [287]. In this thesis, preparation of 5-cyano-2-pivaloylaminopyrrolo[2,3-*d*]pyrimidin-4-one (**8**) was achieved in 80% yield.

2-Amino-4-methoxy-5-cyanopyrrolo[2,3-*d*]pyrimidine (**9**) was prepared from preQ$_0$ (**1**) in one step, as depicted in Scheme 3.11. PreQ$_0$ was treated with sodium methoxide in methanol at reflux, as described in literature [288, 289]. Purification by recrystallization did not yield sufficiently pure material. Purification by column chromatography was impeded by the limited solubility of compound **9**. The product could not be quantitatively isolated from the column. The isolated yield obtained after purification was therefore low.

Synthesis starting from a pyrrole precursor

A number of preQ$_0$ analogues were prepared starting from a pyrrole precursor, as depicted in Scheme 3.12. The pyrrole precursor, 2-amino-5-bromo-3,4-dicyanopyrrole (**10**), is formed by the reaction of tetracyanoethylene with hydrogen bromide. The reaction was first described by saturating a cooled solution of tetracyanoethylene in acetone with anhydrous hydrogen bromide gas [290]. Higher yields are achieved when tetracyanoethylene is dissolved in acetone and ethyl acetate and hydrogen bromide in acetic acid is added to the solution [291]. In this reaction step, tetracyanoethylene is first reduced to tetracyanoethane by hydrogen bromide. Subsequently, additional hydrogen bromide adds to the tetracyanoethane to form the pyrrole. The bromine formed in the reduction step is consumed by acetone. No pyrrole product was observed when tetrahydrofuran or methyl formate were used instead of acetone as solvent. Therefore, the bromine has to be removed from the reaction mixture to prevent reoxidation of tetracyanoethane to tetracyanoethylene. This reaction mechanism was proven by successfully preparing 2-amino-5-bromo-3,4-dicyanopyrrole (**10**) in the reaction of tetracyanoethane with hydrogen bromide [290]. 2-Amino-5-bromo-3,4-dicyanopyrrole (**10**) is soluble in dilute aqueous sodium hydroxide and can be reprecipitated upon acidification. This purification step removes hydrogen bromide and water soluble impurities [290, 291]. In this thesis, 2-amino-5-bromo-3,4-dicyanopyrrole (**10**) was synthesized in excellent yield and purity.

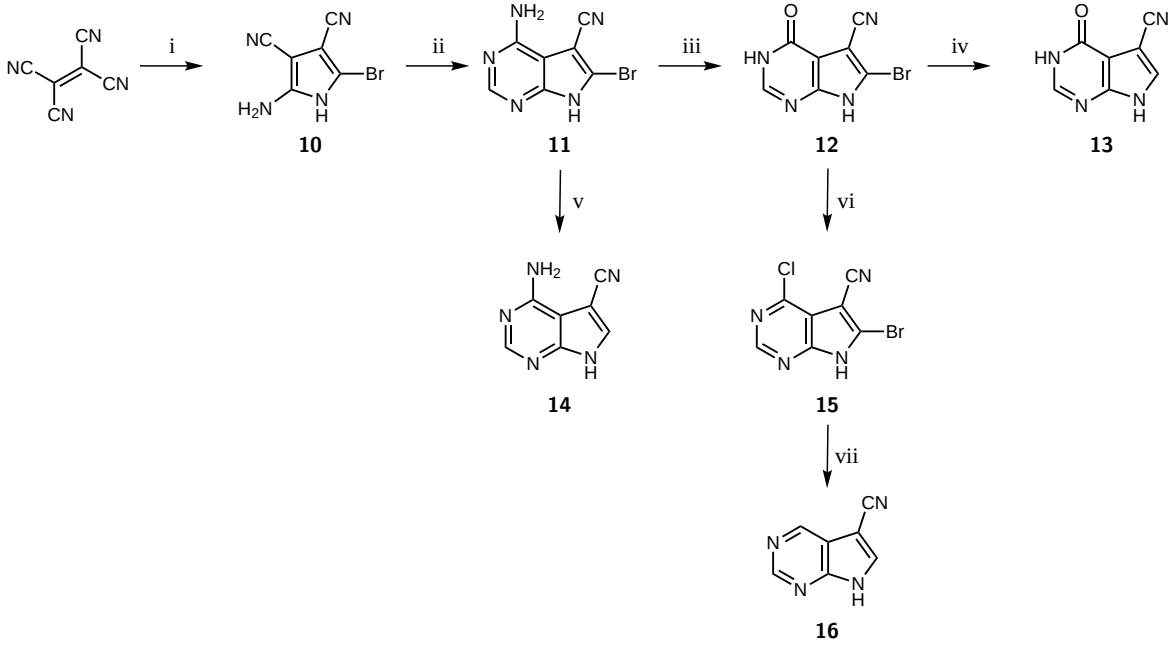

Scheme 3.12 Synthesis of preQ$_0$ analogues starting from a pyrrole precursor. (i) HBr in acetic acid, acetone, ethyl acetate, 0°C, (ii) formamidine acetate salt, ethoxyethanol, reflux, (iii) $NaNO_2$, acetic acid, deionized water, reflux, (iv) and (v) Pd/C, H_2, aqueous ammonia solution, ethanol, room temperature, (vi) $POCl_3$, acetonitrile, triethylamine, (vii) Pd/C, 100bar H_2, ethanol, $NaHCO_3$, 70°C.

4-Amino-6-bromo-5-cyanopyrrolo[2,3-*d*]pyrimidine (**11**) was prepared in the next synthetic step in a condensation reaction of 2-amino-5-bromo-3,4-dicyanopyrrole (**10**) with a suitable reagent (Scheme 3.12). This reaction was first described by Tolman *et al.* in 1969 and produced 4-amino-6-bromo-5-cyanopyrrolo[2,3-*d*]pyrimidine (**11**) in 51% yield [292]. In later publications the same

reaction is described with up to 65% yield [293–295]. An alternative method for ring annulation is available in literature. 2-Amino-5-bromo-3,4-dicyanopyrrole (**10**) reacts with triethylorthoformate to form 2-bromo-5-(ethoxymethylene)iminopyrrole-3,4-dicarbonitrile. This intermediate is then dissolved in saturated ethanolic ammonia solution and heated in a sealed steel reaction vessel to give 4-amino-6-bromo-5-cyanopyrrolo[2,3-*d*]pyrimidine (**11**) in 71% yield [296, 297]. In this thesis, 4-amino-6-bromo-5-cyanopyrrolo[2,3-*d*]pyrimidine (**11**) was prepared by condensation with formamidine acetate in moderate yield.

6-Bromo-5-cyanopyrrolo[2,3-*d*]pyrimidin-4-one (**12**) was achieved by diazotizing 4-amino-6-bromo-5-cyanopyrrolo[2,3-*d*]pyrimidine (**11**) with sodium nitrite in aqueous acetic acid, as depicted in Scheme 3.12. This reaction was described for the preparation of 5-cyanopyrrolo[2,3-*d*]pyrimidin-4-one by Uematsu *et al.* [298]. Deamination is proposed to proceeed faster and with less decomposition of 4-amino-6-bromo-5-cyanopyrrolo[2,3-*d*]pyrimidine (**11**) when 4-amino-6-bromo-5-cyanopyrrolo[2,3-*d*]pyrimidine (**11**) was reprecipitated *in situ*, by addition of acetic acid to a basic solution of the starting material, before the deamination procedure [292]. Employing an *in situ* reprecipitation procedure 77% yield was achieved in literature, while 95% yield was achieved by direct deamination [292, 299]. In this thesis, 6-bromo-5-cyanopyrrolo[2,3-*d*]pyrimidin-4-one (**12**) was prepared in 80% yield, applying the procedure without *in situ* reprecipitation of the starting material.

Chlorination of 6-bromo-5-cyanopyrrolo[2,3-*d*]pyrimidin-4-one (**12**) was achieved with phosphorus oxychloride, as depicted in Scheme 3.12. The starting material was suspended in acetonitrile and triethylamine, followed by heating to reflux and addition of phosphorus oxychloride. 6-bromo-4-chloro-5-cyanopyrrolo[2,3-*d*]pyrimidine (**15**) was prepared in good yields and purities. In literature the reaction is also described in neat phosphorus oxychloride at reflux [292, 299].

Dehalogenation of compounds **11**, **12**, and **15** was achieved by catalytic hydrogenation, as depicted in Scheme 3.12. Dehalogenation of 6-bromo-5-cyanopyrrolo[2,3-*d*]pyrimidin-4-one (**12**) is described in ethanol/aqueous ammonia solution 1/1 using palladium on charcoal as catalyst and 2.8bar hydrogen pressure [292]. These conditions were successfully applied for the dehalogenation of 4-amino-6-bromo-5-cyanopyrrolo[2,3-*d*]pyrimidine (**11**) and 6-bromo-5-cyanopyrrolo[2,3-*d*]pyrimidin-4-one (**12**). Simultaneous dehalogenation of the bromo- and chloro-functionality of 6-bromo-4-chloro-5-cyanopyrrolo[2,3-*d*]pyrimidine (**15**) was accomplished with 100bar hydrogen pressure and a palladium on charcoal catalyst with sodium bicarbonate in ethanol. These conditions are described for the dehalogenation of 2-amino-4-chloro-5-cyanopyrrolo[2,3-*d*]pyrimidine [281]. 5-Cyanopyrrolo[2,3-*d*]pyrimidine (**16**) was first prepared in this thesis.

An alternative route for the preparation of 4-amino-5-cyanopyrrolo[2,3-*d*]pyrimidine (**14**) is described in literature [300, 301]. In this synthesis, tetracyanoethylene is reacted with hydrogen sulfide to give 2,5-diamino-3,4-dicyanothiophene [290]. 2,5-Diamino-3,4-dicyanothiophene is rearranged to 2-mercapto-3,4-dicyano-5-aminopyrrole in a base-catalyzed reaction. 2-Mercapto-3,4-dicyano-5-aminopyrrole reacts with trimethyl orthoformate and subsequently ammonia. The expected reaction product was 4-amino-5-cyano-6-mercaptopyrrolo[2,3-*d*]pyrimidine, however, NMR spectroscopy indicated a free mercapto-group was not present. The product was identified as 4-amino-5-cyano-6-methylmercaptopyrrolo[2,3-*d*]pyrimidine which can easily be desulphurized by Raney-Nickel to give 4-amino-5-cyanopyrrolo[2,3-*d*]pyrimidine (**14**) [300, 301].

3.2 Pyrrolo[3,2-*c*]pyridines and pyrrolo[2,3-*b*]pyridines

Pyrrolo[3,2-*c*]pyridines and pyrrolo[2,3-*b*]pyridines, 5- and 7-azaindoles, respectively, are structural analogues of pyrrolo[2,3-*d*]pyrimidines, differing only in the absence of one ring nitrogen in the six-membered ring. The most common synthetic routes to azaindoles are Fischer, Madelung and Reissert synthesis. However, these syntheses are originally indole syntheses and often cannot be effectively applied to the synthesis of the corresponding azaindoles [153, 302].

Pyrrolo[3,2-*c*]pyridines

4-Hydroxypyrrolo[3,2-*c*]pyridine was prepared starting from pyrrole-2-carboxaldehyde in several literature procedures, as depicted in Scheme 3.13 [302–304]. *N*-Benzylpyrrole-2-carbaldehyde is condensed with malonic acid to give the acrylic acid derivative **17**. The acid is then transformed into an acyl azide. Subsequent Curtius arrangement gives 1-benzyl-4-hydroxy[3,2-*c*]pyridine [302–304]. Introduction of an aldehyde functionality in position 3, which can be further converted into the corresponding oxime, and dehydrated to the nitrile, and final deprotection gives the desired 3-cyano-4-hydroxypyrrolo[3,2-*c*]pyridine.

This synthesis, depicted in Scheme 3.13, was carried out by Cornelia Hojnik in her master thesis [305]. A protection group was introduced on the pyrrole nitrogen of pyrrole-2-carbaldehyde. A benzyl-protecting group and a phenylsulfonyl-protecting group were used. The phenylsulfonyl-protecting group has the advantage of milder reaction conditions for the deprotection than those required for benzyl-deprotection. Deprotection of the phenylsulfonyl-protecting group is achieved in aqueous sodium hydroxide solution, whereas benzyl-deprotection, is described with sodium in aqueous ammonia [302–304, 306]. The next step to the acrylic acid derivatives (**17**) was successfully carried out in good yield of 60%. However, the formation of the acyl azide and especially subsequent Curtius rearrangement proved to be tedious. Consequently, the synthetic pathway was not further pursued.

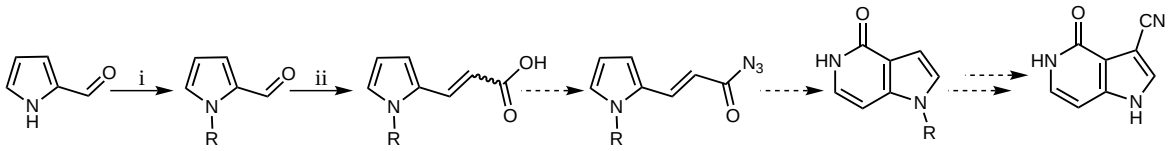

Scheme 3.13 Synthesis of 3-cyano-4-hydroxypyrrolo[3,2-*c*]pyridine starting from a pyrrole precursor. Full line arrows indicate completed synthetic steps, dashed line arrows indicate synthetic steps in progress, (i) NaH, benzylbromide, acetonitrile or NaOH, DCM, benzenesulfonyl chloride, reflux, (ii) malonic acid, aniline, ethanol, reflux or malonic acid, pyridine, piperidine, reflux.

A new synthetic pathway for the synthesis of 3-cyano-4-hydroxypyrrolo[3,2-*c*]pyridine starting from a substituted pyridine precursor was developed. This pathway, depicted in Scheme 3.14, yields the pyrrolo[3,2-*c*]pyridine ring system in only one step, whereas four steps are necessary when starting from a pyrrole precursor as in Scheme 3.13. The condensation of 2,4-diamino-6-hydroxypyridine with chloroacetaldehyde was previously described to yield only polymeric products [307]. The condensation reaction of 4-amino-2-hydroxypyridine with chloroacetaldehyde was carried out analogously to the synthesis of $preQ_0$. 4-Hydroxypyrrolo[3,2-*c*]pyridine was formed

in the reaction. However, only 10.5% of product could be isolated after column chromatography [305].

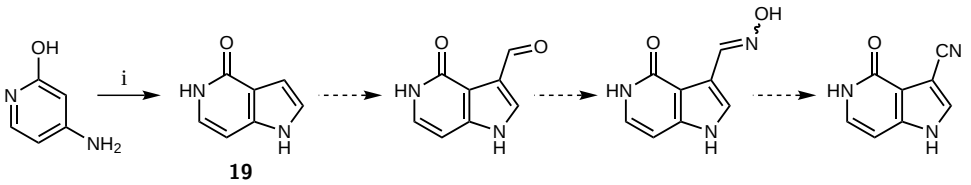

Scheme 3.14 Synthesis of 3-cyano-4-hydroxypyrrolo[3,2-*c*]pyridine starting from a pyridine precursor. Full line arrows indicate completed synthetic steps, dashed line arrows indicate synthetic steps in progress, (i) chloroacetaldehyde, sodium acetate, water 80°C.

Pyrrolo[2,3-*b*]pyridines

A straight forward synthesis of 7-azaindoles, starting from inexpensive succinonitrile, was described in literature (Scheme 3.15) [161, 308]. In the first synthetic step, succinonitrile and ethylformate are condensed in the presence of sodium methoxide or potassium *t*-butoxide to give the corresponding salt of 2-hydroxymethylenebutyronitrile. This salt is then treated with an appropriate amine to yield an aminomethylenesuccinonitrile. The pK_a-value of the amine used (pK_a range 1.02-10.64) was not found to have an effect on the yield [308]. The base catalyzed internal condensation to the *N*-protected 2-amino-4-cyanopyrrole was carried out using potassium ethoxide or potassium hydroxide as base [161, 308]. The 7-azaindole ring system was then built up by reaction of the *N*-protected 2-amino-4-cyanopyrrole with 1,1,3,3-tetramethoxypropane in the presence of a catalytic amount of acid, either hydrochloric acid or *p*-toluenesulfonic acid yielding *N*-protected 3-cyanopyrrolo[2,3-*b*]pyrimidine [161].

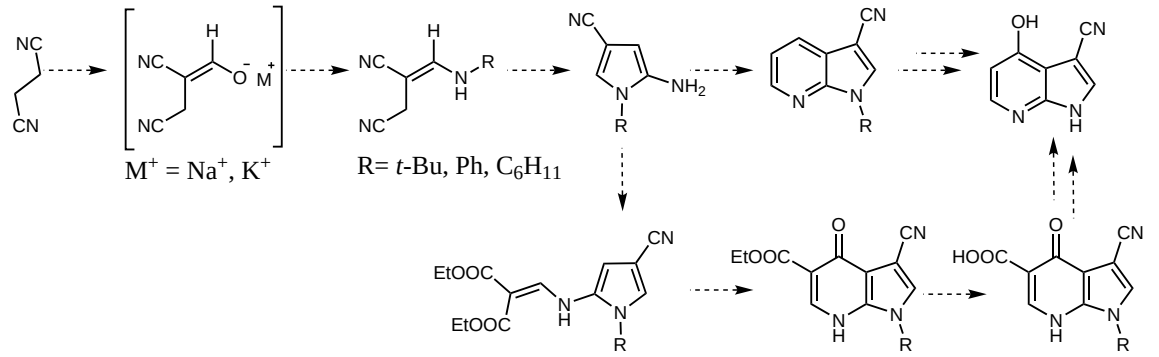

Scheme 3.15 Synthesis of 3-cyano-4-hydroxypyrrolo[2,3-*b*]pyridine starting from a pyrrole precursor. Dotted line arrows indicate synthetic steps in progress.

Formation of the 7-azaindole ring system by preparation of 2-bisethoxycarbonylvinylamino-pyrroles and subsequent cyclization, as depicted in Scheme 3.15. The *N*-protected 2-amino-4-cyanopyrrole is reacted with ethoxymethylenemalonates and the cyclization of the resulting 2-bisethoxycarbonylvinylaminopyrroles occurs by heating in diphenyl ether to give ethyl 3-cyano-4-oxopyrrolo[2,3-*b*]pyrimidin-5-carboxylate [308]. Ester hydrolysis and subsequent decarboxylation yields the *N*-protected 3-cyano-4-hydroxypyrrolo[2,3-*b*]pyridine. After deprotection, the desired 3-cyano-4-hydroxypyrrolo[2,3-*b*]pyridine is achieved [309]. In Cornelia Hojnik's master thesis 2-((benzylamino)methylene)succinonitrile was prepared, however in rather low yield and purity.

This synthetic pathway over seven steps was then abandoned in favour of a shorter synthesis starting from a substituted pyridine [305].

Preparation of 4-hydroxypyrrolo[2,3-*b*]pyridine starting form a pyridine precursor is not described in literature. The condensation reaction of 2-amino-4-hydroxypyridine with chloroacetaldehyde gave 1-(2-chloroethenyl)-4-hydroxypyrrolo[2,3-*b*]pyridine instead of the desired 4-hydroxypyrrolo[2,3-*b*]pyridine, as depicted in Scheme 3.16. This product was formed in the reaction of a second equivalent of chloroacetaldehyde with the amino-group of 2-amino-4-hydroxypyridine.

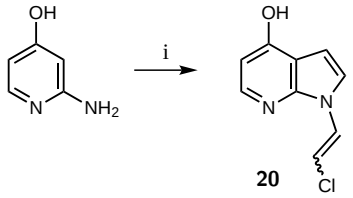

Scheme 3.16 Synthesis of 1-(2-chloroethenyl)-4-hydroxypyrrolo[2,3-*b*]pyridine. (i) chloroacetaldehyde, sodium acetate, water, reflux.

A number of pyridine precursors were prepared for the condensation with chloroacetaldehyde, as depcited in Scheme 3.17. The chloro-group of 2-amino-4-chloropyridine was substituted with a methoxy group and an azide group, respectively [310, 311]. The azide was then reduced to the corresponding amine.

The differently substituted pyridine precursors **21**, **22**, and **23** where then used for condensation reactions with chloroacetaldehyde. The condensation reaction of 2-hydroxy-4-methoxypyridine (**21**) gave a mixture of undesired products. The condensation reaction of 2,4-diaminopyridine (**23**) gave the desired product 4-aminopyrrolo[2,3-*b*]pyrimidine (m/z = 134) and a byproduct with m/z = 212. The mass of the byproduct corresponds to the condensation of a second molecule of chloroacetaldehyde to 4-aminopyrrolo[2,3-*b*]pyrimidine. Both, the desired product 4-aminopyrrolo[2,3-*b*]pyrimidine and the byproduct were formed in approximately 15% conversion after one hour reaction time. With increasing reaction time, only the amount of byproduct increased to up to 50% after four hours, while the amount of 4-aminopyrrolo[2,3-*b*]pyrimidine remained constant and did not exceed 15% to 20%.

In the condensation reaction of 2-amino-4-azidopyridine (**22**) with chloroacetaldehyde, 1,2-bis(4-azidopyrrolo[2,3-*b*]pyridin-1-yl)ethene (**24**) was formed as sole product and could be isolated in 54% yield (Scheme 3.17). The preparation of this bridged pyrrolo[2,3-*b*]pyridine system has so far not been reported in literature. The bridged pyrrolo[2,3-*b*]pyridine acts as protection group of the pyrrole nitrogen, and therefore provides several advantages over the unprotected pyrrolo[2,3-*b*]pyridine, including better solubility.

A variety of reactions for the direct introduction of a nitrile group to an indole ring are found in literature, such as Sandmeyer and Rosenmund von Braun reactions, as well as metal-catalyzed cyanation reactions by coupling aryl halides with cyanating reagents or oxidative cyanation through C-H bond activation using metal cyanides like $Zn(CN)_2$ or CuCN [312]. Directly introducing the nitrile group to 1,2-bis(4-azidopyrrolo[2,3-*b*]pyridin-1-yl)ethene (**24**) with chlorosulfonylisocyanate or CuCN, as described for indole, was not successful [313, 314]. Bromination and chlorination of 1,2-bis(4-azidopyrrolo[2,3-b]pyridin-1-yl)ethene (**24**) with *N*-bromosuccinimide or *N*-chlorosuccinimide, respectively, were carried out in good yields (Scheme 3.17). Reduction of the

azide group of compound **24** was achieved with palladium on charcoal in a steel autoclave with moderate hydrogen pressure of 25 bar, analogously to a literature procedure for the reduction of 4-azidopyrrolo[2,3-*b*]pyridine [315].

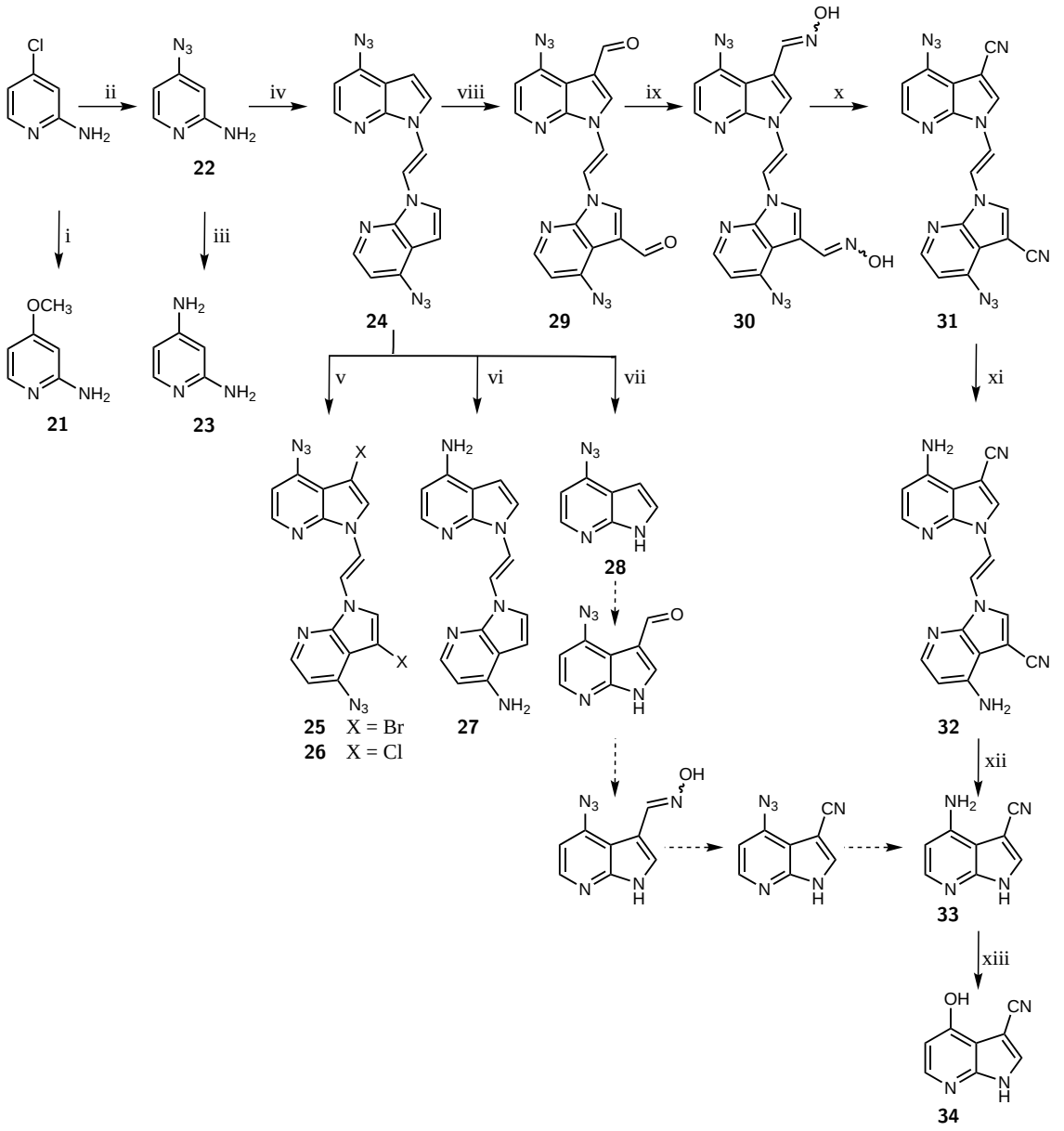

Scheme 3.17 Synthesis of 3-cyano-4-hydroxypyrrolo[2,3-*b*]pyridine starting from a pyridine precursor. Full line arrows indicate completed synthetic steps, dashed line arrows indicate synthetic steps in progress, (i) sodium methoxide, methanol, reflux, (ii) sodium azide, DMF, ammonium formate, 120°C, (iii) Pt/C 10%m/m, acetic acid, hydrogen, (iv) chloroacetaldehyde, sodium acetate trihydrate, water, reflux, (v) NBS or NCS in THF, (vi) Pd/C 10%m/m, ethanol, 25bar hydrogen, (vii) and (xii) $NaIO_4$, $NaClO_2$, OsO_4, acetonitrile/water 1/1 , (viii) $POCl_3$, DMF, (ix) hydroxylamine hydrochloride, ethanol, aqeuous NaOH, (x) 1. acetic anhydride, 2. acetic acid, reflux, (xi) Pt/C, acetic acid, hydrogen or Pd/C, THF, hydrogen, (xiii) $NaNO_2$, acetic acid/water 1/1, 100°C.

Cleavage of the ethylene bridge of 1,2-bis(4-azidopyrrolo[2,3-*b*]pyridin-1-yl)ethene (**24**) was achieved by dihydroxylation and subsequent periodate cleavage, as depicted in Scheme 3.17. The reaction with osmium tetraoxide, *N*-methylmorpholine *N*-oxide (NMO) and sodium periodate in *t*-butanol/water/acetone (1/5/2) showed product formation on TLC and HPLC-MS, however the

product was not successfully isolated [316]. A number of alternative conditions for the reaction and work-up are described in literature. Dioxane/water (3/1 to 10/1) is commonly used as reaction solvent [317, 318]. *N*-Methylmorpholine in combination with *meta*-chloroperoxybenzoic acid can be used instead of NMO for the reoxidation of osmiumtetraoxide, however epoxidation occurs as competing reaction [319]. Recently, sodium chlorite ($NaClO_2$) was described as oxidative reagent in a periodate cleavage. For work-up, isopropanol and potassium hydroxide was used, as isopropanol is easily oxidized to acetone by osmium tetroxide in the presence of potassium hydroxide. This reducing system was applied as recycling system in literature [320]. Cleavage of the ethylene bridge of compound **24** was successful using osmium tetroxide, sodium periodate, sodium chlorite in water/acetonitrile 1/1 and for work-up the isopropanol and potassium hydroxide system. Dihydroxylation and periodate cleavage leads to a formyl group, in case of 1,2-bis(4-azidopyrrolo[2,3-*b*]pyridin-1-yl)ethene (**24**) as starting material to a formyl-group on the pyrrole nitrogen. The basic conditions of the isopropanol and potassium hydroxide work up quantitatively cleaved the formyl group, leading to 4-azidopyrrolo[2,3-*b*]pyridine (**28**) as product, as depicted in Scheme 3.17.

Introduction of a nitrile group to 1,2-bis(4-azidopyrrolo[2,3-*b*]pyridin-1-yl)ethene (**24**) was not successful, therefore an aldehyde group was introduced which in turn can be converted to the oxime and further dehydrated to the nitrile, as depicted in Scheme 3.17. For the formylation of azaindoles Duff reaction is frequently used in literature [321–325]. Duff reaction was first described in 1932 for the preparation of 3- and 5-formylsalicylic acids [326]. In the original procedure salicylic acid and hexamethylenetetramine in deionized water are boiled under reflux and subsequently acidified with 4N HCl [326]. This procedure was then improved by heating the starting material and hexamethylenetetramine in acetic acid solution or boric acid in glycerol and subsequent hydrolysis with hydrochloric acid [327–330]. The reaction proceeds in a series of equilibrium reactions, with iminium ion intermediates. First secondary amines are formed with hexamethylenetetramine. Dehydrogenation of these amines by heating in hexamethylenetetramine in acetic acid produces Schiff bases which can be hydrolyzed to aldehydes. The hydrolysis of secondary amines from hexamethylenetetramine is similar to the Sommelet reaction, which allows the preparation of aldehydes from alkyl- or arylalkyl halides [331, 332]. 4-Azido-3-formylpyrrolo[2,3-*b*]pyridine was successfully prepared in a Duff reaction, however the yield was rather low and several side products were formed. Vilsmeier reaction was investigated as alternative formylation reaction. Higher yield and product purity was achieved in the Vilsmeier reaction, however still a number of side products were observed [333]. The Vilsmeier reaction starting from 1,2-bis(4-azidopyrrolo[2,3-*b*]pyridin-1-yl)ethene (**24**) gave the formylated product **29** in good yield of 54% and high purity. The subsequent step to the oxime **30** 1,2-bis(4-azido-3-(hydroxyiminomethyl)pyrrolo[2,3-*b*]pyridin-1-yl)ethene proceeded in excellent yield of 82% and gave the *(E)-/(Z)*-isomers in a ratio of 1/0.63.

Dehydratisation of 1,2-bis(4-azido-3-(hydroxyiminomethyl)pyrrolo[2,3-*b*]pyridin-1-yl)ethene to the corresponding nitrile **31** was carried out with acetic anhydride, as depicted in Scheme 3.17. The *(Z)*-oxime was quantitatively converted to the nitrile, however the *(E)*-isomer was *O*-acetylated under the reaction conditions. The *O*-acetylated *(E)*-oxime was then converted into the nitrile by reflux in acetic acid. In literature, dehydratisation of 4-chloro-7-azaindole-3-carbaldehyde oxime to the corresponding nitrile is described with thionyl chloride [219]. Thionyl chloride is

also used for the dehdyratisation of 4-chloropyrrolo[2,3-*d*]pyrimidin-5-carbaldehyde oxime [334]. Dehydratisation with thionylchloride might therefore increase the yield of this synthetic step, by avoiding the acetylation of the *(E)*-isomer in the dehydratisation.

Reduction of the azide group of 1,2-bis(4-azido-3-cyanopyrrolo[2,3-*b*]pyridin-1-yl)ethene (**31**) to the corresponding amino-group was carried out with platinum or palladium on charcoal and hydrogen, as depicted in Scheme 3.17. Cleavage of the ethylene bridge was achieved as demonastrated on 1,2-bis(4-azidopyrrolo[2,3-*b*]pyridin-1-yl)ethene (**24**). In the final synthetic step the 4-amino-substituent of 4-amino-3-cyanopyrrolo[2,3-*b*]pyridine (**33**) was converted to a hydroxy group in a diazotisation reaction in excellent yield of 87%, similarly to the diazotisation reaction used for the preparation of 5-cyanopyrrolo[2,3-*d*]pyrimidin-4-one (**13**). The desired product was obtained in nine steps in good to excellent yields.

3.3 Thieno[2,3-*d*]pyrimidines

Thieno[2,3-*d*]pyrimidines are structural analogues of pyrrolo[2,3-*d*]pyrimidines, differing only in the heteroatom in the five-membered ring. By replacing the NH of the pyrrole ring of the natural substrate $preQ_0$ with a sulphur in the thiophene ring, the influence of NH as hydrogen bond donor compared to S as a hydrogen bond acceptor can be investigated. 2-Amino-5-cyanothieno[2,3-*d*]pyrimidin-4-one and 5-cyanothieno[2,3-*d*]pyrimidin-4-one are therefore suitable compounds to evaluate the influence of the pyrrole-nitrogen on substrate binding in nitrile reductase queF (active site models of nitrile reductase queF are depicted in chapter 5 in Figure 5.3 and Figure 5.7).

Synthesis starting from a pyrimidine precursor

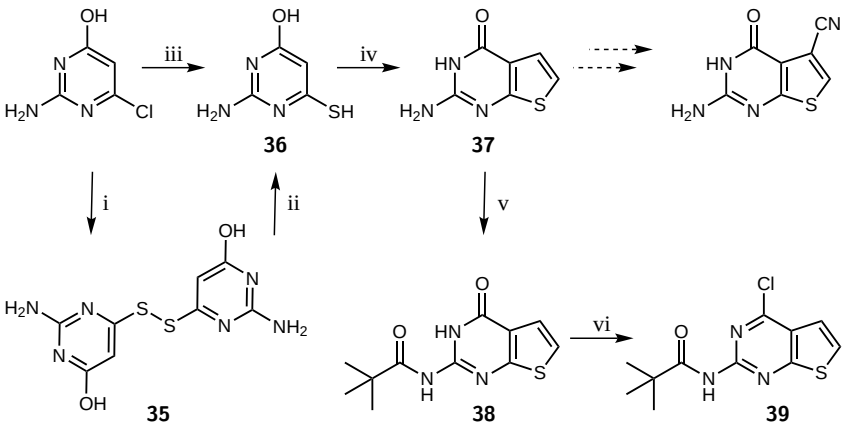

Scheme 3.18 Synthesis of 2-amino-4-hydroxythieno[2,3-*d*]pyrimidines. Full line arrows indicate completed synthetic steps, dashed line arrows indicate synthetic steps in progress, (i) sodium hydrosulfide, ethylene glycol, reflux, (ii) 1. $NaBH_4$, DMF, 2. aqueous HCl, (iii) sodium hydrosulfide, ethylene glycol, reflux, inert atmosphere, (iv) sodium acetate, water, chloroacetaldehye, reflux, or potassium carbonate, DMF, chloroacetaldehyde, 90°C, (v) pivaloylchloride, triethylamine, pyridine, DMF, 85°C, (vi) $POCl_3$, DMF, 55°C.

In this thesis, a synthetic pathway starting from a pyrimidine-precursor was developed, as depicted in Scheme 3.18. In the first synthetic step, 2-amino-6-hydroxy-4-mercaptopyrimidine (**36**) was prepared from 2-amino-4-chloro-6-hydroxypyrimidine, according to a literature procedure [335–338].

2-Amino-6-hydroxy-4-mercaptopyrimidine (**36**) dimerized, forming a disulfide bond. Dimerization could be avoided by carrying out the substitution reaction under inert conditions, and proceeding with the next synthetic step without isolation of the product. Alternatively, the disulfide bond was cleaved with sodium borohydride. The thiophene ring was then formed by condensation of 2-amino-6-hydroxy-4-mercaptopyrimidine (**36**) with chloroacetaldehyde. The condensation of a suitable pyrimidine precursor with chloroacetaldehyde is commonly found in literature for the formation of pyrrolo[2,3-*d*]pyrimidines [339, 340]. For thieno[2,3-*d*]pyrimidines, condensation of haloketones, such as chloroacetone or 3-bromo-2-butanone, to pyrimidine-precursors is described in literature [180, 181, 341, 342]. In a recent patent, ethyl 4-chloro-5-hydroxy-2-methylthieno[2,3-*d*]pyrimidine-6-carboxylate was prepared in one step from ethyl 4,6-dichloro-2-methylpyrimidine-5-carboxylate and thioglycolate [343]. Pivaloyl-protection of the amino-group in position 2 of 2-amino-4-hydroxythieno[2,3-*d*]pyrimidine (**37**) was achieved with pivaloylchloride in moderate yields. In patent literature, pivaloyl protection of this compound is described with trimethylacetic anhydride in 61% yield [191]. Vilsmeier conditions yielded a chloro-substitution in position 4 instead of the desired formylation. Intentional chlorination was also achieved using phosphorous oxychloride [191]. All steps in this synthetic pathway were completed in moderate yields of 20% to 35% yield. The formation of disulfide bonds in the pyrimidine starting material certainly decreased yield.

Syntheses starting from a thiophene precursor

Thieno[2,3-*d*]pyrimidines are commonly prepared starting from 2-aminothiophene-precursors. A number of synthetic methods for the preparation of 2-aminothiophenes are known, including the condensation of ethyl chloroacetoacetate with isothiocyanates in the presence of sodium hydride, cyclization of thioamides and their *S*-alkylates, or Hofmann or Schmidt reaction [344]. These reactions, however, involve difficult preparation of the starting materials and multi-step synthesis [344]. 2-Aminothiophenes can be conveniently prepared in one step, using the Gewald reaction [345]. The Gewald reaction was originally reported using α-mercaptoketones or α-mercaptoaldehydes, and α-methylene activated nitriles bearing an electron withdrawing group in DMF or alcohol as solvent with catalytic amounts of piperidine or triethylamine yielding 2-amino-3,4,5-tetrasubstituted thiophenes [345]. Similar 2-amino-3,4,5-tetrasubstituted thiophenes were prepared from 4-halocrotononitrile and sodium hydrosulfide [345]. A convenient one-pot Gewald reaction is described in literature. This procedure uses aldehydes, ketones, or 1,3-dicarbonyl compounds with activated nitriles, such as malonitrile, cyanoacetic aesters, cyanoacetamide, or its *N*-substituted derivatives, heteroarylacetonitriles, α-cyanoketones and sulphur, in the presence of amine at room temperature [344]. This method replaces the use of α-mercaptoketones or α-mercaptoaldehydes by simpler, more stable starting materials and improves yields [344]. The scope and limitations of Gewald reaction has been thoroughly investigated. The Gewald reaction involves only one step, and proceeds in high yields and short reaction times. The Gewald reaction is, however, limited to activated nitriles and proceeds more readily with cyclic ketones than with linear aldehydes or ketones [344]. Ethyl 2-amino-4,5,6,7-tetrahydrobenzo[2,3-*d*]thiophene-3-carboxylate was prepared in a Gewald synthesis starting from cyclohexanone in excellent yields [175].

2-Aminothieno[2,3-*d*]pyrimidin-4-one was prepared starting from methyl 2-aminothiophene-3-

carboxylate and chloroformamidine, as depicted in Scheme 3.19. Chloroformamidine was prepared *in situ* from cyanamide [174, 191, 346, 347]. 2,4-Diaminothieno[2,3-*d*]pyrimidine was prepared analogously [185]. In this thesis, this synthetic pathway was not successful. A major limitation of this reaction is the preparation of chloroformamidine from cyanamide, as it requires gaseous hydrochloric acid, or organic solvents saturated with hydrochloric acid, and cyanamide itself is prone to hydrolysis to dicyandiamide and melamin.

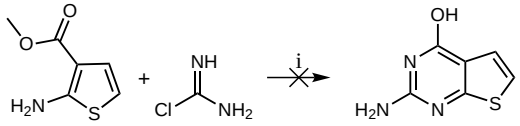

Scheme 3.19 Synthesis of 2-aminothieno[2,3-*d*]pyrimidin-4-one. (i) DMSO, 160°.

4-Hydroxythieno[2,3-*d*]pyrimidine (**40**) was prepared in literature from methyl 2-aminothiophene-3-carboxylate and formamide, as depicted in Scheme 3.20 [174, 188]. Both, 2-aminothiophene-3-carboxylate and formamide, are commercially available. In this thesis, the reaction proceeded in good yields. Vilsmeier formylation yielded not the desired 3-formyl-4-hydroxythieno[2,3-*d*]pyrimidine, but 4-chlorothieno[2,3-*d*]pyrimidine (**41**) in good yield of 70%. Substitution of the chloro-substituent by a methoxy-group and subsequent Vilsmeier reaction again only yielded 4-chlorothieno[2,3-*d*]pyrimidine. Formylation by Duff reaction was not successful.

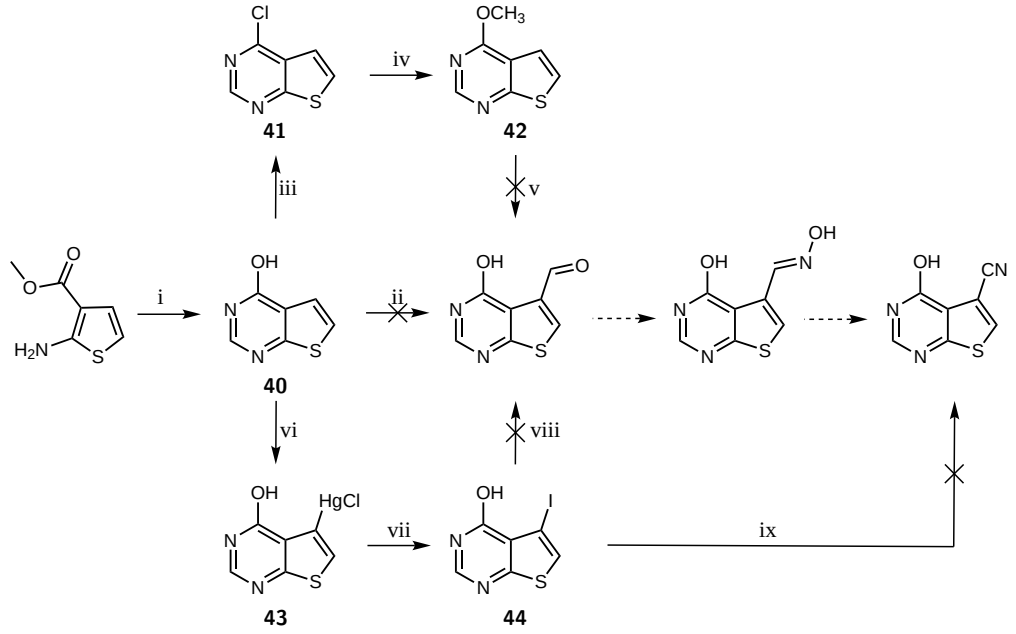

Scheme 3.20 Synthesis of 4-hydroxythieno[2,3-*d*]pyrimidines. Full line arrows indicate completed synthetic steps, dashed line arrows indicate synthetic steps in progress, (i) formamide, ammonium formate, 150°, (ii), (iii) and (v) $POCl_3$, DMF, 100°C, (iv) sodium methoxide, methanol, reflux, (vi) mercury(II)acetate, acetic acid, 100°C, (vii) iodine, chloroform, 50°C, (viii) 1. $Pd(dba)_2$ or $Pd_2(dba)_3$, triphenylphosphine, CO, toluene, 2. 50°C, tributyltin hydride, (ix) 1. CH_3MgCl in THF, -65°C, 2. *i*-PrMgCl·LiCl in THF, toluene, -65°C, 3. tosylcyanide, -65°C to room temperature.

4-Hydroxy-5-iodothieno[2,3-*d*]pyrimidine was prepared as a starting material for palladium catalyzed formylation or cyanation. Direct iodination of 4-hydroxythieno[2,3-*d*]pyrimidine with *N*-iodosuccinimide in THF was not successful, probably due to the limited solubility of the starting

material in THF. Direct bromination of 2-amino-4-hydroxy-6-methylthieno[2,3-*d*]pyrimidine with *N*-bromosuccinimide or bromine was not possible using a variety of reaction conditions [183]. Direct bromination of 2-amino-4-hydroxy-6-methylthieno[2,3-*d*]pyrimidine was reported using bromine in acetic acid under microwave irradiation [184]. Iodination by chloromercuration and subsequent substitution with iodine was reported for 2-pivaloylaminopyrrolo[2,3-*d*]pyrimidine [348]. This procedure was successfully applied for the preparation of 2-amino-6-ethyl-4-hydroxy-5-iodothieno[2,3-*d*]pyrimidine [183]. In this thesis, iodination of 4-hydroxythieno[2,3-*d*]pyrimidine was successful using this two-step procedure, however a mixture of mono-iodinated and di-iodinated products in a ratio of 1/0.64 was formed.

Palladium catalyzed reductive carbonylation was discovered by Schoenberg and Heck in 1974 [349, 350]. This formylation reaction was successfully applied for the formylation of pyrrolo[2,3-*d*]pyrimidine nucleosides [339, 351, 352]. In this thesis, the palladium catalyzed formylation of 4-hydroxy-5-iodothieno[2,3-*d*]pyrimidine with $Pd(dba)_2$ or $Pd_2(dba)_3$ as catalysts was not successful.

Aromatic nitriles can be prepared from aryl halides. In the Rosenmund-von Braun reaction, aromatic nitriles are prepared by cyanation of aryl halides with an excess of copper(I) cyanide in a polar high-boiling solvent such as DMF, nitrobenzene, or pyridine at reflux. Stoichiometric amounts of copper cyanide, however, led to equimolar amounts of heavy metal waste. Transition metal catalyzed cyanation of aryl halides is therefore a valuable alternative [353]. The order or reactivity of the aryl halides derivatives is I∼OTf>Br>Cl, reverse to the bond dissociation energy of the C-X bond. Electron withdrawing substituents on the aryl ring increase reactivity, while electron donating substituents decrease reactivity [353]. The cyanation of aryl bromides and iodides has been performed using potassium cyanide, sodium cyanide, trimethylsilyl cyanide, tributyltin cyanide (Bu_3SnCN), and zinc cyanide ($Zn(CN)_2$) [353]. No differences were observed between palladium(II) or palladium(0) pre-catalysts [353]. Catalyst deactivation by excess cyanide ions is one of the main reasons for low productivity and activity of palladium catalysts in the cyanation of aryl halides when compared to other C-C coupling reactions [353]. The concentration of cyanide ions can be circumvented by continuous dosage of cyanide to the reaction mixture, applying a two-phase system or by adjusting the solubility of the cyanide source by choosing an appropriate solvent [353].

Preparation of 7-cyano-4-oxo-2-pivaloylamino-9-[2',3',5'-*O*-tribenzoyl-β-*D*-ribofuranosyl]-9*H*-pyrrolo[2,3-*d*]pyrimidine from the corresponding iodide was achieved using Turbo-Grignard conditions [351]. Turbo-Grignard uses the reagent *i*-PrMgCl·LiCl [354, 355]. Lithium chloride can greatly accelerate ortholithiation reactions of arenes containing halogen-based directing groups [356]. The so called salt effect of lithium chloride is exploited in the Turbo Grignard reagent, which exhibits enhanced magnesiating power towards aromatics and heterocycles and shows a greater functional group tolerance [356]. The stoichiometry of the *i*-PrMgCl·LiCl was found to have a dramatic influence on reaction time and conversion [354, 357]. In the Turbo Grignard reaction, the aryl iodide is first deprotonated with CH_3MgCl and then converted into the Grignard compound by addition of *i*-PrMgCl·LiCl. The Grignard-reagent can then be trapped by addition of tosylcyanide [351].

In this thesis, cyanation of 4-hydroxy-5-iodothieno[2,3-*d*]pyrimidine (**44**) was carried out using to Turbo Grignard conditions (Scheme 3.20). The reagents CH_3MgCl and *i*-PrMgCl·LiCl were

obtained from Sigma-Aldrich and the concentration of the reagents was determined by titration, as described by Martin Peters [357]. The reaction was carried out analogously to the preparation of the nucleoside 7-cyano-4-oxo-2-pivaloylamino-9-[2',3',5'-*O*-tribenzoyl-β-*D*-ribofuranosyl]-9*H*-pyrrolo[2,3-*d*]pyrimidine [351]. Cyanation of 4-hydroxy-5-iodothieno[2,3-*d*]pyrimidine (**44**) was not successful using this method.

A synthetic pathway for the synthesis of 5-cyano-4-hydroxythieno[2,3-*d*]pyrimidine, introducing a hydroxymethyl group in the thiophene precursor, was developed in this thesis (Scheme 3.21). In the first synthetic step, 3-chloro-2-oxopropyl acetate (**45**) was prepared starting from dichloroacetone or starting from 2-chloro-2-propen-1-ol, according to modified literature procedures [358, 359]. The substitution reaction starting from dichloroacetone proceeded very slowly at 0°C. The reaction was progressively warmed, thereby increasing reaction rate. At temperatures over 70°C or upon addition of DMF, 2-oxopropane-1,3-diyl diacetate (1,3-diacetoxyacetone) was formed. The reaction starting from 2-chloro-2-propen-1-ol was carried out at room temperature to improve reaction rates.

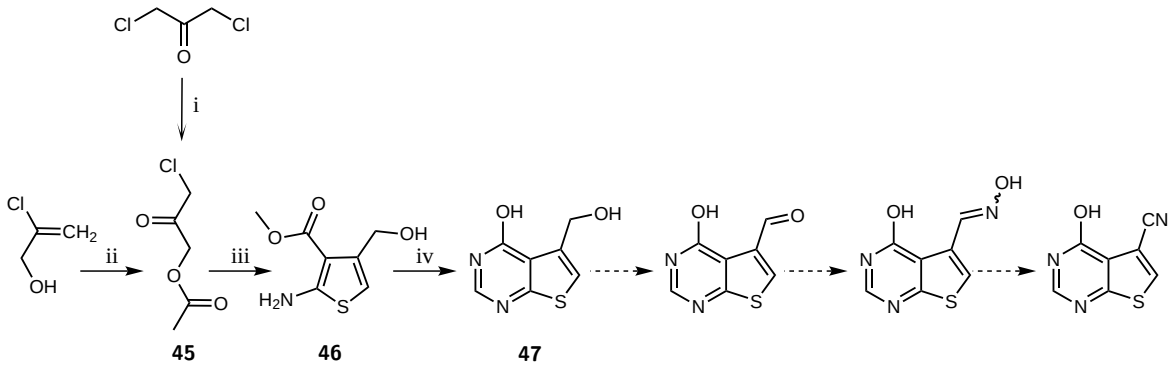

Scheme 3.21 Synthesis of 4-hydroxy-5-hydroxymethylthieno[2,3-*d*]pyrimidine. Full line arrows indicate completed synthetic steps, dashed line arrows indicate synthetic steps in progress, (i) potassium acetate, acetic acid, 70°C, (ii) acetone, acetic acid, aqueous sodium hypochlorite solution, (iii) methylcyano acetate, sodium sulfide nonahydrate, methanol, 0°C to room temperature, (iv) formamide, ammonium formate, 180°C.

In the next synthetic step, depicted in Scheme 3.21 methyl 2-amino-4-hydroxymethylthiophene-3-carboxylate (**46**) was prepared in good yields of 60% [360, 361]. Condensation of this thiophene precursors with formamide yields 4-hydroxy-5-hydroxymethylthieno[2,3-*d*]pyrimidine (**47**). The hydroxy group can subsequently be oxidized to the corresponding aldehyde which in turn can be converted into an oxime and dehydrated to the desired nitrile. The desired compound 5-cyanothieno[2,3-*d*]pyrimidin-4-one can therefore be prepared in the three subsequent reaction steps.

3.4 Cyclopenta[*d*]pyrimidines

2-Amino-5-cyanocyclopenta[*d*]pyrimidin-4-one differs from $preQ_0$ only in the absence of the nitrogen in the five-membered ring. 2-Amino-5-cyanocyclopenta[*d*]pyrimidin-4-one, as well as 5-cyanocyclopenta[*d*]pyrimidin-4-one are new compounds, therefore for their preparation, novel synthetic pathways were developed, as depicted in Scheme 3.22 and Scheme 3.23.

Synthesis of 2-amino-6,7-dihydrocyclopenta[*d*]pyrimidin-4-one (**48**) is described in literature as condensation reaction of ethyl 2-oxocyclopentanecarboxylate with an appropriate guanidine salt

such as guanidine hydrochloride or carbonate. For the preparation of 2-amino-6,7-dihydrocyclopenta[*d*]pyrimidin-4-one, the reaction with guanidine hydrochloride is described using sodium ethoxide as base, while the reaction with guanidine carbonate was carried out without addition of base [192, 194]. The condensation of guanidine hydrochloride to substituted indanones is described analogously and yields indeno[1,2-*d*]pyrimidin-5-one [203]. The condensation of guanidine carbonate with an aromatic aldehyde and cyclopentanone in the presence of sodium hydroxide is described for the preparation of quinazoline derivatives [362]. Alternatively, condensation of thiourea or formamide to ethyl 2-oxocyclopentanecarboxylate are found in literature [192, 198, 200].

In this thesis, condensation reactions of ethyl 2-oxocyclopentanecarboxylate with different precursors were evaluated (Scheme 3.22). The condensation reaction with guanidine carbonate was not successful, however the condensation with guanidine hydrochloride yielded the desired product 2-amino-5-cyano-6,7-dihydrocyclopenta[*d*]pyrimidin-4-one (**48**) in high purities, albeit moderate yields. In the reaction of ethyl 2-oxocyclopentanecarboxylate with thiourea, 85% yield was achieved and the removal of the thiol group in position 2 was almost quantitative, as summarized in Table 3.3.

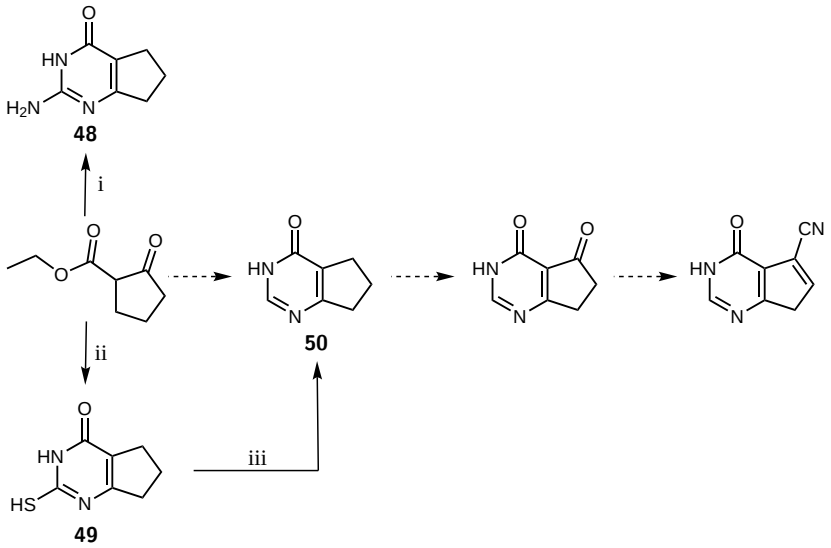

Scheme 3.22 Synthesis of 5-cyanocyclopenta[*d*]pyrimidin-4-one. Full line arrows indicate completed synthetic steps, dashed line arrows indicate synthetic steps in progress, (i) guanidine hydrochloride, sodium ethoxide, ethanol, reflux, (ii) thiourea, sodium methoxide, methanol, reflux, (iii) Raney nickel, water, reflux.

In the next synthetic step, depicted in Scheme 3.22, a keto-group is introduced to the cyclopentane ring. A keto-functionality can be introduced in the benzylic position of indane by oxidation, e.g. with potassium permanganate.[363] The oxidation of the cyclopentane ring of 2-acetoxymethyl-7,8-dihydrocyclopenta[*g*]quinazolin-6-one to the corresponding 4,6-dione is described with bis(tri-phenylsilyl) chromate ($(Ph_3SiO)_2CrO_2$) and *t*-butyl hydroperoxide in dichloromethane [364]. Several other methods for allylic and benzylic oxidation are found in literature, including allylic oxidation with chromium trioxide and pyrazole [365], and allylic or benzylic oxidation using copper catalysts [366]. Alternatively, a hydroxy- or keto-functionality can be introduced by Gif-chemistry [367].

Table 3.3 Reaction conditions for the synthesis of 6,7-dihydrocyclopenta[*d*]pyrimidin-4-one, *yield over two steps, after cleavage of the thiol substituent

method	reagents	reaction conditions	product	yield	reference
A	guanidine carbonate, ethanol	reflux, 23h	**48**	no product isolated	[192]
B	guanidine hydrochloride, sodium ethoxide, ethanol	reflux for 5h, then room temperature for 48h	**48**	34.8%	[194]
C	thiourea, sodium methoxide, methanol	reflux, 20h	**50**	80.1%*	[192, 200]

Preparation of the desired compound 5-cyanocyclopenta[*d*]pyrimidin-4-one from 6,7-dihydrocyclopenta[*d*]pyrimidin-4-one requires only one synthetic step, as depicted in Scheme 3.22. The formation of an α,β-unsaturated nitriles from a keto-group was not yet demonstrated for 6,7-dihydrocyclopenta[*d*]pyrimidin-4-one. Indenecarbonitriles, however, can be synthesized from indanones. Substituted indanones were treated with trimethylsilylcyanide, and subsequent elimination of the trimethylsilyloxyl group is catalyzed by trifluoroacetic acid or amberlyst-15 in toluene or benzene [368–370]. The formation of α,β-unsaturated nitriles from ketones can also be achieved by cyanophosphorylation. Cyanophosphonates are formed from aromatic ketones with diethyl cyanophosphonate in the presence of lithium cyanide and are subsequently readily converted into α,β-unsaturated nitriles by treatment with boron trifluoride etherate [371].

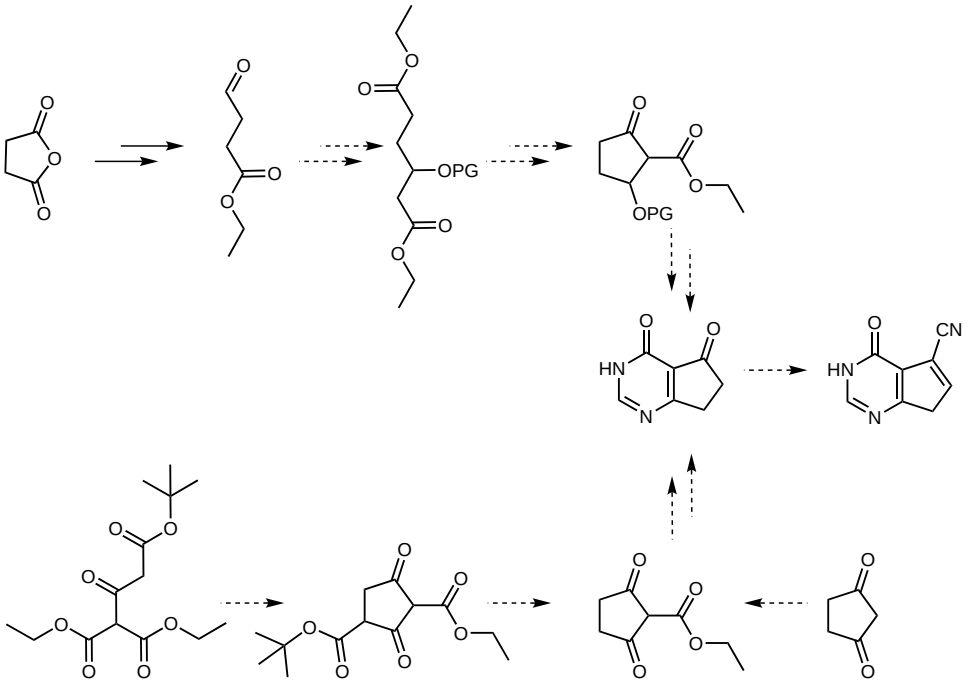

Scheme 3.23 Alternative synthetic pathways for the synthesis of 5-cyanocyclopenta[*d*]pyrimidin-4-one. Full line arrows indicate completed synthetic steps, dashed line arrows indicate synthetic steps in progress.

To circumvent oxidation of the unfunctionalized cyclopentane ring, a hydroxy- or keto-

functionality can be introduced in the cyclopentane-precursor, as depicted in Scheme 3.23. These cyclopentane precursors are not commercially available, however can be prepared according to a variety of synthetic pathways, as summarized in Scheme 3.23. Ethyl 2-hydroxy-5-oxocyclopentanecarboxylate, bearing a hydroxy protecting group, can be prepared from succinic anhydride by opening the anhydride with sodium ethoxide in ethanol, creating the succinic acid monoethyl ester. This ester can in turn be converted into the acid chloride and subsequently reduced to ethyl 4-oxobutanoate [372, 373]. Reduction of the acid chloride to the corresponding aldehyde was not successful using the Rosenmund reduction. Reduction using a palladium on charcoal catalyst and 2,6-lutidine yielded the desired aldehyde in excellent yield [374].

In the next synthetic step, diethyl 3-hydroxyhexanedioate is prepared in a Reformatzky reaction and a hydroxyl-protecting group is introduced, as depicted in Scheme 3.23 [375]. Dieckmann condensation then yields the respective phcyclopentane precursor. This cyclopentane precursor reacts in a condensation reaction with thiourea. Subsequent desulphurisation and deprotection of the hydroxy group yields 5-hydroxy-6,7-dihydrocyclopenta[*d*]pyrimidin-4-one which can be oxidized to the ketone, or the hydroxy group can be directly replaced by a cyanogroup yielding 5-cyano-6,7-dihydrocyclopenta[*d*]pyrimidin-4-one. A similar synthesis of 2,6-dimethyl-6,7-dihydrocyclopenta[*d*]pyrimidin-4-one is described in literature [197].

In literature, ethyl 2,5-dioxocyclopentanecarboxylate was prepared in two steps from 3-*tert*-butyl 1,1-diethyl 2-oxopropane-1,1,3-tricarboxylate. The cyclisation was achieved in a Dieckmann condensation and the resulting 1-*tert*-butyl 3-ethyl 2,4-dioxocyclopentane-1,3-dicarboxylate was treated with *p*-toluenesulfonic acid in benzene to yield ethyl 2,5-dioxocyclopentanecarboxylate in 33% yield over two steps [376]. Ethyl 2,5-dioxocyclopentanecarboxylate could also be prepared from 1,3-cyclopentandione using Mander's reagent. Mander's reagent is known for the site selective preparation of β-ketoesters by acylation of enolates with methyl cyanoformate [377]. Cyclopenta[*d*]pyrimidin-4,5-dione can then be prepared in the condensation reaction of 2,5-dioxocyclopentanecarboxylate with a suitable fragement, e.g., thiourea and subsequent removal of the thiol group. 5-Cyanocyclopenta[*d*]pyrimidin-4-one can be prepared in only four synthetic steps. Similarly, 2-amino-5-cyanocyclopenta[*d*]pyrimidin-4-one can be prepared in three steps, when guanidine hydrochloride is used in the condensation.

A variety of cyclopentane precursors can be used for the synthesis of cyclopenta[*d*]pyrimidines. Condensation of 2-(bis(methylthio)methylene)cyclopentane-1,3-dione or 2-benzylidenecyclopentane-1,3-dione with guanidine salts yield 2-amino-4-arylcyclopenta[*d*]pyrimidin-5-ones [202, 206, 207]. Starting from 2-vinylcyclopentane-1,3-dione, 5-vinylcyclopenta[*d*]pyrimidin-5-one can be prepared. The vinyl group can then be dihydroxylized and cleaved to the corresponding aldehyde, which could then be further reacted to the oxime and dehydrated to the nitrile.

The synthesis of 5-cyano-6,7-dihydrocyclopenta[*d*]pyrimidin-4-one will be continued by Stefan Faschauner in his master thesis [378].

3.5 3-Cyanopyrazolo[3,4-*d*]pyrimidines

5-Cyanopyrazolo[3,4-*d*]pyrimidin-4-one differs from $preQ_0$ in an additional nitrogen heteroatom in the five membered ring and the missing amino group in position 2 and would therefore be a potential substrate for nitrile reductase queF.

3-Cyanopyrazolo[3,4-*d*]pyrimidin-4-one can be synthesized analogously to 5-cyanopyrrolo[2,3-*d*]pyrimidin-4-one, as depicted in Scheme 3.24. First, 5-amino-3,4-dicyanopyrazole is formed from tetracyanoethylene and semicarbazide, according to a literature procedure [379]. The condensation of tetracyanoethylene with a variety of hydrazine derivatives to give *N*-substituted 5-amino-3,4-dicyanopyrazoles is found in patent literature by DuPont and Sterling Winthrop Inc [214, 380, 381]. In the next synthetic step, the pyrimidine ring is formed in a condensation reaction. The reaction of dimethylformamide diethylacetal with 5-amino-3,4-dicyanopyrazole and subsequent treatment with ammonia is described in 50% to 60% yield [382]. Analogously, the condensation of triethyl orthoformate to 5-amino-3,4-dicyanopyrazole with subsequent treatment with ammonia is described to yield the desired 4-amino-3-cyanopyrazolo[3,4-*d*]pyrimidine in 83% yield [383]. Similarily, diethoxymethyl acetate was used in the condensation reaction with 5-amino-3,4-dicyano-1-methylpyrazole to give 4-amino-3-cyano-1-methylpyrazolo[3,4-*d*]pyrimidine in 74% yield [384]. The condensation of 5-amino-4-cyanopyrazole and 5-amino-4-cyano-3-methyl-1-phenylpyrazole with formamide is also described in literature in 56% to 68% yield [385, 386]. The amino group in position 4 can then be converted into an hydroxy group in a diazotization reaction using sodium nitrite and hydrochloric acid [383].

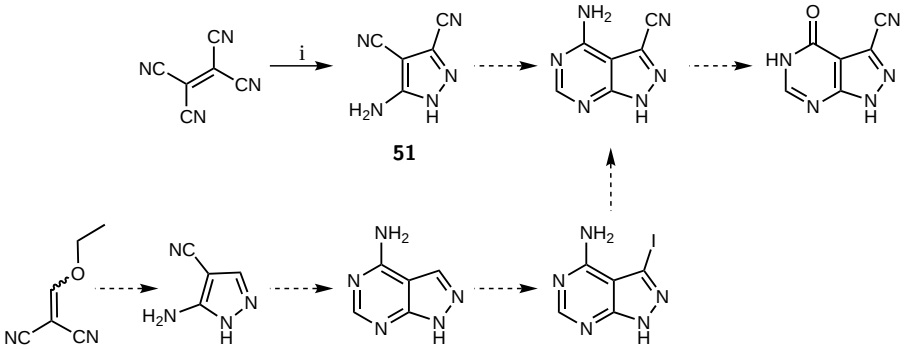

Scheme 3.24 Synthesis of 3-cyanopyrazolo[3,4-*d*]pyrimidin-4-one. Full line arrows indicate completed synthetic steps, dashed line arrows indicate synthetic steps in progress, (i) 1. semicarbazide hydrochloride, ethanol, triethylamine, 2. water, reflux.

3-Cyanopyrazolo[3,4-*d*]pyrimidin-4-one can be prepared by first synthesizing 4-aminopyrazolo[3,4-*d*]pyrimidine and introducing the cyano-substituent in position 3 later in the synthetic pathway, as depicted in Scheme 3.24. In the first synthetic step, 1,1-dicyano-2-ethoxyethylene (ethoxymethylene malononitrile) is reacted with hydrazine to give 3-amino-4-cyanopyrazole [387–389]. This reaction was also performed successfully in a flow microwave system and with substituted hydrazines [390–392]. The formation of the bicyclic pyrazolo[3,4-*d*]pyrimidine ring system starting from 3-amino-4-cyanopyrazole or 5-amino-3,4-dicyanopyrazole as precursor, is described with dimethylformamide diethylacetal, triethyl orthoformate, or formamide [222, 382, 383, 385, 393]. Iodination in position 3 can be achieved with *N*-iodosuccinimide in DMF in excellent yields of up to 89% [218, 222, 393, 394]. The iodide substituent can then be substituted by a nitrile group in a palladium catalyzed reaction with a tris-(dibenzylideneacetone)dipalladium(0) and dichloro(1,1'-bis(diphenylphosphanyl)ferrocene)palladium(II) dichloromethane adduct and zinc cyanide in DMF [395].

3-cyanopyrazolo[3,4-*d*]pyrimidin-4-one can also be prepared from 1,1-dicyano-2,2-bis(methyl-

thio)-ethylene, as depicted in Scheme 3.25. The reaction of 1,1-dicyano-2,2-bis(meth-ylthio)-ethylene with hydrazine to 5-amino-4-cyano-3-methylthiopyrazole and the subsequent condensation reaction with formamide were carried out according to a literature procedure in excellent yields of 89% and 75%, respectively [396]. The thioether can then be oxidized to the sulfon which in turn can be substituted by a nitrile group, as described for pyrazolo[1,5-*a*]pyridines [397]. The last synthetic step is the substitution of the amino group in position 4 with a hydroxy group [383]. The synthesis of 5-cyanopyrazolo[3,4-*d*]pyrimidin-4-one will be continued by Wilfried Sailer-Kronlachner in his master thesis [398].

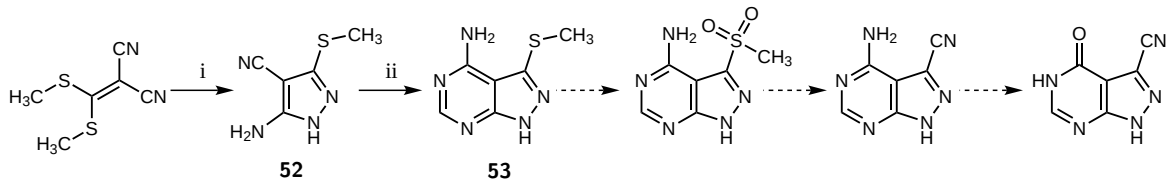

Scheme 3.25 Synthesis of pyrazolo[3,4-*d*]pyrimidines starting from 1,1-dicyano-2,2-bis(methylthio)ethylene. Full line arrows indicate completed synthetic steps, dashed line arrows indicate synthetic steps in progress, (i) hydrazine hydrate, methanol, (ii) formamide, 180°C

3.6 Monocyclic compounds

Monocyclic substrates, resembling either the pyrrole part or the pyrimidine part of $preQ_0$ (**1**), of the natural substrate of nitrile reductase queF were prepared in this thesis (Scheme 3.26). 5-Cyanomethyl-2,4-diamino-6-hydroxypyrimidine (**54**) resembles the pyrimidine part of the natural substrate $preQ_0$ and bears the cyano-group in similar distance to the pyrimidine ring as $preQ_0$. 2-Hydroxybenzylcyanide (**55**) also resembles the pyrimidine part of $preQ_0$, however, is devoid of the heteroatoms. 3-Cyanopyrrole represents the pyrrole part of the natural substrate $preQ_0$.

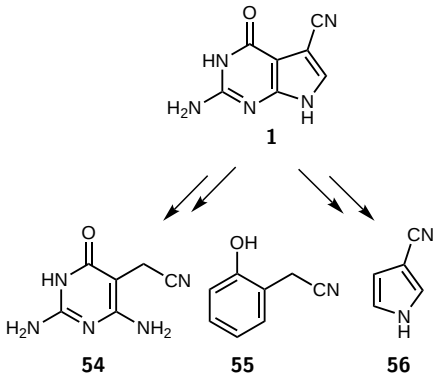

Scheme 3.26 Monocyclic structural analogues of $preQ_0$

In this thesis, 5-cyanomethyl-2,4-diamino-6-hydroxypyrimidine (**54**) was prepared in one step from 2,6-diamino-4-hydroxypyrimidine. Pyrimidines can be regioselectively monoalkylated in the C-5 position by strong electrophiles bearing an electron-withdrawing group. The cyanomethyl group was therefore introduced by reacting 2,4-diamino-6-hydroxypyrimidine with bromoacetonitrile in DMF in the presence of sodium bicarbonate [399].

2-Hydroxybenzylcyanide (**55**) is accessible in one step either by cleavage of the methoxy ether of 2-(2-methoxyphenyl)acetonitrile or by substitution of the primary alcohol of 2-(hydroxymethyl)-

phenol, as depicted in Scheme 3.27. In this thesis, cleavage of the methoxy ether of commercially available 2-(2-methoxyphenyl)acetonitrile was carried out with boron tribromide in dichloromethane, as described in literature for similar compounds [400]. However, not only cleavage of the methoxy ether, but also hydrolysis of the cyano functionality to the corresponding carboxylic acid was observed. The hydroxy group and carboxylic acid reacted intramolecularly to yield benzofuranone. Preparation of 2-hydroxybenzylcyanide was then achieved by displacement of the primary alcohol of commercially available 2-(hydroxymethyl)phenol by cyanide using sodium cyanide or potassium cyanide in DMF [401–403].

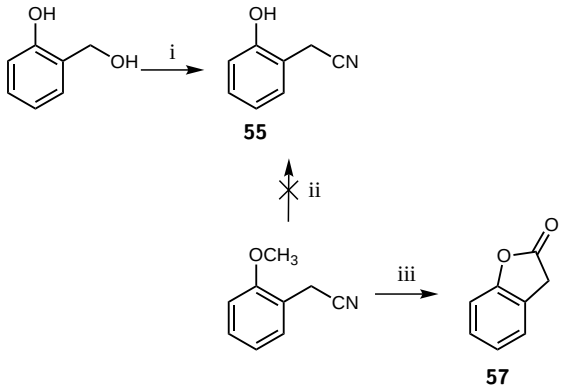

Scheme 3.27 Synthesis of 2-hydroxybenzylcyanide. (i) KCN, DMF, 130°C, (ii) and (iii) BBr_3 in dichloromethane, 0°C to 60°C.

In this thesis, 3-cyanopyrrole (**56**) was prepared from 2-(trichloroacetyl)pyrrole in a three step synthesis by Loader *et al.* [404, 405], depicted in Scheme 3.28. 2-(Trichloroacetyl)pyrrole is used as starting material to exploit the directing properties of the trichloroacetyl electron withdrawing group. The cyano-group is introduced by chlorosulfonyl isocyanate and DMF. Chlorosulfonyl isocyanate reacts with 2-(trichloroacetyl)pyrrole, and on warming with DMF gives the nitrile **58**. The trichloroacetyl group can easily be converted into the carboxylic acid by treatment with base, followed by acidification. Subsequent decarboxylation gave 3-cyanopyrrole.

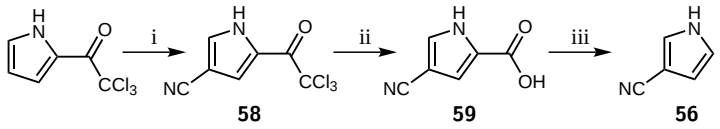

Scheme 3.28 Synthesis of 3-cyanopyrrole. (i) 1. acetonitrile, chlorosulfonyl isocyanate, 0°C, 2. DMF, 50°C, (ii) 1. NaOH, 0°C, 2. conc. HCl, (iii) copper chromite catalyst, quinoline, 160°C.

3.7 2-Amino-5-formylpyrrolo[2,3-*d*]pyrimidin-4-one

Several different strategies for the synthesis of the aldehyde bearing the $preQ_0$ core structure were developed in this thesis (Scheme 3.29). This aldehyde, 2-amino-5-formylpyrrolo[2,3-*d*]pyrimidin-4-one, can be synthesized by first preparing the $preQ_0$ core structure devoid of the substituent at C-5 and subsequent formylation. Another strategy is condensation of a precursor bearing an aldehyde group, e.g. 2-chloromalonaldehyde (2-chloro-1,3-propandial) to 2,4-diamino-6-hydroxypyrimidine. Alternatively, a compound bearing a functional group at C-5 which can easily be converted into an aldehyde can be prepared. An ester or a cyano-group can be transformed into aldehydes by

reduction or an alcohol can be oxidized to the aldehyde.

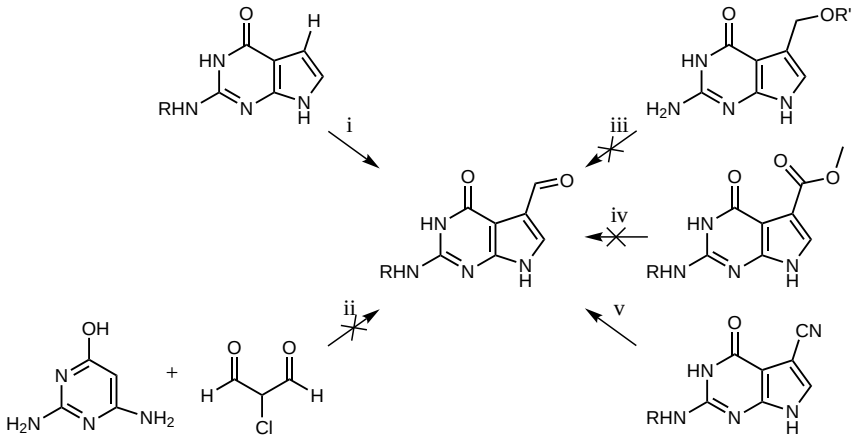

Scheme 3.29 Synthetic strategies for the synthesis of 2-amino-5-formylpyrrolo[2,3-*d*]pyrimidin-4-one. R = H, Piv or Trt, R' = Bn or $SiPh_2t$−Bu, (i) formylation reactions, i.e., Vilsmeier reaction, Duff reaction, Pd catalyzed formylation, (ii) condensation reaction, (iii) ether cleavage and subsequent oxidation, (iv) reduction with LAH or DIBAL-H, (v) reduction with DIBAL-H or Raney-Ni/H_2.

Synthesis of the aldehyde by formylation

The $preQ_0$ core structure 2-aminopyrrolo[2,3-*d*]pyrimidin-4-one (**60**) can be prepared in a condensation reaction of 2,4-diamino-6-hydroxypyrimidine and chloroacetaldehyde as depicted in Scheme 3.30. A variety of reaction conditions is found in literature for this condensation reaction. Reaction temperatures range from room temperature to 65°C .[339, 406]. A mixture of DMF and water is commonly used as solvent with or without sodium acetate added to the reaction mixture [285, 339, 340, 407]. Water as reaction solvent and addition of sodium acetate is found in recent patent literature [406, 408, 409] In this thesis, water with addition of sodium acetate as reaction solvent at 85°C were found to be the optimum reaction conditions. 2,4-Diamino-6-hydroxypyrimidine is poorly soluble in water at room temperature, however solubility increases with higher temperatures. When only water is used as reaction solvent, the product can be isolated by precipitation from the reaction mixture in high purity. When DMF is used, DMF has to be removed quantitatively before crystallization of the product. Alternatively, the product can be isolated by extraction. Isolation by extraction led to lower yields due to the poor solubility of the product 2-aminopyrrolo[2,3-*d*]pyrimidin-4-one (**60**) in the extraction solvents ethyl acetate and dichloromethane. The crude product isolated by extraction contained impurities and was purified by column chromatography, whereas the product obtained from precipitation did not require further purification.

Formylation of aromatic systems can be achieved by Duff reaction. The Duff reaction is commonly found in literature for the formylation of 7-azaindoles [321–325]. The formylation of pyrrolo[2,3-*d*]pyrimidine by Duff reaction is also described in literature [280]. However, in this thesis, Duff reaction starting from 2-aminopyrrolo[2,3-*d*]pyrimidin-4-one (**60**) did not yield the desired product.

Pivaloyl protection of 2-aminopyrrolo[2,3-*d*]pyrimidin-4-one (**60**) was carried out analogously to pivaloyl protection of $preQ_0$, as described in chapter 3.1.3.

Vilsmeier-Haack reaction was described for the preparation of 5-formyl-2-pivaloylaminopyr-

rolo[2,3-*d*]pyrimidin-4-one (**61**) [114]. Vilsmeier and Haack published this formylation procedure in 1927. In the original procedure, the formylation reagent is formed from DMF and phosphorus oxychloride. The starting material is then added dropwise to the formylation reagent and the resulting reaction mixture is heated moderately [410]. The reaction of phosphorus oxychloride with DMF produces an electrophilic iminium cation which can react with the aromatic starting material in an electrophilic aromatic substitution to give an iminium ion intermediate. This intermediate is hydrolysed during work-up to the corresponding aldehyde [330, 410]. The Vilsmeier-Haack reagent can also be formed *in situ*, by dropwise addition of phosphorus oxychloride to a solution of the starting material in DMF [411]. In the procedure described for the preparation of 5-formyl-2-pivaloylaminopyrrolo[2,3-*d*]pyrimidin-4-one (**61**), the starting material 2-pivaloylaminopyrrolo[2,3-*d*]pyrimidin-4-one is heated in a mixture of two equivalents of *N,N*-dimethylformamide and a large excess of phosphorus oxychloride (60 equivalents) to give 95% of the desired aldehyde [114]. In this thesis, only traces of the desired product were found when the starting material 2-pivaloylaminopyrrolo[2,3-*d*]pyrimidin-4-one (**62**) was dropwise added to the Vismeier reagent and subsequently heated to 55°C. The addition of a sixfold excess of phosphorus oxychloride to the starting material in DMF showed conversion to the desired aldehyde **61**, as well as to the byproduct **63**. HPLC-MS analysis indicated a ratio of 1/2 of aldehyde **61** to byproduct **63**. The highest conversion to aldehyde **61** was achieved by dissolving the starting material in DMF, dropwise addition of 2.7 equivalents of phosphorus oxychloride to the cold solution and subsequent heating to 55°C. Under these conditions HPLC-MS analysis indicated conversion to the aldehyde **61** and byproduct **63** in a ratio of 2.4/1. Purification of the starting material, byproduct and aldehyde by column chromatography is difficult due to the similar polarity of the compounds. The purified aldehyde **61** was isolated in only 6% yield after column chromatography. Therefore, alternative methods for the preparation of 5-formyl-2-pivaloylaminopyrrolo[2,3-*d*]pyrimidin-4-one (**61**) were investigated.

Iodination of pyrrolo[2,3-*d*]pyrimidine compounds in position 5 is an important reaction to prepare precursors for palladium catalyzed cross couplings, e.g., for the preparation of antifolate compounds [412]. Iodination of 4-chloro-2-pivaloylaminopyrrolo[2,3-*d*]pyrimidine **63** is described in literature using *N*-iodosuccinimide as iodination reagent. The reaction is described in DMF or THF with yields of approximately 60% to 80% [284, 285, 339, 413–416]. In this thesis, iodination was accomplished with *N*-iodosuccinimide in THF. TLC indicated complete conversion, however only 23% yield were isolated after column chromatography.

The 4-oxo group can be re-established after halogenation. The oxo-substituent was achieved in one step by Klepper *et al.* by using caesium acetate, 1,4-diazabicyclo[2.2.2]octane (DABCO), and triethylamine in DMF [339]. The chloro-substituent can also be substituted by an alkoxy-derivative by treating the chloro derivatives with alkali alkoxides. Subsequently, the alkoxide is dealkylated with sodium thiocresylate and hexamethylphosphoramide (HMPA) or with sodium and potassium hydroxide [412]. Displacement of the chloro-group with caesium acetate and DABCO did not yield the desired product in this thesis.

Iodination of 2-pivaloylaminopyrrolo[2,3-*d*]pyrimidin-4-one (**62**) with *N*-iodosuccinimide in DMF does not proceed regioselectively and yields a mixture of 5- and 6-iodo-substituted product, along with the 5,6-di-iodo product and starting material [286, 412]. Introduction of a chloro-

mercurio-substituent and subsequent substitution with iodine also yielded a mixture of 5- and 6-substituted products [348]. Selective reduction to the monosubstituted 5-iodo-2-pivaloylaminopyrrolo[2,3-*d*]pyrimidin-4-one **64** is described in literature with a mixture of zinc powder and glacial acetic acid [286]. Regioselective iodination in position 5 of 4-oxopyrrolo[2,3-*d*]pyrimidines is reported in literature by silylation of the 4-oxopyrrolo[2,3-*d*]pyrimidine compound with two equivalents of bis(trimethylsilyl)acetamide (BSA) in DMF at the 4-oxo and N-7 position. Silylation creates the electronic configurational requirements for regioselective halogenation at C-5. Selective iodination at position 5 of the silylated starting material was achieved with *N*-iodosuccinimide. The N-7 and *O*-silyl substitutens in the halogenated product were found highly unstable towards hydrolysis. Desilylation occurs spontaneously during work-up [412]. In this thesis, iodination of 2-pivaloylaminopyrrolo[2,3-*d*]pyrimidin-4-one (**62**) was carried out analogously to the iodination of the corresponding 4-chloro-compound. However, only 14% of the desired product were isolated after column chromatography.

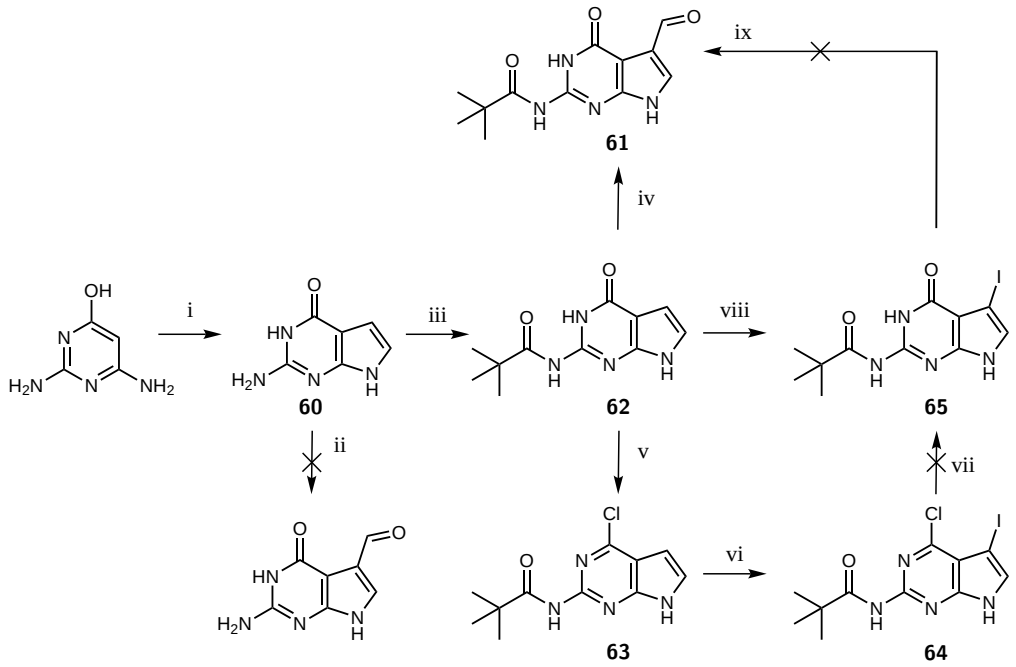

Scheme 3.30 Preparation of 2-amino-5-formylpyrrolo[2,3-*d*]pyrimidin-4-one by formylation. (i) chloroacetaldehyde, sodium acetate, water, 85°C, (ii) HMTA, acetic acid, reflux, (iii) pivaloyl chloride, pyridine, triethyl amine, 90°C, (iv) and (v) $POCl_3$, DMF, 55°C, (vi) and (viii) *N*-iodosuccinimide, THF, (vii) DABCO, caesium acetate, triethyl amine, DMF (ix) $Pd(dba)_2$ or $Pd_2(dba)_3$, triphenylphosphine, carbon monoxide, $SnBu_3H$, toluene.

Palladium catalyzed carbonylation was described to produce aldehydes from aryl, heterocyclic and vinylic halides. The method was first described using a palladium(0) catalyst and a gas mixture of carbon monoxide and hydrogen by Schoenberg and Heck in 1974. The palladium(0) complex undergoes oxidative addition with the organic halide, inserts carbon monoxide, and is finally reduced by hydrogen [349]. High pressures of 80 bar to 100 bar of hydrogen pressure and temperatures of 80°C to 150°C were essential to convert aryl and vinyl bromides or iodides to the corresponding aldehydes using a $PdX_2(PPh_3)_2$ catalyst [350]. Milder conditions were described by Baillargeon and Stille using tributyltin hydride as hydrogen transfer agent instead of hydrogen gas [417]. The palladium catalyzed formylation of a variety of organic substrates, including aryl

iodides, benzyl halides, vinyl iodides, vinyl triflates and allylic halides with tributyltin hydrid and 1-3atm carbon monoxide gas tolerated a number of functional groups. Electron donating or withdrawing substituents did not affect the formylation reaction, however a *para*-nitro substituent on the aryl halide impaired the yield of aldehyde. Yields were also found to be diminished by steric hinderance of the electrophile. The formylation of unsymmetrical allyl hydrides is regioselective, taking place at the less substituted allylic position, with retention of geometry at the allylic double bond. Retention of the double bond geometry also is observed in the formylation of vinyl iodides [418, 419]. Silyl hydrides were reported as alternative to tributyltin hydride. Polymethylhydrosiloxane (PMHS) was used as mild, air stable, and inexpensive reducing agent for the palladium catalyzed carbonylation of iodobenzene [420]. Triethylsilane was used for the carbonylation of aryl iodides catalyzed by palladium-cobalt bimetallic systems [421]. A selection of palladium catalysts were tested for a number of aryl bromides and iodides using triethylsilane as reducing agent. High yields of aldehyde were achieved with catalysts containing bidentate phosphine ligands, such as [$PdCl_2$(dppp)], [$PdBr_2$(BINAP)], or [$PdCl_2$(dppf)]. Chelate ring size was identified as important factor in catalyst choice. Bidentate phosphine ligands with a small bite angle, like [$PdCl_2$(dppe)], were found inactive in the carbonylation reaction. Pre-formed catalysts exceeded over those generated *in situ* from palladium acetate and the ligand. A general optimization of conditions to produce the highest yield of aldehyde is not a viable approach as each substrate poses different challenges. In literature, the amount of catalyst was varied in the range of 1 mol% to 5 mol% with little effect on the distribution of products, at 1 mol% or lower, the reaction was noticeably slower. Generally two equivalents of triethylsilane and 2.1 equivalents of base were used. Reducing either triethylsilane or base to one equivalent improved yields of aldehyde, however reducing the quantity of both, silane and base, had a detrimental effect. Carbonmonoxide pressure was lowered to 3bar, further decrease in pressure led to the formation of a dehalogenated side product. Aryl iodide starting materials showed increased activity towards the oxidative addition step of the reductive carbonylation reaction. High yields were achieved for substrates with an electronically neutral substituent in position 4. Substrates with an electron withdrawing group in position 4 gave similar results, except for 1-bromo-4-nitrobenzene. Nitro-substituted aromatic systems are known to show abnormal reactivity due to their coordinating ability and high electron deficiency. Substrates with an electron withdrawing group in position 2 promoted reductive debromination over reductive carbonylation. Substrates with electron-donating groups required higher temperature for the reaction to take place. Again yields were lower when the substituent is in position 2, rather than in position 4 [422]. The oxidative addition step was intensively studied, amongst others in the Buchwald-Hartwig amination. Strongly donating phosphines bearing bulky substituents like $PtBu_3$ are considered advantageous, explained by the relative stability of the Pd(0) and Pd(II) complexes [423]. The carbonyl insertion step consists of initial substitution of carbon monoxide into the coordination sphere and then insertion into the Pd-C bond. The hydrogen transfer step and the reductive elimination from the aryl and acyl intermediates are less understood [422, 424].

Palladium catalyzed formylation was described for the nucleosides 4-chloro-5-iodo-2-pivaloylamino-7-[(2,3,5-tribenzoyl)-β-*D*-ribofuranosyl]-7*H*-pyrrolo[2,3-*d*]pyrimidine and 5-iodo-4-oxo-2-pivaloylamino-7-[(2,3,5-tribenzoyl)-β-*D*-ribofuranosyl]-7*H*-pyrrolo[2,3-*d*]pyrimidine. $Pd_2(dba)_3$

was used as catalyst with triphenylphosphane as ligand and tributyltin hydride as reducing agent [339, 351, 352]. In this thesis, analogous conditions were chosen for the formylation of 5-iodo-2-pivaloylaminopyrrolo[2,3-*d*]pyrimidin-4-one (**65**), as depicted in Scheme 3.30. The reaction was carried out in degassed toluene under 1bar of carbonmonoxide pressure with $Pd(dba)_2$ or $Pd_2(dba)_3$ as catalyst and triphenylphosphine as ligand. The reaction was heated to 50°C upon addition of tributyltin hydride. Traces of product were observed by HPLC-MS besides large amounts of unreacted starting material. The reaction was probably affected by the limited solubility of the starting material **65** in toluene.

Synthesis of the aldehyde by preparation of an alcohol and subsequent oxidation

2-Amino-5-formylpyrrolo[2,3-*d*]pyrimidin-4-one (**66**) can be prepared by oxidation of the corresponding 2-amino-5-hydroxmethylpyrrolo[2,3-*d*]pyrimidin-4-one. This alcohol can be prepared in a condensation reaction of a suitable precursor with 2,4-diamino-6-hydroxypyrimidine [352, 425, 426]. 2-Bromo-3-hydroxypropanal, bearing a protected hydroxy-group, was chosen as suitable precursor for the preparation of 2-amino-5-hydroxmethylpyrrolo[2,3-*d*]pyrimidin-4-one. Several hydroxy protecting groups were investigated in literature. Benzyl and *tert*-butyldiphenylsilyl (TBDPS) allowed the preparation of the β-alkoxy-α-bromoaldehydes in good yiels. TBDMS, TIPS, benzoyl, and trityl mono-protected 1,3-propanediols were smoothly oxidated, however bromiation led to decomposition of starting material [425]. In this thesis, 2-amino-5-hydroxmethylpyrrolo[2,3-*d*]pyrimidin-4-one bearing a benzyl, as well as a TBDPS protecting group, was synthesized.

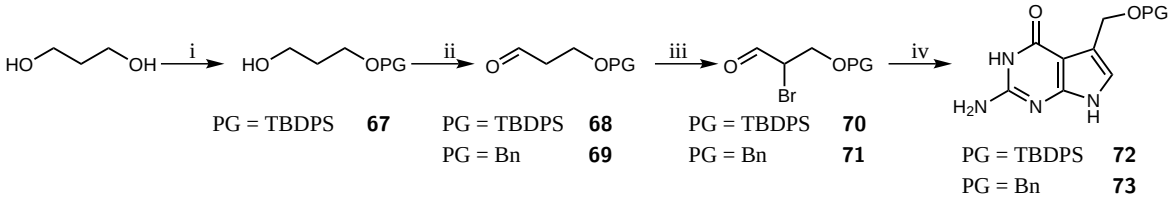

Scheme 3.31 Synthesis of hydroxy-protected 2-amino-5-hydroxymethylpyrrolo[2,3-*d*]pyrimidin-4-one. (i) *t*-$BuPh_2SiCl$, triethylamine, DCM, 0°C to room temperature, (ii) oxalyl chloride, DMSO, triethyl amine, DCM, -78°C or TEMPO, DCM, (iii) bromine, dioxane, diethyl ether or trimethylsilyl bromide, DMSO, (iv) 2,4-diamino-6-hydroxypyrimidine, acetonitrile, sodium acetate, water or 2,4-diamino-6-hydroxypyrimidine, sodium acetate, water

The benzyl-protected alcohol was prepared starting from commercially available 3-benzyloxy-1-propanol, according to a literature procedure [426]. In the first synthetic step, depicted in Scheme 3.31, the alcohol was oxidized with TEMPO in combination with trichloroisocyanuric acid. This method was previously described for oxidations under mild, basic conditions [427]. The resulting product 3-benzyloxy-1-propanal was used in the next synthetic step without purification. Bromination was achieved with trimethylsilylbromide in a mixture of acetonitrile and DMSO. The brominated product was not isolated and 2,4-diamino-6-hydroxypyrimidine in an aqueous sodium acetate solution was added to the reaction mixture. The resulting product 2-amino-5-(benzyloxy)methylpyrrolo[2,3-*d*]pyrimidin-4-one (**73**) was isolated in 5.2% yield after purification by column chromatography.

The synthesis of the TBDPS-protected alchol was started from 1,3-propandiol. The TBDPS protecting group was introduced with TBDPSCl and triethylamine in dichloromethane according

to a literature procedure [428, 429]. Various similar procedures using different bases e.g. n-BuLi, sodium hydride, or imidazole, are found in literature [430–433]. A Swern oxidation of 3-((*tert*-butyldiphenylsilyl)oxypropan-1-ol gave the corresponding aldehyde in 87.7% yield. Swern oxidation is applied throughout literature for this step [431, 432, 434]. The bromination of 3-((*tert*-butyldiphenylsilyl)oxy)propanal is described by using *N,N*'-dibromobarbituric acid in acetonitrile [425]. In this thesis, the bromination was carried out with bromine in dioxane and diethyl ether and gave the desired 2-bromo-3-((*tert*-butyldiphenylsilyl)oxy)propanal in 69.8% yield. The product was used for the next synthetic step without purification. The condensation reaction with 2,4-diamino-6-hydroxypyrimidine was carried out in acetonitrile and aqueous sodium acetate solution. The desired product 2-amino-5-((*tert*-butyldiphenylsilyl)oxymethyl)pyrrolo[2,3-*d*]pyrimidin-4-one (**72**) was isolated in 15.3% yield after column chromatography. The yield over all synthetic steps was 6.6%. Both alcohols, (**73**) and (**72**), were obtained in rather low yields. Deprotection and subsequent oxidation to the corresponding aldehyde was therefore not pursued.

Synthesis of the aldehyde by preparation of an ester and subsequent reduction

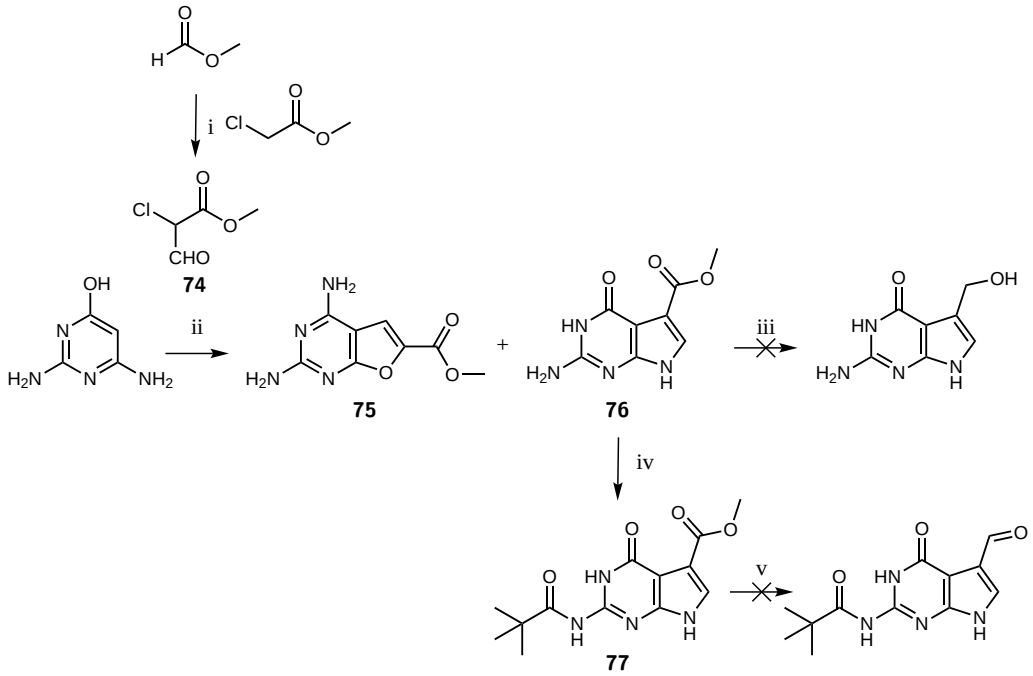

Scheme 3.32 Synthesis of methyl 2-amino-4-oxopyrrolo[2,3-*d*]pyrimidin-5-carboxylate. (i) NaH, THF, (ii) sodium acetate, water, 75°C, (iii) LAH, diethyl ether, room temperature to reflux, (iv) pyridine, triethylamine, pivaloylchloride, 90°C, (v) DIBAL-H, toluene, THF, room temperature or for reduction to the alcohol LAH, diethyl ether, reflux.

2-Amino-5-formylpyrrolo[2,3-*d*]pyrimidin-4-one (**66**) can be prepared by reduction of the corresponding ester methyl 2-amino-4-oxopyrrolo[2,3-*d*]pyrimidin-5-carboxylate **76**. This ester is synthesized by condensation of a suitable precursor to 2,4-diamino-6-hydroxypyrimidine, as depicted in Scheme 3.32. In literature, formation of two esters **76** and **75** was observed. The reaction of 2,4-diamino-6-hydroxypyrimidine with methyl 2-chloro-3-oxopropionate (**74**) in DMSO containing potassium carbonate gave the 40% of the desired ester **76** and 25% of **75** (ratio **76**/**75** 1.6/1). Reaction in an aqueous solution of sodium acetate increased the yield of the desired ester **76** to

50%. The ester products **76** and **75** could be separated on small scale by fractional crystallization from methanol. However, on an scale of more than 100mg both products co-crystallized [277]. Gangjee *et al.* obtained the desired methyl 2-amino-4-oxopyrrolo[2,3-*d*]pyrimidin-5-carboxylate **76** as sole product in 62% yield, when reacting 2,4-diamino-6-hydroxypyrimidine in aqeuous sodium acetate solution at 100°C for two hours, as depicted in Scheme 3.32 [259]. In this thesis, under the same reaction conditions, both esters **76** and **75** were found in a ratio of 1.7/1. The amount of the desired ester **76** was slightly increased by using lower temperature and shorter reaction times, as summarized in Table 3.4. Separation of the two esters **76** and **75** was not possible by recrystallization, column chromatography or preparative TLC.

Table 3.4 Comparison of the reaction conditions for the synthesis of methyl 2-amino-4-oxopyrrolo[2,3-*d*]pyrimidin-5-carboxylate

method	reaction conditions	total yield	ratio **75**/**76**
A	100°C for 1.5h, then room temperature over night	50.2%	1/1.70
B	75°C for 1.25h	52.7%	1/2.13

Reduction of methyl 2-amino-4-oxopyrrolo[2,3-*d*]pyrimidin-5-carboxylate **76** with lithium aluminium hydride in diethyl ether was not possible in this thesis. Unsuccessful reduction of this ester using lithium aluminum hydride is also reported in literature [259]. The starting material (**76** and **75**) is unsoluble in the reaction solvents used for the reductions. The esters **76** and **75** were pivaloyl-protected by using pivaloylchloride in pyridine and triethylamine. Pivaloyl-protection increased the solubility of these compounds and allowed the separation of the two esters by column chromatography. Reduction of the pivaloyl-protected compound **77** by lithium aluminium hydride was not possible, neither was selective reduction to the corresponding aldehyde using DIBAL-H in toluene and THF.

Synthesis of the aldehyde by reduction of a nitrile

Direct reduction of the cyano-group in $preQ_0$ to the corresponding aldehyde in 2-amino-5-formylpyrrolo[2,3-*d*]pyrimidin-4-one (**66**) by DIBAL-H is described in literature [263, 435]. In this thesis, reduction of unprotected $preQ_0$ was not successful using DIBAL-H, possibly due to the low solubility of $preQ_0$. Reduction is also described with trityl-protected $preQ_0$ using DIBAL-H in dichloromethane at 0°C [263]. Silylation with hexamethyldisiloxane (HMDS) in refluxing toluene was utilized to further improve solubility of trityl-protected $preQ_0$ for the subsequent reduction with DIBAL-H. The trityl-protected aldehyde was achieved in 42% yield over two steps [435]. In this thesis, the reduction of trityl-protected $preQ_0$ using DIBAL-H in dichloromethane was not successful.

In literature, Raney-nickel is commonly used for the reduction of nitrile groups to aldehydes. Raney-nickel in acetic acid was used for a reductive condensation of cyano-substituted pyrido[2,3-*d*]pyrimidines with anilines. The aldehyde intermediate was not isolated [436]. Raney-nickel in formic acid was used for the reduction of 5-cyano-2,4-diaminopyrrolo[2,3-*d*]pyrimidine to 2,4-diamino-5-formylpyrrolo[2,3-*d*]pyrimidine. The aldehyde was obtained in 63% yield after

reduction for 2h at 80°C [273, 437]. The reduction of nitriles to aldehydes with Raney nickel in pyridine/acetic acid/water 2/1/1 under addition of sodium hypophosphite was described as an improved method for the synthesis of aldehydes. Raney nickel liberates hydrogen from water in the presence of sodium hypophosphite while retaining its activity. Sodium hypophosphite additionally catalyzes the reduction of the nitrile. Moderate excess of sodium hypochlorite and one third to one half of the weight of nitrile in catalyst were found as suitable conditions [438, 439]. These reduction conditions were successfully applied for the reduction of a nitrile group in the synthetic pathway to a precursor of the 14-membered cyclopeptide alkaloid nummularine. Reduction with Raney nickel and aluminium alloy in formic acid was not successful for this compound [440]. The nitrile group of the nucleoside 4-amino-5-cyano-7-(2'-deoxy-β-D-ribofuranosyl)pyrrolo[2,3-*d*]pyrimidine was also successfully reduced to the corresponding aldehyde using Raney-nickel and sodium hypophosphite in pyridine/acetic acid/water 2/1/1 [441].

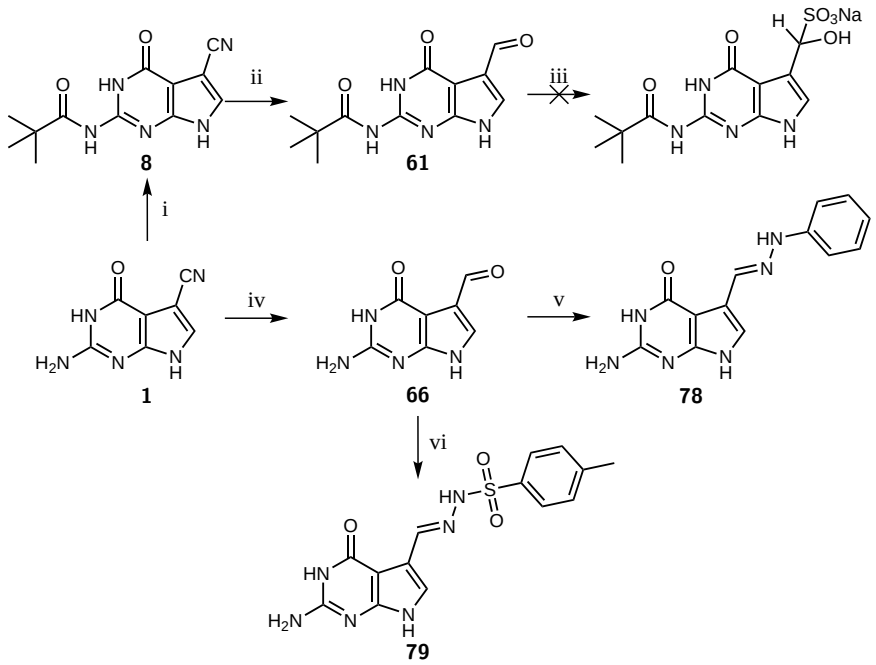

Scheme 3.33 Reduction of preQ$_0$ to 2-amino-5-formylpyrrolo[2,3-*d*]pyrimidin-4-one. (i) pivaloylchloride, pyridine, triethylamine, 90°C, (ii) Raney nickel, acetic acid/water 1/1, 55°C, (iii) $NaHSO_3$, ethanol, water, (iv) Raney nickel, pyridine/acetic acid/water 2/1/1, NaH_2PO_2, (v) phenylhyrdazine, (vi) *p*-toluenesulfonylhydrazide.

In this thesis, the reduction of preQ$_0$ (**1**) with Raney nickel in a variety of solvents with and without the addition of sodium hypophosphite was investigated. The reduction of preQ$_0$ in formic acid was not successful (Table 3.5). Formation of aldehyde **61** was observed when sodium hypophosphite was added to the reaction and diluted acetic acid was used as solvent. However, complete conversion could not be achieved according to reaction control by TLC. Formation of aldehyde **66** was also observed when pyridine/acetic acid/deionised water 2/1/1 was used as solvent and no sodium hypophosphite was added to the reaction mixture. Complete conversion could not be achieved. Reduction of preQ$_0$ to the corresponding aldehyde with Raney nickel is possible when either the appropriate solvent system pyridine/acetic acid/water 2/1/1 is used, or when sodium hypophosphite is added to the reaction in acetic acid. However highest conversions were achieved

when sodium hypophosphite was added to the reaction in pyridine/acetic acid/water 2/1/1. After stirring at room temperature over night 31.07% of aldehyde **66** could be isolated. Increasing the reaction temperature to 55°C further increased the isolated yield to 93.67%. The aldehyde **1** is highly unsoluble in most solvents. Extraction into ethyl acetate of dichloromethane is therefore not possible. Purification by column chromatography led to considerable loss of product, even when using highly polar eluents, such as dimethylformamide. A suitable procedure for work-up and purification of 2-amino-5-formylpyrrolo[2,3-*d*]pyrimidin-4-one was therefore developed. The catalyst was removed by filtration over celite and reaction solvent was evaporated in vacuum under repeated addition of methanol and toluene, to remove acetic acid and water, respectively, as azeotropes. The resulting brown slurry was diluted with 6M aqueous potassium hydroxide solution converting the product **66** into its corresponding potassium salt. Remaining solids were filtered off and the filtrate was neutralized by addition of concentrated hydrochloric acid. The product precipitated from the solution and was isolated by filtration, and washed with copious amounts of water. A second product fraction was isolated after reducing the volume of the filtrate to about one third. A large amount of salts precipitated along with the second product fraction. Salts were easily removed when washing the product with water. When necessary, the product could be further purified by again dissolving it in 6M aqueous potassium hydroxide solution and treating the resulting brown solution with activated charcoal. The activated charcoal was removed by filtration over celite and the product was precipitated from the filtrate by neutralizing with concentrated hydrochloric acid. According to this method, 2-amino-5-formylpyrrolo[2,3-*d*]pyrimidin-4-one (**66**) can easily be prepared in high yields and purity.

Table 3.5 Comparison of the reaction conditions for the synthesis of 2-pivaolylamino- and 2-amino-5-formylpyrrolo[2,3-*d*]pyrimidin-4-one

method	starting material	reagents	solvents	temperature, reaction time	yield
A	**1** ($preQ_0$)	Raney nickel	formic acid	80°C, 3h	no conversion
B	**8** (N-protected $preQ_0$)	Raney nickel, 3.3 eq. $NaPO_2H_2$	acetic acid/water 1/1	55°C, 8h	incomplete conversion
C	**1** ($preQ_0$)	Raney nickel	pyridine/acetic acid/water 2/1/1	room temperature, over night	incomplete conversion
D	**1** ($preQ_0$)	Raney nickel, 3.3 eq. $NaPO_2H_2$	pyridine/acetic acid/water 2/1/1	room temperature, over night	31.07% isolated yield
E	**1** ($preQ_0$)	Raney nickel, 3.3 eq. $NaPO_2H_2$	pyridine/acetic acid/water 2/1/1	55°C, 5h	93.67% isolated yield

A variety of derivates can be prepared from aldehydes to facilitate their isolation. The preparation of semicarbazones was described by Plieninger *et al.* Semicarbazones of indole-3-

acetaldehyde and 2-methylindol-3-acetaldehyde, among other aldehydes, were prepared [442, 443]. Phenylhydrazones are prepared in reduction of nitriles with nickel-catalysts, where phenylhydrazine reacts directly with the aldehyde formed in the reaction [444, 445].

Table 3.6 Reaction conditions for the synthesis of derivatives of 2-amino-5-formylpyrrolo[2,3-*d*]pyrimidin-4-one

method	starting material	reaction conditions	product
A	**61**	$NaHCO_3$, 0.1M HCl, acetic acid, water, methanol, phenylhydrazine	**80**
B	**66**	pyridine/acetic acid/water 2/1/1, pH 5, 2 eq. phenylhydrazine	**78**
C	**1** ($preQ_0$)	pyridine/acetic acid/water 2/1/1, 3 eq. NaH_2PO_2, Raney-nickel, 2 eq. phenylhydrazine	**78**
D	**1** ($preQ_0$)	pyridine/acetic acid/water 2/1/1, 3 eq. NaH_2PO_2, Raney-nickel, 2 eq. *p*-toluenesulfonyl hydrazide	**79**

In this thesis, 2-pivaloyl-protected, or unprotected 2-amino-5-formylpyrrolo[2,3-*d*]pyrimidin-4-one was easily converted into the corresponding phenylhydrazone. The aldehyde was either isolated and subsequently converted into the phenylhydrazone, or converted *in situ* during the reduction of $preQ_0$ to 2-amino-5-formylpyrrolo[2,3-*d*]pyrimidin-4-one, as summarized in Table 3.6. The formation of the phenylhydrazone was clearly visible on TLC. During *in situ* formation of the phenylhydrazone, no free aldehyde was detected on TLC or HPLC, indicating the aldehyde was quantitatively transformed into the phenylhydrazone. However, the phenylhydrazone could not be isolated, as significant amounts of product degraded during work-up. Therefore, *p*-toluenesulfonyl hydrazide was used for derivatization. Again, formation of the hydrazone was easily observed by TLC, however the toluenesulfonyl hydrazone also degraded during work up.

3.8 2-Amino-5-methyliminopyrrolo[2,3-*d*]pyrimidin-4-one and 2-amino-4-oxopyrrolo[2,3-*d*]pyrimidin-5-aldoxime

Several benzylimines with the $preQ_0$ core structure are available in literature. These 2-amino-5-aryliminopyrrolo[2,3-*d*]pyrimidin-4-ones, have different chloro- or fluoro-substituents in *ortho*- and/or *para*-position on the benzylring. These imines were prepared starting from 5-formyl-2-tritylaminopyrrolo[2,3-*d*]pyrimidin-4-one by addition of the corresponding amine in ethanol in the presence of sodium carbonate in yields of 57% to 80% [263].

In this thesis, 2-amino-5-methyliminopyrrolo[2,3-*d*]pyrimidin-4-one (**81**) was prepared starting from 2-amino-5-formylpyrrolo[2,3-*d*]pyrimidin-4-one, as depicted in Scheme 3.34. The reaction of the aldehyde with methyl amine was carried out at room temperature under inert atmosphere. The product was isolated in good yield of 56%.

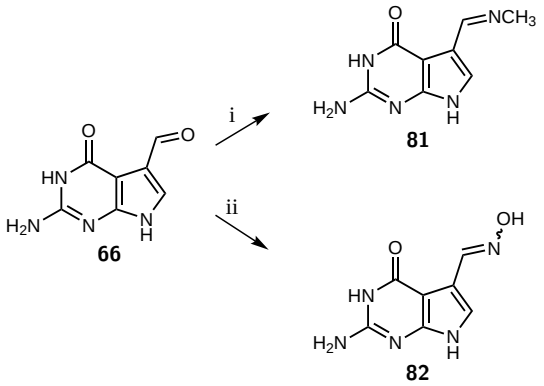

Scheme 3.34 Synthesis of imines and oximes. (i) methylamine, ethanol, room temperature, (ii) hydroxylamine hydrochloride, aqueous sodium hydroxide solution, room temperature to 50°C.

2-amino-4-oxopyrrolo[2,3-*d*]pyrimidin-5-aldoxime is a new compound. In literature, the similar oxime 4-chloropyrrolo[2,3-*d*]pyrimidin-5-aldoxime was prepared from the corresponding aldehyde using hydroxylamine hydrochloride and sodium hydroxide in ethanol [334, 446]. In this thesis, 2-amino-4-oxopyrrolo[2,3-*d*]pyrimidin-5-aldoxime (**82**) was prepared analogously and was isolated in excellent yield of 76%.

4

Results and Discussion II
Enzymes

4.1 *Geobacillus kaustophilus* nitrile reductase

4.1.1 Cloning, expression, purification

Nitrile reductase from *Geobacillus kaustophilus* is the first cloned and characterized nitrile reductase from a thermophile. It was identified in a BLAST search based on the sequence of nitrile reductase queF from *B. subtilis* [447]. Nitrile reductase from *G. kaustophilus* belongs to the type I (YkvM) subfamily, and shows 83% sequence identity and 93% sequence homology, respectively, to nitrile reductase from *B. subtilis*.

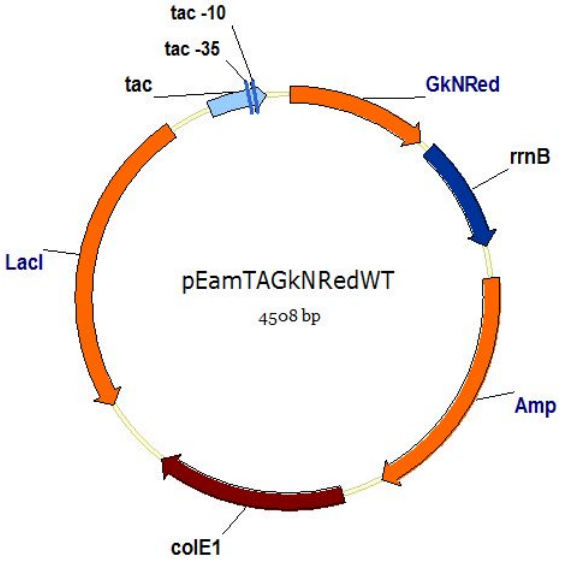

Figure 4.1 pEamTAGkNRedWT vector.

Nitrile reductase from *G. kaustophilus* was amplified from genomic *G. kaustophilus* DNA. The PCR products were gel purified. The DNA fragment was A-tailed and ligated with the Eam1105I linearised pEamTA vector to give the new vector pEamTAGkNRedWT, depicted in Figure 4.1. The ligation mixtures were transformed into electrocompetent *E. coli* K12 Top10F' cells

and positive transformations were selected on LB-ampicillin agar plates. Colonies with correctly integrated inserts were confirmed by digestions of plasmid DNA with NdeI and HindIII fast digest restriction enzymes and verified by sequencing. The plasmid pEamTAGkNRedWT was employed as template for site directed mutagenesis to generate the following mutants: F95A, H96A, H96F, E97A, E97S. Retransformation of the plasmids, carrying wild type or mutant nitrile reductase genes, into chemically competent *E. coli* BL21 (DE3) resulted in the *G. kaustophilus* nitrile reductase expression strains [264, 447, 448].

Main cultures of wild type and mutant nitrile reductase expression strains were cultured in LB-medium to an OD of 0.7, induced with IPTG and incubated for 24 hours at 16°C. The cells were harvested by centrifugation and disrupted by ultrasonication. Cell debris was removed by ultracentrifugation [264, 447, 448].

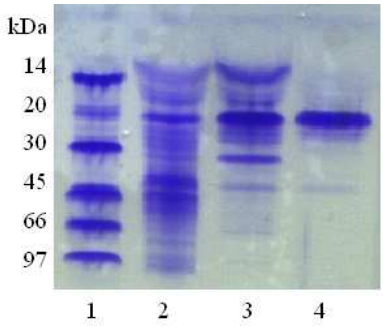

Figure 4.2 SDS-PAGE of stages in purification of wild type queF from *G. kaustophilus*. lane 1: low molecular weight standard (GE Healthcare), lane 2: cell-free extract, lane 3: partially purified wild type queF from *G. kaustophilus* after thermo-precipitation, lane 4: purified wild type queF from *G. kaustophilus* after ion-exchange chromatography.

Nitrile reductase from *G. kaustophilus* was purified by heat precipitation of the host proteins at 70°C or 75°C for ten minutes. Nitrile reductase was then stored at -20°C and used for substrate screening reactions. Nitrile reductase used for enzyme characterization and determination of kinetic parameters was further purified by ion exchange chromatography as depicted Figure 4.2 [449].

4.1.2 Enzyme characterization

The pH dependence of nitrile reductase from *G. kaustophilus* was investigated in a range of pH 5.5 to pH 10. *G. kaustophilus* queF exhibits a bell-shaped pH profile with maximal activity at pH 7.5, as depicted in Figure 4.3 [264, 449]. A similar bell shaped pH profile over a range from pH 5.4 to pH 9.4, with maximal activity at pH 7.50, was reported for *B. subtilis* queF [13]. The pH-dependence of *E. coli* queF was investigated in a range of pH 6 to pH 9. Optimum activity was reported at pH 7 [92].

The temperature dependence of nitrile reductase from *G. kaustophilus* was investigated for temperatures between 25°C and 65°C. Enzymatic activity increased 12-fold in response to a change in temperature from 25°C to 65°C. Determination of specific activities at higher temperatures are increasingly affected by NADPH degradation [264, 449]. Initial activity of *E. coli* queF was also

found to increase with an increasing temperature from 25°C to 50°C. However, at 50°C half life time of the enzyme was only six minutes [92].

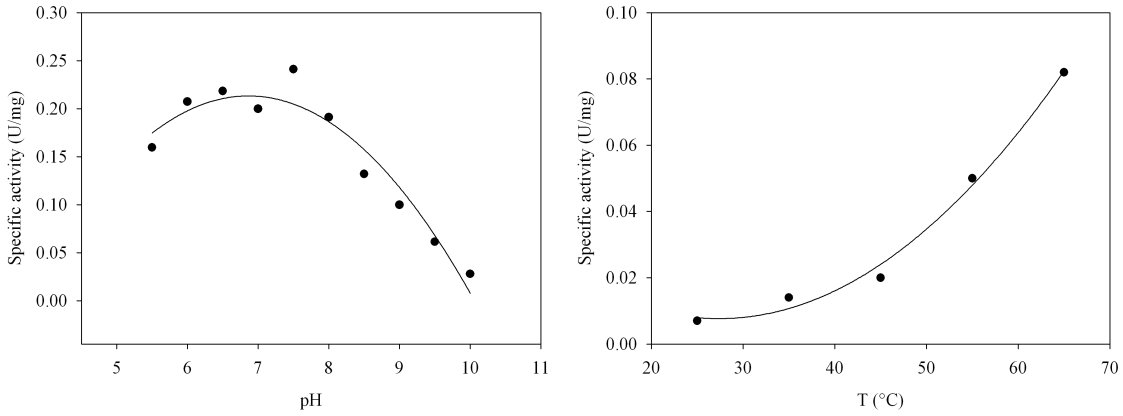

Figure 4.3 pH profile (left) and temperature dependence (right) of wild type queF from *G. kaustophilus*

Enzyme stability of *G. kaustophilus* queF was determined by incubation at 55°C and spectrophotometric determination of specific activities at every hour. Enzyme deactivation followed exponential decay and half-life times of 43 hours and 15 hours were determined with and without TCEP, respectively [264, 449]. Half-life times of 28.2h and 12.8h, at 37°C and 40°C, respectively, were reported for *E. coli* queF [92].

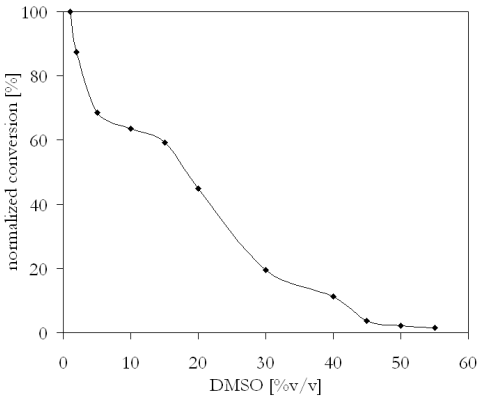

Figure 4.4 DMSO stability of wild type queF from *G. kaustophilus*.

DSMO stability was determined by incubation of wild type nitrile reductase with the natural substrate $preQ_0$ and NADPH at 30°C. DMSO concentrations of 1% v/v DMSO to 55% v/v DMSO were tested. The enzyme retains approximately 90% activity with 2% v/v DMSO and 10% activity up to 40% v/v DMSO, as depicted in Figure 4.4. Reports of DMSO stability for queF are not found in literature.

Biotransformations of the natural substrate with wild type nitrile reductase queF using NADH as cofactor were investigated. NADH as cofactor led to 20-fold lower conversions compared to biotransformations with NADPH. When the amount of NADH was increased to ten equivalents, similar conversions as in reactions with 2.5 equivalents of NADPH were found.

4.2 *Escherichia coli* nitrile reductase

4.2.1 Cloning, expression, purification

The nitrile reductase gene from *E. coli* (gene ID: 947270) was amplified by PCR from the genomic DNA of *E. coli* strain K-12. For the purification of the nitrile reductase, several tagging strategies were investigated. Enzymes with a C-terminal Strep-tag or His-tag with Factor X cleavage site did not express well and the enzyme with the Strep-tag was not functional. The C-terminus of the protein is located at the dimer interface, likely to complicate purification by affinity chromatography. The gene was therefore NcoI-HindIII-cloned into the pEHISTEV vector, providing the sequence for an N-terminal 6xHis-tag, followed by a TEV protease cleavage site [450]. The ligation product was transformed into electrocompetent *E. coli* TOP10 F' cells and plated on LB-agar supplemented with kanamycin. The resulting plasmid pEHISTEV HISEcNRedWT was isolated and the sequence was confirmed by LGC Genomics [447, 448, 451].

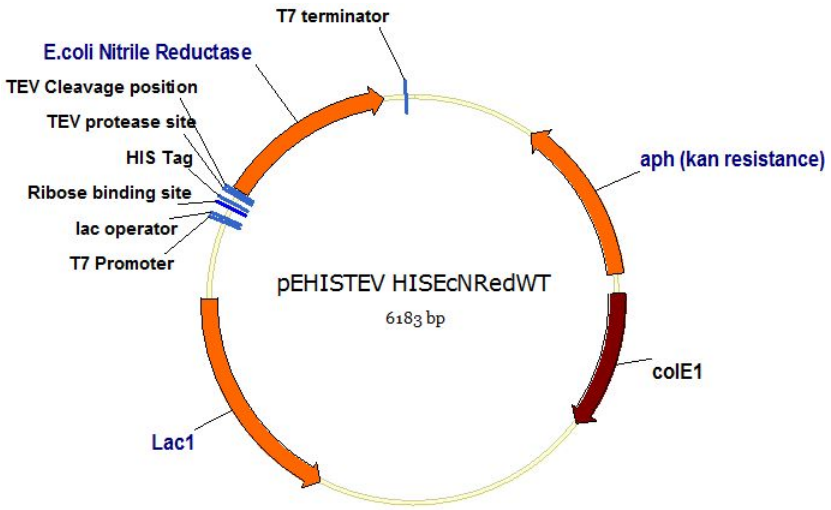

Figure 4.5 pEHISTEV HISEcNRedWT vector.

The plasmid pEHISTEV HISEcNRedWT was employed as template for site directed mutagenesis generating the following mutants: E89A, E89L, S90A, C190A, D197N, D197N + L201I, F228W, H229A, E230Q. Plasmids from wild type and mutants with the correct sequence were transformed into *E. coli* BL21 (DE3). Main cultures were grown to an OD of 0.6-0.8, induced with IPTG, and incubated for 18 hours to 20 hours at 37°C and 130rpm. Expression worked well at temperatures from 16°C, to 37°C, as depicted in Figure 4.6. The cells were harvested by centrifugation and disrupted by ultrasonication. Cell debris was removed by ultracentrifugation [447, 448, 451].

The cell-free extract was purified on a Ni sepharose 6 fast flow column, as depicted in Figure 4.7. The collected protein fractions were concentrated and used directly for screening reactions [447, 448, 451]. Activity of the wild type enzyme decreased tremendously during storage. After twelve months of storage at -70°C wild type nitrile reductase retained only around 1% activity [449]. To ensure optimum activity, the cell-free extract was purified immediately after cell disruption, without intermediate storage or freezing steps, and the enzyme was used for screening reactions directly after purification.

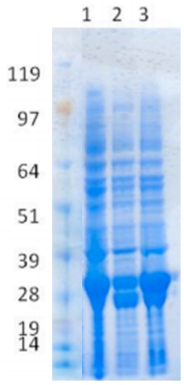

Figure 4.6 Expression study for wild type nitrile reductase from *E. coli*.
SeeBlue 2 Standard (Invitrogen), cell free extract, lane 1: expression at 16°C, lane 2: expression at 25°C, lane 3: expression at 37°C.

SDS-PAGE analysis (Figure 4.6) and Caliper chromatograms (Figure 4.8) of *E. coli* nitrile reductase show two overexpressed bands, corresponding in size to *E. coli* queF with tag (35.9kDa) and without tag (32.6kDa), respectively [448]. Either the His-tag is cleaved off during lysate preparation or the enzyme is partly expressed without the tag, as a second ATG is present in the vector directly before the gene. Both bands are still present after purification over a Ni sepharose column, even though only protein with a His-tag should bind to the column while all other protein is washed off. However, the native state of nitrile reductase from *E. coli* is a dimer of dimers. Therefore, a tagged dimer might dimerize with an untagged dimer, leading to a dimer of dimers bearing the His-tag on only one of the dimer units and therefore binding to the Nickel-sepharose column.

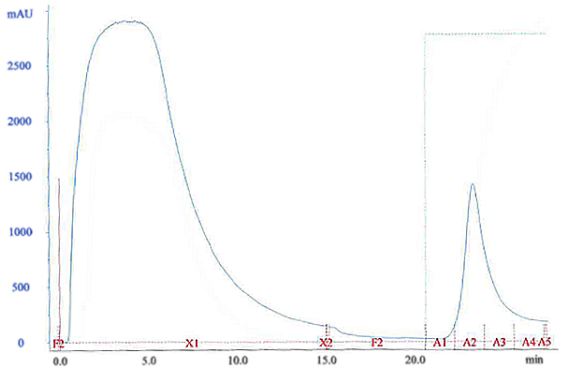

Figure 4.7 Purification of wild type and mutant nitrile reductase from *E. coli* - Äkta elution profile.

The two protein bands of the purified nitrile reductase queF from *E. coli* were further investigated by Caliper measurements. Caliper assays are suitable for protein samples of 14kDa to 200kDa and can provide relative protein concentrations, molecular size, and percent purity. When the His-tag was cleaved from purified wild type nitrile reductase queF by TEV protease, the fraction of the protein in the lower band increased compared to the wild type enzyme before His-tag cleaveage, as depicted in Figure 4.8 [448].

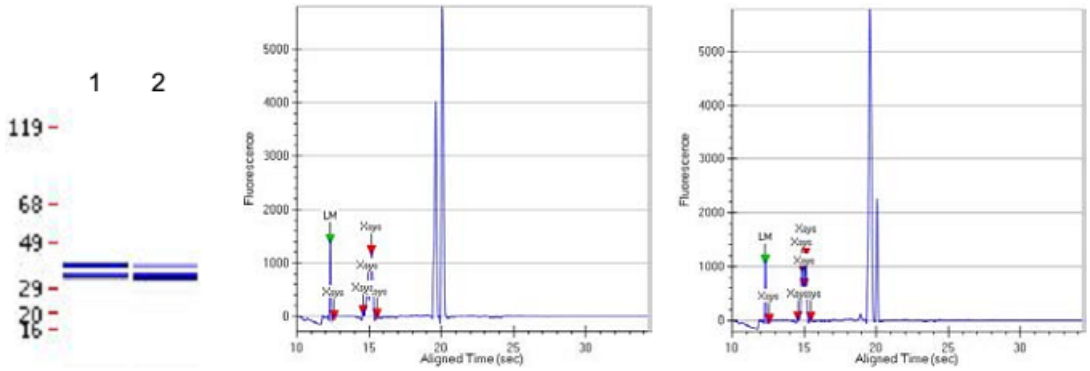

Figure 4.8 Caliper anaylsis of the TEV cleavage of the His-Tag from wild type nitrile reductase from *E. coli*. Lane 1 wild type enzyme without cleavage of the tag, lane 2 wild type enzyme after cleavage of the tag and HisTrap run, chromatograms correspond to lane 1 (left) and lane 2 (right), respectively.

The absence of a His-tag in the lower band was investigated by Western blot [448]. A Western blot uses gel electrophoresis to separate proteins which are then transferred to a membrane, where they are stained with antibodies specific to the target protein. A His-tag selective Western blot therefore shows only bands of His-tagged proteins. The Ponceau S staining, depicted in Figure 4.9 shows the double band of the wild type enzyme and the S90A mutant with N-terminal His-tags, as well as a single band for the wild type enzyme were the His-tag was cleaved off, and for the enzyme with Strep-tag or C-terminal His-tag. Ponceau S staining can be removed with water washes, facilitating subsequent immunological detection. The Western blot against the His-tag showed only the upper band of the double band, verifying that the lower band does not contain His-tagged protein.

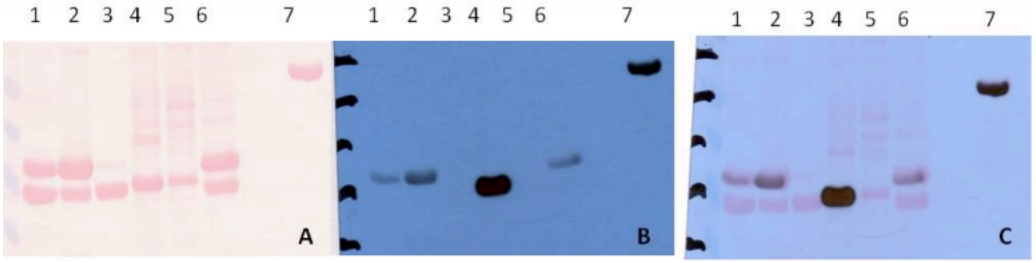

Figure 4.9 Western blot for the detection of His-Tags in wild type nitrile reductase from *E. coli*. A: Ponceau S staining of the membrane, B: Western blot against the His-tag, C: overlay A and B. Lane 1: purified wild type queF with N-terminal His-tag, lane 2: purified S90A mutant queF with N-terminal His-tag, lane 3: purified wild type queF after cleavage of the His-tag, lane 4: cell free extract of wild type queF with C-terminal His-tag, lane 5: cell free extract of wild type queF with C-terminal Strep-tag, lane 6: cell free extract of wild type queF with N-terminal His-tag, lane 7: positive control.

5

Results and Discussion III
Biocatalytic Screening Reactions

5.1 Nitrile reduction

Nitrile hydrolysing enzymes have been successfully applied in chemical synthesis and chemical industries for several years, however biological nitrile reduction has become possible only with the discovery of nitrile reductase queF. A number of nitriles are suggested as non-natural substrates for nitrile reductase queF in a patent by Dirk Iwata-Reuyl [93]. Besides this patent, no applications of nitrile reductase queF in biocatalysis are available in literature.

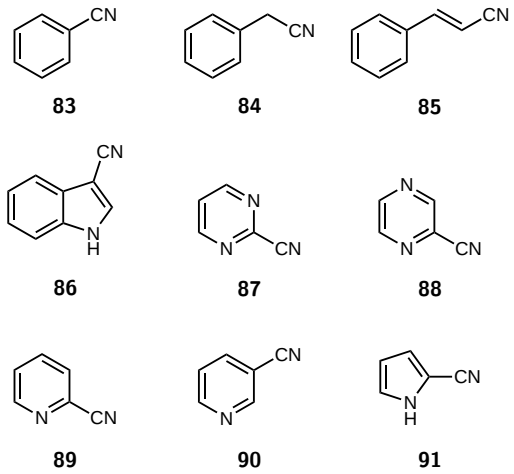

Figure 5.1 Set of nitriles used for initial screenings with wild type nitrile reductase queF from *B. subtilis*, *G. kaustophilus* and *E. coli*.

In this thesis, a number of simple, commercially available nitriles were chosen for an initial substrate screening. This first set of nitriles included two of the compounds suggested as substrates in Iwata-Reuyl's patent [93], namely phenylacetonitrile (**84**) and 3-cyanoindole (**86**), and a variety of aromatic, aliphatic and heterocyclic nitriles, as depicted in Figure 5.1. Aromatic nitriles, like benzonitrile (**83**), bear the nitrile group directly at the aromatic ring, while phenylacetonitrile (**84**) has the nitrile group in an aliphatic open chain fragment in comparable distance to the natural substrate $preQ_0$. Cinnamonitrile (**85**) bears the nitrile group on a double bond in a conjugated unsaturated sytem. Heterocyclic nitriles included 3-cyanoindole (**86**), resembling the bycyclic core-

structure of the natural substrate $preQ_0$, as well as monocyclic five- or six-membered rings.

Initial screenings were carried out with wild type nitrile reductase type I from *B. subtilis*, and *G. kaustophilus*, and type II from *E. coli*. Biotransformation reactions with the natural substrate $preQ_0$ were done as positive controls to ensure enzyme activity. Nitrile reductase from *B. subtilis*, *G. kaustophilus*, and *E. coli* was found active for the reduction of $preQ_0$. However, none of the nitriles shown in Figure 5.1 were accepted as substrate, indicating high substrate specificity. The substrate scope and substrate binding of nitrile reductase queF was then investigated by synthesis and screening of structural analogues of the natural substrate $preQ_0$ and by introducing rational mutations to the active site.

5.1.1 *Geobacillus kaustophilus* nitrile reductase

Active site mutations of *G. kaustophilus* queF were chosen based on an active site model of *B. subtilis* queF. *G. kaustophilus* queF shows 83% sequence identity and 93% sequence similarity with *B. subtilis* queF. A homology model of *B. subtilis* queF was published based on the crystal structure of *E. coli* GTP-CH-I. Sequence identity and similarity of *B. subtilis* queF with *E. coli* GTP-CH-I is 14% and 26%, respectively. The location of the active site was predicted at the intersubunit interface. In one monomer, the docked substrate interacts with two conserved side chains of Glu97 and Cys55, as well as with Phe95 and the backbone NH of His96. In the other monomer the side chain of Ser97 and the backbone CO of Val77 were identified to interact with the substrate [73]. Additionally to substrate binding, Cys55 was proposed to play an essential role in the covalent catalysis mechanism [13].

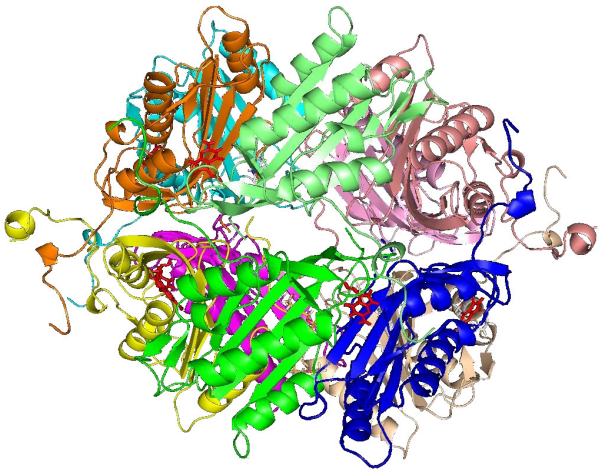

Figure 5.2 Homology model of nitrile reductase queF from *Geobacillus kaustophilus*, based on the crystal structure of *B. subtilis* queF.

The crystal structure of *B. subtilis* queF was solved in 2012. The crystal structure of wild type enzyme with $preQ_0$ bound (4F8B), as well as the structure of a C55A mutant (4FGC) was published [89]. The structure reveals a homodecamer of two head-to-head facing pentamers. Based on the crystal structures, an homology model of *G. kaustophilus* queF was calculated, as depicted in Figure 5.2 [452]. The active sites are located at the intersubunit interfaces. Two of the ten active sites in the *B. subtilis* queF structure were found unoccupied, providing insight into the differences

in active site structure with or without substrate bound [89]. The model of *G. kaustophilus* queF, depicted in Figure 5.3 clearly shows the conformational change associated with $preQ_0$ binding. $PreQ_0$ binding is therefore suggested to stabilize the functional decamer.

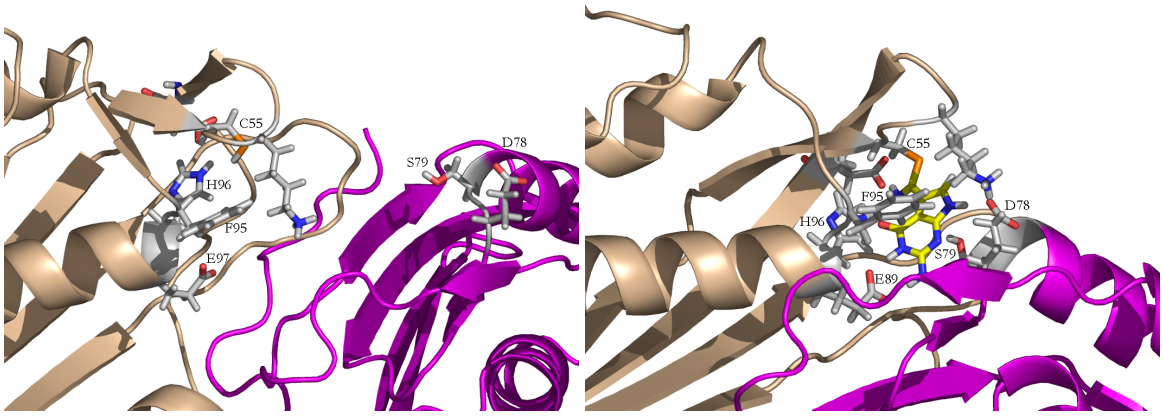

Figure 5.3 Active site of *G. kaustophilus* nitrile reductase. Left: open active site, without substrate bound, right: closed active site with $preQ_0$ bound.

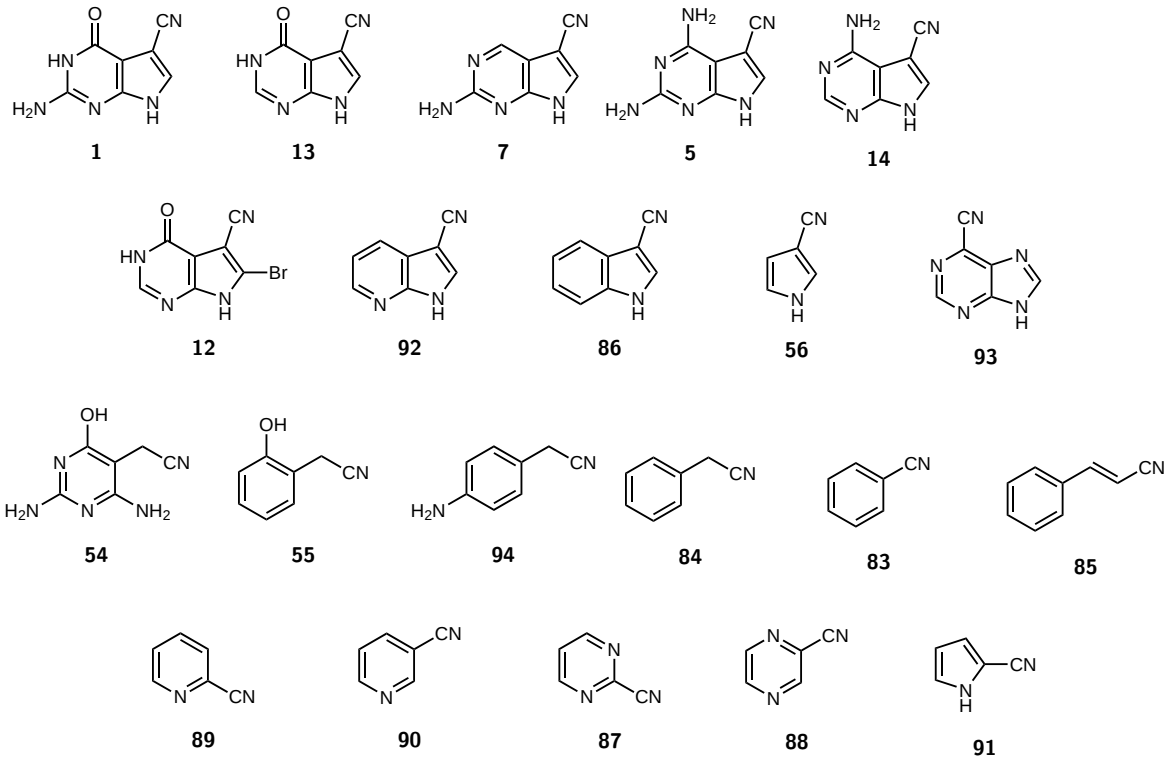

Figure 5.4 Full range of nitriles used for screening reactions with wild type and mutant nitrile reductase queF from *Geobacillus kaustophilus*, including nitriles depicted in Figure 5.1

The homology model of *B. subtilis* queF and the crystal structure published subsequently, suggest similar amino acid residues that interact with the substrate. In active site mutations, the amino acids identified to interact with the substrate were replaced. His96 and Glu97, coordinating to the keto- and amino- functionality of the natural substrate $preQ_0$, respectively, and Phe95, holding the substrate in place by π-π stacking, were exchanged by smaller amino acid residues. Furthermore, Cys55 was replaced by Ala to verify its essential role in the catalytic mechanism.

A number of structural analogues of the natural substrate $preQ_0$ were prepared in chemical synthesis, as discussed in chapter 3. Those compounds are differing from $preQ_0$ in their functional groups. Nitriles **13** and **7** resemble the natural substrate $preQ_0$ (**1**) except for the keto- and amino- substituents, respectively, on the pyrimidine ring. Nitriles **5**, **14** and **12**, show the same core structure as $preQ_0$, but differ in their substituents. Compounds **5** and **14** have an amino-functionality instead of the keto-functionality in position 4, compound **12** shows a bromo-substituent in position 6. Additionally to these pyrrolo[2,3-*d*]pyrimidines, nitriles resembling only the pyrimidine part of $preQ_0$, as compounds **54**, **55** and **94**, as well as resembling only the pyrrole part, as compound **56** were prepared. The full range of nitriles screened is depicted in Figure 5.4.

Substrate screening was carried out in 96-well plates to simultaneously screen the complete set of substrates with one variant in a multiple determinations. Screenings were carried out with purified enzyme, as described in chapter 7. Reactions were started by addition of NADPH. The consumption of NADPH was then monitored at 340nm on a plate reader. Subsequently, the samples were analyzed by HPLC-MS to monitor product formation. Enzymatic activity can therefore be detected by decrease of NADPH absorption and validated by the analysis of product formation by HPLC-MS.

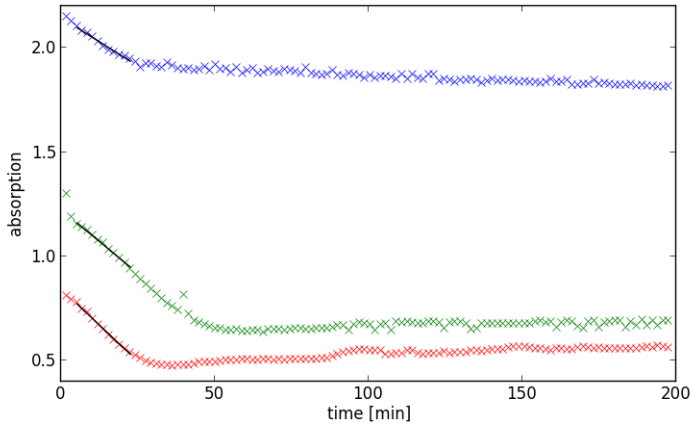

Figure 5.5 NADPH depletion in the conversion $preQ_0$ (**1**, green), 5-cyanopyrrolo[2,3-*d*]pyrimidin-4-one (**13**, red) and 2-amino-5-cyanopyrrolo[2,3-*d*]pyrimidine (**7**, blue) with wild type queF from *G. kaustophilus*

The natural substrate $preQ_0$ as well as two non-natural substrates were successfully reduced to their corresponding primary amines by nitrile reductase queF from *G. kaustophilus*. These two non-natural substrates **13** and **7**, are the first non-natural substrates reduced by nitrile reductase queF. Compounds **13** and **7**, differ from the natural substrate $preQ_0$ in absence of the amino- or keto-substituent on the pyrimidine ring, respectively. Conversions of substrate **13**, missing the amino-group, were comparable to those of the natural substrate $preQ_0$, whereas conversions of substrate **7** were significantly lower (Table 5.1). Reaction rates for the reduction of compound **13** were similar compared to those of the natural substrate $preQ_0$, whereas the reduction of compound **7** proceeded slower, as depicted in Figure 5.5.

Based on the screening results, *G. kaustophilus* queF exhibits high substrate specificity. Monocyclic substrates were not reduced, even those closely resembling the natural substrate, e.g. compounds **56** or **54**. The bicyclic structure of the natural substrate $preQ_0$ might be necessary to stabilize the functional protein. However, bicyclic substrates, such as compounds **92**, and **86**

were neither accepted as substrates, indicating the importance of the functional groups on the six-membered ring for substrate binding.

Substrate analogues differing from the natural substrate $preQ_0$ in their number of ring heteroatoms will be used to investigate the influence of the ring heteroatoms on substrate binding. 3-Cyanopyrrolo[3,2-*c*]pyridines and 3-cyanopyrrolo[2,3-*b*]pyridines differ from the natural substrate $preQ_0$ in the number of ring heteroatoms in the six membered ring. Screening of these compounds will give insight into the influence of the pyrimidine nitrogens on substrate binding. 5-Cyanothieno[2,3-*d*]pyrimidines and 5-cyanocyclopenta[*d*]pyrimidines were designed to probe the influence of the pyrrole nitrogen on substrate binding. In thieno[2,3-*d*]pyrimidines, the NH of the pyrrole ring of the natural substrate$preQ_0$ is replaced with a sulfur in the thiophene ring, thereby NH as a hydrogen bond donor is replaced by S as a hydrogen bond acceptor. 3-Cyanopyrazolo[3,4-*d*]pyrimidines have an additional nitrogen heteroatom in the five membered ring compared to the natural substrate $preQ_0$.

Table 5.1 HPLC-MS based screening results of wild type and mutant nitrile reductase queF from *G. kaustophilus*.

	1	**13**	***7***	other substrates
wild type	95 %	100 %	< 5 %	n. c.
wild type His Tev	85 %	40 %	< 5 %	n. c.
C55A	n.c.	n. d.	n. d.	n. d.
F95A His Tev	< 5 %	14 %	< 5 %	n. c.
H96A	67 %	100 %	< 5 %	n. c.
H96F	29 %	32 %	< 5 %	n. c.
E97A	96 %	75 %	< 5 %	n. c.
E97S	> 99 %	74 %	< 5 %	n. c.

n. c. = no conversion, n. d. = not determined.

All mutants, except Cys55Ala, were found to be active for the reduction of $preQ_0$ and nitriles **13** and **7**. The Cys55Ala mutant was inactive for the conversion of all substrates, including $preQ_0$, proving the essential role of Cys55 in the catalytic mechanism. All other mutants accepted the same substrates as the wild type enzyme, however conversions differed (Table 5.1). Conversions with Phe95Ala were considerably lower, probably due to the loss of π-π stacking between Phe95 and the substrate. Two different mutations were done on His96. His96Phe exchanges the histidine against an amino acid of comparable size, whereas His96Ala exchanges histidine against the small amino acid alanine. His96 is proposed to coordinate to the keto-group of $preQ_0$ by main chain interaction. His96Phe, and His96Ala should therefore still coordinate to the substrate, however, His96Ala might increase the space available in the active site. Comparing His96Phe and His96Ala, higher conversions were achieved with His96Ala. However, no additional substrates were found to be accepted by the His96Ala mutant. Mutations of Glu98 in *B. subtilis* queF, equivalent to Glu97 in *G. kaustophilus* queF, were reported to potentially change substrate specificity [93]. Glu97Ala

exchanges the charged gluatmic acid residue by the neutral residue alanine, whereas Glu97Ser replaces the C-6 amino acid glutamic acid by the C-3 amino acid serine. Serine still provides an OH-group and could therefore coordinate to an amino-group in the substrate. Glu97Ala and Glu97Ser mutants of *G. kaustophilus* queF showed similar conversions as wild type enzyme and did not show changed substrate specificity compared to wild type enzyme (Table 5.1).

Table 5.2 Apparent kinetic parameters for wild type nitrile reductase queF from *G. kaustophilus*, measured at 55°C.

	1	**13**	**7**
K_m, substrate [μM]	11 ± 5	336 ± 37	> 1000
k_{cat} [min^{-1}]	3.9 ± 0.6	9.3 ± 1.8	n.d.
k_{cat}/K_m [$min^{-1}\mu M^{-1}$]	0.35	0.028	3.2*10^{-6} [a]
K_m, NADPH [μM]	34 ± 7	60 ± 9	n.d.

[a] Saturation of substrate was not achieved, therefore, initial rates were recorded under conditions in which pseudo first-order kinetics can be assumed. k_{cat}/K_m was determined from the linear part of the Michaelis-Menten curve. n. d. = not determined.

Apparent kinetic parameters were determined for wild type nitrile reductase queF from *G. kaustophilus* to compare the non-natural substrates **13** and **7** to the natural substrate $preQ_0$ (**1**) [449]. The non-natural substrates both showed higher K_m-values than the natural substrate, indicating weaker substrate binding in the active site. The k_{cat}-value of the non-natural substrate **13** is higher than for the natural substrate, possibly due to weaker substrate binding. K_m- and k_{cat}- values for the natural substrate $preQ_0$ with *G. kaustophilus* queF are higher than those reported in literature for *B. subtilis* queF [13]. The turn over number (k_{cat}/K_m) of *G. kaustophilus* queF is 5.5-fold increased compared to *B. subtilis* queF. The higher K_m-value of *G. kaustophilus* queF was attributed to the higher temerature (55°C) in initial rate measurements. The high sequence homology between *B. subtilis* queF and *G. kaustophilus* queF suggests similar substrate binding. Substrate binding is a temperature sensitive step, as hydrophobic interactions form endothermically and are weakened by a deacrease in temperature, whereas electrostatic interactions form exothermically and are stabilized at low temperature [453]. The higher K_m-value of *G. kaustophilus* queF, compared to *B. subtilis* queF is therefore most likely due to weakened interactions in the substrate binding site.

Inhibition studies were performed to further evaluate the structural features necessary for substrate binding [449]. The set of compounds chosen for inhibitor screenings is depicted in Figure 5.6, and included monocyclic compounds resembling the natural substrate $preQ_0$ in the functional groups (**55**, **94**), and bicyclic compounds differing from $preQ_0$ in the number of heteroatoms and functional groups (**37**, **19**, **20**, **92**). Three inhibitors were identified, namely compounds **60**, **94**, and **37**. 2-Aminopyrrolo[2,3-*d*]pyrimidin-4-one represents the $preQ_0$-core structure, differing from $preQ_0$ only in the absence of the cyano-group. All three inhibitors bear an amino-group in similar position as $preQ_0$. Among the 15 compounds tested as inhibitors, three possessed an amino-group in relevant position, these three compounds were all identified as inhibitors (**60**, **94**, **37**), as summarized in Table 5.3. The amino-group in position 2 of the natural

substrate might therefore have a significant effect on substrate binding.

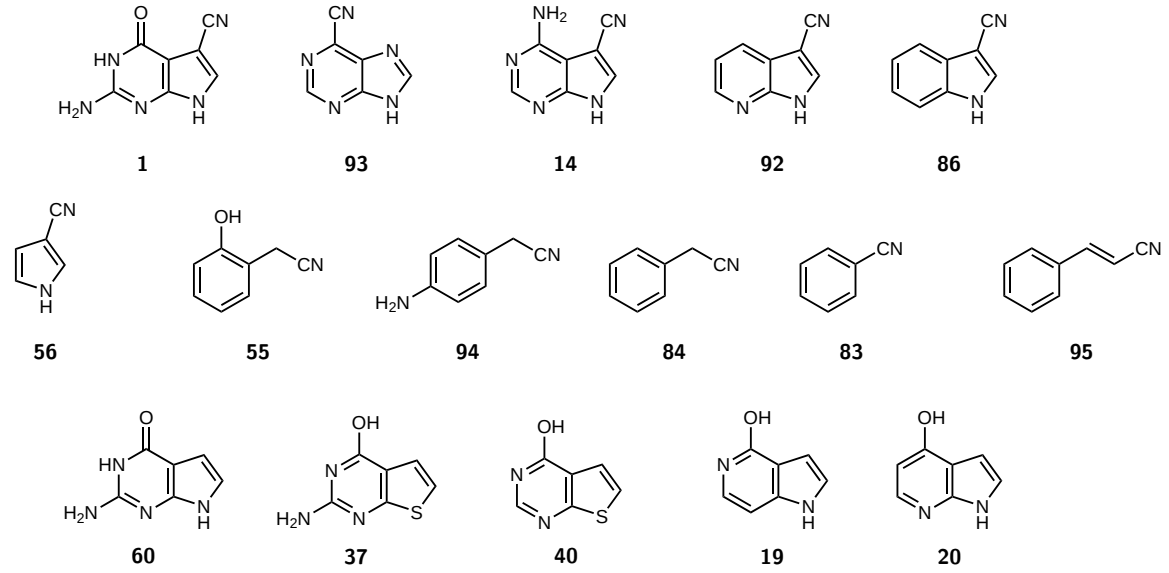

Figure 5.6 Compounds used for inhibition studies with wild type and mutant nitrile reductase queF from *G. kaustophilus*

Table 5.3 Screening for *G. kaustophilus* nitrile reductase inhibitors. Residual activities refer to nitrile reductase activities obtained with 10 μM $preQ_0$ (K_m $preQ_0$)

compound [mM]	residual activity [%]
6-cyanopurine, **93**, [0.5mM]	107
4-amino-5-cyano-7*H*-pyrrolo[2,3-*d*]pyrimidine, **14**, [5mM]	90
7-aza-3-cyanoindole, **92**, [2mM]	101
3-cyanoindole, **86**, [2mM]	87
3-cyano-1*H*-pyrrole, **56**, [10mM]	93
2-hydroxybenzylcyanide, **55**, [10mM]	100
4-aminobenzylcyanide, **94**, [10mM]	0
phenylacetonitrile, **84**, [20mM]	120
benzonitrile, **83**, [20mM]	99
cinnamonnitrile, **95**, [20mM]	122
2-amino-7*H*-pyrrolo[2,3-*d*]pyrimidine-4-one, **60**, [5mM]	17
2-amino-4-hydroxythieno[2,3-*d*]pyrimidine, **37**, [1.67mM]	72
4-hydroxythieno[2,3-*d*]pyrimidine, **40**, [5mM]	101
5-aza-4-hydroxyindole, **19**, [5mM]	94
7-aza-4-hydroxyindole, **20**, [2mM]	109

5.1.2 *Escherichia coli* nitrile reductase

An homology model of *E. coli* queF was calculated based on the crystal structure of *V. cholerae* queF (3RZQ), as depicted in Figure 5.7 [452]. Sequence identity between the two enzymes is 65%, while sequence similarity is 76%. Although *V. cholerae* queF is not experimentally characterized it is likely to possess the same enzymatic activity and is therefore considered a good model for studies of type II nitrile reductase. *V. cholerae* queF crystallizes as dimer of dimers, solution data suggest the protein is a dimer and exists in equilibrium with its monomer. The substrate is bound to each of the four monomers in a cavity near the dimer interface. However, only one molecule of NADPH can bind to a dimer and serves only one of the two sites occupied by substrate. Consequently, the dimer is considered a minimal biological unit and queF should exhibit half-site reactivity [91].

According to the active site model depicted in Figure 5.7, the substrate is oriented by a series of hydrogen bonds and a ring-stacking interaction with Phe228. The ring nitrogen in position 1 is coordinated to the main chain of Ser90, while the Glu230 residue coordinates to the amino-functionality in position 2, as well as to the ring nitrogen in position 3. The amino-group in position 2 is also interacting with the main chain of Ile88. The ring-nitrogen in position 7 is coordinated by Glu89. Finally, the keto-functionality in position 4 is interacting with His229. These amino acid residues might therefore be involved in substrate specificity.

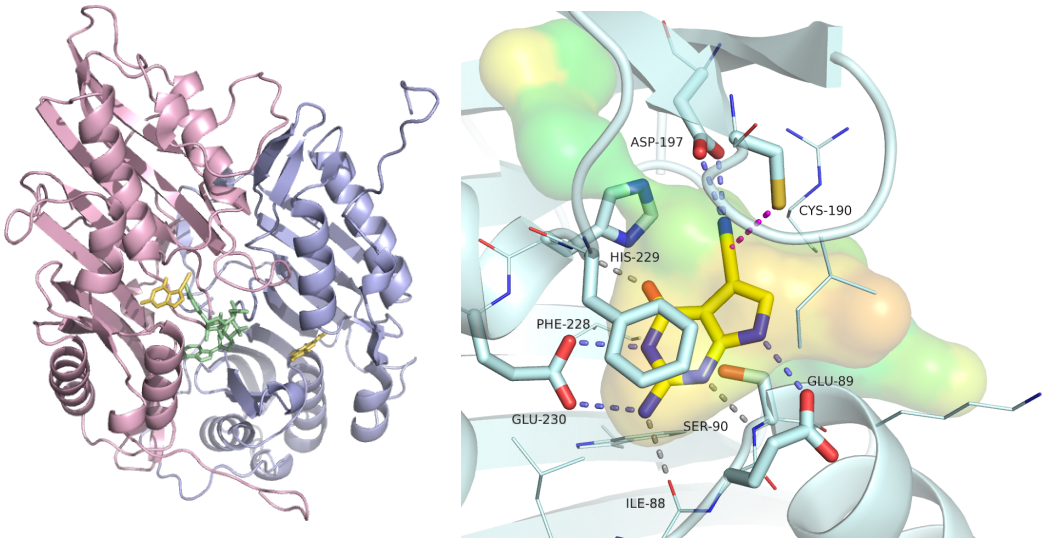

Figure 5.7 Homology model of nitrile reductase queF from *E. coli*, based on the crystal structure of *Vibrio cholerae* queF. Left: dimeric queF, right: energy minimized model of the active site of wild type nitrile reductase queF from *E. coli*. The cavity is shown as transparent surface and coloured hydrophobicity values (red hydrophobic, green less hydrophilic, blue hydrophilic). Distances to binding residues are shown as dashed lines. Grey dashed lines indicate interactions with the main chain of the amino acid, while blue dashed lines indicate interactions with the side chain. The magenta dashed line indicates where the active site Cys190 should attack the substrate to form the covalent reaction intermediate.

His229, Asp197, found in its close proximity, and Cys190 are amino acids involved in the mechanism proposed. The reduction of $preQ_0$ to its corresponding primary amine requires four protons and four electrons transferred to the substrate. The inital step of the reduction of $preQ_0$ involves formation of a covalent adduct by nucleophilic attack of the Cys190 residue on the cyano-residue of the substrate. This covalent bond is then postulated to hold the substrate in place while

two molecules NADPH donate hydrides to the substrate. These two hydride transfers account for two protons and four electrons. The inital proton is transferred to the substrate during formation of the covalent adduct. The final proton is then provided by His229 [13, 91].

Additionally to natural substrate analogues screened with nitrile reductase queF from *G. kaustophilus*, new natural substrate analogues were chosen for screening reactions with nitrile reductase queF from *E. coli*, as depicted in Figure 5.8. Two non-natural substrates (**13**, **7**) could be identified in screenings with nitrile reductase from *G. kaustophilus*. These two substrates differ from the natural substrate in the absence of the amino- or keto- functionality, respectively, on the pyrimidine ring. Consequently, for screenings with nitrile reductase from *E. coli*, natural substrate analogues bearing protecting groups on these functionalities were prepared. The keto-functionality was substituted for a methoxy-group (**9**), while the amino-group was protected with a pivaloyl-group (**8**). Furthermore, a natural substrate analogue missing both functional groups on the pyrimidine ring, 5-cyanopyrrolo[2,3-*d*]pyrimidine (**16**), was prepared.

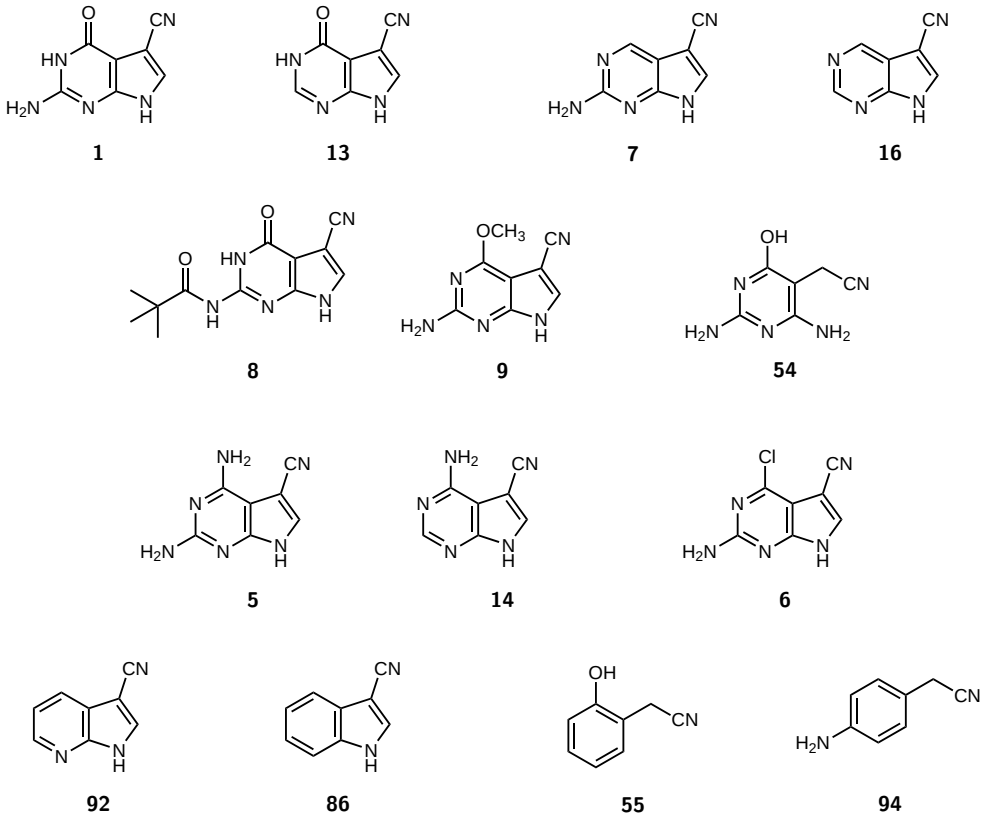

Figure 5.8 Full set of nitriles used for screening reactions with wild type and mutant nitrile reductase queF from *Escherichia coli*.

Wild type nitrile reductase queF from *E. coli* was found to be active for the conversion of its natural substrate preQ$_0$ (**1**), as well as the two non-natural substrate 5-cyanopyrrolo[2,3-*d*]pyrimidin-4-one (**13**) and 2-amino-5-cyanopyrrolo[2,3-*d*]pyrimidine (**7**), as summarized in Table 5.4 and Table 5.5. While the natural substrate **1** and nitrile **13** were quantitatively reduced to their corresponding amines, the reduction of nitrile **7** was not detectable by HPLC-MS (Table 5.4). These results are consistent with spectrophotometric determinations of specific activities. Specific activities for substrates **1** and **13** are in the same range, however, specific activity for substrate **7**

was found to be significantly lower. Docking simulations, depicted in Figure 5.9 indicate substrate **13** is coordinated to the active site similarly to the natural substrate $preQ_0$. However, the Glu230 residue is coordinating to the N-3 ring heteroatom only, as the substrate differs from the natural substrate in the absence of the amino group in position 2. In substrates **7** and **16** substrate binding is further decreased by the absence of the keto- functionality and therefore missing coordination by the His229 residue.

Table 5.4 HPLC-MS based screening results of wild type and mutant nitrile reductase queF from *E. coli*.

	1	**13**	**7, 16**	other substrates
wild type	100 %	100 %	n. c.	n. c.
E89A	< 2 %	< 2 %	n. c.	n. c.
E89L	< 2 %	< 2 %	n. c.	n. c.
S90A	100 %	> 98 %	n. c.	n. c.
C190A	n. c.	n. c.	n. c.	n. c.
D197N	n. c.	n. c.	n. c.	n. c.
D197N + L201I	n. c.	n. c.	n. c.	n. c.
F228W	100 %	> 98 %	n. c.	n. c.
H229A	98 %	> 98 %	n. c.	n. c.
E230Q	< 5 %	< 5 %	n. c.	n. c.

n. c. = no conversion

Substrate analogues differing from the natural substrate $preQ_0$ in their number of ring heteroatoms will be used to investigate the influence of the ring heteroatoms on substrate binding. These substrate analogues include 3-cyanopyrrolo[3,2-*c*]pyridines, 3-cyanopyrrolo[2,3-*b*]pyridines, 5-cyanothieno[2,3-*d*]pyrimidines, 5-cyanocyclopenta[*d*]pyrimidines and 3-cyanopyrazolo[3,4-*d*]-pyrimidines. Several amino acid residues were identified to coordinate to the ring heteroatoms. Interaction of Glu230 with N-3, and coordination of Ser90 to N-1 and Glu89 to N-7 respectively, are indicated in the active site model depicted in Figure 5.7.

In order to verify their proposed role in the catalytic mechanism, enzyme variants with amino acid exchanges at Cys190, Asp197 and His229 were prepared. The substitution of the active site nucleophile Cys190 by alanine resulted in a protein that was no longer active for the conversion of neither the natural substrate, nor any of the non-natural substrates (Table 5.4). The essential role of the cysteine residue was previously proven by Cys55Ala and Cys55Ser mutant of *B. subtilis* queF [13]. Crystallization of a Cys55Ala mutant from *B. subtilis* showed non-covalently bound $preQ_0$, while covalently bound substrate was found in the crystal structure of the thioimide complex [89]. However, in this thesis, substitutions of the aspartic acid or histidine residue were done first. The Asp197Asn mutation led to complete loss of activity, confirming its essential role in the catalytic mechanism. However, the His229Ala mutant retained activity, leading to similar conversions as wild type enzyme (Table 5.4). Specific activities, however, were approximately one order of magnitude lower than for the wild type enzyme (Table 5.5). Based on this data, the aspartic acid

residues seems to be essential for reduction of the substrate, while an essential role of the histidine residue in the catalytic mechanism could not be verified.

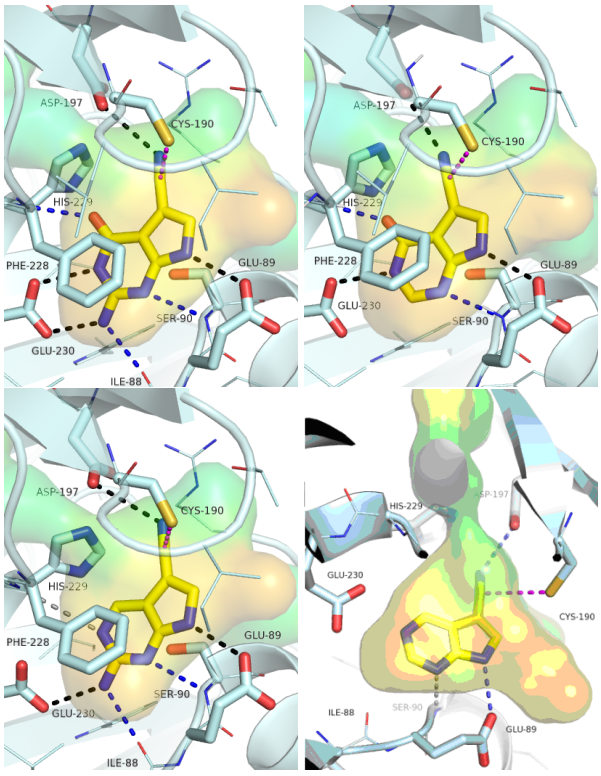

Figure 5.9 Comparison of substrates docked into the *E. coli* nitrile reductase model. Top left: natural substrate $preQ_0$ (**1**), top right: substrate **13**, bottom left: substrate **7**, bottom right: substrate **16**

Table 5.5 Specific activities in mU/mg of wild type and mutant nitrile reductase queF from *E. coli*

	1	**13**	**7**	**16**
wild type	117	90	< 0.1	no activity
S90A	12.9	3.8	< 0.1	< 0.1
F228W	10.2	8.7	< 0.1	no activity
H229A	17.9	14.3	no activity	no activity
E230Q	4.4	3.0	2.2	2.0

Several amino acid residues coordinating the substrate in the active site were substituted to investigate their influence on substrate binding. The Phe228Trp mutant retains the possibility of ring stacking interactions with the substrate and was found active. While conversions were comparable to those with wild type enzyme, specific activities were 90% lower for $preQ_0$ and substrate **13**. The mutation Glu230Gln exchanges two amino acid residues of similar length bearing a carboxylic acid functionality of the glutamate against the amide functionality of the glutamine. This mutation led to lower conversions as well as specific activities for $preQ_0$ and substrate **13**. However, this mutant showed broader substrate specificity; specific activities for substrates **13** and **16** were higher than with wild type enzyme or any other mutant. Exchanges of Glu89 by Ala

or Leu led to a drastic loss in activity. Conversions of the natural substrate were lower than 2%, indicating this amino acid is important for substrate binding. The Ser90Ala mutant showed similar conversions as the wild type enzyme. Specific activities were decreased by 90%, however, four substrates were accepted (**1**, **7**, **13**, **16**). The active site model suggests main chain interactions between Ser90 and the substrate, as depicted in Figure 5.7, consequently alterations in the side chain might have less impact on substrate binding.

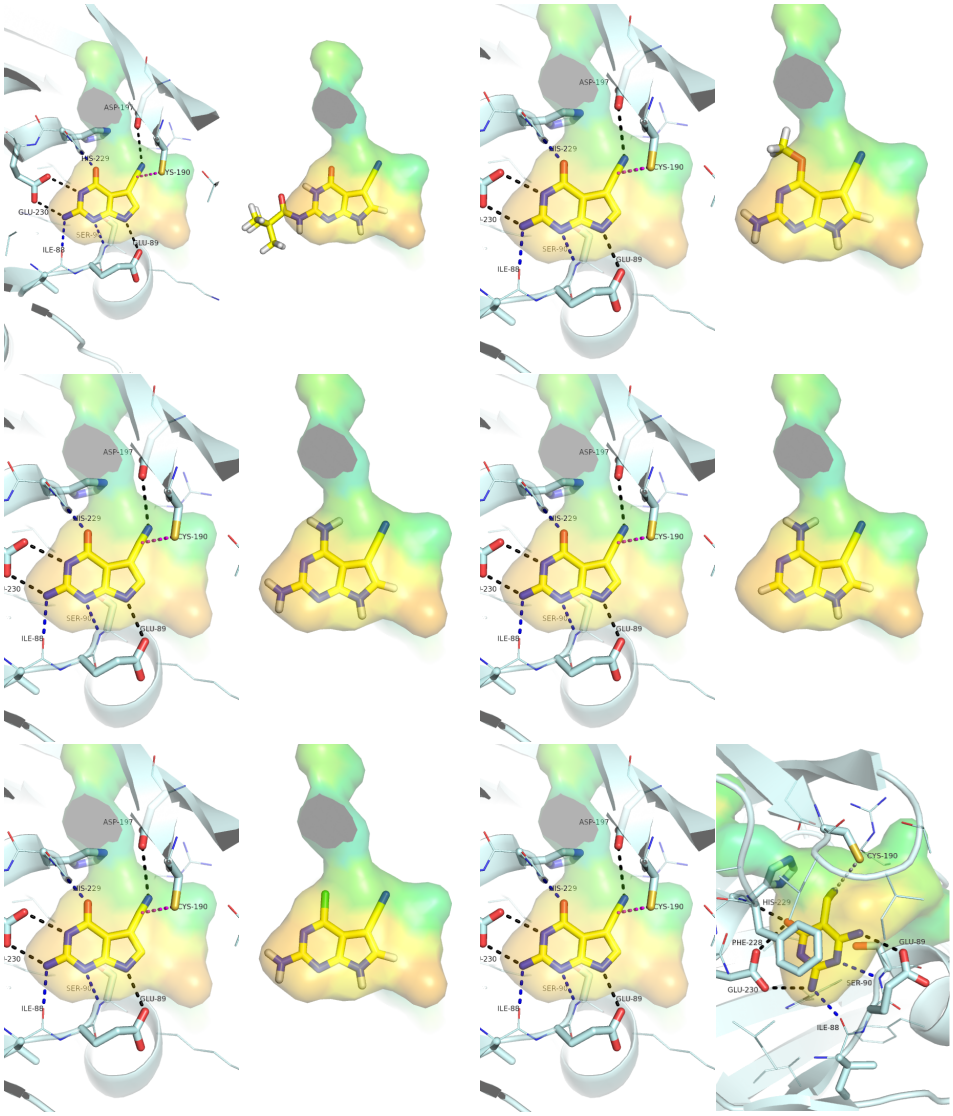

Figure 5.10 Comparison of substrates in the energy minimized model of the binding pocket of *E. coli* nitrile reductase. Top left: pivaloyl-protected preQ$_0$ (**8**), top right: methoxy-protected preQ$_0$ (**9**), centre left: 5-cyano-2,4-diaminopyrrolo[2,3-*d*]pyrimidine (**5**), centre right: 4-amino-5-cyanopyrrolo[2,3-*d*]pyrimidine (**14**), bottom left: 2-amino-4-chloro-5-cyanopyrrolo[2,3-*d*]pyrimidine (**6**), bottom right: 2,6-diamino-5-cyanomethyl-4-hydroxypyrimidine (**54**).

Determination of kinetic parameters for wild type nitrile reductase from *E. coli* showed that k_{cat} values for the natural substrate **1** and the non-natural substrate **13** are in the same range, however, the K_m value for substrate **13** is considerably higher, affecting substrate specificity by a factor of 100 [449]. This is also indicated by the slightly lower specific activities for substrate **13** [449]. The k_{cat}- and K_m-values determined for preQ$_0$ and NADPH are consistent with the values reported in literature [9, 92]. The k_{cat}-value found, is comparable with the two subsequent enzymes in the

pathway of biosynthesis of queuosine [9].

Table 5.6 Kinetic parameters of nitrile reductase queF from *E. coli*

	NADPH	**1**	**13**
K_m [μM]	6.0 ± 0.7	6.1 ± 0.7	176 ± 23
k_{cat} [min^{-1}]	8.5 ± 0.1	6.5 ± 0.2	3.6 ± 0.3
k_{cat} / K_m [$min^{-1}\mu M^{-1}$]		1.1	0.020

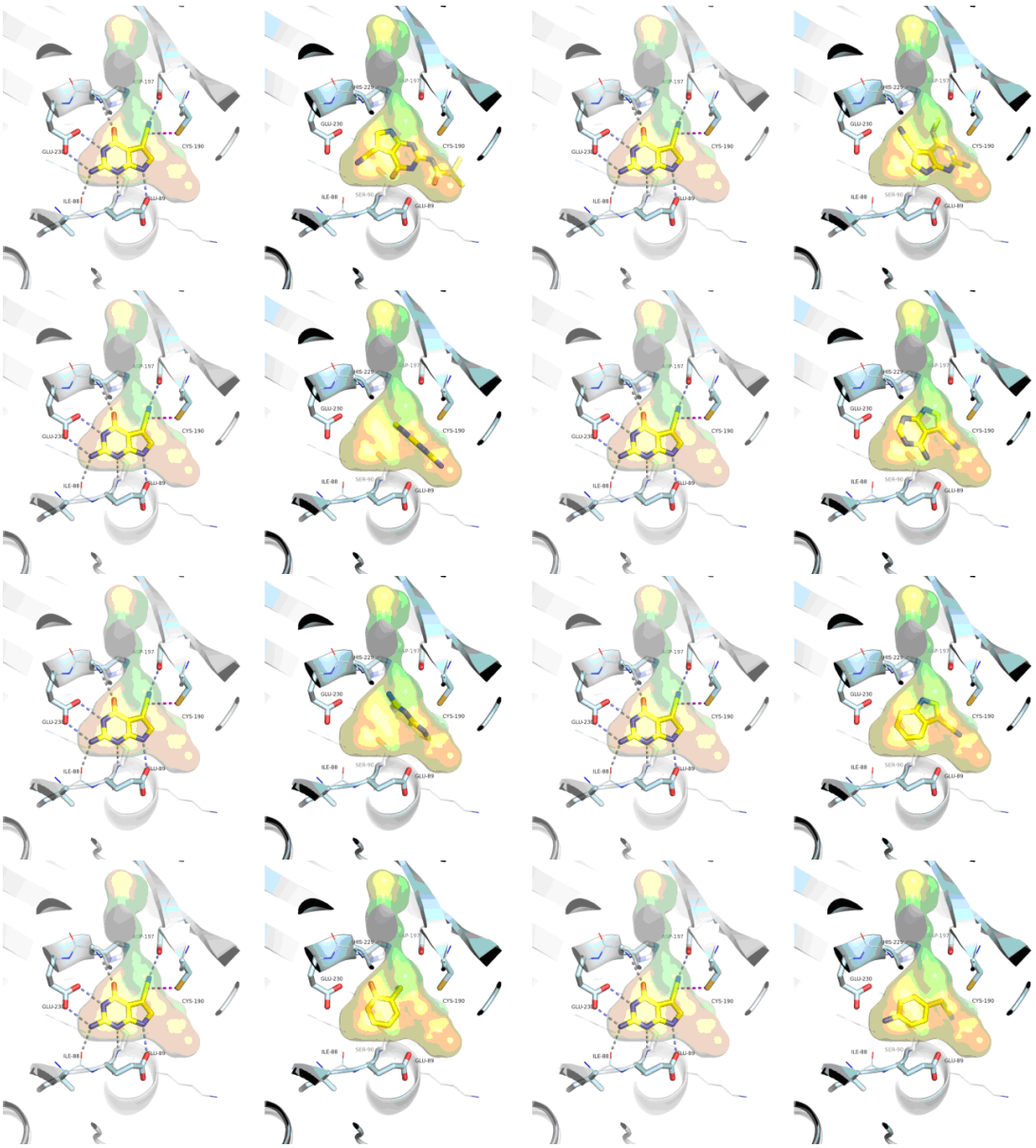

Figure 5.11 Comparison of substrates docked into the *E. coli* nitrile reductase model without productive binding mode. First line left: pivaloyl-protected $preQ_0$ (**8**), first line right: methoxy-protected $preQ_0$ (**9**), second line left: 5-cyano-2,4-diaminopyrrolo[2,3-*d*]pyrimidine (**5**), second line right: 4-amino-5-cyanopyrrolo[2,3-*d*]pyrimidine (**14**), third line left: 2-amino-4-chloro-5-cyanopyrrolo[2,3-*d*]pyrimidine (**6**), third line right: 3-cyanoindole (**86**), forth line left: 2-hydroxybenzylcyanide (**55**), forth line right: 4-aminobenzylcyanide (**94**).

All successfully reduced non-natural substrates (**13**, **7**, **16**) contain the bicyclic pyrrolo[2,3-*d*]pyrimidine ring structure, and differ from the natural substrate $preQ_0$ only in the pyrimidine ring substituents. However, several nitriles containing the pyrrolo[2,3-*d*]pyrimidine ring structure were not accepted as substrates. Comparison of the substrates in the energy minimized model of the binding pocket of *E. coli* nitrile reductase (Figure 5.10) show that the pivaloyl- and methoxy-protected structures (**8** and **9**) are too large to fit into the binding pocket [452]. The 4-amino substitution in **14** and **5** may hinder binding, as it is located close to the main chain NH of the His229 residue. Active site binding of 2-amino-4-chloro-5-cyanopyrrolo[2,3-*d*]pyrimidine **6** and 2,6-diamino-5-cyanomethyl-4-hydroxypyrimidine **54** seem possible, however screening results showed these compounds were not accepted as substrates.

Most of the substrates screened can not only bind to the active site in a productive binding mode, but are also able to bind in a nonproductive complex, as depicted in Figure 5.11 [452]. Formation of a nonproductive complex may account for those compounds not being reduced by nitrile reductase queF.

5.2 Two electron reductions

The catalytic mechanism of nitrile reductase queF indicates two reduction steps. The nitrile is reduced to an imine in the first two electron reduction step, while in the second step the resulting imine is reduced to the corresponding amine, as discussed in chapter 1. In this thesis, imines, and analogous structures were investigated as substrates for nitrile reductase queF.

Imine reductase activity has been reported in literature since the 1980s, only recently, imine reducing enzymes have been considered for biocatalysis. Dihydrofolate reductase (DHFR from *E. coli*) and related enzymes convert dihydrofolate to tetrahydrofolate, by reducing an imine to an chiral amine [454]. The protein PchG from *Pseudomonas aeruginosa* was identified as NADPH dependent imine reductase, catalyzing the reduction of a thiazoline to a thiazolidine in pyochelin biosynthesis [455]. Thiazolinyl imine reductase from *Yersinia enterocolitica* was crystallized [456]. Asymmetric reduction of imines has recently been reported from yeasts [457, 458] and anaerobic bacteria [459]. Enzymes possessing imine reductase activity were also found in *Streptomyces* sp. in the biosynthetic pathways of sibiromycin and tomaymycin [460, 461]. In a search for an imine reductase for the reduction of 2-methyl-1-pyrroline in 261 strains of bacteria, 117 strains of actinomycetes and 84 strains of fungi, imine reductase activity was identified in five filamentous bacteria of *Streptomyces* sp. [241, 462]. *Streptomyces* sp. GF3587 and 3546 showed high enantioselectivity for 2-methyl-1-pyrroline [241, 462]. The structure of NADPH dependent imine reductase Q1EQE0 from *Streptomyces kanamyceticus* was solved and a catalytic mechanism was proposed [242]. These imine reductases are, however, so far restricted to cyclic imines or secondary imines as substrates.

In this thesis, nitrile reductase queF was preliminarily investigated as biocatalyst for the reduction of imines and other C-N and C-O double bonds. Nitrile reductase queF exhibits high substrate specificity. The non-natural nitriles reduced by queF all show the $preQ_0$ core structure. An imine, oxime and aldehyde with $preQ_0$ core structure was prepared as discussed in chapter 3. The imine (**81**), oxime (**82**) and aldehyde (**66**) were then used as substrate for nitrile reductase queF, as depicted in Scheme 5.1.

Biocatalytic imine reduction is limited by the hydrolysis of unsubstituted imines in water [242, 463–465]. In this thesis the mehtylimine 2-amino-5-methyliminopyrrolo[2,3-*d*]pyrimidin-4-one (**81**) was chosen as imine structure. 2-Amino-5-methyliminopyrrolo[2,3-*d*]pyrimidin-4-one (**81**) was quantitatively hydrolyzed to the aldehyde in the aqueous reaction medium. However, the hydrolysis was not enzyme catalyzed, but occurred in blank reactions as well.

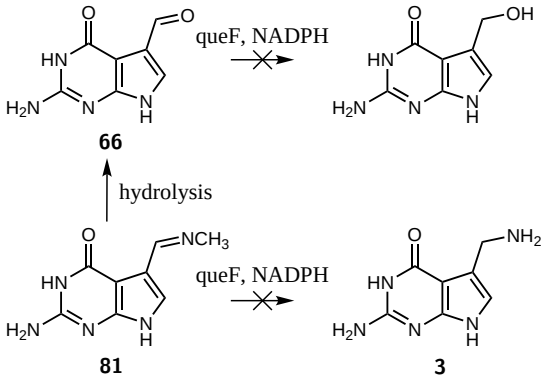

Scheme 5.1 Reduction of aldehyde and imine substrates by nitrile reductase

2-Amino-5-formylpyrrolo[2,3-*d*]pyrimidine (**66**) could not be reduced to the corresponding alcohol with nitrile reductase queF. A substrate concentration of 2mM was used with 2.5 equivalents of NADPH. No product formation was observed, neither at 30°C nor at 55°C with neither 1% v/v nor 10% v/v DMSO and neither wild type nitrile reductase from *G. kaustophilus* nor the C55A mutant. 2-Amino-4-oxopyrrolo[2,3-*d*]pyrimidin-5-carbaldehyde oxime was also not reduced by nitrile reductase queF.

5.3 Oxidations

Nitrile reductase is an oxidoreductase naturally working in reductive direction. In this thesis, 2-amino-5-formylpyrrolo[2,3-*d*]pyrimidine (**66**) was applied as substrate for the preliminary screening reaction in oxidative direction to achieve 2-amino-4-oxopyrrolo[2,3-*d*]pyrimidin-5-carboxylic acid. $NADP^+$ or NAD^+ was used as cofactor in excess of 2.5 equivalents or 10 equivalents. In these preliminary experiments, the reaction conditions, e.g. buffer pH-value, were not optimized. Under these reaction conditions no oxidation of the aldehyde to the carboxylic acid could be observed.

5.4 Nitrile hydrolysis

The enzymatic hydrolysis of the nitrile group of $preQ_0$ was investigated with commercial enzyme preparations of bacterial nitrilases from Codexis, Inc. (NIT-101 - NIT106, NIT-108 - NIT-114) and Prozomix Limited (PRO-E0260 - PRO-E0264). When 2mM substrate was used (2% v/v DMSO) no conversion was observed with any of the Codexis nitrilases NIT-101 to NIT-106, and NIT-108 to NIT-114. When the substrate concentration was decreased to 0.4mM (2% v/v DMSO) or 0.2mM (2% DMSO), NIT-113 was found to hydrolyze $preQ_0$ to its corresponding carboxylic acid in 20%-30% conversion after 23 hours.

6

Conclusions and Outlook

In this thesis, nitrile reductase queF, a novel enzyme found in the biosynthetic pathway to the hypermodified nucleoside queuosine, was investigated towards its application in biocatalysis.

Nitrile reductase from three different bacterial sources, *B. subtilis*, *G. kaustophilus* and *E. coli*, was successfully cloned and expressed in *E. coli*. The nitrile reductase from *G. kaustophilus* was characterized regarding its temperature, pH and co-factor dependence, as described in chapter 4. Initial substrate screenings indicated high substrate specificity of nitrile reductase queF.

A number of structural analogues of the natural substrate preQ$_0$ was prepared in multi-step syntheses, as described in chapter 3. These structural analogues were differently substituted pyrrolo[2,3-*d*]pyrimidines, pyrrolo[2,3-*b*]pyridines, pyrrolo[3,2-*c*]pyridines, thieno[2,3-*d*]pyrimidines, cyclopenta[*d*]pyrimidines, and pyrazolo[3,4-*d*]pyrimidines. A number of compounds was first prepared in this thesis, as summarized in Scheme 6.1, Scheme 6.2 and Scheme 6.3.

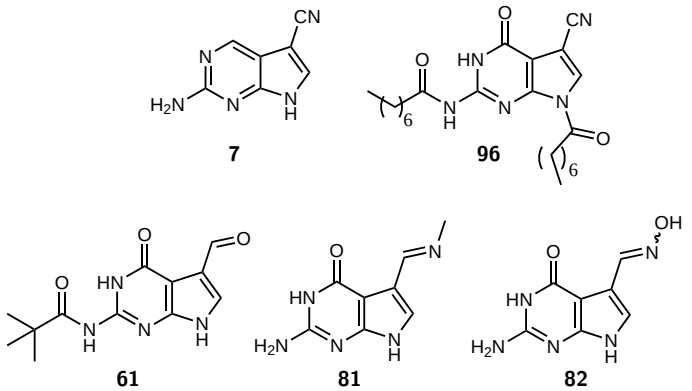

Scheme 6.1 Pyrrolo[2,3-*d*]pyrimidines first synthesized in this thesis.

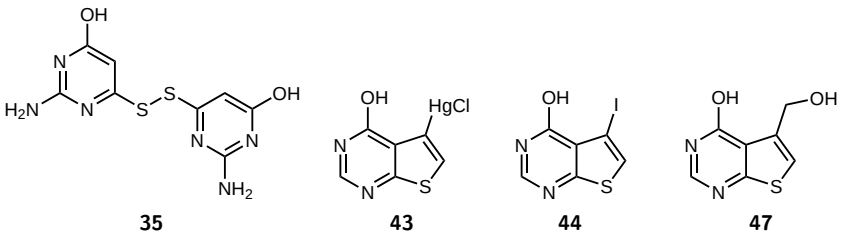

Scheme 6.2 Thieno[2,3-*d*]pyrimidines and its precursors first synthesized in this thesis.

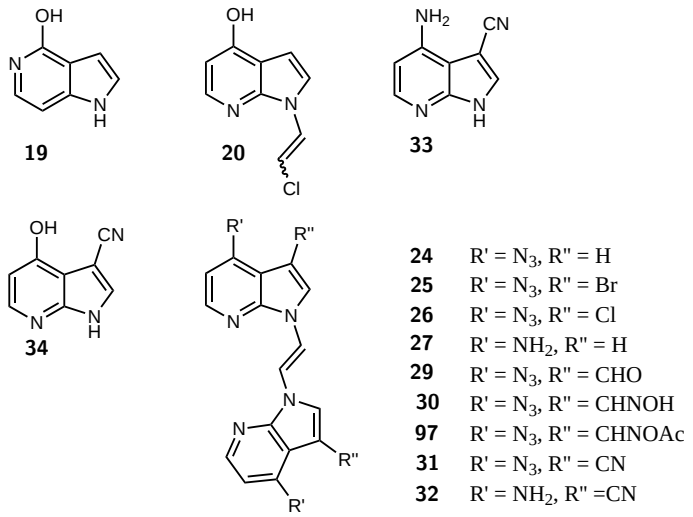

Scheme 6.3 Compounds first synthesized in this thesis, except for compounds **19** and **20**, first reported in Cornelia Hojnik's master thesis [305].

A dual HPLC and photometric screening assay for the screening of nitrile reductase queF with natural and non-natural substrates was developed. This assay is suitable for semi-high-throughput screenings in 96-well plates. Detection of substrate conversion is possible by photometric monitoring of NADPH consumption and additionally HPLC-MS based analysis of product formation.

Three non-natural substrates for nitrile reductase queF were identified. Wild type and mutant nitrile reductase from *G. kaustophilus* catalyzed the reduction of the non-natural substrates 5-cyanopyrrolo[2,3-*d*]pyrimidin-4-one (**13**) and 2-amino-5-cyanopyrrolo[2,3-*d*]pyrimidine (**7**), as depicted in Scheme 6.4. Wild type nitrile reductase from *E. coli* accepted only compound **13** as non-natural substrate. Wild type enzyme and the S90A and E230Q mutants also showed residual activities for compound **7**. Residual activities for the reduction of 5-cyanopyrrolo[2,3-*d*]pyrimidine (**16**) were found with the S90A and E230Q mutants of *E. coli* queF. Determination of the kinetic parameters, for *G. kaustophilus* queF and *E. coli* queF, showed 30-fold higher K_m-values for the non-natural substrate **13** than for the natural substrate $preQ_0$, indicating weakened substrate binding. k_{cat} values for these two substrates were in the same range. Absence of the amino-group of the substrate therefore showed an effect on substrate binding, but not on the reaction rate. Three inhibitors (compounds **60**, **37**, **94**) of wild type queF from *G. kaustophilus* were identified in inhibitor measurements (Scheme 6.4). All three inhibitors possess an amino-group in similar position as the natural substrate $preQ_0$. Among the 15 compounds tested as inhibitors, three possessed an amino-group in relevant position, these three compounds were all identified as inhibitors. The amino-group in position 2 of the natural substrate might therefore have a significant effect on substrate binding.

Several amino acids were identified in the homology models of *G. kaustophilus* and *E. coli* queF to be involved in substrate binding. Two amino acid residues, D197 (*E. coli* queF) and C190 (*E. coli* queF), and the corresponding C55 (*G. kaustophilus* que F) were identified as essential for the catalytic mechanism. Mutations of His96 (*G. kaustophilus* queF) and His229 (*E. coli* queF) respectively retained their activity, indicating this residue is not essential for the catalytic mechanism. Glutamic acid coordinates to the amino-group of the substrate in position 2, the E97A and E97S mutations of *G. kaustophilus* queF showed similar conversions as the wild type enzyme, as

well as similar substrate specificity, whereas the E230Q mutant of *E. coli* queF showed much lower conversions, however broader substrate specificity. Mutations of the phenylalanine, responsible for π-π stacking with the substrate showed different effects. The F95A mutant of *G. kaustophilus* queF increases the available space in the active site, however does not offer the possibility of π-π stacking with the substrate. The F95A mutant was active for the conversion of substrates **1**, **13** and **7**, however conversions were much lower compared to those of the wild type enzyme. The F228W mutant of *E. coli*, still capable of π-π stacking with the substrate, showed similar conversions as the wild type enzyme. Substrate specificity did not change for any of the mutations, compared to the substrate specificity of the wild type enzyme (as discussed in chapter 5).

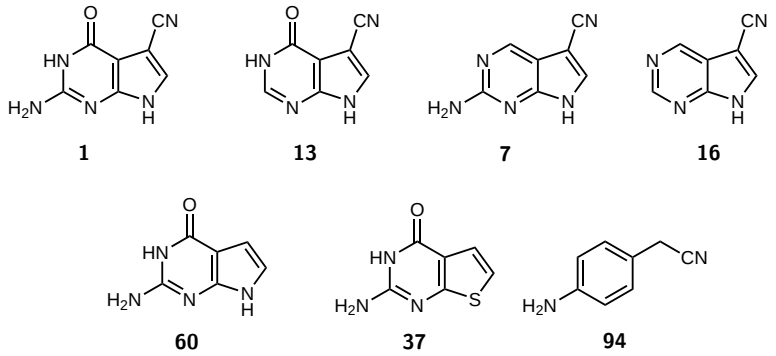

Scheme 6.4 Substrates and inhibitors of nitrile reductase queF. Natural substrate (**1**), non-natural substrates **13**, **7** for nitrile reductase from *G. kautophilus* and *E. coli* and **16**) for nitrile reductase from *E. coli*, and inhibitors **60**, **37**, **94** for wild type nitrile reductase queF from *G. kaustophilus*.

Screenings of substrates differing from the natural substrate in functional groups gave first insight into the substrate scope and substrate binding of nitrile reductase queF. Screening of natural substrate analogues differing in ring heteroatoms, such as pyrrolo[2,3-*b*]pyridines, pyrrolo[3,2-*c*]pyridines, thieno[2,3-*d*]pyrimidines, cyclopenta[*d*]pyrimidines and pyrazolo[3,4-*d*]pyrimidines will provide insight into the contribution of the ring-heteroatoms to substrate binding.

The activity of nitrile reductase queF from *G. kaustophilus* towards the reduction of C-N- and C-O double bonds was preliminarily evaluated using substrates bearing the $preQ_0$ core structure. The enzymatic reduction of imines is significantly complicated by the hydrolysis of unsubstituted imines in aqueous media. The methyl-substituted imine was hydrolysed quantitatively in the reaction buffer. In order to investigate enzymatic imine reduction with free imines or imines bearing small substituents, *in situ* imine formation in the reaction buffer might be a suitable approach. An aldehyde or oxime was not reduced by nitrile reductase queF.

Nitrile reductase queF is an enzyme of high interest for biocatalysis. The first non-natural substrates were identified in this thesis. So far the substrate scope, however, is restricted to structural analogues of the natural substrate. In order to increase the substrate scope further enzyme engineering will be necessary.

The Catalophore approach offers a method to search for similar enzyme activity in protein structures [452]. In the catalophore approach, the amino acid residues essential for the catalytic mechanism and the relevant distances in the structure are used to find similar structural features in other proteins. In this thesis, two amino acid residues were identified as essential for the catalytic mechanism, which might serve as a starting point for a catalophore search.

7

Experimental Procedures

7.1 General remarks

Reagents and starting materials were obtained from commercial suppliers, and used without further purification, except stated otherwise.
All manipulations of air- and/or moisture-sensitive materials were performed under inert atmosphere, using a dual vacuum/nitrogen line, and standard Schlenk techniques.
The following cooling baths were used: ice-water mixtures for a temperature of 0°C, ice/NaCl mixtures for temperatures of 0°C to -20°C, dry ice/acetone mixtures for -78°C.

7.1.1 NMR spectroscopy

^{1}H NMR and ^{13}C NMR spectra were recorded on a Bruker AVANCE III with autosampler (^{1}H NMR 300.36 MHz, ^{13}C NMR 75.53 MHz) or on a Varian Unity Inova 500 MHz NB high resolution FT NMR spectrometer (^{1}H NMR 499.76 MHz, ^{13}C NMR 125.67 MHz). Chemical shifts for ^{1}H NMR are reported in ppm relative to Me_4Si as internal standard. Signal multiplicities are abbreviated as s (singlet), d (doublet), dd (doublet of doublet), t (triplet), dt (doublet of triplet), q (quadruplet), quin (quintet) and m (multiplet), with the prefix b in case of broad signals. When necessary, ^{13}C NMR resonances were assigned by APT, HSQC and HMBC experiments.

7.1.2 Chromatography

Column chromatography

Column chromatography was performed using Merck Silica Gel 60 (40µm - 63µm particle size) or Acros Silica Gel 60 Å(35µm - 70µm particle size).

Thin layer chromatography

Thin layer chromatography was carried out with precoated aluminium silica gel 60 F_{254} plates from Merck, spots were visualized by radiation with UV light ($\lambda = 254$nm) or by treament with cerium ammonium molybdate solution (2.0g $CeSO_4$, 50g $(NH_4)_2MoO_4$, 50mL concentrated H_2SO_4 in 400mL water) and subsequent warming with a heat gun.

Gas chromatography

GC measurements were performed on an Agilent Technologies 6890N (G1530N) GC system with FID detector on an Agilent 19091 J-413 capillary column (30.0m x 320µm x 0.25µm, HP-5, (5% phenyl) methyl siloxane). Inlet temperature: 250°C, injection volume 1.0µL, split mode 20/1, initial temperature 100°C, hold for three minutes, then linear ramp 25°C per minute, final temperature 270°C. Samples were dissolved in dichloromethane and dried over magensium sulphate before injection.

High pressure liquid chromatography (HPLC)

Semi-preparative HPLC was carried out on a Knauer Smartline Instrument with Autosampler 3800, Manager 5000, Pump 1000, UV Diode Array Detector 2600 and Fraction Collector Teledyne Isco Foxy Jr on a Macherey-Nagel VP 125/21 Nucleodur 100-5 C18ec column (762029.210) with a VP 20/16 Nucleodur C18ec pre-column.
Method A: flow 13mL/min, stepwise gradient starting with 90% water and 10% acetonitrile, hold for three minutes, decrease to 30% acetonitrile in twelve minutes, hold for five minutes.
Method B: flow 13mL/min, stepwise gradient starting with 90% water and 10% acetonitrile, hold for three minutes, decrease to 35% acetonitrile in seven minutes, hold for ten minutes.

Analytical HPLC-MS analysis was carried out on an Agilent 1200 series (G1379B Degasser, G1312B Binary Pump SL, G1367C High Performance Autosampler SL, G1330 FC/ALS Thermostat, G1316B Thermostatted Column Compartment SL, G1365C Multiple Wavelength Detector SL) with an Agilent Technologies 6120 quadrupole LC/MS Detector with a G1918B Electrospray Ionization Source. For analytical purposes and HPLC and/or semi-preparative HPLC, demineralized water was filtered through a 0.2 µm cellulose nitrate membrane filter.
HPLC-MS methods: various gradients of acetonitrile and ammonium acetate in water were applied for separation. The following colums and conditions were used: methods C-G: column: phenomenex Gemini-NX 3 C18 110A (150 x 2.0mm) , flow: 0.2mL/min, oven temperature: 20°C, method J: column: Merck SeQuant ZIC-HILIC (150 x 2.1mm, 3.5µm, 200Å), flow: 0.1mL/min, oven temperature: 20°C.
Method C: stepwise gradient starting with 98% 20mM ammonium acetate in water and 2% acetonitrile, hold for eight minutes, increase to 40% acetonitrile in five minutes, and decrease to 2% acetonitrile in two minutes.
Method D: stepwise gradient starting with 95% 20mM ammonium acetate in water and 5% acetonitrile, hold for eight minutes, increase to 40% acetonitrile in five minutes, and decrease to 5% acetonitrile in two minutes.
Method E: stepwise gradient starting with 95% 20mM ammonium acetate in water and 5% acetonitrile, hold for seven minutes, increase to 90% acetonitrile in seven minutes, hold for one minute, and decrease to 5% acetonitrile in one minute.
Method F: stepwise gradient starting with 95% 20mM ammonium acetate in water and 5% acetonitrile, hold for five minutes, increase to 50% acetonitrile in five minutes, increase to 80% acetonitrile in five minutes, and decrease to 5% acetonitrile in one minute.
Method G: stepwise gradient starting with 95% 20mM ammonium acetate in water and 5%

acetonitrile, increase to 10% acetonitrile in three minutes, increase to 40% acetonitrile in two minutes, hold for one minute, increase to 80% acetonitrile in two minutes, hold for two minutes, decrease to 10% acetonitrile in one minute, and decrease to 5% acetonitrile in two minutes.
Method H: stepwise gradient starting with 95% 20mM ammonium acetate in water and 5% acetonitrile, increase to 40% acetonitrile in five minutes, then increase to 80% acetonitrile in five minutes, decrease to 5% acetonitrile in two minutes.
Method I: stepwise gradient starting with 95% 20mM ammonium acetate in water and 5% acetonitrile, hold for six minutes, increase to 40% acetonitrile in seven minutes, then increase to 80% acetonitrile in two minutes, decrease to 5% acetonitrile in one minutes.
Method J: isocratic method with 75% acetonitrile and 25% 5mM ammonium acetate in water.

7.1.3 Biotransformation reactions

Screening reactions were incubated on an Eppendorf comfort thermomixer. Absorption measurements to monitor NADPH depletion were done on a Fluostar plate reader from BMG lab tech at 340nm.
Data from plate reader absorption measurements was plotted using the Python 2D plotting library Matplotlib, linear regressions were calculated with Python library SciPy (scipy.stats) [466].
HPLC-MS data was analyzed using the Agilent LC/MSD ChemStation software.
Photospectrometric determinations of kinetic parameters and specific activities were performed on a Beckman DU-800 spectrophotometer.

7.2 Enzyme cloning, expression, and purification

7.2.1 Nitrile reductase from *G. kaustophilus*

Strains, vectors and growth conditions

Geobacillus kaustophilus HTA426 was grown on LB agar medium. The pEamTA vector [467] was used for recombinant expression. *E. coli* K12 Top10F' (Invitrogen, Carlsbad, CA, USA) was used to amplify and maintain engineered constructs and *E. coli* BL21 (DE3) (Invitrogen, Carlsbad, CA, USA) for protein expression. LB medium and LB agar supplemented with ampicillin when appropriate (100mgL^{-1}) was used for cell cultivation [447, 448].

Vector construction and preparation of mutants

The *Geobacillus kaustophilus* nitrile reductase was amplified from genomic *G. kaustophilus* DNA employing the primers 5'-atg gca gga aga aaa g-3' and 5'-gaa ttc cta gcg gtt gtc gac-3', respectively, and Phusion DNA polymerase (Finnzymes, Espoo, Finland) according to the manufacturer's protocol. All oligonucleotides used were manufactured by Integrated DNA Technologies, San Jose, CA, USA. The amplified PCR product was purified using a preparative gel. The DNA fragment was recovered from the gel using the QIAquick®Gel Extraction Kit (Qiagen, Hilden, Germany). The fragment (31µL) was A-tailed by incubation with 5µL of dNTPs (2mM, each), 8µL of magnesium chloride (25mM), 5µL of Taq buffer and 1µL of Taq Polymerase (5UμL^{-1}, Fermentas, Burlington,

Canada) at 72°C for 30 minutes. Subsequent purification with the QIAquick®PCR Purification Kit (Qiagen, Hilden, Germany) yielded the A-tailed insert in approximately 5ngmL^{-1} concentration. The linear pEamTA vector was prepared by digestion of 44µL of plasmid DNA (isolated with the GeneJET™Plasmid Miniprep Kit from Fermentas, Burlington, Canada) supplemented with 5µL Eam1105I buffer (10X) and 1µL of Eam1105I (Fermentas) at 37°C for four hours. The DNA fragment was recovered from the gel using the QIAquick®Gel Extraction Kit (Qiagen) yielded the linear vector in approximately 40ngmL^{-1} concentration. The insert (110ng, 22µL) was ligated with the vector (80ng, 2µL) in an overnight reaction at 16°C using 3µL T4 DNA ligase buffer and 3µL T4 ligase (Promega, Madison, WI, USA). After heat inactivation (65°C, 20 minutes) and desalting on ultradialysis membranes (Millipore, 0.025µm), the entire ligation mixtures were transformed into 180µL of electrocompetent *E. coli* K12 Top10F' cells (Invitrogen) and selected on LB-ampicillin agar plates. Colonies with correctly integrated inserts were confirmed by digestions of plasmid DNA (isolated with the GeneJET™Plasmid Miniprep Kit from Fermentas) with NdeI and HindIII fast digest restriction enzymes (Fermentas) and verified by sequencing (LCG Genomics, Berlin, Germany) using the primers pEamf1 (5'-ttgtgagcggataacaatttc-3') or pEamr1 (5'-tactgccgccaggcaaattct-3'). Retransformation of 1µL of plasmid into chemically competent *E. coli* BL21 (DE3) (Invitrogen) resulted in the wild type *G. kaustophilus* nitrile reductase expression strain [447, 448].

Site specific mutagenesis

pEamTA, was employed as the template for a two stage mutagenesis reaction protocol. Briefly, 5µL of PfuUltra HF reaction buffer (10X), the template (1µL, 10ng), 1µL dNTP mix (10mM), 1µL of forward OR reverse primer (5mM) and 1µL of PfuUltra High Fidelity DNA polymerase (2.5U µL-1 from Stratagene (La Jolla, CA, USA) were added to 41µL of doubly distilled water (Fresenius, Graz, Austria). The two stage PCR was conducted on a Gene Amp System 2400 thermo cycler (Applied Biosystems, Foster City, CA) under the following conditions: 95°C for one minute, four cycles of 50 seconds at 95°C, 50 seconds at 60°C, five minutes at 68°C, then seven minutes at 68°C for the final elongation step. After these initial four cycles of primer extension, 25µL of the reaction containing the forward primer was combined with 25µL of the reaction containing the reverse primer. Additional 18 cycles were run under the above conditions. Subsequently, dpnI (1µL, Fermentas) was added to digest the template at 37°C for one hour. 2µL of the mixture were transformed into 60µL of electrocompetent *E. coli* K12 Top10F' cells (Invitrogen) and selected on LB-ampicillin agar plates. The mutations were confirmed by sequencing (LCG Genomics). Plasmids from mutants having the correct sequence were replicated and transformed into *E. coli* BL21 (DE3). PAGE purified primers used for site specific mutagenesis: GkNRedC55Af 5'-c cgg agt tta cga cgt tgg cgc caa aaa ccg gac aac cg-3'; GkNRedC55Ar 5'-cgg ttg tcc ggt ttt tgg cgc caa cgt cgt aaa ctc cgg-3' GkNRedF95Af 5'-c ttc cgc aat cat ggc gac gcg cac gaa gac tgc gtc aac a-3'; GkNRedF95Ar 5'-t gtt gac gca gtc ttc gtg cgc gtc gcc atg att gcg gaa g-3'; GkNRedH96Af 5'-gc ttc cgc aat cat ggc gac ttt gcc gaa gac tgc gt-3'; GkNRedH96Ar 5'-ac gca gtc ttc ggc aaa gtc gcc atg att gcg gaa gc-3'; GkNRedH96Ff 5'-gc ttc cgc aat cat ggc gac ttt ttc gaa gac tgc gt-3'; GkNRedH96Fr 5'-ac gca gtc ttc gaa aaa gtc gcc atg att gcg gaa gc-3'; GkNRedE97Af 5'-cat ggc gac ttt cac gca gac tgc gtc aac atc-3'; GkNRedE97Ar 5'-gat gtt gac gca gtc tgc gtg aaa gtc gcc atg-3'; GkNRedE97Sf 5'-gc aat cat ggc gac

ttt cac tca gac tgc gtc aac atc att a-3'; GkNRedE97Sr 5'-t aat gat gtt gac gca gtc tga gtg aaa gtc gcc atg att gc-3' [447, 448].

Protein expression and purification for biocatalytic screening reactions

Wild type nitrile reductase from *G. kaustophilus* and variants were cultivated as follows: overnight cultures (20mL LB/ampicillin, inoculated with a single colony and grown at 37°C in an orbital shaker) were used to inoculate 500mL LB/ampicillin medium in 2L baffled Erlenmayer flasks. These main cultures were grown at 37°C and 130rpm to an optical density of 0.7, induced with 0.5mL of IPTG (1M) and incubated for 24 hours at 16°C and 130rpm. The cells were harvested by centrifugation (4,000 rpm, 4°C, 10min). The pellet was resuspended in reaction buffer (12.1gL^{-1} Tris, 3.73gL^{-1} KCl, 287mgL^{-1} *tris*(2-carboxyethyl)phosphine hydrochloride (TCEP); pH 7.5 adjusted with HCl 37%) and disrupted by ultrasonication. The cell debris was removed by ultracentrifugation at 40,000 rpm for 45 minutes at 4°C. The supernatant (crude lysate) was purified by heat precipitation of host proteins at 70°C for ten minutes and then applied to a centrifugation step (4,000rpm, 4°C, ten minutes). The supernatant contained fairly pure nitrile reductases and was stored at -20°C [447, 448].

Cultivation and purification of enzyme for the determination of kinetic parameters

E. coli BL21 *G. kaustophilus* nitrile reductase was grown in 1000mL baffled shaken flasks containing 200mL of LB media supplemented with 115mg/L ampicillin. Flasks were shaken at 120rpm and 37°C in a Certomat®BS-1 incubator from Sartorius. Recombinant protein production used a standard procedure in which cultures were cooled to 25°C when an optical density of 0.6 (± 10%) was reached. Isopropylthio-β-D-galactoside (IPTG) was added in a concentration of 1.0mM, and the cultivation time after induction was 18 hours. Cells were harvested by centrifugation, washed with physiological NaCl solution, re-centrifuged and diluted into 100mM Tris buffer, pH 7.5, supplemented with 50mM KCl and 1mM TCEP. Cells were disrupted by two passages through a French press (American Instrument Company, Silver Springs, Maryland, USA) operated at an internal cell pressure of 25,000psi. The crude cell extract obtained was clarified by centrifugation (16,000g, 45 minutes, 4°C) prior to enzyme purification. *E. coli* protein was separated from the cell-free extract by incubation at 75°C for ten minutes. Thermo-precipitated protein was centrifuged (16,000g, ten minutes). Recombinant enzyme was further purified by ion exchange chromatography using a QFF from GE Healthcare (bed volume 55mL). The column was equilibrated with 100mM Tris buffer, 50mM KCl, pH 7.5. Adsorbed protein was eluted at a flow rate of 4mLmin^{-1} with a step gradient of 0.1M and 1M KCl. Fractions of 5mL were collected and the 0.1M KCl peak containing most of the *G. kaustophilus* nitrile reductase, as judged by activity measurements and SDS-PAGE, was pooled. The pooled fractions were concentrated in Vivaspin 20mL Concentrator tubes with 10,000 molecular weight cut off to a volume of less than 0.5mL and re-diluted into 100mM Tris containing 50mM KCl and 1mM TCEP [449].

7.2.2 Nitrile reductase from *E. coli*

Vector construction

E. coli queF (gene ID: 947270) was amplified from genomic DNA of *Escherichia coli* strain K-12 including the introduction of restriction sites NcoI and HindIII using Phusion®High-Fidelity DNA polymerase (Finnzymes) and primers 5'- AAT CAC CAT GGC TAT GTC TTC TTA TGC AAA C-3' and 5'-AAT CAA AGC TTT TAT TGC CGA ACC AGT C-3', respectively. The PCR reaction was thermally cycled: 98°C for 30 seconds, followed by 30 cycles of 98°C for ten seconds, 55°C for 15 seconds, and 72°C for 20 seconds, then a final incubation of 72°C for five minutes. The PCR products were gel purified with the QIAquick®Gel Extraction Kit (QIAGEN), digested with NcoI and HindIII restriction enzymes (Fermentas) in Tango buffer (Fermentas) and column purified according to QIAquick®PCR purification protocol (QIAGEN). The gene was ligated into the pEHISTEV vector which was also digested with NcoI and HindIII [450]. The ligation was carried out for three hours at room temperature in the presence of T4 ligase (Fermentas) and T4 ligation buffer (Fermentas). The ligation product was transformed into electrocompetent *E. coli* TOP10 F'cells and plated on LB-agar supplemented with 50 µg kanamycin/mL. The resulting plasmid pEHISTEV:EcNRedWT was isolated with the GeneJET™Plasmid Mininprep Kit (Fermentas) and the sequence was confirmed by LGC Genomics [447, 448, 451].

Site specific mutagenesis

pEHISTEV:EcNRedWT was employed as the template for site directed mutagenesis using the following primers: E89Afw 5'-ACC AGC GTA AAT CTG ATT GCG TCG AAG AGT TTT AAG CTC-3, E89Arv 5'-GAG C TT AAA ACT CTT CGA CGC AAT CAG ATT TAC GCT GGT-3', E89Lfw 5'-GAT TAC ACC AGC GTA AAT CTG ATT CTG TCG AAG AGT TTT AAG CTC TAT-3, E89Lrv 5'-ATA GAG CTT AAA ACT CTT CGA CAG AAT CAG ATT TAC GCT GGT GTA ATC-3', S90Afw 5'- GC GTA AAT CTG ATT GAG GCG AAG AGT TTT AAG CTC TAT C -3', S90Arv 5'- G ATA GAG CTT AAA ACT CTT CGC CTC AAT CAG ATT TAC GC -3', C190Afw 5'- C CTG CTG AAA TCA AAT GCC CTG ATC ACC CAT CAA CCA G -3', C190Arv 5'- C TGG TTG ATG GGT GAT CAG GGC ATT TGA TTT CAG CAG G -3', D197Nfw 5'-C CTG ATC ACC CAT CAA CCA AAT TGG GGT TCG CTC C-3', D197Nrv 5'-G GAGCGA ACC CCA ATT TGG TTG ATG GGT GAT CAG G -3', F228Wfw 5'- GT CAT CAC AAC GAG TGG CAC GAA CAG TGC GTG GAA C -3', F228Wrv 5'- G TTC CAC GCA CTG TTC GTG CCA CTC GTT GTG ATG AC -3', H229Afw 5'- GT C AT CAC AAC GAG TTC GCC GAA CAG TGC GTG GAA C -3', H229rv 5'- G TTC CAC GCA CTG TTC GGC GAA CTC GTT GTG ATG AC -3', E230Qfw 5'- CAT CAC AAC GAG TTC CAC CAA CAG TGC GTG GAA CGC -3' and E230Qrv 5'- GCG TTC CAC GCA CTG TTG GTG GAA CTC GTT GTG ATG -3'. 5µL of PfuUltra HF reaction buffer (10X), the template (1µL, 10ng), 1µL dNTP mix (10mM), 1µL of forward or reverse primer (5mM) and 1µL of PfuUltra High Fidelity DNA polymerase (2.5U µL-1 from Stratagene (La Jolla, CA, USA) were added to 41µL of doubly distilled water (Fresenius, Graz, Austria). The two stage PCR was conducted on a Gene Amp System 2400 thermo cycler (Applied Biosystems, Foster City, CA) under the following conditions: 95°C for one minute, 4 cycles of 50 seconds at 95°C, 50 seconds at 60°C

and 5.5 minutes at 68°C and then seven minutes at 68°C for the final elongation step. After these initial four cycles of primer extension, 25µL of the reaction containing the forward primer was combined with 25µL of the reaction containing the reverse primer. Additional 25 cycles were run under the above conditions. Subsequently, dpnI (1µL, Fermentas) was added to digest the template at 37°C for one hour. 2µL of the mixture were transformed into 60µL of electrocompetent *E. coli* K12 Top10F' cells (Invitrogen) and selected on LB-kanamycin agar plates. The mutations were confirmed by sequencing (LCG Genomics). Plasmids from wild type and mutants having the correct sequence were transformed into *E. coli* BL21 (DE3) [447, 448, 451].

Protein expression and purification

The wild type and the mutant nitrile reductase were cultivated as follows: overnight cultures (20mL LB/ampicillin, inoculated with a single colony and grown at 37°C in an orbital shaker) were used to inoculate 500mL LB/ampicillin medium in 2L baffled Erlenmayer flasks. These main cultures were grown at 37°C and 130rpm to an optical density of 0.7, induced with 0.5mL of IPTG (1M) and incubated for 24 hours at 16°C and 130rpm. The cells were harvested by centrifugation (4,000rpm, 4°C, 10min). The pellet was resuspended in reaction buffer (12.1gL^{-1} Tris, 3.73gL^{-1} KCl, 287mgL^{-1} *tris*(2-carboxyethyl)phosphine hydrochloride (TCEP); pH 7.5 adjusted with HCl 37%) and disrupted by ultrasonication. The cell debris was removed by ultracentrifugation at 40,000rpm for 45 minutes at 4°C. The cell free extract was applied to a 5mL Ni Sepharose 6 Fast Flow column (GE Healthcare, Great Britain) after filtration through a 45µm syringe filter (Milipore). The tagged enzymes were obtained by a one step purification with running buffer A (100mM Tris, 50mM KCl, 1%v/v glycerol, pH 7.5) and elution buffer B (100mM Tris, 50mM KCl, 1%v/v glycerol, 400mM imidazole, pH 7.5). After purification, the enzyme solution was desalted against reaction buffer (100mM Tris, 50mM KCl, 1mM TCEP; pH7.5 adjusted with HCl 37%) using HiTrap Desalting columns (GE Healthcare, Great Britain). TCEP (1mM) was added to the collected protein fractions which were then concentrated by Vivaspin 20 tubes (10,000MWCO, Sartorius) [447, 448, 451].

7.3 Enzyme characterization

Reductase activity measurement and determination of pH stability

Specific reductase activity was assayed spectrophotometrically by monitoring the reduction of NADPH at 340nm. Typically, rates of 0.05 - 0.10 ΔA/min were measured over a time period of five minutes. One unit of enzyme activity refers to 1µmol of NADPH consumed per minute. All measurements were performed with a Beckman DU-800 spectrophotometer thermostated at 55°C. The assay contained 100µM $preQ_0$ and 250µM NADPH. $preQ_0$ was dissolved in DMSO prior to dilution into buffer to give a final DMSO concentration of 1%v/v. Unless otherwise stated, Tris/HCl buffer, pH 7.5 supplemented with 50mM KCl was used. Reactions were always started by the addition of cofactor. Activity measurements for pH studies were performed in either 100mM Tris buffer (pH values 5.5; 6,0; 6.5; 7.0) or Bis-Tris buffer (pH values 7.0; 7.5; 8.0; 8.5; 9.0; 10.0) supplemented with 100mM KCl. Measured rates were corrected for appropriate blank readings accounting for non-specific decomposition of NADPH [449].

Temperature stability

Purified enzyme was diluted to 11mgmL^{-1} in 100mM Tris buffer, pH 7.5, containing 100mM KCl with or without 1mM TCEP. Experiments were carried out in Eppendorf tubes incubated at 55°C and 500rpm in a Thermomixer comfort from Eppendorf. Samples were withdrawn every hour and specific activities were determined as described above [449].

DMSO stability

DMSO stability was determined by measuring the conversions of the reduction of the natural substrate preQ$_0$ to its corresponding amine preQ$_1$ using 1% v/v DMSO to 55% v/v DMSO. A 200mM stock of preQ$_0$ in DMSO and a 250mM stock of NADPH in buffer (100mM Tris, 50mM KCl, 1.15mM TCEP, pH 7.5 adjusted with HCl conc.) were prepared. Biotransformation reactions contained buffer (100mM Tris, 50mM KCl, 1.15mM TCEP, pH 7.5 adjusted with HCl conc.), enzyme (40µM), substrate (2mM) in DMSO, and additional DMSO to adjust the concentration of DMSO to 1%v/v to 55%v/v, in a total reaction volume of 500µL. Reactions were started by addition of cofactor (5mM) and incubated on a thermomixer at 500rpm and 30°C for 19 hours. Reactions were stopped by addition of 200µL methanol. The enzyme was precipitated by heating to 75°C for ten minutes at 1400rpm and subsequent centrifugation. The reactions were then analysed with HPLC-MS. Conversions were calculated by area normalisation. Double determinations were run.

Steady-state enzyme kinetics

All experiments were carried out in 100mM Tris buffer, pH 7.5, supplemented with 50mM KCl, and, unless otherwise stated, at 55°C. Measurements of the initial rates of substrate reduction were performed with a Beckman DU-800 spectrophotometer monitoring the consumption of NADPH over a time period of five minutes. Initial rate data were measured under conditions where substrate (or cofactor) was held at a constant saturating concentration and the cofactor (or substrate) was varied in the range $0.4 < K_m <$ 4-10 fold. Typical reaction mixtures contained 80µM wildtype nitrile reductase from *G. kaustophilus* and about 0.7µM wild type nitrile reductase from *E. coli*. Kinetic parameters were obtained from unweighted non-linear least-square fits of experimental data to equation 7.1 using the program Sigmaplot 2004 for Windows, version 9.0. In equation 7.1 v is the initial rate, *[E]* is the molar concentration of the enzyme subunit (38.8 kDa), *[A]* is the substrate or coenzyme concentration, k_{cat} is the turnover number (min^{-1}) and K_{mA} is an apparent Michaelis-Menten constant [449].

$$v = \frac{k_{cat}[E][A]}{K_{mA} + [A]} \tag{7.1}$$

Two NADPH consumed account for one turnover. All rates were corrected for the appropriate blank readings accounting for the non-specific decomposition of NADPH. Unless otherwise stated, estimates of kinetic parameters had standard errors of $< 20\%$ [449].

$$v = \frac{k_{cat}}{2}\sqrt{(K_{mA} + [E] + [A]) - ((K_{mA} + [E] + [A])^2 - 4[E][A])} \tag{7.2}$$

In case of nitrile reductase from *E. coli*, the used enzyme concentration of 0.7µM was in the range of >0.1-fold of the obtained K_{mA}-values for $preQ_0$ and NADPH. The concentration of the free substrate is, under these conditions, the substrate concentration in the reaction mixture, corrected for the substrate that is bound to the enzyme. We therefore calculated the K_m-values according to equation 7.2.

7.4 Modelling and docking

The structure of *E. coli* nitrile reductase queF was modelled using the program YASARA Structure [468, 469] by applying the standard modelling protocol. For the comparative modelling, the structure of *V. cholerae* queF (PDB Code: 3RZQ) with a sequence identity of 65% and a similarity of 76% was used as a template. The natural substrate of *V. cholerae* queF was retained during modelling and energy minimization. The side chain of the proposed catalytic residue Cys190, which is located in a loop close to the active site, was rotated in the model to match the proposed reaction mechanism. An energy minimization of the complex was performed using the force field AMBER03 [470] by applying the standard YASARA energy minimization protocol. For the docking calculations the program Glide (L.L.C. Schrödinger: Glide, version 5.8. In New York, NY 2012) was used [471]. The substrates were prepared in Maestro (L.L.C. Schrödinger: Maestro, version 9.3. In New York, NY 2012.) and optimized using Jaguar (L.L.C. Schrödinger: Jaguar, version 7.9. In New York, NY 2012) with basis set 6-31G. The docking box for the grid calculation was set to a side length of 10Å with the centre of the box at the active site. The docking was performed with extra precision and with flexible ligands. Receptor hydroxyl and thiol groups within the docking box were allowed to rotate. All pictures were generated using PyMOL (L.L.C. Schrödinger: The PyMOL Molecular Graphics System, version 1.41. In New York, NY 2012). Hydrophobicity values for the visualization of the cavity surface were calculated using VASCo [452, 472].

7.5 Biocatalytic screening reactions

Screenings of nitrile substrates with wild type and mutant nitrile reductase queF

Screening reactions were run in UV star 96 well plates using the following conditions and concentrations: nitrile reductase (55µM of *G. kaustophilus* nitrile reductase (purity 60%-85%) or 45µM of *E. coli* nitrile reductase purity >85%, respectively) in buffer (100mM TRIS, 50mM KCl, 1.15mM TCEP, pH 7.5 adjusted with HCl conc.), substrate in DMSO (2mM, 10%v/v DMSO), NADPH (0.25mM in buffer), total volume 200µL. Blank reactions contained buffer, substrate in DMSO (2mM, 10%v/v DMSO) and NADPH (0.25mM in buffer). Reactions were started by addition of 50µL NADPH (1.0mM stock in buffer). NADPH depletion was monitored at 30°C for 14 hours. Subsequently, additional 4mM of NADPH was added to each well to allow full conversion. The screening reactions were incubated on a thermomixer for 24 hours at 30°C and 500rpm. Samples were then analysed with HPLC-MS to observe possible product formation. For all screening reactions, including blank reactions, multiple parallel determinations were run.

Inhibitor screenings with nitrile reductase queF

Inhibitor screenings were measured spectrophotometrically by monitoring the reduction of NADPH at 340nm. Typically, rates of 0.05 - 0.10 ΔA/min were measured over a time period of five minutes. One unit of enzyme activity refers to 1µmol of NADPH consumed per minute. All measurements were performed with a Beckman DU-800 spectrophotometer thermostated at 55°C. The assay contained 100µM $preQ_0$ and 250µM NADPH. $preQ_0$ was dissolved in DMSO prior to dilution into buffer, to give a final DMSO concentration of 1%v/v. Unless otherwise stated, Tris/HCl buffer, pH 7.5 supplemented with 50mM KCl was used. Reactions were always started by the addition of cofactor. Activities were normalized to $preQ_0$ reductase activity. Assays for inhibitor screening contained 10µM $preQ_0$ and the compounds listed in Figure 5.6. Residual activities refer to reductase activities obtained with 10µM $preQ_0$. Measured rates were corrected for appropriate blank readings accounting for non-specific decomposition of NADPH [449].

Screenings of aldehyde, imine, and oxime substrates with nitrile reductase

Screening reactions were run in Eppendorf tubes using the following conditions and concentrations: nitrile reductase queF from *G. kaustophilus* (90µM) in buffer (100mM Tris, 50mM KCl, 1.15mM TCEP, pH 7.5 adjusted with HCl conc.), substrate in DMSO (2mM, 1%v/v, 5%v/v or 10%v/v DMSO), and NADPH (5mM in buffer). Blank reactions contained buffer, substrate in DMSO (2mM, 1%v/v, 5%v/v or 10%v/v DMSO) and NADPH (5mM in buffer). Reactions were started by addition of NADPH. Blank reactions contained substrate in buffer, substrate and cofactor in buffer, enzyme and substrate, in similar concentrations as the biotransformation reactions. Reactions were incubated on a thermomixer at 30°C or 55°C and 500rpm for 16 hours. The protein was precipitated by addition of 200µL methanol and subsequent centrifugation. The supernatant was transferred to HPLC-vials and analyzed by HPLC-MS.

Screenings of oxidation reactions with nitrile reductase

Screenings of oxidation reactions were done analogously to screenings of aldehyde, imine, and oxime substrates, except $NADP^+$ or NAD^+ was used as cofactor.

Screenings of $preQ_0$ with nitrilase

Screening reactions were run in 96 well plates (total reaction volume 200µL) or eppendorf tubes (total reaction volume 500µL). Stock solutions of substrate in DMSO (10mM, 20mM, 50mM, 100mM) and lypohilized enzyme in buffer (50mM K_2HPO_4, pH 8, 4.0mg/mL enzyme) were prepared. Reactions were started by addition of substrate stock (substrate 0.2mM or 0.4mM, DMSO 2%v/v). The screening reactions were incubated on a thermomixer at 30°C and 800rpm for 24 hours. Subsequently, the protein was precipitated by addition of methanol (40%v/v of the total reaction volume) and centrifugation. The supernatant was transferred in a new 96 well plate or HPLC vials and analyzed by HPLC-MS. For all screening reactions, including blank reactions, double parallel determinations were run.

7.6 Substrate synthesis

7.6.1 Synthesis of pyrrolo[2,3-*d*]pyrimidines

Synthesis of $preQ_0$ and $preQ_1$

2-chloro-3-oxopropanenitrile (2)

2

Method A: NaH (1.0g, 50% in mineral oil) was washed twice with cyclohexane and once with THF and was then suspended in 20mL THF. The suspension was cooled to 0°C and methyl formate (0.90mL, 14mmol) was added. Chloroacetonitrile (0.83mL, 13mmol) was added dropwise to the stirred solution and the solution was stirred for additional 3.5 hours. Afterwards, 20mL deionised water were added and the mixture was extracted twice with ethyl acetate. The layers were separated and the pH value of the aqueous layer was adjusted to pH 4 with 5M HCl. The aqueous layer was then extracted three times with diethyl ether. The combined organic phases from the second extraction were dried over Na_2SO_4 and reduced under pressure to yield of a brown oil which was used for the next synthetic step without further purification.
Yield 1.142g, 85%, brown oil, M=103.5071g/mol.
Method B: 2-Chloro-3-oxopropanenitrile as prepared according to a modified literature procedure [259, 263]. Sodium (524.0mg, 22.79mmol, 1.755eq.) was washed in cyclohexane and added portionwise to methanol (25mL). Formation of the methoxide was complete when all sodium was dissolved. The excess methanol was removed in vacuum. Toluene (15mL) was added to the sodium methoxide and the resulting mixture was cooled to 0°C. Methylformate (900µL, 14.2mmol, 1.09eq.) was added to the cooled reaction mixture. Chloroacetonitrile (830µL, 13.0mmol) was added dropwise to the stirred solution. After 4.5 hours the reaction was quenched by dropwise addition of 15mL deionized water. The resulting mixture was twice extracted with ethyl acetate. The pH value of the aqueous layer was adjusted to pH 4 by addition of aqueous HCl. The aqueous layer was again extracted with ethyl acetate, three times. The combined organic layers from the second extraction were dried over sodium sulphate and reduced in vacuum.
Yield not determined, light yellow oil, M=103.5071g/mol.
Method C: 2-Chloro-3-oxopropanenitrile as prepared according to a modified literature procedure [260, 262]. Sodium (2.299g, 100.0mmol, 1.486eq.) was washed in cyclohexane and added portionwise to methanol (15mL). After complete formation of the sodium methoxide, the excess methanol was removed in vacuum. THF (63mL) was added and the resulting reaction mixture was cooled to 0°C and stirred under nitrogen atmosphere. Methyl formate (4.60mL, 72.4mmol, 1.08eq.) was added to the stirred reaction mixture. Subsequently, chloroacetonitrile (4.30mL, 67.3mmol) was added dropwise over an hour and the resulting reaction mixture was stirred for additional three hours. The reaction was quenched by addition of 7.4mL 10M aqueous HCl. The solvent was reduced by 50% in vacuum. The resulting residue was used directly in the next synthetic step.
Yield not determined, light orange oil, M=103.5071g/mol.

2-amino-5-cyano-7*H*-pyrrolo[2,3-*d*] pyrimidin-4-one (preQ$_0$, 1)

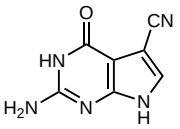

1

2-Amino-5-cyano-7*H*-pyrrolo [2,3-*d*]pyrimidin-4-one (**1**) was prepared according to a literature procedure [259]. Sodium acetate trihydrate (2.693g, 19.79mmol) was dissolved in 40mL deionised water and 2-diamino-6-hydroxypyrimidine (1.225g, 9.32mmol) was added. The suspension was heated to reflux. 2-Chloro-3-oxopropanenitrile (1.142g, 11.03mmol) was dissolved in 20mL deionised water and added dropwise to the reaction mixture. The reaction mixture was stirred at reflux over night. On cooling to room temperature the beige product precipitated from the solution. The product was filtered off, washed with copious amounts of water and acetone.
Yield 840.0mg, 51%, beige to brown solid, M=175.1475g/mol.
TLC R_f 0.53 ($CHCl_3$/MeOH/aq. NH_3 5/4/1)
HPLC-MS t_{ret}= 15.4min (method C)
^{1}H NMR (DMSO-d_6) δ 6.39 (s, 2H, NH_2), 7.62 (s, 1H, H-6), 10.72 (s, 1H, H-7), 11.99 (s, 1H, H-3).
^{13}C NMR (DMSO-d_6) δ 85.53 (C-5), 98.73 (C-4a), 115.87 (CN), 127.77 (C-6), 151.66 (C-7a), 153.72 (C-2), 157.56 (C-4).

2-octanoylamino-7-*N*-octanoylpyrrolo[2,3-*d*]pyrimidin-4-one (96)

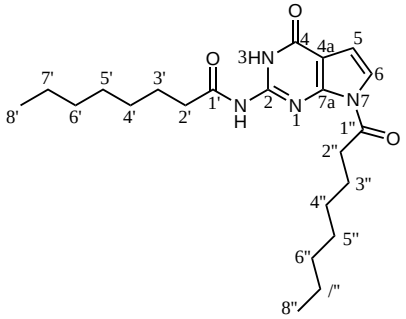

2-Octanoylamino-7-*N*-octanoylpyrrolo[2,3-*d*]pyrimidin-4-one was prepared according to a modified literature procedure [266]. 2-Aminopyrrolo[2,3-*d*]pyrimidin-4-one (7.920g, 52.75mmol) was dissolved in pyridine (51.0mL, 631mmol, 11.9eq.) and octanoyl chloride (26.0mL, 151mmol, 2.86eq.) was added dropwise to the stirred reaction mixture. The reaction mixture was heated to 80°C over night, and subsequently neutralized by addition of aqueous ammonia solution. The product was isolated by filtration and washed with ethanol and diethyl ether.
Yield 6.200g, 29.20%, beige solid, M=402.5304g/mol.
^{1}H NMR (DMSO-d_6) δ 0.87 (s, 6H, H-8', H-8"), 1.28 (s, 16H, H-4', H-5', H-6', H-7', H-4", H-5", H-6", H-7"), 1.65 (m, 4H, H-3', H-3"), 2.48 (m, 4H, H-2', H-2"), 6.61 (s, 1H, H-5), 7.48 (s, 1H, H-6), 11.41 (s, 1H, H-3), 12.08 (s, 1H, NH).
^{13}C NMR (DMSO-d_6) δ 13.88 (C-8', C-8"), 22.03 (C-7', C-7"), 23.98, 24.31 (C-3', C-3"), 28.39, 28.45,

28.67 (C-4', C-5', C-4", C-5"), 31.09, 31.14 (C-6', C-6"), 36.00, 36.59 (C-2', C-2"), 105.29 (C-5), 107.14 (C-4a), 119.44 (C-6), 147.29 (C-2), 147.99 (C-7a), 156.37 (C-4), 171.56, 176.35 (C-1', C-1").

2-amino-5-methylamino-7*H*-pyrrolo[2,3-*d*]pyrimidin-4-one (preQ$_1$, 3)

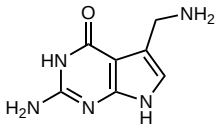

3

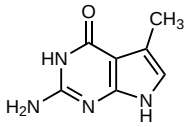

4

PreQ$_1$ was prepared as HPLC reference material for screening reactions.
Method A: PreQ$_0$, **1**, (1.00g, 5.71mmol) was dissolved in 20mL DMF. Aqueous ammonia (4.0mL, 57mmol, 10eq.), triethylamine (200µL, 1.44mmol, 0.25eq.), and Raney-Nickel catalyst were added. The reaction mixture was stirred at 55°C under 40bar of hydrogen pressure for 24 hours. HPLC analysis indicated approximately 60% conversion and no side product formation.
Method B: PreQ$_0$, **1**, (408.0mg, 5.709mmol) was dissolved in 40mL DMF and triethylamine (80.0µL, 0.577mmol, 0.25eq.) and aqeuous ammonia (1.52mL, 23.3mmol, 10.0eq.) were added. The reaction mixture was stirred at 70°C under 100bar of hydrogen pressure over 54 hours. HPLC analysis indicated approximately 40% conversion to preQ$_1$, 15% to a by-product, and 45% remaining preQ$_0$. The by-product was isolated and purified by column chromatography using chloroform/methanol 10/1 as eluent. The by-product was identified as 2-amino-5-methylpyrrolo[2,3-*d*]pyrimidin-4-one (**4**) by NMR spectropscopy.
2-amino-5-methylamino-7*H*-pyrrolo[2,3-*d*]pyrimidin-4-one (preQ$_1$)
TLC R_f 0.24 ($CHCl_3$/MeOH/aq. NH_3 5/4/1)
HPLC-MS t_{ret}= 9.3min (method C)
2-amino-5-methylpyrrolo[2,3-*d*]pyrimidin-4-one (**4**)
TLC R_f ($CHCl_3$/MeOH/aq. NH_3 5/4/1)
^{1}H NMR (DMSO-d_6) δ 2.17 (s, 3H, CH_3, 6.07 (s, 2H, NH_2, 6.33 (s, 1H, H-6), 10.21 (s, 1H, H-7), 10.61 (s, 1H, H-3).
^{13}C NMR (DMSO-d_6) δ 11.36 (CH_3), 99.31 (C-4a), 112.86 (C-5), 113.59 (C-6), 151.03 (C-7a), 152.17 (C-2), 159.50 (C-4).

2-amino-4-oxo-pyrrolo[2,3-*d*]pyrimidin-5-carboxylic acid (98)

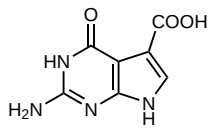

98

2-Amino-4-oxo-pyrrolo[2,3-*d*]pyrimidin-5-carboxylic acid (**98**) was prepared from preQ$_0$ according to a modified literature procedure [104]. 2-Amino-5-cyanopyrrolo[2,3-*d*]pyrimidin-4-one (218.4mg, 1.247mmol) was dissolved in 15mL 6M aqueous KOH. The resulting reaction mixture was stirred at reflux for 16 hours and subsequently at room temperature over night. The reaction mixture was then cooled to room temperature and neutralized by addition of hydrochloric acid. The product

precipitated from the solution, was isolated by filtration and washed with copious amounts of water and acetone
Conversion 42%, light orange solid, M=194.1475g/mol.
HPLC-MS t_{ret}= 14.9min (method C)

Synthesis of preQ$_0$ analogues

2,4-diamino-5-cyano-7*H*-pyrrolo[2,3-*d*]pyrimidine (5)

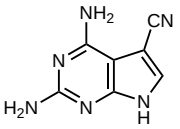

5

2,4-Diamino-5-cyano-7*H*-pyrrolo[2,3-*d*]pyrimidine was prepared similar to preQ$_0$. 2,4,6-triaminopyrimidine (500.0mg, 3.876mmol) and sodium acetate trihydrate (2.693g, 19.79mmol, 5.106eq.) were suspended in 20mL deionized water and heated to 85°C. 2-Chloro-3-oxopropanenitrile (500mg, 4.831mmol, 1.246eq.) was dissolved in 10mL deionised water and added dropwise to the reaction mixture. The reaction mixture was stirred under reflux over night. Subsequently, the reaction mixture was cooled to 0°C. The dark brown product precipitated from the solution, was isolated by filtration and washed with copious amounts of water and acetone.
Yield 272.0mg, 40.29%, dark brown solid, M=174.1624g/mol.
TLC R_f 0.54 (dichloromethane/MeOH 4/1)
HPLC-MS t_{ret}= 8.42min (method D), t_{ret}= 19.07min (method C)
^{1}H NMR (DMSO-d$_6$) δ 5.88 (s, 2H, NH$_2$-2), 6.23 (s, 2H, NH$_2$-4), 7.64 (s, 1H, H-6), 11.79 (bs, 1H, NH).
^{13}C NMR (DMSO-d$_6$) δ 81.97 (C-5), 94.03 (C-4a), 116.77 (CN), 128.81 (C-6), 153.68 (C-7a), 157.23 (C-4), 161.07 (C-2).

2-amino-4-chloro-5-cyano-7*H*-pyrrolo[2,3-*d*]pyrimidine (6)

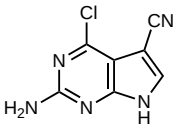

6

2-amino-4-chloro-5-cyano-7*H*-pyrrolo[2,3-*d*]pyrimidine was prepared according to a modified literature procedure [275]. preQ$_0$, **1**, (2.00g, 11.4mmol) was suspended in 12mL acetonitrile. Triethylamine (3.2mL, 23mmol) was added and the suspension was heated to 60°C. Phosphorus oxychloride (2.2mL, 24mmol) was slowly added to the warm reaction mixture. The reaction mixture was stirred at 60°C over night. Subsequently, additional 10mL acetonitrile, phosphorus oxychloride (2.2mL, 24mmol), and triethylamine (3.2mL, 23mmol) were added. The reaction was stirred at reflux for additional 48 hours at which time HPLC-MS analysis showed full conversion. The reaction mixture was cooled to room temperature and ice was slowly added. The pH value

of the reaction mixture was then adjusted to pH 6 using saturated sodium carbonate solution. The mixture was then cooled to 0°C. The brown product precipitated from the solution and was isolated by vacuum filtration and washed with water. The product was purified by recrystallization from methanol and dried in vacuum.
Yield 2.125g, 96.16%, brown solid, M=193.5932g/mol.
TLC R_f 0.78 ($CHCl_3$/MeOH/aq. NH_3 5/4/1)
HPLC-MS t_{ret}= 19.49min (method D), t_{ret}= 14.84min (method E)
^{1}H NMR (DMSO-d_6) δ 6.96 (s, 2H, NH_2), 8.12 (s, 1H, H-6).
^{13}C NMR (DMSO-d_6) δ 83.05 (C-5), 106.10 (C-4a), 115.05 (CN), 134.16 (C-6), 151.09 (C-7a), 154.49 (C-4), 160.38 (C-2).

2-amino-5-cyano-7*H*-pyrrolo[2,3-*d*]pyrimidine (7)

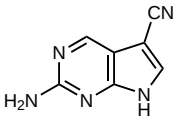

7

2-Amino-4-chloro-5-cyano-7*H*-pyrrolo[2,3-*d*]pyrimidine (650mg, 3.36mmol) was suspended in 80mL ethanol. Palladium on charcoal catalyst (10%m/m, 65mg) and sodium bicarbonate (33.8mg, 4.02mmol) were added. The suspension was stirred at 500rpm at 90°C and 80bar of hydrogen pressure in a steel autoclave for 40 hours. The catalyst was removed by filtration over celite and washed with ethanol. The filtrate was reduced in vacuum until dryness.
Yield 440.0mg, 82.34%, brown solid, M=159.1481g/mol. An analytical sample was purified by preparative HPLC (method B).
TLC R_f 0.81 ($CHCl_3$/MeOH/aq. NH_3 = 5/4/1), R_f 0.62 (ethyl acetate/MeOH = 7/1)
HPLC-MS t_{ret}= 15.10min (method D)
Anal. calcd for $C_7H_5N_5$ C 52.83, H 3.17, N 44.01, found: C 54.30, H 4.23, N 41.47.
^{1}H NMR (DMSO-d_6) δ 6.55 (s, 2H, NH_2), 8.02 (s, 1H, H-6), 8.63 (s, 1H, H-4).
^{13}C NMR (DMSO-d_6) δ 82.83 (C-5), 108.96 (C-4a), 115.45 (CN), 133.01 (C-6), 149.93 (C-4), 153.55 (C-7a), 161.13 (C-2).

2-pivaloylamino-5-cyanopyrrolo[2,3-*d*]pyrimidin-4-one (8)

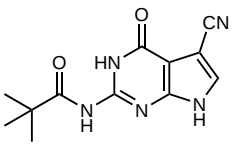

8

$PreQ_0$ (500.0mg, 2.855mmol) was suspended in pyridine (5mL) and triethylamine (1mL) and heated to 90°C. Trimethylacetyl chloride (1.07mL, 8.60mmol, 3.00eq.) was added dropwise to the stirred solution and the reaction mixture was stirred at 90°C over night. Subsequently, the reaction mixture was cooled to room temperature. A white precipitate was removed from the reaction

mixture by filtration. The filtrate was concentrated in vacuum until dryness. The residue was then resuspended in deionised water, cooled to 0°C, and the pH was adjusted to pH 7 by addition of aqueous ammonia. The brown product precipitated from the solution and was isolated by filtration.
Yield 594.2mg, 80.28%, brown solid, M=259.2639g/mol.
TLC R_f 0.89 ($CHCl_3$/MeOH/aq. NH_3 = 5/4/1)
HPLC-MS t_{ret}= 14.99min (method E)
^{1}H NMR (DMSO-d_6) δ 1.19 (s, 3H, CH_3), 7.87 (s, 1H, H-6), 10.93 (s, 1H, H-7), 12.05 (bs, 1H, H-3), 12.55 (s, 1H, NH-Piv).
^{13}C NMR (DMSO-d_6) δ 26.27 (CH_3-Piv), 35.76 (C-Piv), 86.22 (C-5), 103.04 (C-4a), 115.16 (CN), 130.18 (C-6), 148.39, 148.45 (C-2, C-7a), 155.67 (C-4), 181.09 (CO-Piv).

2-pivaloylamino-4-chloro-5-cyanopyrrolo[2,3-*d*]pyrimidine (99)

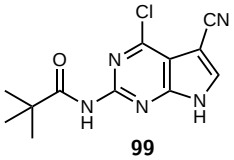

99

2-Pivaloylamino-4-chloro-5-cyanopyrrolo[2,3-*d*]pyrimidine was prepared according to a literature procedure [262]. 2-Pivaloylamino-5-cyanopyrrolo[2,3-*d*]pyrimidin-4-one (710.0mg, 2.739mmol) was suspended in 5mL acetonitrile. Dimethylaniline (1.7mL, 13.4mmol, 4.9eq.), triethylbenzylammonium chloride (368.0mg, 1.616mmol, 0.590eq.) and phosphorus oxychloride (3.0mL, 33mmol, 12eq.) were added to the stirred suspension. The resulting reaction mixture was heated to 90°C for 1.5 hours. Subsequently, the solvent was removed in vacuum and ice water was added to the remaining residue. The pH value was adjusted to pH 4 by addition of aqueous ammonia solution. The brown product precipitated from the solution, was isolated by filtration, washed with copious amounts of water and dried in vacuum.
Yield 450.0mg, 59.17%, brown solid, M=277.7096g/mol.
^{1}H NMR (DMSO-d_6) δ 1.25 (s, 3H, CH_3), 8.53 (d, J=3.8Hz, H-6), 10.33 (s, 1H, H-7), 13.41 (s, 1H, NH-Piv).

2-amino-4-methoxy-5-cyanopyrrolo[2,3-*d*]pyrimidine (9)

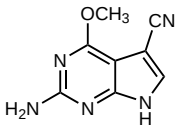

9

2-Amino-4-methoxy-5-cyanopyrrolo[2,3-*d*]pyrimidine was prepared according to a literature procedure [288]. Sodium methoxide was prepared by adding sodium (700.0mg, 30.45mmol, 4.912eq.) to methanol (40mL) under nitrogen atmosphere. 2-Amino-4-chloro-5-cyanopyrrolo[2,3-*d*]pyrimidine (1.200g, 6.198mmol) was then added to the stirred solution. The reaction mixture was heated to reflux and stirred for 6 hours. Subsequently, the solvent was removed in vacuum. The remaining

residue was purified by column chromatography using chloroform/ethyl acetate/methanol 5/1/1 as eluents.
Yield 50.40mg, 4.298%, brown solid, M=189.1714g/mol.
TLC R_f 0.46 (chloroform/ethyl acetate/methanol = 5/1/1).
^{1}H NMR (DMSO-d_6) δ 3.77 (s, 3H, CH_3), 6.25 (s, 2H, NH_2), 7.61 (s, 1H, H-6), 11.95 (s, 1H, H-7).
^{13}C NMR (DMSO-d_6) δ 53.23 (CH_3), 82.35 (C-5), 95.39 (C-4a), 116.11 (CN), 130.25 (C-6), 151.08 (C-7a), 160.69 (C-2), 162.69 (C-4).

2-amino-5-bromo-3,4-dicyano-1*H*-pyrrole (10)

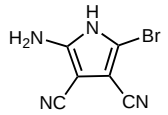

10

2-Amino-5-bromo-3,4-dicyano-1*H*-pyrrole was prepared according to a literature procedure [291]. Tetracyanoethylene (21.00g, 160.7mmol) was added to a stirred mixture of 115mL acetone and 250mL ethyl acetate. The reaction mixture was cooled to -5°C and 118mL of a 33% solution of hydrogen bromide in acetic acid was added dropwise over 2.5 hours during which time a pale yellow solid precipitated from the reaction mixture. The reaction mixture was stirred for additional 30 minutes. The precipitate was collected by vacuum filtration and washed with copious amounts of ethyl acetate. The remaining solid was suspended in 300mL of ice water. The pH of the suspension was adjusted to pH 11 with aqueous 50% sodium hydroxide solution at which point the solid was completely dissolved. The pH value was then adjusted to pH 5 by adding glacial acetic acid to the cooled solution. A beige precipitate formed which was isolated by vacuum filtration.
Yield 28.29g, 83.44%, beige solid, M=211.0188g/mol.
TLC R_f 0.45 ($CHCl_3$/MeOH = 9/1 plus triethylamine)
^{1}H NMR (acetone-d_6) δ 5.90 (bs, 2H, NH_2), 11.14 (s, 1H, NH).
^{13}C NMR (acetone-d_6) δ 73.87 (C-4), 95.64 (C-3), 102.08 (C-5), 113.91 (CN), 114.29 (CN), 149.66 (C-2).

4-amino-6-bromo-5-cyano-7*H*-pyrrolo[2,3-*d*]pyrimidine (11)

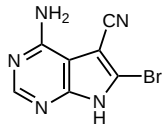

11

4-Amino-6-bromo-5-cyano-7*H*-pyrrolo[2,3-*d*]pyrimidine was prepared according to a literature procedure [292]. 2-Amino-5-bromo-3,4-dicyano-1*H*-pyrrole (26.65g, 126.9mmol) was dissolved in 500mL 2-ethoxyethanol. Formamidine acetate salt (26.63g, 250.8mmol) was added to the stirred solution. The reaction mixture was heated to reflux for 41 hours. The solution was treated with activated charcoal which was subsequently removed by filtration over celite. The filtrate was concentrated in vacuum until dryness. The resulting brown solid was suspended in 300mL

water, cooled to 0°C, and collected by filtration and dried in vacuum. The product was purified by recrystallisation from DMF/methanol.
Yield 7.166g, 23.84%, beige solid, M=238.0442g/mol.
^{1}H NMR (DMSO-d_6) δ 7.21 (bs, 2H, NH_2), 8.23 (s, 1H, H-2), 13.79 (bs, 1H, NH).
^{13}C NMR (DMSO-d_6) δ 83.89 (C-5), 103.14 (C-4a), 115.35 (CN), 124.34 (C-6), 149.03 (C-7a), 149.53 (C-2), 155.46 (C-4).

4-amino-5-cyano-7*H*-pyrrolo[2,3-*d*]pyrimidine (14)

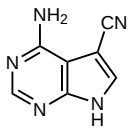

14

4-Amino-6-bromo-5-cyano-7*H*-pyrrolo[2,3-*d*]pyrimidine (1.60g, 6.72mmol) was dissolved in 300mL ethanol and 300mL 33% aqueous ammonium hydroxide solution. Palladium on charcoal catalyst (10% m/m) was added and the reaction mixture was stirred in hydrogen atmosphere (hydrogen balloon) for 12 hours. The catalyst was removed by filtration over celite, and washed with hot ethanol/ammonium hydroxide solution. The filtrate was reduced in vacuum to about one half of the original volume. On cooling a white solid precipitated from the solution. The product was isolated by filtration.
Yield 686.5mg, 63.86%, white solid, M=159.1481g/mol.
TLC R_f 0.77 ($CHCl_3$/MeOH/aq. NH_3 5/4/1)
HPLC-MS t_{ret}= 9.40min (method D), t_{ret}= 19.05min (method C)
^{1}H NMR (DMSO-d_6) δ 6.75 (bs, 2H, NH_2), 8.16 (s, 1H, H-6), 8.20 (s, 1H, H-2), 12.60 (bs, 1H, NH).
^{13}C NMR (DMSO-d_6) δ 82.02 (C-5), 100.89 (C-4a), 115.96 (CN), 132.33 (C-6), 150.88 (C-7a), 153.52 (C-2), 156.89 (C-4).

6-bromo-5-cyano-7*H*-pyrrolo[2,3-*d*]pyrimidin-4-one (12)

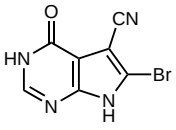

12

6-Bromo-5-cyano-7*H*-pyrrolo[2,3-*d*] pyrimidin-4-one was prepared from 4-amino-6-bromo-5-cyano-7*H*-pyrrolo[2,3-*d*]pyrimidine according to a literature procedure [299]. 4-Amino-6-bromo-5-cyano-7*H*-pyrrolo[2,3-*d*]pyrimidine (1.415g, 5.944mmol) was suspended in a mixture of 30mL deionised water and 30mL acetic acid and heated to 105°C. Sodium nitrite (4.402g, 63.80mmol) was dissolved in 60mL deionised water and added to the reaction mixture dropwise over one hour. The reaction mixture was then stirred at 105°C for additional two hours, cooled to room temperature and stirred at room temperature over night. The reaction mixture was then cooled at 0°C for four

hours. The precipitate was collected by vacuum filtration, resuspended in 60mL deionised water and heated to 100°C for 3.5 hours. The reaction mixture was then cooled to 0°C over night. The product was collected by vacuum filtration.
Yield 1.123g, 79.04%, beige solid, M=239.0289g/mol.
TLC R_f 0.60 ($CHCl_3$/MeOH/aq. NH_3 = 5/4/1)
^{1}H NMR (DMSO-d_6) δ 8.01 (s, 1H, H-2), 12.44 (bs, 1H, NH), 13.84 (bs, 1H, NH).
^{13}C NMR (DMSO-d_6) δ 88.82 (C-5), 108.48 (C-4a), 113.96 (C-6), 115.07 (CN), 146.40 (C-2), 148.93 (C-7a), 155.82 (C-4).

5-cyano-7*H*-pyrrolo[2,3-*d*]pyrimidin-4-one (13)

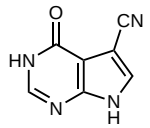

13

5-Cyano-7*H*-pyrrolo[2,3-*d*]pyrimidin-4-one was prepared according to a literature procedure [293]. 6-Bromo-5-cyano-7*H*-pyrrolo[2,3-*d*]pyrimidin-4-one (1.406mg, 5.906mmol) were dissolved in aqueous ammonia solution (250mL). Palladium on charcoal (10% m/m, 0.699g) in 250mL ethanol were added to the stirred solution. The reaction was stirred at room temperature under hydrogen (hydrogen balloon) over night. The catalyst was then removed by filtration over celite and washed with 100mL hot ethanol/aqueous ammonia solution. The clear, light yellow solution was decreased by one half in vacuum and cooled to 0°C at which point the product precipitated from the solution. The white product was isolated by filtration.
Yield 552.0mg, 58.60%, white solid, M=160.1329g/mol. The product was then further purified by preparative HPLC (method A).
TLC R_f 0.62 ($CHCl_3$/MeOH/aq. NH_3 = 5/4/1)
HPLC-MS t_{ret}= 19.07min (method C)
Anal. calcd for $C_7H_4N_4O$: C 58.33, H 2.80, N 38.87, found: C 58.23, H 2.88, N 38.90.
^{1}H NMR (DMSO-d_6) δ 12.14 (bs, 1H, NH-7), 8.02 (s, 1H, H-2), 8.01 (s, 1H, H-6).
^{13}C NMR (DMSO-d_6) δ 85.98 (C-5), 107.13 (C-4a), 115.24 (-CN), 130.82 (C-6), 145.85 (C-2), 148.56 (C-7a), 157.07 (C-4).

6-bromo-4-chloro-5-cyanopyrrolo[2,3-*d*]pyrimidine (15)

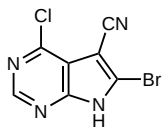

15

6-Bromo-5-cyanopyrrolo[2,3-*d*]pyrimidin-4-one (1.100g, 4.602mmol) was suspended in acetonitrile (10mL) and triethylamine (1.3mL, 9.2mmol, 2.0eq.). Phosphorus oxychloride (0.9mL, 9.7mmol, 2.1eq.) was added dropwise and the resulting reaction mixture was heated to 60°C and stirred over

night. TLC control showed incomplete conversion, consequently additional acetonitrile (5mL), triethylamine (1.3mL, 9.2mmol, 2.0eq.) and phosphorus oxychloride (0.9mL, 9.7mmol, 2.1eq.) were added, and the reaction mixture was heated to 90°C. After 9 hours reaction time at 90°C the reaction mixture was cooled to room temperature. Deionized water (5mL) was added slowly, the pH value of the reaction mixture was then adjusted to pH 6 by addition of saturated Na_2CO_3 solution. The reaction volume was reduced about one half in vacuum at which point the product precipitated from the solution. The product was isolated by filtration and washed with copious amounts of water. The product was purified by recrystallization from methanol.
Yield 455.4mg, 38.43%, brown solid, M=257.4746g/mol.
TLC R_f 0.90 ($CHCl_3$/MeOH/aq. NH_3 = 5/4/1)
^{1}H NMR (DMSO-d_6) δ 8.74 (s, 1H, H-2).
^{13}C NMR (DMSO-d_6) δ 86.24 (C-5), 112.40 (C-4a), 113.23 (CN), 126.07 (C-6), 149.21 (C-7a), 152.01 (C-2), 152.36 (C-4).

5-cyanopyrrolo[2,3-*d*]pyrimidine (16)

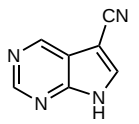

16

6-Bromo-4-chloro-5-cyanopyrrolo[2,3-*d*]pyrimidine (400.0mg, 1.554mmol) was suspended in ethanol (60mL). $NaHCO_3$ (287.0mg, 3.418mmol, 2.2eq.) and Pd/C (10%m/m, 80mg) were added to the suspension. The reaction mixture was stirred in a steel autoclave at 70°C and 100bar hydrogen pressure for 24 hours. Afterwards, the catalyst was removed by filtration over celite. The solvent was removed in vacuum until dryness.
Yield 111.6mg, 49.83%, beige solid, M=144.1335g/mol.
TLC R_f 0.82 ($CHCl_3$/MeOH/aq. NH_3 = 5/4/1)
HPLC-MS t_{ret}= 11.46min (method D)
^{1}H NMR (DMSO-d_6) δ 8.58 (s, 1H, H-6), 8.96 (s, 1H, H-2), 9.22 (s, 1H, H-4), 13.27 (bs, 1H, NH).
^{13}C NMR (DMSO-d_6) δ 83.06 (C-5), 114.53 (C-4a), 117.15 (CN), 137.27 (C-6), 148.81 (C-4), 150.85 (C-5), 152.86 (C-2).

7.6.2 Synthesis of pyrrolo[2,3-*b*]pyridines and pyrrolo[3,2-*c*]pyridines

2-amino-4-azidopyridine (22)

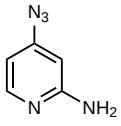

22

2-Amino-4-azidopyridine was prepared according to a literature procedure for the preparation of 2-azido-4-aminopyridine [310, 311]. 2-Amino-4-chloropyridine (5.000g, 37.73mmol) was dissolved in

40mL DMF and stirred under nitrogen atmosphere. Sodium azide (5.100g, 77.66mmol, 2.059eq.) and ammonium chloride (4.200g, 78.52mmol, 2.081eq.) were added to the stirred solution. The resulting reaction mixture was heated to 120°C and stirred over night. Subsequently, the reaction mixture was cooled to room temperature and quenched with 85mL saturated sodium bicarbonate solution. The resulting light brown precipitate was removed by filtration. The filtrate was extracted with ethyl acetate three times. The combined organic layers were then washed with water, dried over sodium sulphate and reduced in vacuum until dryness. The product was purified by recrystallization from cyclohexane/ethyl acetate.
Yield 2.700g, 52.96%, beige solid, M=135.1267g/mol.
^{1}H NMR (DMSO-d_6) δ 6.15 (s, 1H, NH_2), 6.18 (d, 1H, H-3, J=1.9Hz), 6.29 (dd, 1H, H-5, J1=5.5Hz, J2=2.0Hz), 7.91 (d, 1H, H-6, 5.5Hz).
^{13}C NMR (DMSO-d_6) δ 96.51 (C-3), 103.12 (C-5), 148.44 (C-4), 149.59 (C-6), 161.12 (C-2).

2,4-diaminopyridine (23)

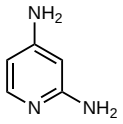

23

2-Amino-4-azidopyridine (100.0mg, 0.7400mmol) was dissolved in 10mL acetic acid. Platinum on charcoal catalyst (10% m/m) was added. The reaction was stirred under hydrogen atmosphere (hydrogen balloon) for one hour at which point TLC indicated full conversion. The catalyst was removed by filtration over celite, and the filtrate was reduced in vacuum until dryness.
Yield 88.00mg, crude product, contains traces of acetic acid, black resin, M=109.1292g/mol.
^{1}H NMR (DMSO-d_6) δ5.39 (bs, 1H, H-3), 5.69 (bs, 1H, H-5), 6.22 (bs, 2H, NH_2), 6.88 (bs, 2H, NH_2), 7.13 (bs, 1H, H-6).
^{13}C NMR (DMSO-d_6) δ 88.94 (C-3), 101.47 (C-5), 140.16 (C-6), 157.14 (C-4), 175.21 (C-2).

2-amino-4-methoxypyridine (21)

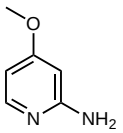

21

2-Amino-4-chloropyridine (970.0mg, 7.178mmol) was dissolved in 50mL methanol. Sodium methoxide was prepared *in situ*, by adding sodium (450.0mg, 19.57mmol, 2.727eq.) in portions to the stirred solution. The reaction mixture was then stirred under reflux for 48 hours at which point TLC-control indicated complete conversion. The reaction mixture was then cooled to room temperature and 10% aqueous hydrochloric acid was added until pH 8. The solvent was removed in vacuum and the remaining residue was resuspended in diethyl ether and the insoluble components were removed by filtration. The solvent was removed in vacuum.
Yield 511.2mg, 57.36%, brown solid, M=124.1405g/mol.

^{1}H NMR (DMSO-d_6) δ 3.72 (s, 3HCH_3), 5.86 (bs, 2H, NH_2), 5.98 (d, J=2.2Hz, H-2), 6.14 (dd, J=2.3Hz, J=5.9Hz, 1H, H-4), 7.72 (d, J=5.9Hz, 1H, H-5).
^{13}C NMR (DMSO-d_6) δ 54.60 (OCH_3), 91.14 (C-5), 100.89 (C-3), 148.37 (C-4), 161.34 (C-6), 166.30 (C-2).

1,2-bis(4-azidopyrrolo[2,3-*b*]pyridin-1-yl)ethene (24)

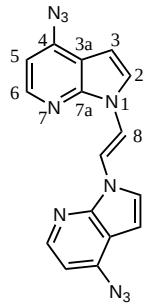

24

2-Amino-4-azidopyridine (4.400g, 32.56mmol) and sodium acetate trihydrate (9.000g, 66.14mmol, 2.031eq.) were suspended in 90mL deionized water and heated to reflux. Chloroacetaldehyde (50%m/m aqueous solution, 5.2mL, 33mmol, 1.0eq.) diluted with 30mL deionized water was added to the reaction mixture over 30 minutes. The reaction was stirred at reflux for three hours and then at room temperature over night. The solvents were removed in vacuum and the remaining residue was resuspended in methanol and filtered over silica gel to remove the remaining salts. The filtrate was reduced in vacuum and the remaining residue was resuspended in boiling toluene. All remaining solids were filtered off in a hot filtration. The product precipitated from the filtrate and was purified by recrystallization from toluene.
Yield 3.000g, 53.83%, beige solid, M=342.3176g/mol.
^{1}H NMR (DMSO-d_6) δ 6.74 (dd, J=2.1Hz, J=7.3Hz, 1H, H-5), 7.29 (d, J=1.9Hz, 1H, H-3), 7.56 (d, J=0.7Hz, 1H, H-2), 7.92 (s, 1H, H-8), 8.58 (d, J=7.3Hz, 1H, H-6).
^{13}C NMR (DMSO-d_6) δ 104.44 (C-3), 106.12 (C-5), 113.11 (C-8), 128.23 (C-6), 133.82 (C-2), 136.63 (C-4), 144.64 (C-7a).

1,2-bis(4-azido-3-bromopyrrolo[2,3-*b*]pyridin-1-yl)ethene (25)

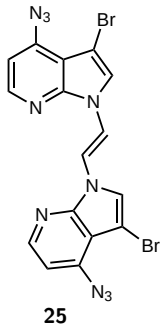

25

1,2-Bis(4-azidopyrrolo[2,3-*b*]pyridin-1-yl)ethene (98.3mg, 0.287mmol) was dissolved in 5mL THF and cooled to 0°C. *N*-Bromosuccinimide (62.6mg, 0.352mmol, 1.22eq.) was added portionwise to

the stirred reaction mixture. After stirring at room temperature over night, TLC control indicated incomplete conversion. Additional *N*-bromosuccinimide (15.3mg, 0.0859mmol, 0.30eq.) was added to the reaction mixture and the reaction mixture was stirred for additional 2.5 hours at room temperature. Subsequently, the reaction was quenched by the addition of 15mL deionised water. The product precipitated from the reaction mixture and was isolated by filtration and washed with copious amounts of deionized water.
Yield 70.1mg, 48.81%, beige solid, M=500.1097g/mol.
^{1}H NMR (DMSO-d_6) δ 6.89 (dd, J=7.3Hz, J=2.0Hz, 1H, H-5), 7.40 (d, J=1.4Hz, 1H, H-2), 7.71 (s, 1H, H-8), 8.35 (d, J=7.3Hz, 1H, H-6).
^{13}C NMR (DMSO-d_6) δ 94.46 (C-3), 104.94 (C-5), 107.71 (C-8), 125.67 (C-6), 134.14 (C-2), 137.48 (C-4), 145.36 (C-7a).

1,2-bis(4-azido-3-chloropyrrolo[2,3-*b*]pyridin-1-yl)ethene (26)

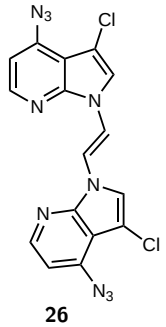

26

1,2-Bis(4-azidopyrrolo[2,3-*b*]pyridin-1-yl)ethene (404.4mg, 1.18mmol) was dissolved in 5mL THF and cooled to 0°C. *N*-Chlorosuccinimide (372.4mg, 2.73mmol, 2.31eq.) was added portionwise to the stirred reaction mixture. The reaction mixture was stirred at room temperature over night. Subsequently, the reaction was quenched by the addition of 30mL saturated sodium bicarbonate solution. The product precipitated from the reaction mixture and was isolated by filtration and washed with copious amounts of deionized water.
Yield 390.0mg, 78.12%, beige solid, M=411.2077g/mol.
^{1}H NMR (DMSO-d_6) δ 6.95 (d, J=6.3Hz, 1H, H-5), 7.44 (s, 1H, H-2), 7.73 (s, 1H, H-8), 8.41 (d, J=6.9Hz, 1H, H-6).
^{13}C NMR (DMSO-d_6) δ 86.36 (C-3), 105.05 (C-5), 107.64 (C-8), 124.70 (C-6), 130.73 (C-2), 137.42 (C-4), 144.12 (C-7a).

1,2-bis(4-aminopyrrolo[2,3-*b*]pyridin-1-yl)ethene (27)

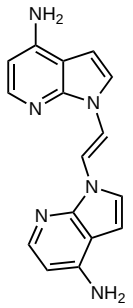

27

The reaction was carried out analogously to a literature proceudure [315]. 1,2-Bis(4-azidopyrrolo[2,3-*b*]pyridin-1-yl)ethene (500.0mg, 1.156mmol) was dissolved in 20mL ethanol and 50mg palladium on charcoal (10%m/m) was added. The reaction was stirred in a steel autoclave at 30°C under 25bar hydrogen pressure over night. Subsequently, the catalyst was removed by filtration over celite and the filtrate was reduced in vacuum until dryness. The product was purified by column chromatography using a gradient of ethyl acetate/methanol 9/1 to 5/1 as eluent.
Yield 330.2mg, 88.04%, orange solid, M=324.3124g/mol.
^{1}H NMR (DMSO-d_6) δ 5.61 (bs, 2H, NH_2), 6.34-6.40 (m, 2H, H-3, H-5), 7.18 (d, J=0.8Hz, 1H, H-6), 7.51 (s, 1H, H-8), 8.15 (m, 1H, H-2).
^{13}C NMR (DMSO-d_6) δ 92.31 (C-5), 106.40 (C-3), 110.30 (C-8), 126.67 (C-6), 131.36 (C-2), 146.30 (C-4), 147.07 (C-7a).

1,2-bis(4-azido-3-formylpyrrolo[2,3-*b*]pyridin-1-yl)ethene (29)

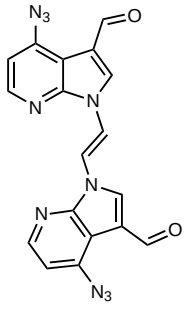

29

1,2-Bis(4-azidopyrrolo[2,3-*b*]pyridin-1-yl)ethene (2.362g, 6.900mmol) was dissolved in 40.0µL DMF and stirred under nitrogen atmosphere. Phosphorus oxychloride (4.6mL, 23mmol, 3.3eq.) was added to the stirred reaction mixture over 1.5 hours. The reaction mixture was then heated to 70°C and stirred over night. Subsequently, the reaction mixture was heated to 80°C for one hour. The reaction was then cooled in an ice bath and quenched by slow addition of 150mL of deionised water. The product was precipitated by adjusting the pH value to pH 10 by addition of sodium hydroxide. The product was isolated by filtration and washed with copious amounts of water. An additional product fraction was obtained by extracting the filtrate with dichloromethane. The product was dissolved in dichloromethane and the combined organic layers were washed with 0.05M aqueous

hydrochloric acid to remove not reacted starting material. The combined organic layers were dried over sodium sulphate and reduced in vacuum until dryness.
Yield 1.5985mg, 53.59%, beige solid, M=432.3276g/mol.
^{1}H NMR (DMSO-d_6) δ 7.05 (dd, J=2.0Hz, J=7.3Hz, 1H, H-5), 7.53 (d, J=1.6Hz, 1H, H-8), 8.44 (s, 1H, H-2), 9.25 (d, J=7.3Hz, 1H, H-6), 9.81 (s, 1H, CHO).
^{13}C NMR (DMSO-d_6) δ 105.29 (C-8), 109.54 (C-5), 124.61 (C-3), 129.16 (C-6), 142.46 (C-4), 148.06 (C-2), 149.42 (C-7a), 178.31 (CHO).

1,2-bis(4-azido-3-(hydroxyiminomethyl)pyrrolo[2,3-*b*]pyridin-1-yl)ethene (30)

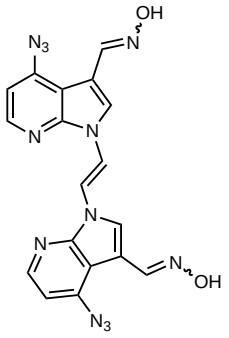

30

1,2-Bis(4-azido-5-formylpyrrolo[2,3-*b*]pyridin-1-yl)ethene (106.0mg, 0.2452mmol) and hydroxylamine hydrochloride (76.00mg, 1.094mmol, 4.461eq.) were dissolved in 4mL ethanol and 1.9mL 0.64M aqueous sodium hydroxide solution was added. The resulting reaction mixture was stirred at room temperature over night. The reaction mixture was then heated to 65°C for two hours. Subsequently, the solvent was removed in vacuum until dryness. The remaining residue was resuspended in deionized water and isolated by filtration. The product was washed with copious amounts of ice water and dried in vacuum.
Yield 93.11mg, 82.13%, *(E)*/*(Z)*=1/0.63, orange solid, M=462.3569g/mol.
(Z)-1,2-bis(4-azido-5-(hydroxyiminomethyl)pyrrolo[2,3-*b*]pyridin-1-yl)ethene
^{1}H NMR (DMSO-d_6) δ 6.84 (dd, J=2.0Hz, J=7.3Hz, 1H, H-5), 7.32 (d, J=1.7Hz, 1H, H-8), 8.06 (s, 1H, H-2), 8.29 (s, 1H, C*H*NOH), 8.84 (d, J=7.4Hz, 1H, H-6), 11.74 (s, 1H, CHNO*H*).
^{13}C NMR (DMSO-d_6) δ 104.89 (C-8), 107.24 (C-5), 116.97 (C-3), 126.58 (C-6), 132.47 (C-2), 138.58 (C-4), 140.14 (*C*HNOH), 145.02 (C-7a).
(E)-1,2-bis(4-azido-5-(hydroxyiminomethyl)pyrrolo[2,3-*b*]pyridin-1-yl)ethene
^{1}H NMR (DMSO-d_6) δ 6.94 (dd, J=2.1Hz, J=7.4Hz, 1H, H-5), 7.36 (d, J=1.6Hz, 1H, H-8), 8.39 (s, 1H, C*H*NOH), 8.99 (d, J=7.4Hz, 1H, H-6), 11.18 (s, 1H, CHNO*H*).
^{13}C NMR (DMSO-d_6) δ 104.96 (C-8), 107.70 (C-5), 118.41 (C-3), 128.81 (C-6), 138.27 (C-4), 138.47 (C-2), 139.72 (*C*HNOH), 147.03 (C-7a).

1,2-bis(4-azido-3-cyanopyrrolo[2,3-*b*]pyridin-1-yl)ethene (31)

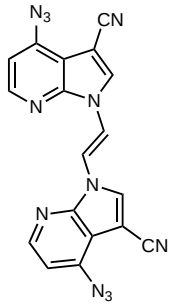

31

Method A: A mixture of *(E)*- and *(Z)*-1,2-bis(4-azido-5-(hydroxyiminomethyl)pyrrolo[2,3-*b*]pyridin-1-yl)ethene (2.295g, 7.077mmol) was dissolved in 20mL acetic anhydride and stirred at 70°C for six hours and then at room temperature over night. Subsequently, the reaction mixture was cooled to 0°C and quenched by addition of 200mL of deionised water. The reaction mixture was neutralized by addition of sodium hydroxide. The product precipitated from the reaction mixture at neutral pH. The product was isolated by filtration. An additional product fraction was isolated by extracting the filtrate with dichloromethane. The crude product was then redissolved in dichloromethane and the combined organic layers washed with 0.05M aqueous HCl. The organic layer was dried over sodium sulphate and reduced in vacuum to dryness. The isolated product consisted of 1,2-bis(4-azido-3-cyanopyrrolo[2,3-*b*]pyridin-1-yl)ethene and *O*-acetylated *(E)*-1,2-bis(4-azido-5-(hydroxyiminomethyl)pyrrolo[2,3-*b*]pyridin-1-yl)ethene which were separated by column chromatography using ethyl acetate/cyclohexane 10/1 as eluent.
Yield 462.8mg, 16.67%, yellow solid, M=392.3365g/mol.
Method B: A mixture of *O*-acetylated *(E)*-1,2-bis(4-azido-5-(hydroxyiminomethyl)pyrrolo[2,3-*b*]-pyridin-1-yl)ethene (**97**) and 1,2-bis(4-azido-3-cyanopyrrolo[2,3-*b*]pyridin-1-yl)ethene (**31**) was then dissolved in acetic acid and refluxed for three hours. Subsequently, the reaction mixture was cooled to room temperature and neutralized by addition of sodium hydroxide. The product precipitated from the reaction mixture and was isolated by filtration. The crude product was then redissolved in dichloromethane and the combined organic layers washed with 0.05M aqueous HCl. The organic layer was dried over sodium sulphate and reduced in vacuum to dryness.
Yield not determined, yellow solid, M=392.3365g/mol.
1,2-bis(4-azido-3-cyanopyrrolo[2,3-*b*]pyridin-1-yl)ethene (**31**)
^{1}H NMR ($CDCl_3$) δ 6.74 (dd, J=7.2Hz, J=2.0Hz, 1H, H-5), 7.33 (d, J=1.5Hz, 1H, H-8), 8.07 (s, 1H, H-2), 8.22 (d, J=7.2Hz, 1H, H-6).
^{13}C NMR ($CDCl_3$) δ 99.97 (C-3), 105.91 (C-8), 109.39 (C-5), 110.88 (C-3a), 115.99 (CN), 126.57 (C-6), 142.00 (C-7a), 143.40 (C-2), 147.08 (C-4).

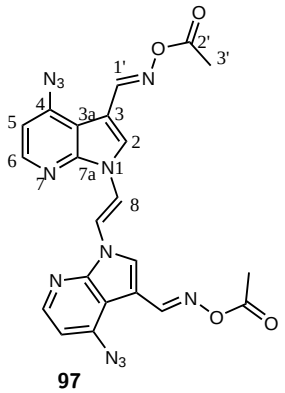

97

O-acetylated *(E)*-1,2-bis(4-azido-5-(hydroxyiminomethyl)pyrrolo[2,3-*b*]pyridin-1-yl)ethene (**97**)
^{1}H NMR ($CDCl_3$) δ 2.17 (s, 3H, H-3'), 6.72 (dd, J=2.0Hz, J=7.3Hz, 1H, H-5), 7.28 (d, J=1.6Hz, 1H, H-2), 7.87 (s, 1H, H-1'), 8.49 (s, 1H, H-8), 9.19 (d, J=7.3Hz, 1H, H-6).
^{13}C NMR ($CDCl_3$) δ 18.46 (C-3'), 104.05 (C-8), 107.52 (C-5), 115.27 (C-3), 129.73 (C-6), 140.08 (C-4), 141.65 (C-1'), 144.27 (C-2), 148.33 (C-7a), 166.98 (C-2').

1,2-bis(4-amino-3-cyanopyrrolo[2,3-*b*]pyridin-1-yl)ethene (32)

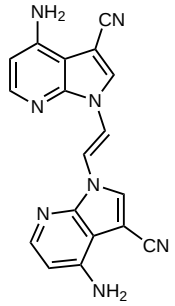

32

Method A: 1,2-Bis(4-azido-3-cyanopyrrolo[2,3-*b*]pyridin-1-yl)ethene (101.3mg, 0.296mmol) was dissolved in acetic acid. Pt/C (10%m/m, 10.8mg) was added to the stirred reaction mixture. The resulting reaction mixture was stirred under hydrogen atmosphere over night (hydrogen balloon). Subsequently, the catalyst was removed by filtration over celite. The pH value of the filtrate was adjusted to pH 9 by addition of sodium carbonate and then extracted with dichloromethane, to remove unreacted starting material, and subsequently with ethyl acetate to extract the product. The combined ethyl acetate layers were dried over sodium sulphate and reduced in vacuum until dryness.
Yield 18.5mg, 18.37%, beige solid, 340.3415g/mol.
Method B: 1,2-Bis(4-azido-3-cyanopyrrolo[2,3-*b*]pyridin-1-yl)ethene (706.3mg, 2.063mmol) was suspended in 25mL THF in an ultrasonic bath. Pd/C (10%m/m, 70.7mg) was added to the stirred reaction mixture. The resulting reaction mixture was stirred under hydrogen atmosphere over night (hydrogen balloon). Subsequently, the catalyst was removed by filtration over celite. The celite pad was washed with ethyl acetate. The resulting filtrate was dried over sodium sulphate and reduced in vacuum until dryness.
Yield 610.9mg, 86.99%, beige solid, 340.3415g/mol.

^{1}H NMR (DMSO-d_6) δ 6.34 (s, 2H, NH_2), 6.62 (d, J=1.5Hz, 1H, H-2), 6.71 (dd, J=7.2Hz, 1.8Hz, 1H, H-5), 8.14 (s, 1H, H-8), 8.27 (d, J=7.2Hz, 1H, H-6).
^{13}C NMR (DMSO-d_6) δ 93.17 (C-8), 94.41 (C-3), 108.33 (C-5), 112.68 (CN), 126.48 (C-6), 143.37 (C-2), 149.86 (C-4), 149.93 (C-7a).

4-amino-3-cyanopyrrolo[2,3-*b*]pyridine (33)

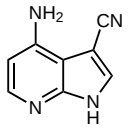

33

1,2-Bis(4-amino-3-cyanopyrrolo[2,3-*b*]pyridin-1-yl)ethene (**32**, 691.6mg, 2.032mmol) was dissolved in acetonitrile/deionised water 1/1 (19mL). Sodium chlorite (918.8mg, 8.127mmol, 4.00eq.) and sodium periodate (437.0mg, 2.043mmol, 1.005eq.) were added to the reaction mixture. Subsequently, osmium tetroxide (catalytic amount) was added to the reaction mixture, which was stirred at room temperature for three hours. The reaction was then quenched by addition of sodium bisulfite (1.1048g, 10.62mmol, 5.308eq.). The product was precipitated from the reaction mixture by neutralizing the reaction mixture by addition of sodium carbonate. The product was isolated by filtration and washed with deionised water. The crude product was then redissolved in ethyl acetate and washed with saturated sodium thiosulphate solution and subsequently with deionized water. The organic layer was dried over sodium sulphate and reduced in vacuum to dryness.
Yield 368.1mg, 57.27%, light brown solid, M=158.16g/mol.
^{1}H NMR (DMSO-d_6) δ 6.63 (s, 2H, NH_2), 6.85 (d, J=7.2Hz, 1H, H-5), 8.20 (s, 1H, H-2), 8.30 (d, J=7.2Hz, 1H, H-6).
^{13}C NMR (DMSO-d_6) δ 96.66 (C-3), 97.93 (C-3a), 107.73 (C-5), 111.95 (CN), 125.11 (C-6), 143.23 (C-2), 145.29 (C-4), 146.44 (C-7a).

4-amino-3-cyanopyrrolo[2,3-*b*]pyridine (34)

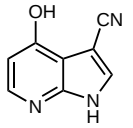

34

4-Amino-3-cyanopyrrolo[2,3-*b*]pyridine (**33**, 350.7mg, 2.217mmol) was dissolved in acetic acid/deionized water 1/1 (30mL). The solution was heated to 100°C. Subsequently, sodium nitrite (1.9648g, 28.48mmol, 12.84eq.) in 30mL water was added dropwise to the stirred solution. After complete addition (approximately two hours), the reaction mixture was stirred at 100°C for additional two hours. Subsequently, the reaction mixture was cooled to room temperature and neutralized by addition of sodium hydroxide. The product precipitated from the reaction mixture, was isolated by filtration and washed with deionized water. A second product fraction was obtained by extracting the filtrate with dichloromethane. The combined organic phases were dried over sodium sulphate

and reduced in vacuum until dryness.
Yield 306.3mg, 86.80%, brown solid, M=159.1448g/mol.
^{1}H NMR (DMSO-d_6) δ 7.28 (d, J=7.4Hz, 1H, H-5), 7.47 (d, J=7.4Hz, 1H, H-6), 8.32 (s, 1H, H-2).

4-azidopyrrolo[2,3-*b*]pyridine (28)

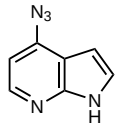

28

The reaction was carried out under inert atmosphere. 1,2-Bis(4-azidopyrrolo[2,3-*b*]pyridin-1-yl)ethene (995.8mg, 2.909mmol) was suspended in acetonitrile/deionised water 1/1 (16mL). Sodium chlorite (1.0542g, 9.325mmol, 3.21eq.) and sodium periodate (643.1mg, 3.007mmol, 1.033eq.) were added to the reaction mixture. Subsequently, osmium tetroxide (catalytic amount) was added to the reaction mixture, which was stirred at room temperature for 25 hours. The reaction was then quenched by dropwise addition of sodium bisulfite solution (2.0mL, 5.9M aqueous solution) and stirred over night. The product was precipitated from the reaction mixture by neutralizing the reaction mixture by addition of aqueous sodium hydroxide solution. The product was isolated by filtration and washed with deionised water. The crude product was then redissolved in ethyl acetate and washed with saturated sodium thiosulphate solution. The organic layer was dried over sodium sulphate and reduced in vacuum to dryness.
Yield 499.0mg, 53.89%, beige solid, M=159.1481g/mol.
^{1}H NMR (CDCl3) δ 6.58 (dd, J=7.3Hz, J=2.0Hz, 1H, H-5), 7.17 (d, J=1.4Hz, 1H, H-3), 7.45 (s, 1H, H-2), 7.95 (d, J=7.3Hz, 1H, H-6).
^{13}C NMR (CDCl3) δ 104.35 (C-3), 106.52 (C-5), 116.83 (C-3a), 122.68 (C-6), 129.79 (C-2), 136.98 (C-4), 143.59 (C-7a).

4-hydroxypyrrolo[3,2-*c*]pyridine (19)

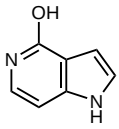

19

4-Hydroxypyrrolo[3,2-*c*]pyridine was prepared by Cornelia Hojnik [305]. 4-Amino-2-hydroxypyridine (600.0mg, 5.449mmol) and sodium acetate trihydrate (2.400g, 17.64mmol, 3.237eq.) were suspended in 27mL deionised water and heated to 80°C. Chloroacetaldehyde (50%m/m in water, 840µL, 5.35mmol, 0.982eq.) in 6mL deionized water, was added dropwise to the reaction mixture, and the resulting mixture was stirred under reflux for 18 hours. Subsequently, the reaction mixture was cooled to room temperature and neutralized by addition of aqueous ammonia solution. The reaction mixture was then extracted with ethyl acetate three times. The combined organic layers were dried over sodium sulphate, and concentrated in vacuum until dryness. The product was

purified by column chromatography using dichloromethane/methanol 20/1 as eluent.
Yield 77.00mg, 10.54%, brown solid, M=134.1353g/mol.
TLC R_f 0.66 (ethyl acetate/ethanol/acetone/deionized water 20/2/2/1)
^{1}H NMR (DMSO-d_6) δ 6.37 (d, J=5.6Hz, 1H, H-6), 6.59 (bs, OH), 7.00 (d, J=2.4Hz, H-3), 7.68 (d, J=2.4Hz, 1H, H-2), 7.76 (d, J=5.6Hz, 1H, H-7).
^{13}C NMR (DMSO-d_6) δ 103.33 (C-3), 104.28 (C-7), 140.55 (C-3a), 144.58 (C-2), 149.83 (C-7a), 163.36 (C-6), 172.10 (C-1).

1-(2-chloroethenyl)-4-hydroxypyrrolo[2,3-*b*]pyridine (20)

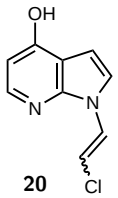

20

7-(2-Chloroethenyl)-4-hydroxypyrrolo[2,3-*b*]pyridine was prepared in Cornelia Hojnik's master thesis [305]. 2-Amino-4-hydroxypyridine (500.0mg, 4.541mmol) and sodium acetate trihydrate (2.200g, 16.17mmol, 3.560eq.) were suspended in 25mL deionised water and heated to 80°C. Chloroacetaldehyde (50%m/m in water, 700.0µL, 4.459mmol, 0.9819eq.) was added dropwise to the stirred reaction mixture. The reaction mixture was stirred under reflux for 24 hours and subsequently cooled to room temperature. The reaction mixture was neutralized by addition of aqueous ammonia solution and the solvent was evaporated until dryness. The remaining residue was purified by column chromatography using dichloromethane/methanol 20/1 as eluent.
Yield 58.11mg, 6.57%, yellow solid, M=194.6177g/mol.
TLC R_f 0.33 (ethyl acetate/ethanol/acetone/deionized water 20/2/2/1)
^{1}H NMR (DMSO-d_6) δ 4.48 (dd, J=2.1Hz, J=10.5Hz, 1H, *(E)*-H-2'), 4.71 (m, 1H, *(Z)*-H-2'), 5.64 (d, J=5.1Hz, 1H, H-1'), 6.83 (d, J=7.3Hz, 1H, H-5), 7.49 (d, J=0.9Hz, 1H, H-3), 7.92 (d, J=1.1Hz, 1H, H-2), 8.55 (d, J=7.3Hz, 1H, H-6).
^{13}C NMR (DMSO-d_6) δ 69.23 (C-1'), 80.27 (C-2'), 100.87 (C-3), 110.99 (C-3a), 112.67 (C-6), 129.22 (C-2), 132.06 (C-5), 142.93 (C-7a), 157.82 (C-4).

7.6.3 Synthesis of thieno[2,3-*d*]pyrimidines

bis(2-amino-6-hydroxypyrimidin-4-yl)disulfide (35)

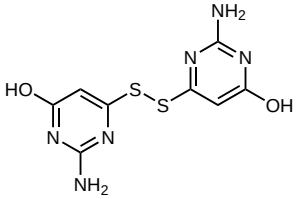

35

2-Amino-6-chloropyrimidin-4-one (3.280g, 22.54mmol) was suspended in 15mL ethylene glycol. Sodium hydrosulfide (6.030g, 107.6mmol, 4.773eq.) was added in portions over 1.5 hours. The resulting reaction mixture was heated to 130°C for 6.5 hours. 15mL of each, ethanol and acetic acid, were added. The resulting mixture was stirred at room temperature over night. Subsequently, the reaction mixture was cooled to 0°C and the product precipitated from the solution. The product was isolated by filtration and used in the next synthetic step without further purification.
Yield: crude product, contained ethylene glycol 3.330g, light yellow solid, M=284.3181g/mol.
TLC R_f 0.67 (ethyl acetate/ethanol/acetone/deionized water = 20/2/2/1)
^{1}H NMR (DMSO-d_6) δ 5.47 (s, 1H, H-5), 7.49 (bs, NH_2), 11.32 (bs, 1H, OH/NH).
^{13}C NMR (DMSO-d_6) δ 97.97 (C-5), 152.75 (C-2), 161.77 (C-4), 175.75 (C-6).

2-amino-6-hydroxy-4-mercaptopyrimidine (36)

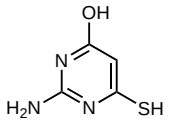

36

Method A: 2-Amino-6-hydroxy-4-mercaptopyrimidine was prepared according to a literature procedure [337]. 2-Amino-6-chloropyrimidin-4-one (500.0mg, 3.435mmol) and sodium hydrosulfide (770.0mg, 13.73mmol, 3.998eq.) were suspended in 2mL ethylene glycol and stirred under nitrogen atmosphere at 135°C for seven hours. The product was not isolated and used directly for the next synthetic step.
Method B: The cleavage of the disulfide bond was achieved in a procedure similar to those described by Yui et al [473]. Bis(2-amino-6-hydroxypyrimidin-4-yl)disulfide (1.015g, 3.570mmol) was suspended in 15mL DMF. Sodium borohydride (71.40mg, 1.887mmol, 2.115eq.) in 10mL DMF were added to the stirred reaction mixture. After 30 minutes at room temperature the reaction mixture was acidified to pH 3 by addition of 2M HCl and stirred for further 15 minutes. Subsequently, the reaction mixture was neutralised by addition of potassium carbonate and used for the next synthetic step without further purification.
Dark yellow to greenish liquid. M=143.1670g/mol.
TLC R_f 0.34 (chloroform/methanol/aqueous ammonia = 5/4/1)

2-amino-4-hydroxythieno[2,3-*d*]pyrimidine (37)

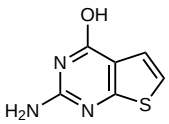

37

Method A: Sodium acetate trihydrate (0.900g, 6.614mmol, 1.925eq.) was dissolved in 12.9mL deionized water. The reaction mixture of the previous synthetic step, containing 2-amino-6-hydroxy-4-mercaptopyrimidine, was added to the stirred solution. Chloroacetaldehyde (50%m/m solution in water, 540µL, 3.44mmol, 1.00eq.) was added dropwise to the reaction mixture. The

reaction mixture was stirred under nitrogen at 100°C over night. Subsequently, ethyl acetate was added to the reaction mixture and the remaining solids were removed by filtration. The filtrate was reduced in vacuum until dryness. The crude product was purified by column chromatography using chloroform/methanol/aqueous ammonia 5/4/1 as eluent.
Yield not determined, dark brown solid, M=167.1884g/mol.
Method B: Potassium carbonate (1.100g, 7.959mmol, 1.115eq.) was added to the reaction mixture containing 2-amino-6-hydroxy-4-mercapopyrimidine, prepared according to method B. Chloroacetaldehyde (50%m/m solution in water, 900µL, 5.73mmol, 0.803eq.) were added dropwise to the stirred solution. After complete addition the suspension was heated to 40°C for one hour and then to 90°C for 4.5 hours. Subsequently, the reaction mixture was cooled to room temperature. The solvent was removed in vacuum and the crude product was purified by column chromatography using dichloromethane/methanol 10/1 as eluent.
Yield 210mg, 21.91%, M=167.1884g/mol.
TLC R_f 0.67 (ethyl acetate/ethanol/acetone/deionized water = 20/2/2/1)
^{1}H NMR (DMSO-d_6) δ 6.55 (s, 2H, NH_2), 6.97 (d, J=5.8Hz, 1H, H-5), 7.11 (d, J=5.9Hz, 1H, H-6), 10.93 (bs, 1H, NH).
^{13}C NMR (DMSO-d_6) δ 115.62 (C-4a), 116.32 (C-5), 121.24 (C-6), 153.10 (C-2), 158.25 (C-4), 168.25 (C-7a).

4-hydroxy-2-pivaloylaminothieno[2,3-*d*]pyrimidine (37)

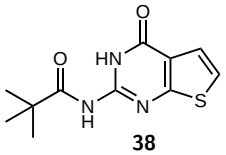

38

2-Amino-4-hydroxythieno[2,3-*d*]pyrimidine (479.0mg, 2.865mmol) was dissolved in 5mL DMF und 15mL pyridine. Triethylamine (2.8mL, 20mmol, 7.0eq.) was added. The resulting solution was cooled to 0°C and pivaloylchloride (1.2mL, 9.6mmol, 3.4eq.) was added dropwise over five minutes. The reaction mixture was warmed to room temperature and was then stirred at 50°C for 30 minutes and subsequently at 85°C for 3.5hours. For work-up, the reaction solvent was removed in vacuum and 20mL deionized water were added to the remaining residue. The pH value of the mixture was adjusted to pH 2. The aqueous mixture was then extracted with ethyl acetate three times. The combined organic layers were dried over sodium sulphate and reduced in vacuum until dryness. The crude product was purified by column chromatography using cyclohexane/ethyl acetate 3/1 as eluent.
Yield 270.0mg, 33.03%, white solid, M=285.2946g/mol.
^{1}H NMR (DMSO-d_6) δ 1.26 (s, 3H, CH_3), 7.33 (d, J=5.8Hz, 1H, H-5), 7.41 (d, J=5.8Hz, 1H, H-6), 11.20 (bs, 1H, H-3), 12.21 (bs, 1H, NH-Piv).
^{13}C NMR (DMSO-d_6) δ 26.24 (CH_3-Piv), 40.00 (C-Piv), 120.26 (C-4a), 121.36 (C-5), 121.59 (C-6), 148.11 (C-2), 156.27 (C-4), 164.70 (C-7a), 181.24 (CO-Piv).

4-chloro-2-pivaloylaminothieno[2,3-*d*]pyrimidine (39)

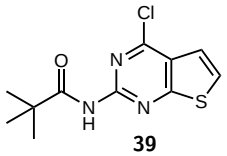

39

4-Hydroxy-2-pivaloylaminothieno[2,3-*d*]pyrimidine (121.4mg, 0.4255mmol) was dissolved in phosphorous oxychloride (5mL, 24.87mmol, 58.44eq.) and stirred under nitrogen atmosphere. DMF (75.0µL, 0.9688mmol, 2.277eq.) was added dropwise to the stirred reaction mixture. The resulting reaction mixture was heated to 55°C for 1.5 hours. The solvents were removed in vacuum and ice water was added to the remaining residue. The resulting mixture was neutralized by addition of aqueous ammonia solution. The aqueous phase was then extracted with ethyl acetate four times. The combined organic layers were dried over sodium sulphate and the solvent removed in vacuum. The crude product was purified by column chromatography using dichloromethane/methanol 60/1 as eluent.

Yield 31.10mg, 23.33%, M=313.3047g/mol.

^{1}H NMR (DMSO-d_6) δ 1.26 (s, 3H, CH_3), 7.36 (d, J=6.0Hz, 1H, H-5), 7.73 (d, J=6.0Hz, 1H, H-6), 8.59 (bs, 1H, NH-Piv).

^{13}C NMR (DMSO-d_6) δ 28.23 (CH_3-Piv), 38.06 (C-Piv), 119.33 (C-5), 122.92 (C-4a), 125.66 (C-6), 153.49 (C-2), 162.30 (C-7a), 169.35 (C-4), 171.82 (CO-Piv).

4-hydroxythieno[2,3-*d*]pyrimidine (40)

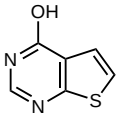

40

4-Hydroxythieno[2,3-*d*]pyrimidine was prepared according to a literature procedure [188]. Methyl 2-aminothiophene-3-carboxylate (5g, 30.85mmol) and ammonium formate (6.318g, 100.2mmol, 3.3eq.) were added to formamide (25mL, 625.7mmol, 20eq.) and the resulting mixture was heated to 150°C for six hours. The reaction mixture was then cooled to room temperature and stored at 4°C over night. The brown product precipitated from the reaction mixture and was isolated by filtration. The product was purified by recrystallization from acetone/water.

Yield 2.753g, 56.8%, brown solid, M=152.1738g/mol.

TLC R_f 0.67 (ethyl acetate/ethanol/acetone/deionized water = 20/2/2/1)

HPLC-MS t_{ret}= 10.12min (method G), t_{ret}= 8.98min (method F)

^{1}H NMR (DMSO-d_6) δ 7.41 (d, 1H, J=5.8Hz, H-5), 7.59 (d, 1H, J=5.8Hz, H-6), 8.14 (s, 1H, H-2), 12.51 (bs, 1H, NH/OH).

^{13}C NMR (DMSO-d_6) δ 121.60 (C-5), 123.80 (C-6), 124.59 (C-4a), 145.58 (C-2), 157.46 (C-4), 164.20 (C-7a)

5-chloromercurio-4-hydroxythieno[2,3-*d*]pyrimidine (43) and 5,6-dichloromercurio-4-hydroxythieno[2,3-*d*]pyrimidine (100)

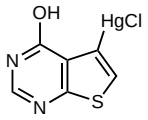

43

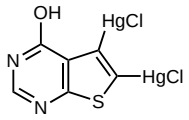

100

The chloromercurio-substituted thieno[2,3-*d*]pyrimidine was prepared similar to a literature procedure for thieno[2,3-*d*]pyrimidines, and for pyrrolo[2,3-*d*]pyrimidines [183, 348]. 4-Hydroxythieno[2,3-*d*]pyrimidine (1.001g, 6.578mmol) was dissolved in 15mL acetic acid and mercury(II) acetate (3.141g, 9.856mmol, 1.50eq.) was added. The reaction mixture was stirred under nitrogen at 100°C for three hours. Subsequently the reaction was cooled to room temperature and 15mL brine was added. Twenty minutes after the addition of brine, the precipitate was isolated by filtration and washed with water and cyclohexane. The product was dried in vacuum.
Yield not determined, **43**/100=1/0.64, brown solid,
M(**43**)=387.2088g/mol, M(100)=622.2439g/mol.
^{1}H NMR (DMSO-d_6) δ 7.53 (s, 0.5H, H-6), 8.06 (s, 1H, H-2), 12.30 (bs, 1H, OH/NH).

4-hydroxy-5-iodothieno[2,3-*d*]pyrimidine (44) and 4-hydroxy-5,6-diiodothieno[2,3-*d*]pyrimidine (101)

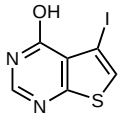

44

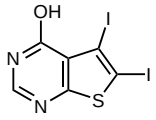

101

The iodo-substituted thieno[2,3-*d*]pyrimidine was prepared similar to a literature procedure for differently substituted thieno[2,3-*d*]pyrimidines, and for pyrrolo[2,3-*d*]pyrimidines [183, 348]. The product mixture of the previous reaction step consisting of 5-chloromercurio-4-hydroxythieno[2,3-*d*]pyrimidine and 5,6-dichloromercurio-4-hydroxythieno[2,3-*d*]pyrimidine (619.0mg, 1.302mmol1/0.6) was suspended in 8mL chloroform in a flask protected from light and iodine (609.0mg, 2.399mmol, 1.90eq.) was added. The reaction mixture was stirred at 50°C over night. Subsequently, the solvent was removed in vacuum. The remaining residue was resuspended in 2N aqeuous sodium thiosulphate solution. The product was isolated by filtration and dried in vacuum.
Yield 367.0mg, 86.78%, **44**/101=1/0.64, beige solid,
M(**44**)=278.0703g/mol, M(101)403.9668=g/mol.
4-hydroxy-5-iodothieno[2,3-*d*]pyrimidine (**44**)
^{1}H NMR (DMSO-d_6) δ7.66 (s, 1H, H-6), 8.10 (s, 1H, H-2), 12.63 (s, OH).
^{13}C NMR (DMSO-d_6) δ 76.28 (C-5), 126.65 (C-4a), 130.80 (C-6), 145.99 (C-2), 155.76 (C-7a), 168.31 (C-4).
4-hydroxy-5,6-diiodothieno[2,3-*d*]pyrimidine (**101**)
^{1}H NMR (DMSO-d_6) δ 8.16 (s, 1H, H-2), 12.63 (s, OH)

^{13}C NMR (DMSO-d_6) δ 88.45 (C-6), 89.74 (C-5), 124.56 (C-4a), 146.02 (C-2), 154.99 (C-7a), 167.98 (C-4).

4-chlorothieno[2,3-*d*]pyrimidine (41)

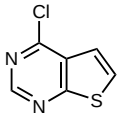

41

4-Hydroxythieno[2,3-*d*]pyrimidine (1.000g, 6.571mmol) was suspended in 3.9mL acetonitrile. Triethylamine (1.83mL, 13.12mmol, 2.00eq.) was added dropwise to the stirred reaction mixture. Subsequently, phosphorus oxychloride (1.26mL, 13.48mmol, 2.051eq.) was added dropwise. The reaction mixture stirred at 100°C for one hour and then cooled to room temperature. The reaction was quenched by addition of ice water. The product precipitated from the solution and was isolated by filtration.
Yield 785.0mg, 70.01%, beige solid, M=170.6194g/mol.
^{1}H NMR (DMSO-d_6) δ 7.61 (d, J=6.0Hz, 1H, H-5), 8.16 (d, J=6.0Hz, 1H, H-6), 8.97 (s, 1H, H-2).
^{13}C NMR (DMSO-d_6) δ 119.67 (C-5), 129.06 (C-4a), 130.68 (C-6), 152.78 (C-4), 153.94 (C-7a), 168.42 (C-2).

4-methoxythieno[2,3-*d*]pyrimidine (42)

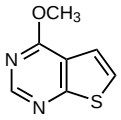

42

4-Methoxythieno[2,3-*d*]pyrimidine was prepared according to a literature procedure [474]. A solution of sodium methoxide in methanol was prepared by adding sodium (348.0mg, 15.14mmol, 2.996eq.) to methanol. 4-Chlorothieno[2,3-*d*]pyrimidine (862.0mg, 5.052mmol) was then dissolved in 5mL methanol and the sodium methoxide solution was added dropwise over 15 minutes. The resulting reaction mixture was stirred at reflux for four hours. The methanol was then removed in vacuum and deionized water (5.1mL) was added to the remaining residue. The product precipitated from the mixture, was isolated by filtration and washed with ice water.
Yield 744.0mg, 88.60%, beige solid, M=166.2003g/mol.
^{1}H NMR (DMSO-d_6) δ 4.15 (s, 3H, CH_3), 7.52 (d, J=5.9Hz, 1H, H-5), 7.90 (d, J=5.9Hz, 1H, H-6), 8.75 (s, 1H, H-2).
^{13}C NMR (DMSO-d_6) δ 54.02 (CH_3), 118.36 (C-5), 118.38 (C-4a), 126.40 (C-6), 153.17 (C-2), 163.57 (C-7a), 167.80 (C-4).

3-chloro-2-oxopropyl acetate (45)

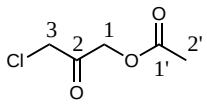

45

Method A: 3-Chloro-2-oxopropyl acetate was prepared from 1,3-dichloroacetone according to a modified literature procedure [358]. 1,3-Dichloroacetone (10.46g, 78.26mmol) and potassium acetate (9.70g, 98.8mmol, 1.2eq.) were dissolved in 100mL acetic acid. The reaction mixture was heated to 70°C for four days. The reaction was monitored with GC, after four days GC indicated 51% conversion and no formation of any side products. Subsequently, the reaction mixture was heated to 130°C over night. The amount of product formed did not increase, however 2-oxopropane-1,3-diacetate was formed. According to GC analysis 19.3% of remaining 1,3-dichloroacetone, 51.4% of the desired product 3-chloro-2-oxopropyl acetate, and 29.3% of 2-oxopropane-1,3-diacetate was found in the reaction mixture. The reaction was cooled to room temperature and the solvent was removed in vacuum. The resulting dark brown residue was purified by vacuum distillation.

Yield 5.30g, 40.90%, purity (GC) 79.8%, dark orange oil, M=132.1146g/mol.

Method B: 3-Chloro-2-oxopropyl acetate was prepared from 2-chloro-2-propen-1-ol according to a modified literature procedure [359]. 2-Chloro-2-propen-1-ol (1.000g, 9.728mmol) was added to mixture of 20mL acetone, 8mL acetic acid and sodium hypochlorite solution (10%-15% in water, 5.5mL, 11mmol, 1.1eq.). The resulting reaction mixture was stirred at 0°C for 12 hours and subsequently at room temperature for 6 days. The reaction was monitored by GC. When GC analysis indicated complete conversion, the 50mL saturated sodium bicarbonate solution was added to the reaction mixture. The reaction mixture was then diluted with dichloromethane, until two layers were visible. The layers were separated and the aqueous layer was extracted with dichloromethane twice. The combined organic layers were dried over sodium sulphate and reduced in vacuum until dryness. The product was purified by vacuum distillation.

Yield not determined, dark orange oil, M=132.1146g/mol.

GC t_{ret}(**45**)= 4.64min, t_{ret}(2-chloro-2-propen-1-ol)= 2.40min, t_{ret}(dichloroacetone)= 3.27min, t_{ret}(2-oxopropane-1,3-diacetate)= 6.30min.

^{1}H NMR ($CDCl_3$) δ 2.11 (s, 3H, H-2'), 4.10 (2H, H-3), 4.84 (s, 2H, H-1).

^{13}C NMR ($CDCl_3$) δ 20.36 (C-2'), 45.64 (C-3), 66.41 (C-1), 170.20 (C-1'), 196.44 (C-2).

methyl 2-amino-4-hydroxymethylthiophene-3-carboxylate (46)

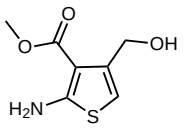

46

Methyl 2-amino-4-hydroxymethylthiophene-3-carboxylate was prepared according to a literature procedure [360, 361]. Methyl cyanoacetate (2.8mL, 31.42mmol, 0.98eq.) was dissolved in 40mL

methanol and sodium sulfide nonahydrate (8.48g, 35.31mmol, 1.10eq.) was added. The reaction mixture was cooled to 0°C. 3-Chloro-2-oxopropyl acetate (4.23g, 32.01mmol) was added dropwise to the stirred reaction mixture. After complete conversion, the ice bath was removed and triethylamine (4.8mL, 34.44mmol, 1.1eq.) was added dropwise. The reaction mixture was stirred at room temperature over night. Subsequently, the reaction mixture was diluted with deionised water and extracted with ethyl acetate. Brine was added to facilitate separation of the layers. The combined organic layers were dried over sodium sulphate and reduced in vacuum until dryness.
Yield 3.487g, 59.29%, brown solid, M=187.2163g/mol.
^{1}H NMR (DMSO-d_6) δ 3.41 (s, 3H, CH_3), 3.93 (d, J=6.2Hz, OH), 5.08 (s, 2H, CH_2), 6.31 (s, 1H, H-5), 7.44 (s, 2H, NH_2).
^{13}C NMR (DMSO-d_6) δ 50.55 (CH_3), 62.24 (CH_2), 101.61 (C-3), 104.78 (C-5), 133.95 (C-4), 164.72 (C-2), 165.54 ($COOCH_3$).

4-hydroxy-5-hydroxymethylthieno[2,3-*d*]pyrimidine (47)

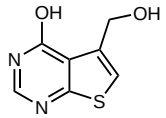

47

Methyl 2-amino-4-hydroxymethylthiophene-3-carboxylate (240.0mg, 1.282mmol) and ammonium-formate (261.4mg, 4.145mmol, 3.233eq.) were dissolved in formamide (4.2mL, 82mmol) and heated to 180°C for six hours and then at room temperature over night. Subsequently, the reaction mixture was diluted with deionised water and any insoluble material was filtered off. The filtrate was extracted with dichloromethane four times. The combined organic layers were washed with brine, dried over sodium sulphate and reduced in vacuum until dryness. The crude product contained impurities, visible on TLC and NMR.
Yield 62.90mg, 26.93%, yellow oil, M=182.1997g/mol. TODO
^{1}H NMR (DMSO-d_6) δ 5.22 (s, 2H, CH_2), 5.79 (s, 1H, OH), 7.53 (s, 1H, H-6), 8.61 (d, J=0.9Hz, 1H, H-2), 11.40 (OH/NH). TODO
^{13}C NMR (DMSO-d_6) δ 61.66 (CH_2), 120.54 (C-6), 132.46 (C-4a), 145.91 (C-2), 147.26 (C-5), 157.73 (C-4), 163.73 (C-7a).

7.6.4 Synthesis of cyclopenta[*d*]pyrimidines

2-amino-6,7-dihydrocyclopenta[*d*]pyrimidin-4-one (48)

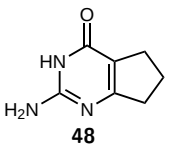

48

2-Amino-6,7-dihydrocyclopenta[*d*]pyrimidin-4-one was prepared according to a literature procedure [194]. Sodium ethoxide was prepated *in situ* by adding sodium (68.0mg, 2.96mmol) to

5mL ethanol. Guanidine hydrochloride (284.0mg, 2.973mmol) was added to the solution. The resulting solution was stirred for ten minutes. Subsequently, ethyl 2-oxocyclopentanecarboxylate (500µL, 3.04mmol) was added to the reaction mixture. The reaction mixture was stirred at room temperature over night and subsequently refluxed for five hours. The reaction mixture was then cooled to room temperature and the product precipitated from the reaction mixture. The product was isolated by filtration and washed with water.
Yield 155.4mg, 34.76%, white solid, M=151,1659g/mol.
^{1}H NMR (DMSO-d_6) δ 1.91 (quin, J=7.3Hz, 2H, H-6), 2.55 (m, 4H, H-5, H-7), 6,44 (bs, 2H, NH_2), 10.64 (NH).

2-mercapto-6,7-dihydrocyclopenta[*d*]pyrimidin-4-one (49)

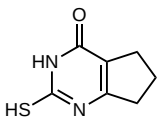

49

2-Mercapto-6,7-diyhdrocyclopenta[*d*]pyrimidin-4-one (**49**) was prepared according to a literature procedure [192]. Sodium methoxide was prepared by adding sodium (1.860g, 2.660mmol, 2.67eq.) portionwise to 20mL methanol. Formation of the methoxide was complete when all sodium was dissolved. Ethyl 2-oxocyclopentanecarboxylate (5mL, 30mmol) and thiourea (12.160g, 159.7mmol, 5.253eq.) were added to the stirred solution. The resulting reaction mixture was stirred under reflux for 20 hours. Subsequently, 70mL ice water were slowly added to the reaction mixture. Ethanol was removed in vacuum. The product was precipitated from the aqueous solution by adjusting the pH value to pH 4 by addition of acetic acid. The product was isolated by filtration and purified by recrystallization from water.
Yield 4.3716g, 85.45%, white solid, M=168.2162g/mol.
TLC R_f 0.69 (chloroform/methanol 9/1)
^{1}H NMR (DMSO-d_6) δ 1.97 (quin, J=7.1Hz, 2H, H-6), 2.49 (t, J=6.8Hz, 2H, H-5), 2.70 (t, J=7.1Hz, 2H, H-7), 12.20, 12.58 (SH, NH).
^{13}C NMR (DMSO-d_6) δ 20.78 (C-6), 26.59 (C-5), 30.97 (C-7), 115.53 (C-4a), 156.44 (C-2), 159.50 (C-7a), 175.57 (C-4).

6,7-dihydrocyclopenta[*d*]pyrimidin-4-one (50)

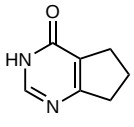

50

6,7-Dihydrocyclopenta[*d*]pyrimidin-4-one (**50**) was prepared according to a literature procedure [192]. 2-Mercaptocyclopenta[*d*]pyrimidin-4-one (80.2mg, 0.487mmol) was dissolved in 1mL deionized water and Raney nickel in water was added. The reaction was stirred under reflux for three hours at which time TLC indicated complete conversion. The Raney-nickel catalyst was removed

by filtration over celite. The filtrate was dried in vacuum until dryness. The remaining residue was recrystallized from ethanol. The product can be further purified by converting it into the corresponding potassium salt by dissolving the product in 5M potassium hydroxide solution and reprecipitating it by neutralizing the solution by addition of hydrochloric acid.
Yield 62.2mg, 93.72%, white solid, M=136.1512g/mol.
TLC R_f 0.46 (chloroform/methanol 9/1)
HPLC-MS t_{ret}= 11.36min (method H)
^{1}H NMR (DMSO-d_6) δ 1.96 (quin, J=7.3Hz, 2H, H-6), 2.63 (t, J=6.5Hz, 2H, H-5), 7.75 (t, J=7.0Hz, 2H, H-7), 8.03 (s, 1H, H-2), 11.87 (bs, 1H, NH).
^{13}C NMR (DMSO-d_6) δ 20.47 (C-6), 27.12 (C-5), 34.15 (C-7), 124.40 (C-4a), 149.14 (C-2), 159.89 (C-7a), 168.56 (C-4).

7.6.5 Synthesis of pyrazolo[3,4-*d*]pyrimidines

5-amino-4-cyano-3-(methylthio)pyrazole (102)

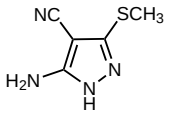

102

5-amino-4-cyano-3-(methylthio)pyrazole was prepared according to a literature procedure [396]. 2-[Bis(methylthio)methylene]malononitrile (5.000g, 28.49mmol) was dissolved in 100mL methanol. Hydrazine hydrate (50%-60%, 3.5mL, 56mmol, 2.0eq.) was added and the resulting reaction mixture was heated to reflux for three hours. Subsequently, the solvent was removed in vacuum. The remaining residue was recrystallized from methanol.
Yield 3.907g, 88.95%, beige solid, M=154.1929g/mol
^{1}H NMR (DMSO-d_6) δ 2.45 (s, 3H, CH_3), 6.46 (bs, 2H, NH_2), 11.97 (bs, 1H, NH).
^{13}C NMR (DMSO-d_6) δ 13.90 (CH_3), 72.63 (C-4), 114.66 (CN), 147.16 (C-3), 154.41 (C-5).

4-amino-3-(methylthio)pyrazolo[3,4-*d*]pyrimidine (103)

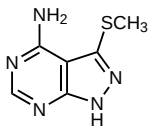

103

5-amino-4-cyano-3-(methylthio)pyrazole (3.800g, 24.64mmol) was suspended in formamide (4.0mL, 50mmol, 2.0eq.) and heated to 180°C. The reaction mixture was stirred at 180°C for four hours and subsequently at 150°C for additional 24 hours. The reaction mixture was then cooled to 0°C and the product precipitated. The product was isolated by filtration and washed with water.
Yield 3.330g, 74.56%, beige solid, M=181.2183g/mol
HPLC-MS t_{ret}= 14.1min (method I)
^{1}H NMR (DMSO-d_6) δ 2.62 (s, 3H, CH_3), 7.14 (bs, 2H, NH_2), 8.20 (s, 1H, H-6), 13.50 (bs, 1H,

NH).
^{13}C NMR (DMSO-d_6) δ 15.50 (CH_3), 98.77 (C-3a), 139.07 (C-3), 156.03 (C-7a), 156.20 (C-6), 157.58 (C-4).

5-amino-3,4-dicyanopyrazole (51)

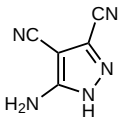

51

5-Amino-3,4-dicyanopyrazole was prepared according to a literature procedure [379]. Semicarbazide hydrochloride (8.726g, 76.67mmol) was dissolved in 150mL ethanol and triethylamine (10.9mL, 78.15mmol) was added. The resulting solution was stirred for 90 minutes at romm temperature and subsequently cooled to 0°C. Tetracyanoethylene (10.00g, 76.51mmol) was added to the reaction mixture. The reaction mixture was stirred at 0°C for three hours, at which time TLC indicated complete conversion. The reaction mixture was heated to reflux for 30 minutes. A beige solid, 5-amino-3,4-dicyanopyrazol-1-carboxamide, precipitated from the solution upon cooling to room temperature, was isolated by filtration, and washed with cold ethanol. Deionized water was heated to reflux and 5-amino-3,4-dicyanopyrazol-1-carboxamide was added in small portions. The resulting mixture was refluxed for 15 minutes. Upon cooling to 0°C, the product precipitated from the solution and was isolated by filtration. The product was purified by recrystallization from dioxane.
Yield 3.74g, 36.69%, white solid, M=133.1108g/mol.
^{1}H NMR (DMSO-d_6) δ 7.03 (s, 2H, NH_2), 13.18 (s, 1H, NH).
^{13}C NMR (DMSO-d_6) δ 75.24 (C-4), 112.40, 112.56 (CN), 125.20 (C-3), 153.28 (C-5).

7.6.6 Synthesis of monocyclic compounds

5-(2,2,2-trichloroacetyl)-1*H*-pyrrole-3-carbonitrile (58)

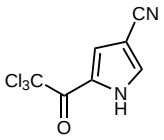

58

5-(2,2,2-Trichloroacetyl)-1*H*-pyrrole-3-carbonitrile was prepared according to a literature procedure [404]. 2-(Trichloroacetyl)pyrrole (2.000g, 9.319mmol) was dissolved in 10mL acetonitrile and the solution was cooled to 0°C. Chlorosulfonyl isocyanate (2.0mL, 22mmol, 2.4eq.) in 3mL acetonitrile was added dropwise, over a period of fifteen minutes, to the stirred solution. When addition was completed, the brown reaction mixture was warmed to room temperature and stirred over night. The reaction mixture was then again cooled to 0°C and 20mL DMF were slowly added. The resulting mixture was then stirred at 50°C for one hour and subsequently at room temperature over

night. The orange/brown solution was then poured onto ice (115g) and extracted with chloroform three times. The combined organic layers were then twice washed with deionised water and once with saturated $NaHCO_3$ solution. The organic layer was dried over sodium sulphate and reduced in vacuum. The resulting dark orange oil was used for the next step without further purification.
Yield (crude product) 7.640g, >100 %, dark orange oil, M=237.4705g/mol.
TLC R_f 0.55 (cyclohexane/ethyl acetate 2:1)
^{1}H NMR ($CDCl_3$) δ 7.54 (m, 1H, H-2), 8.09 (m, 1H, H-4), 11.67 (bs, 1H, NH).

4-cyano-1*H*-pyrrole-2-carboxylic acid (59)

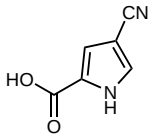

59

4-Cyano-1*H*-pyrrole-2-carboxylic acid was prepared according to a literature procedure [404]. 5-(2,2,2-trichloroacetyl)-1*H*-pyrrole-3-carbonitrile (6.800g, 28.64mmol) was added to 2M aqueous NaOH cooled to 0°C. After complete addition, the cloudy orange solution was stirred at room temperature for two hours. The solution was then acidified to pH 1 by dropwise addition of aqueous HCl. The solution was cooled to 0°C and the light brown, solid product precipitated from the solution. The product was isolated by filtration and washed with water. The light brown product was dried at 80°C over the weekend.
Yield 2.249g, 57.70%, light brown solid, M=136.1082g/mol.
^{1}H NMR (DMSO-d_6) δ 7.13 (s, 1H, H-3), 7.77 (s, 1H, H-5), 12.40 (H-1).
^{13}C NMR (DMSO-d_6) δ 92.78 (C-4), 114.86 (CN), 117.03 (C-3), 124.92 (C-2), 130.50 (C-5), 160.89 (COOH).

1*H*-pyrrole-3-carbonitrile (56)

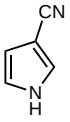

56

1*H*-Pyrrole-3-carbonitrile was prepared according to a literature procedure [404]. 4-Cyano-1*H*-pyrrole-2-carboxylic acid (450.0mg, 3.306mmol) and 300mg copper chromite catalyst in 3mL quinoline were heated to 160°C and stirred at 160°C for three hours. Subsequently, the reaction mixture was cooled to room temperature and 50mL diethyl ether were added. The catalyst was removed by filtration. The filtrate was washed with 1M aqueous HCl three times. The organic phase was then washed with saturated sodium bicarbonate solution, dried over sodium sulphate and reduced to dryness. The resulting brown oil was purified by column chromatography using cyclohexane/ethyl acetate/triethyl amine 5/1/0.025 as eluent.
Yield 114.0mg, 37.44%, orange oil, M=92.0987g/mol.

TLC R_f 0.25 (cyclohexane/ethyl acetate = 3/1)
^{1}H NMR ($CDCl_3$) δ 6.40 (m, 1H, H-4), 6.73 (m, 1H, H-5), 7.24 (m, 1H, H-2).
^{13}C NMR ($CDCl_3$) δ 91.59 (C-3), 110.57 (C-4), 116.19 (CN), 118.19 (C-5), 124.88 (C-2).

2-hydroxybenzylcyanide (55)

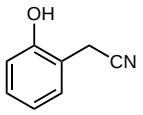

55

2-Hydroxybenzylcyanide was prepared according to a literature procedure, except potassium cyanide was used instead of sodium cyanide [401, 402]. A similar procedure using potassium cyanide was recently described. [403]. 2-Hydroxybenzylcyanide (5.000g, 39.87mmol) and potassium cyanide (3.240g, 48.26mmol, 1.2eq.) were dissolved in 65mL DMF and heated to 130°C. The reaction was stirred at 130°C over night. The reaction mixture was then cooled to room temperature and an aqueous solution of NaOH (20%m/m, 10mL) was added. The resulting mixture was reduced in vacuum to a volume of 20mL. The residue was then diluted with deionized water and acidified by addition of acetic acid to pH 4. The HCN gas was captured by two successive traps of aqueous NaOH (20%m/m). The solution was then stirred in a fume hood over night. The residue was then extracted with chloroform three times, and the combined organic layers were washed with deionized water. The organic phase was then dried over sodium sulphate and reduced in vacuum until dryness. The crude product was purified by column chromatography using cyclohexane/ethyl acetate = 5/1 as eluent.
Yield 2.089g, 39.3%, grey solid, M=133.1473g/mol
TLC R_f 0.49 (cyclohexane/ethyl acetate = 2/1)
HPLC-MS t_{ret}= 9.46min (method F)
^{1}H NMR (DMSO-d_6) δ 3.79 (s, 2H, CH_2), 6.83 (m, J=7.5Hz, 1H, H-4), 6.88 (d, J=7.6Hz, 1H, H-3), 7.18 (m, J=7.5Hz, 1H, H-5), 7.26 (d, J=7.6Hz, 1H, H-6), 9.95 (s, 1H, OH).
^{13}C NMR (DMSO-d_6) δ 17.79 (CH_2), 115.09 (C-6), 117.39 (CN), 118.98 (C-2), 119.21 (C-4), 129.08 (C-3), 129.46 (C-5), 159.96 (C-1).

2,4-diamino-5-cyanomethyl-6-hydroxypyrimidine (54)

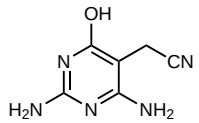

54

2,4-Diamino-5-cyanomethyl-6-hydroxypyrimidine was prepared according a modified literature procedure [399]. 2,4-Diamino-6-hydroxypyrimidine (1.04g, 7.92mmol) and sodium acetate trihydrate (2.24g, 16.5mmol) were dissolved in deionised water (20mL) and heated to 85°C. Bromoacetonitrile (650µL, 9.07mmol) was added dropwise to the solution. The reaction mixture was stirred at 85°C for two days. Subsequently, solvent was removed in vacuum. Water and acetic

acid were removed as azeotrops by addition of toluene and water respectively. The residue was then resuspended in deionised water (25mL) and the pH value was adjusted to pH 7 by addition of aqueous ammonia solution. The beige product precipitated from the solution and was isolated by filtration. The crude product was purified by recrystallization from water/ethanol.
Yield 725.0mg, 55.45%, beige solid, M=165.1527g/mol
TLC R_f 0.46 ($CHCl_3$/MeOH/aq. NH_3 = 5/4/1)
HPLC-MS t_{ret}= 11.9min (method J)
^{1}H NMR (DMSO-d_6) δ 3.13 (s, 2H, CH2), 6.15 (bs, 2H, NH2), 6.32 (bs, 2H, NH2), 10.09 (bs,1H, NH or OH).
^{13}C NMR (DMSO-d_6) δ 16.48 (CH2), 87.45 (C-5), 119.54 (CN), 153.07 (C-2), 163.11, 163.35 (C-4 and C-6).

7.6.7 Synthesis of the 2-amino-5-formylpyrrolo[2,3-*d*]pyrimidin-4-one

3-((*tert*-butyldiphenylsilyl)oxypropan-1-ol (67)

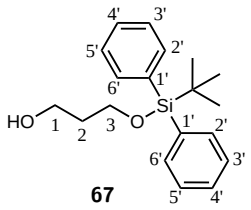

67

3-((*tert*-Butyldiphenylsilyl)oxypropan-1-ol was prepared according to a modified literature procedure [428, 429]. 1,3-Propanediol (480µL, 6.51mmol) was added dropwise to a stirred solution of triethylamine (920µL, 6.60mmol, 1.01eq.) in 5mL dry dichloromethane. The resulting solution was stirred for twenty minutes at room temperature and subsequently cooled to 0°C. A solution of *tert*-butyldiphenylsilylchloride (1.74mL, 6.69mmol, 0.973eq.) in 5mL dry dichloromethane was added dropwise to the stirred solution. After two hours at 0°C, the reaction mixture was warmed to room temperature and stirred at room temperature over night. Subsequently, 40mL of dichloromethane were added to the reaction mixture and the reaction mixture was washed with saturated sodium bicarbonate solution and brine. The organic layer was then dried over sodium sulphate and the solvent evaporated in vacuum until dryness. The crude product was purified by column chromatography using cylcohexane/ethyl acetate 8/1 as eluent.
Yield 1.440g, 70.34%, colourless oil, M=314.4940g/mol.
^{1}H NMR ($CDCl_3$) δ 0.98 (s, 9H, CH_3), 1.73 (quin, J=5.6Hz, 2H, H-2), 2.22 (bs, 1H, OH), 3.77 (t, J=5.6Hz, 4H, H-1, H-3), 7.28-7.40 (m, 6H, H-3', H4', H-5'), 7.57-7.64 (m, 4H, H-2', H-6').
^{13}C NMR ($CDCl_3$) δ 18.06 (C-1"), 25.80 (CH_3), 33.22 (C-2), 60.95 (C-3), 62.26 (C-1), 126.74 (C-3', C-5'), 128.76 (C-4'), 132.22 (C-1'), 134.53 (C-2', C-6').

3-((*tert*-butyldiphenylsilyl)oxy)propanal (68)

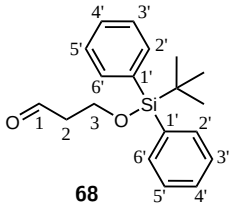

68

3-((*tert*-Butyldiphenylsilyl)oxypropanal was prepared according to a literature procedure [434]. Oxalyl chloride (2.20mL, 25.6mmol, 2.16eq.) was dissolved in 108mL dichloromethane and cooled to -78°C. DMSO (3.75mL, 52.8mmol, 4.44eq.) was added dropwise to the stirred solution. After complete addition the solution was stirred for further 30 minutes at -78°C. Subsequently, 3-((*tert*-butyldiphenylsilyl)oxypropan-1-ol (3.740g, 11.89mmol) in 13mL dichloromethane was added dropwise to the reaction mixture. After additional 45 minutes at -78°C triethylamine (13.3mL, 95.4mmol, 8.02eq.) was added to the reaction mixture. The reaction mixture was kept at -78°for further 30 minutes. The reaction mixture was then warmed to room temperature and 120mL deionized water were added. The resulting layers were separated and the aqueous layer was extracted twice with dichloromethane. The combined organic layers were washed with water and brine, dried over sodium sulphate and concentrated in vacuum until dryness. The crude product was purified by column chromatography using cyclohexane/ethyl acetate 8/1 as eluent.
Yield 3.260g, 87.73%, light yellow oil, M=312.4782g/mol.
^{1}H NMR ($CDCl_3$) δ 0.99 (s, 3H, CH_3), 2.53 (dt, J=2.1Hz, J=6.0Hz, 2H, H-2), 3.95 (t, J=6.0Hz, 2H, H-3), 7.25-7.40 (m, 6H, H-3', H-4', H-5'), 7.55-7.67 (m, 4H, H-2', H-6'), 9.74 (s, 1H, H-1).
^{13}C NMR ($CDCl_3$) δ 18.11 (C-1"), 25.72 (CH_3), 45.34 (C-2), 57.27 (C-3), 126.74 (C-3', C-5'), 128.79 (C-4'), 133.77 (C-1'), 134.52 (C-2', C-6'), 200.89 (C-1).

2-amino-5-((*tert*-butyldiphenylsilyl)oxymethyl)pyrrolo[2,3-*d*]pyrimidin-4-one (72)

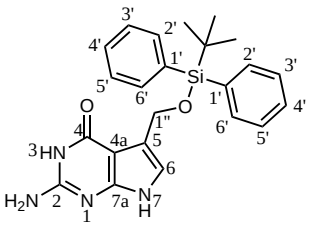

72

3-((*tert*-Butyldiphenylsilyl)oxypropanal (524mg, 1.677mmol) was dissolved in 3mL of dry diethyl ether and dioxane (5.5µL, 0.064mmol, 0.038eq.). The resulting solution was cooled to 0°C and bromine (80.0µL, 1.56mmol, 0.931eq.) was added. The reaction mixture was stirred at 0°C for five minutes and subsequently warmed to room temperature. When TLC control indicated complete conversion, saturated sodium carbonate solution was added. The layers were separated and the organic layer was dried over sodium sulphate and concentrated in vacuum until dryness. The resulting product was used in the next synthetic step without further purification.
Yield 458.0mg, 69.78%, yellow oil, M=391.3742g/mol.

2-Amino-5-((*tert*-butyldiphenylsilyl)oxymethyl)pyrrolo[2,3-*d*]pyrimidin-4-one was prepared as described in literature [425]. 2-Bromo-3-((*tert*-butyldiphenylsilyl)oxy)propanal (1.10g, 2.811mmol) in 20mL acetonitrile was added dropwise to a suspension of 2,6-diamino-4-hydroxypyrimidine (812.0mg, 6.181mmol, 2.199eq.) and sodium acetate trihydrate (1.170g, 8.598mmol, 3.059eq.) in 20mL water. The resulting reaction mixture was stirred at room temperature over night. Subsequently, the solvent was removed in vacuum and the product was purified by column chromatography using dichloromethane/methanol 10/1 as eluent.
Yield 180mg, 15.30%, white solid, M=418,5636g/mol.
^{1}H NMR (DMSO-d_6) δ 1.00 (s, 3H, CH_3), 4.88 (s, 1H, H-1"), 6.05 (s, 2H, NH_2), 6.56 (s, 1H, H-6), 7.42-7.51 (m, 6H, H-3', H-4', H-5'), 7.66-7.73 (m, 4H, H-2', H-6'), 10.24 (s, 1H, H-7), 10.86 (s, 1H, H-3).

3-benzyloxy-1-propanal (69)

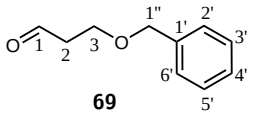

69

3-Benzyloxy-1-propanal was prepared according to a literature procedure [426]. A similar procedure starting from 2-bromo-3-benzyloxypropanal is also described in literature [425]. 3-Benzyloxy-1-propanol (960µL, 5.88mmol) was dissolved in 35mL dichloromethane and the resulting solution was cooled to 0°C. TEMPO (129.0mg, 0.0809mmol, 0.0138eq.) was added to the reaction mixture. After further ten minutes at 0°C, the reaction mixture was warmed to room temperature. The reaction mixture was stirred at room temperature for 30 minutes and subsequently filtered over celite. The filtrate was washed with 1N HCl, saturated sodium carbonate solution and brine. The organic layer was dried over sodium sulphate and reduced in vacuum until dryness. The resulting product was used for the next synthetic step without further purification.
^{1}H NMR ($CDCl_3$) δ 2.62 (dt, J=1.8Hz, J=6.1Hz, 2H, H-2), 3.74 (t, J=6.1Hz, 2H, H-3), 4.46 (s, 2H, H-1") 7.17-7.31 (m, 5H, H-2', H-3', H-4', H-5', H-6'), 7.72 (t, J=1.8Hz, 1H, H-1).

2-amino-5-(benzyloxy)methylpyrrolo[2,3-*d*]pyrimidin-4-one (73)

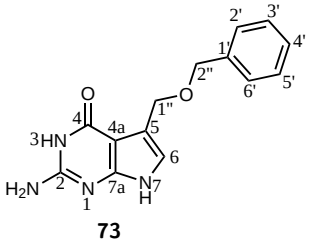

73

2-Amino-5-(benzyloxy)methylpyrrolo[2,3-*d*]pyrimidin-4-one was prepared according to a literature procedure [426]. 3-Benzyloxy-1-propanal was dissolved in 18mL acetonitrile and the resulting solution was cooled to 0°C. DMSO (290µL, 4.08mmol, 0.695eq.) and trimethylsilylbromide (850µL, 5.55mmol, 0.705eq.) was added to the stirred solution. The reaction mixture was stirred over night during which time the reaction mixture warmed to room temperature. Subsequently,

2,6-diamino-4-hydroxypyrimidine (544.0mg, 4.14mmol, 0.705eq.) and sodium acetate trihydrate (896.8mg, 6.590mmol, 1.12eq.) were suspended in 18mL deionized water and the suspension was added to the reaction mixture. The reaction mixture was stirred at room temperature for six hours. Afterwards, the solvents were removed in vacuum and the crude product was purified by column chromatography using dichloromethane/methanol 10/1 as eluent.
Yield 82.0mg, 5.162% over three steps, light yellow solid, M=270.2866g/mol.
^{1}H NMR (DMSO-d_6) δ 4.45 (s, 2H, H-1"), 4.51 (s, 2H, H-2"), 6.00 (s, 2H, NH_2), 6.55 (d, J=2.0Hz, H-6), 7.24-7.29 (m, 5H, H-2', H-3', H-4', H-5', H-6'), 10.20 (s, 1H, H-7), 10.85 (s, 1H, H-3).
^{13}C NMR (DMSO-d_6) δ 64.29 (C-1"), 70.80 (C-2"), 98.43 (C-4a), 115.02 (C-6), 115.61 (C-6), 127.14 (C-4'), 127.39 (C-2', C-6'), 128.11 (C-3', C-5'), 138.99 (C-1'), 151.29 (C-7a), 152.33 (C-2), 159.04 (C-4).

2-amino-7*H*-pyrrolo[2,3-*d*]pyrimidin-4-one (60)

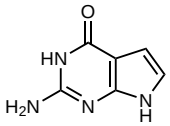

60

Sodium acetate trihydrate (22.50g, 165.3mmol) and the pyrimidine precursor 2,6-diaminopyrimidin-4-one (10.00g, 76.12mmol) were suspended in 310mL deionised water. The reaction mixture was heated to 85°C at which point most of the solids dissolved. Chloroacetaldehyde (12mL, 76.43mmol, 50%m/m solution in deionised water) in 140mL deionised water was added dropwise to the stirred reaction mixture. The reaction was stirred over night at 85°C. After cooling to room temperature the pH value of the reaction mixture was adjusted to pH 7.5 using aqueous ammonia solution. The purple product precipitated from the solution and was isolated by vacuum filtration.
Yield 5.910g, 51.71%, purple solid, M=150.1380g/mol.
TLC R_f 0.65 ($CHCl_3$/MeOH/aq. NH_3 5/4/1)
^{1}H NMR (DMSO-d_6) δ 6.09 (s, 1H, NH_2), 6.20 (dd, J1=1.1 Hz, J2=2.2Hz, 1H, H-5), 6.63 (dd, J1=1.1 Hz, J2=2.2Hz, 1H, H-6), 10.29 (s, 1H, H-7), 11.00 (s, 1H, H-3).
^{13}C NMR (DMSO-d_6) δ 99.83 (C-4a), 101.56 (C-5), 116.66 (C-6), 151.13 (C-7a), 152.20 (C-2), 158.92 (C-4).

2-pivaloylaminopyrrolo[2,3-*d*]pyrimidin-4-one (62)

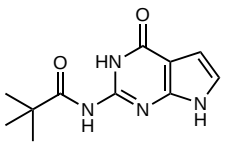

62

2-Pivaloylaminopyrrolo[2,3-*d*]pyrimidin-4-one was prepared according to a modified literature procedure [286]. 2-Aminopyrrolo[2,3-*d*]pyrimidin-4-one (3.530g, 23.51mmol) was suspended in pyridine (35.3mL, 437mmol, 18.6eq.) and triethyl amine (7.1mL, 51mmol, 2.2eq.). The reaction

mixture was heated to 90°C and pivaloylchloride (8.7mL, 70mmol, 3.0eq.) was added dropwise to the stirred reaction mixture. The reaction mixture was stirred at 90°C over night and then cooled to room temperature. All solids were removed by filtration and the filtrate was neutralized by addition of aqueous ammonia solution. The solvent was removed in vacuum until dryness. The resinous residue was resuspended in diethyl ether. The product was isolated by filtration and washed with diethyl ether.
Yield 3.775g, 68.54%, beige solid, M=234.2545g/mol.
HPLC-MS t_{ret}= 14.84min (method E)
^{1}H NMR (DMSO-d_6) δ 1.19 (s, 9H, $(CH_3)_3$), 6.36 (s, 1H, H-5), 6.90 (s, 1H, H-6), 10.73 (s, H-7), 11.52 (s, 1H, H-3), 11.78 (s, 1H, NHPiv).
^{13}C NMR (DMSO-d_6) δ 26.38 $(CH_3)_3$), 102.20 (C-5), 103.86 (C-4a), 119.69 (C-6), 146.47 (C-2), 147.77 (C-7a), 157.01 (C-4), 180.84 (C-Piv).

4-chloro-2-pivaloylaminopyrrolo[2,3-*d*]pyrimidine (63)

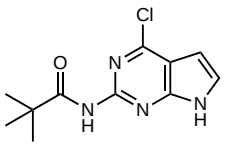

63

2-Pivaloylaminopyrrolo[2,3-*d*]pyrimidin-4-one (1.800g, 7.684mmol) was suspended in dimethylformamide (1.2mL, 15mmol, 2.0eq.) and phosphorus oxychloride (44.7mL, 490mmol, 63.7eq.) was added. The resulting reaction mixture was stirred at 55°C over night. The solvent was removed in vacuum and ice water was added slowly to the resulting residue. The resulting suspension was refluxed for one hour and subsequently the pH value was adjusted to pH 5 by addition of aqueous ammonia solution. The product precipitated from the aqueous solution and was isolated by filtration.
Yield 1.18g, 60.77%, brown solid, M=252.7007g/mol.
HPLC-MS t_{ret}= 15.34min (method E)
^{1}H NMR (DMSO-d_6) δ 1.25 (s, 3H, CH_3), 8.53 (d, J=2.8Hz, H-6), 10.33 (s, 1H, H-7), 13.41 (s, 1H, NH-Piv).
^{13}C NMR (DMSO-d_6) δ 26.87 (CH_3), 98.63 (C-4a), 113.20 (C-5), 127.37 (C-6), 150.21 (C-7a), 151.32 (C-2), 152.71 (C-4), 175.88 (C-Piv).

4-chloro-5-iodo-2-pivaloylaminopyrrolo[2,3-*d*]pyrimidine (64)

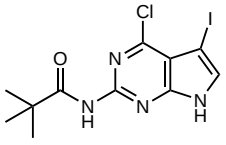

64

4-Chloro-5-iodo-2-pivaloylaminopyrrolo[2,3-*d*]pyrimidine was prepared according to a literature procedure [339]. 4-Chloro-2-pivaloylaminopyrrolo[2,3-*d*]pyrimidine (500.0mg, 1.979mmol) was

dissolved in dry THF under nitrogen atmosphere. The flask was covered in aluminium foil to exclude light from the reaction mixture. *N*-Iodosuccinimide (490.0mg, 2.069mmol, 1.046eq.) was added to the stirred solution. After one hour at room temperature the reaction mixture was diluted with dichloromethane and deionized water was added. The layers were separated and the aqeuous layer was extracted with dichloromethane. The combined organic layers were dried over sodium sulphate and reduced in vacuum until dryness. The resulting crude product was purified by column chromatography using a gradient of dichloromethane to dichloromethane/methanol 10/1 as eluent.
Yield 168.5mg, 22.49%, light yellow solid, M=378.5967g/mol.
HPLC-MS t_{ret}= 16.04min (method E)
^{1}H NMR (DMSO-d_6) δ 1.24 (s, 9H, $(CH_3)_3$), 7.78 (d, J=2.2Hz, 1H, H-6), 10.14 (s, 1H, H-7), 12.72 (s, 1H, NH-Piv).
^{13}C NMR (DMSO-d_6) δ 26,82 (($CH_3)_3$)), 51.64 (C-5), 112.33 (C-4a), 132.74 (C-6), 150.67 (C-7a), 151.42 (C-4), 152.52 (C-2), 175.82 (C-Piv).

5-iodo-2-pivaloylaminopyrrolo[2,3-*d*]pyrimidin-4-one (65)

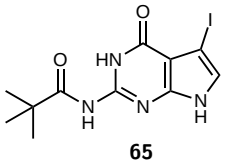

65

2-Pivaloylaminopyrrolo[2,3-*d*]pyrimidin-4-one (500.0mg, 2.134mmol) was suspended in dry THF under nitrogen atmosphere. The flask was covered in aluminium foil to exclude light from the reaction mixture. *N*-Iodosuccinimide (528.0mg, 2.230mmol, 1.045eq.) was added to the stirred reaction mixture. After stirring at room temperature over night, the reaction mixture was diluted with dichloromethane and deionized water. The layers were separated and the aqueous layer was extracted with dichloromethane. The combined organic layers were dried over magnesium sulphate and reduced in vacuum until dryness. The resulting crude product was purified by column chromatography using a gradient of dichloromethane to dichloromethane/methanol 100/1 as eluent.
Yield 107.1mg, 13.93%, light yellow solid, M=360.1510g/mol.
TLC R_f 0.44 (cyclohexane/ethyl acetate/ethanol = 6/5/1)
^{1}H NMR (DMSO-d_6) δ 1.29 (s, 9H, $(CH_3)_3$), 7.22 (d, J=2.2Hz, 1H, H-6), 10.91 (s, 1H, H-7), 11.89 (s, 1H, H-3), 11.99 (s, NHPiv).
^{13}C NMR (DMSO-d_6) δ 26.33 (($CH_3)_3$), 54.15 (C-5), 103.81 (C-4a), 124.91 (C-6), 146.85 (C-2), 147.85 (C-7a), 156.48 (C-4), 180.91 (C-Piv).

methyl 2-chloro-3-oxopropionate (74)

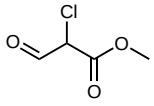

74

Methyl 2-chloro-3-oxo-propionate was prepared according to a modified literature procedure [259]. NaH (5.0g) was washed with cyclohexane and THF and subsequently suspended in 50mL THF. The suspension was cooled to 0°C. Methylformate (3.5mL, 55mmol, 0.97eq.) was added to the stirred solution. Methyl chloroacetate (5.0mL, 56mmol) in 20mL THF were added dropwise to the reaction mixture over ten minutes. The resulting mixture was stirred for five hours at 0°C. Subsequently, 50mL deionized water was added and the mixture was extracted twice with diethyl ether. The pH value of the resulting aqueous phase was adjusted to pH 4 by addition of concentrated HCl. The aqueous layer was extracted with diethyl ether three times. The combined organic phases were dried over sodium sulphate and reduced in vacuum until dryness. The resulting yellow oil was used for the next synthetic step without further purification.
Yield 6.37g, 84.73%, yellow oil, M=136.5337g/mol.

Methyl 2-amino-4-oxopyrrolo[2,3-*d*]pyrimidin-5-carboxylate (76) and methyl 2,4-diaminofuro-[2,3-*d*]pyrimidin-5-carboxylate (75)

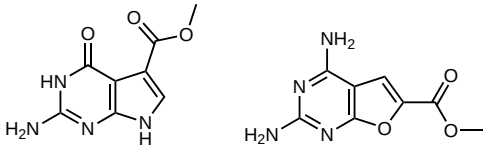

76 **75**

Methyl 2-amino-4-oxopyrrolo[2,3-*d*]pyrimidin-5-carboxylate (**76**) and methyl 2,4-diaminofuro[2,3-*d*]pyrimidin-5-carboxylate (**75**) were prepared according to a literature procedure [259, 277]. Sodium acetate trihydrate (2.99g, 22.0mmol, 0.52eq.) and 2,4-diamino-6-hydroxypyrimidine (5.540g, 42.17mmol) were suspended in 50mL deionized water and heated to 75°C. Methyl 2-chloro-3-oxo-propionate (6.00g, 44.0mmol, 1.04eq.) in 20mL deionized water was added dropwise to the stirred solution. After 75 minutes, the reaction mixture was cooled to room temperature, and the product was isolated by filtration. The precipitate was washed with copious amounts of deionized water, acetone, and diethyl ether. The off-white solid was dried in vacuum. The amount of methyl 2,4-diaminofuro[2,3-*d*]pyrimidin-5-carboxylate (**75**) formed in the reaction remained between 32% and 39% **75** when reaction temperatures between 72°C to 100°C were used and work-up was done either directly afterwards or after stirring at room temperature over night.
Yield 4.63g, 52.70% (**75**/**76**=1/2.13), beige to greenish solid, M=208.1741g/mol.
TLC R_f 0.47 (**76**), 0.81 (**75**) ($CHCl_3$/MeOH/aq. NH_3 = 5/4/1)
methyl 2-amino-4-oxopyrrolo[2,3-*d*]pyrimidin-5-carboxylate (**76**)
^{1}H NMR (DMSO-d_6) δ 3.69 (s, 3H, CH_3), 6.25 (s, 2H, NH_2), 7.37 (d, J= 2.6Hz, 1H, H-6), 10.40 (s, 1H, H-7), 11.67 (s, 1H, H-3).
^{13}C NMR (DMSO-d_6) δ 50.69 (CH_3), 93.07 (C-4a), 109.76 (C-6), 124.92 (C-5), 152.86 (C-2), 153.21 (C-7a), 157.36 (C-4), 169.54 ($COOCH_3$).
methyl 2,4-diaminofuro[2,3-*d*]pyrimidin-5-carboxylate (**75**)
^{1}H NMR (DMSO-d_6) δ 3.81 (s, 3H, CH_3), 6.57 (s, 2H, NH_2), 7.34 (s, 2H, NH_2), 7.65 (s, H-5).
^{13}C NMR (DMSO-d_6) δ 51.66 (CH_3), 97.37 (C-4a), 113.98 (C-5), 136.14 (C-6), 158.84 (C-2), 159.68 ($COOCH_3$), 163.17 (C-7a), 163.43 (C-4).

Methyl 2-amino-4-oxopyrrolo[2,3-*d*]pyrimidin-5-carboxylate (77)

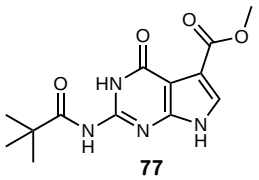

77

A mixture of methyl 2-amino-4-oxopyrrolo[2,3-*d*]pyrimidin-5-carboxylate (**76**) and methyl 2,4-diaminofuro[2,3-*d*]pyrimidin-5-carboxylate (**75**) (1.980g, 9.511mmol, **75**/**76**=1/1.56) was dissolved in 20mL pyridine and triethylamine (4.0mL, 29mmol, 3.0eq.) was added. The resulting mixture was heated to 90°C. Pivaloylchloride (5.0mL, 40mmol, 4.2eq.) was added dropwise to the reaction mixture and the reaction mixture was stirred at 90°C over night. Upon cooling to room temperature, the product precipitated from the reaction mixture. The product was resuspended in deionized water and the pH was adjusted to pH 7 with aqueous ammonia solution. The product was isolated by filtration and washed with copious amounts of deionized water. Methyl 2-amino-4-oxopyrrolo[2,3-*d*]pyrimidin-5-carboxylate (**77**) was purified by column chromatography using cyclohexane/ethyl acetate 1/1 as eluent.

Yield 2.900g, 33.81% beige solid, M=292.2905g/mol.

^{1}H NMR (DMSO-d_6) δ 1.12 (s, 9H, Piv−$(CH_3)_3$), 3.91 (s,3H, CH_3), 7.70 (s, 1H, H-6), 10.18 (s, 1H, H-7), 10.68 (s, 1H, H-3), 12.03 (bs, 1H, Piv-NH).

^{13}C NMR (DMSO-d_6) δ 26.53 (C(CH_3)$_3$), 37.67 (C(CH_3)$_3$), 52.45 (COOCH_3), 103.69 (C-4a), 115.76 (C-6), 140.51 (C-5), 155.05 (C-2), 155.74 (C-7a), 158.51 (C-4), 168.47 (COOCH$_3$), 179.33 (CO-Piv).

5-formyl-2-pivaloylaminopyrrolo[2,3-*d*]pyrimidin-4-one (61)

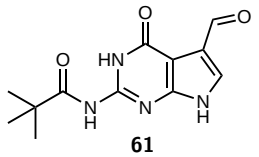

61

2-Pivaloylamino-5-cyanopyrrolo[2,3-*d*]pyrimidin-4-one (**8**) (160mg, 0.617mmol) was suspended in pyridine/acetic acid/deionized water 2/1/1. Alternatively, acetic acid/deionized water 1/1 can be used as reaction solvent. Sodium hypophosphite dihydrate (400.0mg, 3.774mg, 6.115eq.) was added. The resulting reaction mixture was stirred under nitrogen at 55°C for two hours. Subsequently, Raney-Ni (200mg, suspension in water) was added. After four hours TLC indicated complete conversion. The catalyst was removed by filtration over celite. The filtrate was reduced in vacuum until dryness. The remaining residue was redissolved with methanol and the product was precipitated by addition of diethyl ether.

Yield 117.18mg, 36.2%, beige solid, M=262.2646g/mol.

HPLC-MS t_{ret}= 17.0min (method E)

2-amino-5-formylpyrrolo[2,3-*d*]pyrimidin-4-one (66)

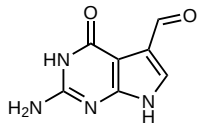

66

Method A: $PreQ_0$ (555.4mg, 3.171mmol) and $Na_2H_2PO_2$ dihydrate (1.087g, 10.25mmol, 3.233eq.) were dissolved in 15mL pyridine/acetic acid/deionized water 2/1/1 and stirred under nitrogen atmosphere. Raney-Ni catalyst (slurry in water, approx. 500mg) was added to the stirred reaction mixture. Upon addition of Raney-Ni the brown reaction mixture started to foam. The reaction mixture was stirred under nitrogen over night. Subsequently, the catalyst was removed by filtration over celite. The resulting filtrate was reduced in vacuum under addition of first methanol, and secondly toluene to remove acetic acid and water, respectively, as azeotropic mixtures. The remaining brown slurry was dissolved in 6M aqueous potassium hydroxide solution and filtered. The resulting filtrate was cooled to 0 °C and neutralized by addition of concentrated aqueous HCl. The product precipitated from the solution and was isolated by filtration. A second fraction of product precipitated from the solution after reducing the solvent volume in vacuum. The product was washed with ice water. An analytical sample was redissolved in 6M aqueous potassium solution and treated with charcoal. Charcoal was removed by filtration over celite, and the product was precipitated from the solution by neutralizing the filtrate by addition of concentrated aqeuous HCl.
Yield 175.5mg, 31.07%, brown solid, M=178.1481g/mol.
Method B: $PreQ_0$ (807,8mg, 4.612mmol) and $Na_2H_2PO_2$ dihydrate (1.4359g, 13.55mmol, 2.937eq.) were dissolved in 15mL pyridine/acetic acid/deionized water 2/1/1 and stirred under nitrogen atmosphere. Raney-Ni catalyst (slurry in water, approx. 500mg) was added to the stirred reaction mixture. The resulting reaction mixture was heated to 50°C for 5 hours. Subsequently, the reaction mixture was cooled to room temperature. Work-up was done analogously as described above for method A. The product was washed with water and acetone.
Yield 769.9mg, 93.67%, brown solid, M=178.1481g/mol.
TLC R_f 0.47 ($CHCl_3$/MeOH/aq. NH_3 = 5/4/1)
HPLC-MS t_{ret}= 10.0min (method C)
^{1}H NMR (DMSO-d_6) δ 6.35 (bs, 2H, NH_2), 7.49 (s, 1H, H-6), 10.04 (s, 1H, CHO), 10.72 (bs, 1H, H-7), 11.96 (bs, 1H, H-3).
^{13}C NMR (DMSO-d_6) δ 98.36 (C-5), 120.34 (C-6), 124.50 (C-4a), 153.40 (C-2), 153.83 (C-7a), 159.02 (C-4), 185.47 (CHO).

2-amino-4-oxopyrrolo[2,3-*d*]pyrimidin-5-carbaldehyde phenylhydrazone (78)

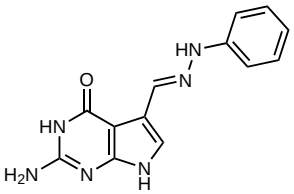

78

2-Amino-5-formylpyrrolo[2,3-*d*]pyrimidin-4-one is prepared as described above. When phenylhydrazine (2eq.) is added to the reaction mixture, complete conversion to 2-amino-4-oxopyrrolo[2,3-*d*]pyrimidin-5-carbaldehyde phenylhydrazone (**78**) is observed on TLC. When the Raney-Ni catalyst was removed by filtration over celite, the product degraded to 2-amino-5-formylpyrrolo[2,3-*d*]pyrimidin-4-one and phenylhydrazine, which are both clearly visible on TLC. Therfore, the product was not isolated.
Yield not determined, M=268.2740g/mol.
TLC R_f 0.77 (chloroform/methanol/aqeuous ammonia 5/4/1)

7.6.8 Synthesis of the 2-amino-5-methyliminopyrrolo[2,3-*d*]pyrimidin-4-one and 2-amino-4-oxopyrrolo[2,3-*d*]pyrimidin-5-carbaldehyde oxime

2-amino-5-methyliminopyrrolo[2,3-*d*]pyrimidin-4-one (81)

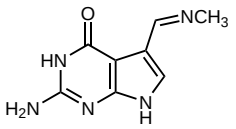

81

2-Amino-5-formylpyrrolo[2,3-*d*]pyrimidin-4-one (280.0mg, 1.572mmol) was suspended in 5mL ethanol and stirred under nitrogen atmosphere. Methylamine (33%m/m in ethanol, 163µL, 17.3mmol, 1.10eq.) was added dropwise to the reaction mixture. The reaction mixture was stirred at room temperature for 44 hours. Subsequently, the reaction mixture was cooled on an ice bath and the product precipitated from the reaction mixture. The product was isolated by filtration and washed with deionised water and aceton.
Yield 169.3mg, 56.34%, beige solid, M=191.1900g/mol.
TLC R_f 0.47 ($CHCl_3$/MeOH/aq. NH_3 = 5/4/1)
HPLC-MS t_{ret}= 16.8min (method C)

2-amino-4-oxopyrrolo[2,3-*d*]pyrimidin-5-carbaldehyde oxime (82)

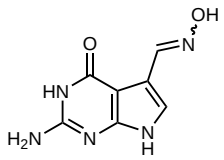

82

2-Amino-5-formylpyrrolo[2,3-*d*]pyrimidin-4-one (450.0mg, 2.526mmol) and hydroxylamine hydrochloride (210.6mg, 3.031mmol, 1.20eq.) were suspended in 5mL ethanol and stirred under nitrogen atmosphere. Aqueous sodium hydroxide solution (5M, 606µL, 3.03mmol, 1.20eq.) was added to the stirred reaction mixture. After 30 minutes at room temperature, the reaction mixture was heated to 50°C over night. Subsequently, the reaction mixture was cooled first to room temperature and then to 0°C. The product precipitated from the reaction mixture and was isolated by filtration. The product was washed with copious amounts of water and acetone and dried in

vacuum.
Yield 372.1mg, 76.26%, brown solid, M=227.1526g/mol.
TLC R_f 0.38 ($CHCl_3$/MeOH/aq. NH_3 = 5/4/1)
HPLC-MS t_{ret}= 15.6min, 16.7min (method C)

7.7 HPLC analysis of commercially available compounds

Several commercial nitriles were used for screening reactions. The HPLC-methods applied are summarized in Table 7.1.

Table 7.1 HPLC-MS methods for commercially available compounds

compound name	HPLC method	retention time
benzonitrile (**83**)	method E	18.42min
	method F	17.67min
phenylacetonitrile (**84**)	method F	17.93min
cinnamonitrile (**85**)	method F	19.06min
3-cyanoindole (**86**)	method G	11.23min
2-cyanopyrimidine (**87**)	method D	7.24min
	method G	7.27min
cyanopyrazine (**88**)	method D	6.75min
	method G	6.67min
2-cyanopyridine (**89**)	method D	11.67min
	method G	10.70min
3-cyanopyridine (**90**)	method D	9.29min
	method G	9.10min
2-cyanopyrrole (**91**)	method G	12.57min
3-cyano-7-azaindole (**92**)	method G	10.47min
6-cyanopurine (**93**)	method C	11.50min
4-aminobenzylcyanide (**94**)	method F	9.17min

8

Publications

8.1 Journal articles

Birgit Wilding, Margit Winkler, Barbara Petschacher, Regina Kratzer, Sigrid Egger, Georg Steinkellner, Andrzej Lyskowski, Bernd Nidetzky, Karl Gruber, Norbert Klempier: Targeting the substrate binding site of *E. coli* nitrile reductase queF by modeling, substrate and enzyme engineering, *Chemistry a European Journal* **2013**, *19 (22)*, 7007-7012.[287]

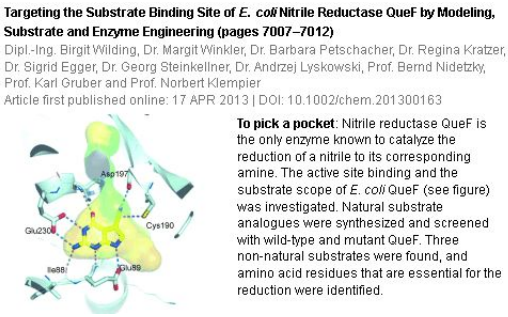

Birgit Wilding, Margit Winkler, Barbara Petschacher, Regina Kratzer, Anton Glieder, Norbert Klempier: Nitrile Reductase from Geobacillus kaustophilus: A Potential Catalyst for a New Nitrile Biotransformation Reaction, *Advanced Synthesis and Catalysis* **2012**, *354*, 2191-2198. [264]

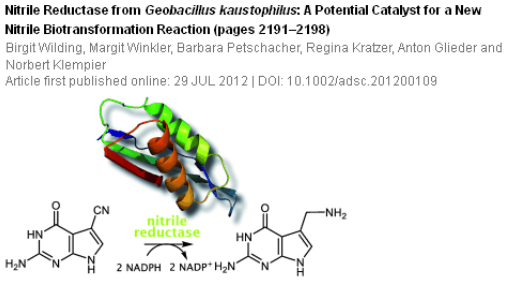

CHEMISTRY

A EUROPEAN JOURNAL

19/22 2013

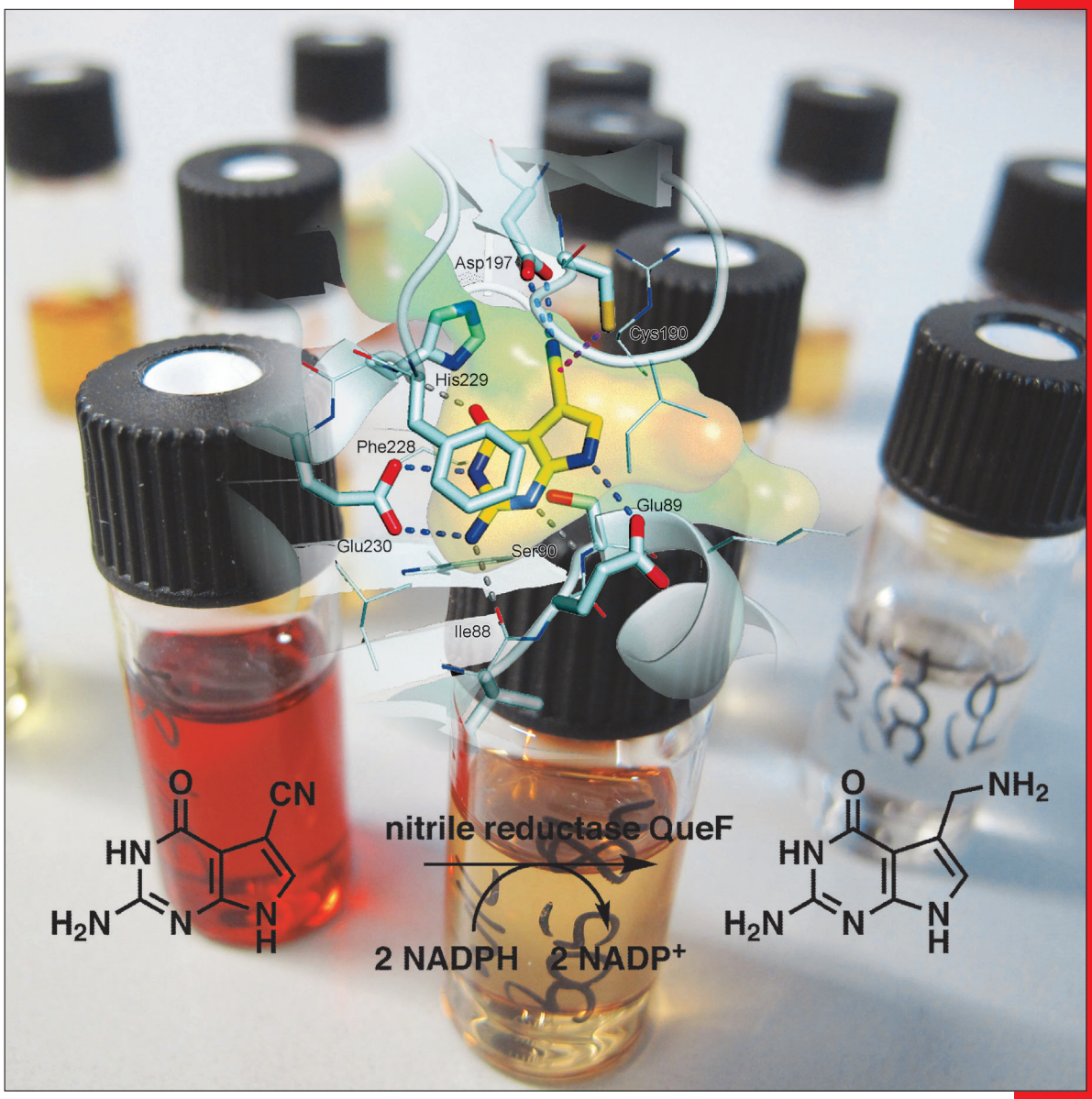

A Journal of

ChemPubSoc Europe

Supported by ACES

Nitrile reductase QueF…

… catalyzes the reduction of a nitrile to its corresponding amine. In their Full Paper on page 7007 ff., N. Klempier et al. report on the investigation of active-site binding and the substrate scope of *E. coli* QueF by modeling, enzyme, and substrate engineering. The active-site residues and structural features of the substrates essential for catalysis were identified in spectrophotometric and HPLC-MS based screenings of active-site mutants and natural substrate analogues.

WILEY-VCH

www.chemeurj.org

CHEMISTRY
A EUROPEAN JOURNAL

FULL PAPER

DOI: 10.1002/chem.201300163

Targeting the Substrate Binding Site of *E. coli* Nitrile Reductase QueF by Modeling, Substrate and Enzyme Engineering

Birgit Wilding,[a] Margit Winkler,[b] Barbara Petschacher,[b] Regina Kratzer,[c] Sigrid Egger,[c] Georg Steinkellner,[d] Andrzej Lyskowski,[d] Bernd Nidetzky,[c] Karl Gruber,[d] and Norbert Klempier*[a]

Abstract: Nitrile reductase QueF catalyzes the reduction of 2-amino-5-cyanopyrrolo[2,3-*d*]pyrimidin-4-one ($preQ_0$) to 2-amino-5-aminomethyl-pyrrolo[2,3-*d*]pyrimidin-4-one ($preQ_1$) in the biosynthetic pathway of the hypermodified nucleoside queuosine. It is the only enzyme known to catalyze a reduction of a nitrile to its corresponding primary amine and could therefore expand the toolbox of biocatalytic reactions of nitriles. To evaluate this new oxidoreductase for application in biocatalytic reactions, investigation of its substrate scope is prerequisite. We report here an investigation of the active site binding properties and the substrate scope of nitrile reductase QueF from *Escherichia coli*. Screenings with simple nitrile structures revealed high substrate specificity. Consequently, binding interactions of the substrate to the active site were identified based on a new homology model of *E. coli* QueF and modeled complex structures of the natural and non-natural substrates. Various structural analogues of the natural substrate $preQ_0$ were synthesized and screened with wild-type QueF from *E. coli* and several active site mutants. Two amino acid residues Cys190 and Asp197 were shown to play an essential role in the catalytic mechanism. Three non-natural substrates were identified and compared to the natural substrate regarding their specific activities by using wild-type and mutant nitrile reductase.

Keywords: active site model · amines · biocatalysis · enzyme catalysis · nitrile reductase

Introduction

Nitrile reductase QueF shows the unique enzymatic activity of reducing the nitrile group of 7-cyano-7-deazaguanine (2-amino-5-cyanopyrrolo[2,3-*d*]pyrimidin-4-one, $preQ_0$) to its corresponding primary amine $preQ_1$ (Scheme 1). This enzyme was found in the biosynthetic pathway to the modified nucleoside queuosine (Q) and represents the first example of a biological conversion of a nitrile to the corresponding amine.[1]

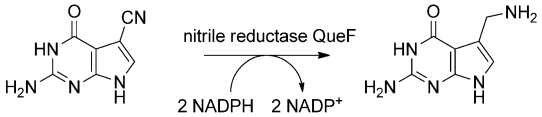

Scheme 1. Enzymatic reduction of 2-amino-5-cyanopyrrolo[2,3-*d*]pyrimidin-4-one $preQ_0$.

Currently, two types of nitrile reductase QueF are known; type I, single-domain proteins, first found in *Bacillus subtilis* (YkvM), and type II, two-domain proteins, found, for example, in *E. coli* and *Vibrio cholerae* (YqcD).[1,2] Both types of nitrile reductase QueF belong to the T-fold superfamily. The structure of QueF from *V. cholerae* was determined at 1.53 Å resolution and was found to crystallize as a tetramer, a dimer of dimers.[2] The structure of *B. subtilis* QueF, determined at 2.5 Å, revealed a homodecamer of two-head to head-facing pentamers.[3,4]

These crystal structures provide additional insight into the catalytic mechanism. Three amino acid residues, Asp197, His229 and Cys190 are considered to be involved in the catalytic mechanism proposed. The initial step is a nucleophilic attack of Cys190 on the cyano functionality of the substrate to form a thioimide intermediate, as proven by a crystal structure of this intermediate from *B. subtilis* QueF.[4] This covalent bond of the cysteine residue to the substrate is then proposed to hold the substrate in place, whereas two molecules of NADPH consecutively donate hydrides to the substrate. The mechanism requires two protons in addition to the two hydrides from NADPH. The initial proton is

[a] Dipl.-Ing. B. Wilding, Prof. N. Klempier
ACIB GmbH, c/o Institute of Organic Chemistry
Graz University of Technology, Stremayrgasse 9, 8010 Graz (Austria)
E-mail: klempier@tugraz.at

[b] Dr. M. Winkler, Dr. B. Petschacher
ACIB GmbH, c/o Institute of Molecular Biotechnology
Graz University of Technology, Petersgasse 14, 8010 Graz (Austria)

[c] Dr. R. Kratzer, Dr. S. Egger, Prof. B. Nidetzky
Institute of Biotechnology and Biochemical Engineering
Graz University of Technology, Petersgasse 12, 8010 Graz (Austria)

[d] Dr. G. Steinkellner, Dr. A. Lyskowski, Prof. K. Gruber
ACIB GmbH, c/o Institute of Molecular Biosciences
University of Graz, Humboldtstrasse 50/III, 8010 Graz (Austria)

Supporting information for this article is available on the WWW under http://dx.doi.org/10.1002/chem.201300163.

© 2013 Wiley-VCH Verlag GmbH & Co. KGaA, Weinheim

transferred to the substrate during formation of the covalent adduct. The final proton is discussed to be either provided by His229[2] or by Asp197.[5]

An enzymatic process allows the reduction of nitriles at ambient temperatures and physiological pH values and could therefore be a valuable alternative to chemical nitrile reduction. Chemical nitrile reduction generally involves either molecular hydrogen under pressure in the presence of metal catalysts, such as Pt, Pd, or Raney-Ni, or expensive borane or hydride reagents, for example, $NaBH_4$ or $LiAlH_4$.[6] Furthermore, a nitrile reductase could expand the toolbox of biocatalytic reactions of nitriles, for example, hydrolysis by nitrilases and nitrile hydratases,[7] and synthesis of α-hydroxynitriles by hydroxynitrile lysases.[8]

We recently reported the first application of nitrile reductase QueF from thermophilic origin in biocatalytic screening reactions. Two non-natural substrates, structural analogues of the natural substrate $preQ_0$, were found to be reduced to their corresponding amines by *Geobacillus kaustophilus* nitrile reductase QueF.[9]

Here, the substrate scope of *E. coli* QueF is investigated by synthesis and screening of several natural substrate analogues, as well as design and screening of active site mutants. The active site was modeled and modeled complex structures including the natural as well as non-natural substrates were investigated.

Results and Discussion

Cloning, expression and purification: Wild-type (WT) nitrile reductase and eight active site mutants were cloned, overexpressed in *E. coli* and purified, as described in the experimental section. The thus prepared enzymes were used directly after purification for screening reactions and determination of kinetic parameters, as activity decreased during storage. Wild-type enzyme retained only around 1% activity after twelve months of storage at −70 °C.

Active site model: A homology model of QueF from *E. coli* was built based on the crystal structure of the enzyme from *V. cholerae* and a docking simulation of the natural substrate $preQ_0$ (**1**) was performed. The sequence identity and the sequence similarity to the template were found to be 65 and 76%, respectively.

According to the active site model, the substrate is oriented by a series of hydrogen bonds and a ring-stacking interaction with Phe228 (Figure 1). The side chain of Glu89 and the main chain of Ser90 coordinate the ring nitrogen atoms in positions 7 and 1, respectively.[10] The carboxylate group of Glu230 interacts with the heteroatom in position 3, as well as the amino-functionality in position 2. The main chain of His229 coordinates the keto-functionality in position 4. These amino acids may therefore be involved in substrate specificity.

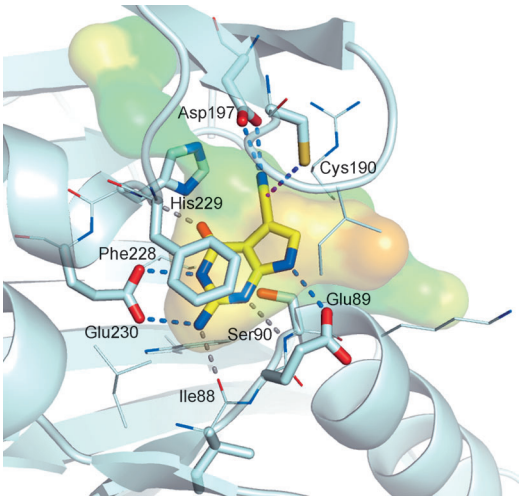

Figure 1. Energy minimized model of the active site of wild-type nitrile reductase QueF from *E. coli*. The cavity is shown as a transparent surface and is colored by hydrophobicity values (red hydrophobic, green less hydrophilic, blue hydrophilic). Grey dashed lines indicate interactions with the main chain of the amino acid, whereas blue dashed lines indicate interactions with the side chain. The magenta dashed line indicates where the active site Cys190 should attack to form the covalent reaction intermediate.

Screening reactions: Screening reactions of wild-type and mutant nitrile reductase from *E. coli* with the natural substrate $preQ_0$ (**1**) and non-natural substrates (**2**–**14**) were analyzed by spectrophotometric monitoring of NADPH depletion, as well as by HPLC-MS based measurements of product formation. Specific activities were assayed spectrophotometrically (see the Experimental Section).

Simple, commercially available nitriles used in screening reactions were not accepted as substrates by wild-type nitrile reductase from *E. coli*. These nitriles included aromatic nitriles, like benzonitrile, aliphatic nitriles, for example, phenylacetonitrile, as well as a variety of heterocyclic nitriles, including 2-cyanopyrrole, 3-cyanoindole, and cyanopyridines. The full range of commercially available nitriles used for screening reactions is depicted in Figure S1 in the Supporting Information.

Consequently, the range of substrates investigated in screening reactions with wild-type and mutant nitrile reductase from *E. coli* were focused on natural substrate analogues. Natural substrate analogues **2**, **3**, and **4** differ from $preQ_0$ in the number of functional groups on the pyrimidine ring. 5-Cyanopyrrolo[2,3-*d*]pyrimidin-4-one (**2**) and 2-amino-5-cyanopyrrolo[2,3-*d*]pyrimidine (**3**) are devoid of the amino- and the keto-substituent, respectively, whereas 5-cyanopyrrolo[2,3-*d*]pyrimidine (**4**) has neither amino- nor keto-substituent. Furthermore, the amino- and keto-functionality were protected by a pivaloyl- (**5**), and methyl-protecting group (**6**). Nitriles **8** and **10** differ from $preQ_0$ in the substituent in position 4. The keto-substituent is replaced by an amino- (**8**) and chloro-substituent (**10**), respectively. 4-Amino-5-cyanopyrrolo[2,3-*d*]pyrimidine (**9**) shows only one substituent on the pyrimidine ring, an amino group in posi-

 © 2013 Wiley-VCH Verlag GmbH & Co. KGaA, Weinheim

tion 4. 2,4-Diamino-5-cyanomethyl-6-hydroxypyrimidine (**7**) resembles the natural substrate $preQ_0$ (**1**) in its substitution pattern on the pyrimidine ring, however, bears the nitrile functionality on an open chain fragment. 2-Hydroxybenzylcyanide (**13**) and 4-aminobenzylcyanide (**14**) are additionally devoid of the ring nitrogen atoms. 3-Cyano-7-azaindole (**11**) and 3-cyanoindole (**12**) show the bicyclic ring structure of the substrate, however, are devoid of the functional groups and one or both nitrogen atoms in the six-membered ring (Figure 2).

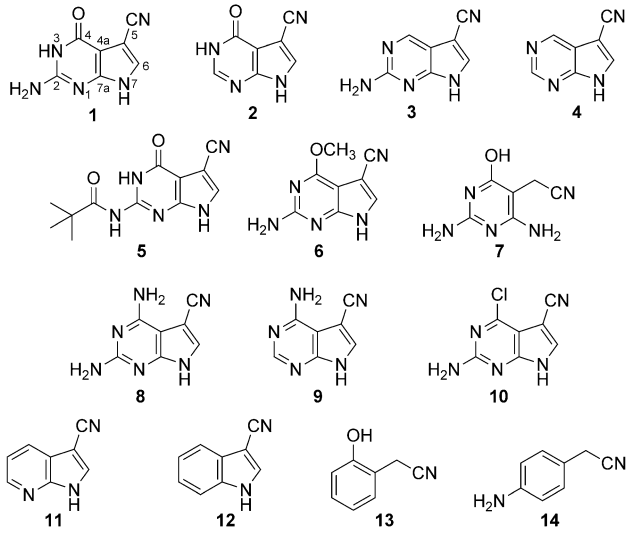

Figure 2. Range of natural substrate analogues screened with wild-type and mutant nitrile reductase QueF from *E. coli*.

Wild-type nitrile reductase QueF from *E. coli* was found to be active for the conversion of its natural substrate $preQ_0$ (**1**), as well as the two non-natural substrates 5-cyanopyrrolo[2,3-*d*]pyrimidin-4-one (**2**) and 2-amino-5-cyanopyrrolo[2,3-*d*]pyrimidine (**3**). Specific activities for the natural substrate **1** and non-natural substrate **2** are in the same range, whereas the specific activity for non-natural substrate **3** is significantly lower and was not detectable by HPLC-MS (Tables 1 and 2). These results are consistent with previous screenings in which two non-natural substrates (**2** and **3**) were identified to be accepted as substrates by wild-type and mutant nitrile reductase from *G. kaustophilus*.[9]

Nitriles **5**–**14** were not accepted as substrate by wild-type or any mutant nitrile reductase from *E. coli* (Table 1). All successfully reduced substrates contain the bicyclic pyrrolo-[2,3-*d*]pyrimidine ring system, differing in their pyrimidine ring substituents. Although substrates **2** and **3**, differing in the missing amino- and keto-functionality on the pyrimidine ring, respectively, were accepted as substrates, nitriles **5** and **6** bearing protecting groups on these functionalities were not converted. Neither nitrile differing from the guanine-substitution pattern, as in substrates **8**–**10**, or monocyclic nitriles, including 2,4-diamino-5-cyanomethyl-6-hydroxypyrimidine (**7**), were accepted as substrate.

Table 1. HPLC-MS based screening results, conversions based on area normalization.[a]

	1	**2**	**3–14**
wild type	+++	+++	–
Glu89Ala	+	+	–
Glu89Leu	+	+	–
Ser90Ala	+++	+++	–
Cys190Ala	–	–	–
Asp197Asn	–	–	–
Phe228Trp	+++	+++	–
His229Ala	+++	+++	–
Glu230Gln	++	++	–

[a] +++, conversion over 95%; ++, conversion 2–10%; +, conversion <2%; –, no conversion.

In order to verify their proposed role in the catalytic mechanism, enzyme variants with amino acid exchanges at Cys190, Asp197 and His229 were prepared. The substitution of the active site nucleophile Cys190 by alanine resulted in a protein that was no longer active for the conversion of neither the natural substrate, nor any of the non-natural substrates (Table 1). The essential role of the cysteine residue was previously proven by Cys55Ala and Cys55Ser variants of *B. subtilis* QueF. Crystallization of a Cys55Ala variant from *B. subtilis* showed $preQ_0$ to be bound noncovalently, whereas covalently bound substrate was found in the crystal structure of the thioimide complex.[5] Additionally, a Cys55Ala variant of *G. kaustophilus* QueF was also inactive for the conversion of $preQ_0$.[10] However, so far no mutations of the aspartic acid or histidine residue are available in the literature. The Asp197Asn mutation led to complete loss of activity, confirming its essential role in the catalytic mechanism. However, the His229Ala mutant retained activity, leading to similar conversions as wild-type enzyme (Table 1). Specific activities, however, were approximately one order of magnitude lower than for the wild-type enzyme (Table 2). Based on these data, an essential role of this histidine residue in the catalytic mechanism could not be verified.

Several amino acid residues coordinating the substrate in the active site were exchanged to investigate their influence on substrate binding. The Phe228Trp variant retains the possibility of ring stacking interactions with the substrate. This variant was found to be active. Although conversions were comparable to wild-type enzyme, specific activities were 90% lower for substrate **1** and **2**. The mutation Glu230Gln exchanges two amino acid residues of similar length, ex-

Table 2. Specific activities [$mU\,mg^{-1}$] determined in spectrophotometric measurements.

	1	**2**	**3**	**4**
wild type	117	90	<0.1[a]	–
Ser90Ala	12.9	3.8	<0.1[a]	<0.1[a]
Phe228Trp	10.2	8.7	<0.1[a]	–
His229Ala	17.9	14.3	–	–
Glu230Gln	4.4	3.0	2.2[a]	2.0[a]

[a] Specific activities for substrates **3** and **4** were significantly lower than for substrates **1** and **2**, therefore no product could be detected by HPLC-MS for substrates **3** and **4**.

 © 2013 Wiley-VCH Verlag GmbH & Co. KGaA, Weinheim

changing the carboxylic acid functionality of the glutamate with the amide functionality of the glutamine. This mutation led to lower conversions as well as specific activities for substrates **1** and **2**. However, this variant showed marginally broader substrate specificity; specific activities for substrates **3** and **4** were higher than with wild-type enzyme or any other variant. Exchanges of Glu89 by Ala or Leu mutations led to a drastic loss in activity. Conversions of the natural substrate (**1**) were lower than 2%, indicating that this amino acid is important for substrate binding. The Ser90Ala variant showed similar conversions as the wild-type enzyme. Specific activities were decreased by 90%, however, nitriles **1**–**4** were accepted as substrate. The active site model suggests main-chain interactions between Ser90 and the substrate (Figure 1), consequently alterations in the side chain might have less impact on substrate binding.

Determination of kinetic parameters for wild-type nitrile reductase from *E. coli* showed that k_{cat} values for substrate **1** and **2** are in the same range, however, the K_M value for substrate **2** is considerably higher, affecting substrate specificity by a factor of 100 (Table 3). This is also indicated by the slightly lower specific activities for substrate **2**. Comparable k_{cat} values were obtained when $preQ_0$ (or NADPH) was held at a constant saturating concentration and the NADPH (or $preQ_0$) was varied, proving internal consistency of kinetic parameters. The K_M value determined for NADPH (Table 3) is consistent with the values found in the literature.[1]

Table 3. Apparent kinetic parameters for wild-type nitrile reductase from *E. coli*.

	NADPH	**1**	**2**
K_M [μM]	6.0±0.7	6.1±1.1	176±23
k_{cat} [min^{-1}]	8.5±0.1	6.5±0.2	3.6±0.3

Conclusion

Type II nitrile reductase QueF from *E. coli* was cloned, expressed, purified, and investigated regarding its active site binding properties and substrate scope. A homology model, calculated based on the crystal structure of *V. cholerae* and modeled complex structures allowed the identification of several active site residues coordinating the substrate. To gain insight into active site binding, variants of the amino acid residues considered important for substrate binding were prepared and screened with various synthesized natural substrate analogues. Several structural elements were found to be essential for binding. All three non-natural substrates converted contain the pyrrolo[2,3-*d*]pyrimidine ring core structure. Substrate **2**, containing the keto-functionality in position 4 showed comparable specific activities to the natural substrate $preQ_0$ (**1**). Monocyclic nitriles **7**, **13**, and **14** were not accepted as substrates, even though nitrile **7** contained similar functional groups and ring hetero-atoms as the natural substrate, indicating the importance of the pyrrolo[2,3-*d*]pyrimidine ring for binding. The active site variant Glu230Gln showed a broader substrate scope than wild-type enzyme, was, however, still restricted to pyrrolo-[2,3-*d*]pyrimidine substrates.

Three amino acids Cys190, Asp197, and His229 were proposed to partake in the catalytic mechanism. The essential role of the cysteine residue was proven previously for type I QueF in screenings of Cys55 variants of *B. subtilis* and *G. kaustophilus* QueF. The screening results of this study support an essential role of Cys190 and Asp197 in nitrile reductase type II, however, could not confirm the essential role of His229.

The present work verifies the catalytic mechanism proposed and provides insight into structural properties of possible substrates and is therefore a first step towards application of nitrile reductase in biocatalytic reactions.

Experimental Section

General procedures: Reagents and starting materials were obtained from commercial suppliers, and used without further purification. Thin layer chromatography was carried out with precoated aluminium silica gel 60 F_{254} plates and column chromatography with Merck silica gel 60 (0.040–0.063 mm). ^1H and ^{13}C NMR spectra were recorded on a Bruker Avance III with autosampler (^1H NMR 300.36 MHz, ^{13}C NMR 75.53 MHz). Chemical shifts for ^1H NMR are reported in ppm relative to Me_4Si as internal standard. Screening reactions were run on an Eppendorf comfort thermomixer. Absorption measurements were obtained with a Fluostar plate reader (BMG Lab Tech) at 340 nm, and HPLC-MS analysis was carried out with an Agilent 1200 series by using a phenomenex Gemini-NX3 C18 110 Å (150 mm × 2.0 mm) column and ammonium acetate (20 mM) in water and acetonitrile as eluents, except for 2,4-diamino-5-cyanomethyl-6-hydroxypyrimidine (**7**) for which a Merck SeQuant ZIC-HILIC column (150 mm × 2.1 mm, 3.5 μm, 200 Å) with ammonium acetate (5 mM) in water and acetonitrile as eluents was used.

Enzyme cloning, expression and purification: *E. coli* queF (gene ID: 947270) was amplified from the genomic DNA of *E. coli* str. K-12 with the introduction of restriction sites NcoI and HindIII by using Phusion® High-Fidelity DNA polymerase (Finnzymes) and primers 5′-AAT CAC CAT GGC TAT GTC TTC TTA TGC AAA C-3′ and 5′-AAT CAA AGC TTT TAT TGC CGA ACC AGT C-3′, respectively. The PCR reaction was thermally cycled: 98 °C for 30 s, followed by 30 cycles of 98 °C for 10 s, 55 °C for 15 s, and 72 °C for 20 s, then a final incubation of 72 °C for 5 min. The PCR products were gel purified with the QIAquick® gel extraction kit (Qiagen), digested with NcoI and HindIII restriction enzymes (Fermentas) in Tango buffer (Fermentas), and column purified according to the QIAquick® PCR purification protocol (Qiagen). The gene was ligated into the pEHISTEV vector,[18] which was also digested with NcoI and HindIII. The ligation was carried out for 3 h at room temperature in the presence of T4 ligase (Fermentas) and T4 ligation buffer (Fermentas). The ligation product was transformed into electrocompetent *E. coli* TOP10 F′ cells and plated on LB-agar supplemented with 50 μg kanamycin per mL. The resulting plasmid pEHISTEV:EcNRedWT was isolated with the GeneJET™ plasmid mininprep kit (Fermentas) and the sequence was confirmed by LGC Genomics.

pEHISTEV:EcNRedWT was employed as the template for site directed mutagenesis with the following primers (exchanged nucleotides underlined): E89Afw, 5′-ACC AGC GTA AAT CTG ATT GCG TCG AAG AGT TTT AAG CTC-3′; E89Arv, 5′-GAG CTT AAA ACT CTT CGA CGC AAT CAG ATT TAC GCT GGT-3′; E89Lfw, 5′-GAT TAC ACC AGC GTA AAT CTG ATT CTG TCG AAG AGT TTT AAG CTC TAT-3′; E89Lrv, 5′-ATA GAG CTT AAA ACT CTT CGA CAG AAT CAG ATT TAC GCT GGT GTA ATC-3′; S90Afw, 5′-GC GTA AAT CTG ATT GAG GCG AAG AGT TTT AAG CTC TAT C-3′; S90Arv, 5′-G ATA GAG CTT AAA ACT CTT CGC CTC AAT CAG ATT TAC GC-3′; C190Afw, 5′-C CTG CTG AAA TCA AAT GCC CTG ATC

© 2013 Wiley-VCH Verlag GmbH & Co. KGaA, Weinheim

ACC CAT CAA CCA G-3′; C190Arv, 5′-C TGG TTG ATG GGT GAT CAG GGC ATT TGA TTT CAG CAG G-3′; D197Nfw, 5′-C CTG ATC ACC CAT CAA CCA AAT TGG GGT TCG CTC C-3′; D197Nrv, 5′-G GAG CGA ACC CCA ATT TGG TTG ATG GGT GAT CAG G-3′; F228Wfw, 5′-GT CAT CAC AAC GAG TGG CAC GAA CAG TGC GTG GAA C-3′; F228Wrv, 5′-G TTC CAC GCA CTG TTC GTG CCA CTC GTT GTG ATG AC-3′; H229Afw, 5′-GT CAT CAC AAC GAG TTC GCC GAA CAG TGC GTG GAA C-3′; H229rv, 5′-G TTC CAC GCA CTG TTC GGC GAA CTC GTT GTG ATG AC-3′; E230Qfw, 5′-CAT CAC AAC GAG TTC CAC CAA CAG TGC GTG GAA CGC-3′; and E230Qrv, 5′-GCG TTC CAC GCA CTG TTG GTG GAA CTC GTT GTG ATG-3′. Briefly, PfuUltra HF reaction buffer (5 μL; 10×), the template (1 μL, 10 ng), dNTPs mix (1 μL;10 mM), either forward or reverse primer (5 mM; 1 μL) and PfuUltra High Fidelity DNA polymerase (1 μL; 2.5 U μL^{-1}; Stratagene, La Jolla, CA, USA) were added to doubly distilled water (41 μL; Fresenius, Graz, Austria). The two-stage PCR was conducted on a Gene Amp System 2400 thermo cycler (Applied Biosystems, Foster City, CA) under the following conditions: 95 °C for 1 min, 4 cycles of 50 s at 95 °C, 50 s at 60 °C, 5 min 30 s at 68 °C, and then 7 min at 68 °C for the final elongation step. After these initial four cycles of primer extension, the reaction containing the forward primer (25 μL) was combined with the reaction containing the reverse primer (25 μL). Additional 25 cycles were run under the above conditions. Subsequently, DpnI (1 μL, Fermentas) was added to digest the template at 37 °C for 1 h. An aliquot of the mixture (2 μL) was transformed into electrocompetent *E. coli* K12 Top10F' cells (60 μL; Invitrogen). SOC medium (500 μL) was added to the cells immediately after transformation. After regeneration for 45 min at 37 °C, 50 μL + 510 μL of the transformation mixture were plated on LB/kanamycin agar plates for selection of positive transformants. The mutations were confirmed by sequencing (LCG Genomics). Plasmids from WT and mutants with the correct sequence were transformed into *E. coli* BL21 (DE3). The WT and the mutant nitrile reductase were cultivated as follows: overnight cultures (20 mL LB/kan, inoculated with a single colony and grown at 37 °C in an orbital shaker) were used to inoculate LB/kan medium (500 mL) in baffled Erlenmeyer flasks (2 L). These main cultures were grown at 37 °C and 130 rpm to an OD of 0.7, induced with IPTG (0.5 mL; 1 M) and incubated for 18–20 h at 37 °C and 130 rpm. The cells were harvested by centrifugation (2800 g, 4 °C, 10 min). The pellet was resuspended in buffer (10 mM Tris, 50 mM KCl, 1% v/v glycerol; pH 7.5 adjusted with HCl 37%) and disrupted by ultrasonication. Cell debris was removed by ultracentrifugation at 164 400 g for 45 min at 4 °C. The cell-free extract was applied to an Ni Sepharose 6 fast flow column (5 mL; GE Healthcare, UK). The tagged enzymes were obtained by a one-step purification by using the buffers recommended in the manual. After purification, the enzyme solution was desalted against reaction buffer (100 mM Tris, 50 mM KCl, 1 mM TCEP, 1% v/v glycerol; pH 7.5 adjusted with HCl 37%) by using HiTrap Desalting columns (GE Healthcare, UK). The collected protein fractions were concentrated tenfold by Vivaspin 20 tubes (10 000 MWCO, Sartorius) and then used for enzymatic assays without intermediate freezing steps.

Modeling and docking: The structure of *E. coli* nitrile reductase QueF was modeled by using the program YASARA Structure[11] by applying the standard modeling protocol. For the comparative modeling, the structure of *V. cholerae* QueF (PDB ID: 3RZQ) with a sequence identity of 65% and a similarity of 76% was used as a template. The natural substrate of *V. cholerae* QueF was retained during modeling and energy minimization. The side chain of the proposed catalytic residue Cys190, which is located in a loop close to the active site, was rotated in the model to match the proposed reaction mechanism. An energy minimization of the complex was performed by using the force field AMBER03[12] by applying the standard YASARA energy minimization protocol. For the docking calculations the program Glide[13] was used. The substrates were prepared in Maestro[14] and optimized by using Jaguar[15] with basis set 6-31G. The docking box for the grid calculation was set to a side length of 10 Å with the center of the box at the active site. The docking was performed with extra precision and with flexible ligands. Receptor hydroxyl and thiol groups within the docking box were allowed to rotate. Substrates **1**–**14** were docked into the model. Compounds **1** and **2** as well as **4**, **8** and **11** showed reasonable binding modes consistent with the proposed reaction mechanism with **1** and **2** yielding the best docking scores (Figures S2 and S3 in the Supporting Information). All pictures were generated by using PyMOL.[16] Hydrophobicity values for the visualization of the cavity surface were calculated with VASCo.[17]

Substrate synthesis: 7-Aza-3-cyanoindole (**11**), 3-cyanoindole (**12**) and aminobenzylcyanide (**14**) are commercially available and were purchased from Sigma–Aldrich. 2-Amino-5-cyanopyrrolo[2,3-*d*]pyrimidin-4-one (preQ$_0$, **1**), 5-cyanopyrrolo[2,3-*d*]pyrimidin-4-one (**2**), 2-amino-5-cyanopyrrolo[2,3-*d*]pyrimidine (**3**), 2,4-diamino-5-cyanomethyl-6-hydroxypyrimidine (**7**), 2,4-diamino-5-cyanopyrrolo[2,3-*d*]pyrimidine (**8**), 4-amino-5-cyanopyrrolo[2,3-*d*]pyrimidine (**9**), 2-amino-4-chloro-5-cyanopyrrolo[2,3-*d*]pyrimidine (**10**) and 2-hydroxybenzylcyanide (**13**) were prepared according to previously published procedures.[9] Syntheses of 5-cyano-2-pivaloylaminopyrrolo[2,3-*d*]pyrimidin-4-one (**5**), and 2-amino-5-cyano-4-methoxypyrrolo[2,3-*d*]pyrimidine (**6**) are described in the Supporting Information.

5-Cyanopyrrolo[2,3-*d*]pyrimidine (4): 6-Bromo-4-chloro-5-cyanopyrrolo-[2,3-*d*]pyrimidine (400 mg, 1.554 mmol) was suspended in ethanol (60 mL). $NaHCO_3$ (2.2 equiv, 3.418 mmol, 287 mg) and 10% Pd/C (80 mg) were added to the suspension. The reaction mixture was stirred in a steel autoclave at 70 °C and 100 bar hydrogen pressure for 24 h. Afterwards, the catalyst was removed by filtration over Celite. The solvent was removed in vacuum until dryness to obtain the beige, solid product. Yield 111.6 mg, 49.83%. $R_f = 0.82$ ($CHCl_3$/MeOH/aq. NH_3); ^{1}H NMR ([D$_6$]DMSO): $\delta = 8.58$ (s, 1H, H-6), 8.96 (s, 1H, H-2), 9.22 (s, 1H, H-4), 13.27 ppm (bs, 1H, NH); ^{13}C NMR ([D$_6$]DMSO): $\delta = 83.06$ (C-5), 114.53 (C-4a), 117.15 (CN), 137.27 (C-6), 148.81 (C-4), 150.85 (C-5), 152.86 ppm (C-2); elemental analysis calcd (%) for $C_7H_4N_4$: C 58.33, H 2.80, N 38.87; found C 52.90, H 3.31, N 34.56.

Screening reactions of natural and non-natural substrates: Screening reactions were run in UV star 96-well plates by using the following conditions and concentrations: nitrile reductase (45 μM, purity >85%) in buffer (100 mM Tris, 50 mM KCl, 1.15 mM TCEP, pH 7.5 adjusted with HCl conc.), substrate in DMSO (2 mM, 10% v/v DMSO), NADPH (0.25 mM in buffer), total volume 200 μL. Blank reactions contained buffer, substrate in DMSO (2 mM, 10% v/v DMSO) and NADPH (0.25 mM in buffer). Reactions were started by addition of NADPH (50 μL; 1.0 mM stock in buffer). NADPH depletion was monitored at 30 °C for 14 h. Subsequently, more NADPH (4 mM) was added to each well to allow full conversion. The screening reactions were incubated on a thermomixer for 24 h at 30 °C and 500 rpm. Samples were then analyzed with HPLC-MS to observe product formation. For all screening reactions, including blank reactions, multiple parallel determinations were obtained.

Determination of specific activities: Specific reductase activity was assayed spectrophotometrically by monitoring the oxidation of NADPH at 340 nm. Typically, rates of 0.01–0.10 $\Delta A\,min^{-1}$ were measured over a time period of 5 to 60 min. One unit of enzyme activity refers to 1 μmol of NADPH consumed per minute. All measurements were performed with a Beckman DU-800 spectrophotometer thermostated at 30 °C. The assay contained preQ$_0$ (100 μM) and NADPH (250 μM). PreQ$_0$ was dissolved in DMSO prior to dilution into buffer to give a final DMSO concentration of 1% (v/v). Unless otherwise stated, Tris/HCl buffer, pH 7.5 supplemented with KCl (50 mM) was used. Reactions were always started by the addition of cofactor. Measured rates were corrected for appropriate blank readings accounting for nonspecific decomposition of NADPH.

Steady-state enzyme kinetics: All experiments were carried out in Tris buffer (100 mM), pH 7.5, supplemented with KCl (50 mM) and, unless otherwise stated, at 30 °C. Measurements of the initial rates of substrate reduction were performed with a Beckman DU-800 by monitoring the consumption of NADPH over a time period of 5–10 min. Two equiv NADPH consumed account for one turnover. Initial rate data were measured under conditions in which substrate (or coenzyme) was held at a constant saturating concentration and the coenzyme (or substrate) was varied. Reaction mixtures contained wild-type nitrile reductase (0.7 μM) from *E. coli*. Blank readings accounting for the nonspecific decomposition of NADPH were <10% under these conditions and were neglected.

 © 2013 Wiley-VCH Verlag GmbH & Co. KGaA, Weinheim

The kinetic parameters were obtained from unweighted nonlinear least-square fits of experimental data to Equation (1) by using the program Sigmaplot 2004 (for Windows, version 9.0):

$$v = \frac{k_{cat} \cdot [E] \cdot [A]}{K_{MA} + [A]} \quad (1)$$

where v is the initial rate, [E] is the molar concentration of the enzyme dimer (71.8 kDa), [A] is the substrate or coenzyme concentration, k_{cat} is the turnover number, and K_{MA} is an apparent Michaelis–Menten constant.

The used enzyme concentration of 0.7 μM was in the range of >0.1-fold the obtained K_{MA} values for preQ$_0$ and NADPH. The concentration of the free substrate is, under these conditions, the substrate concentration in the reaction mixture reduced by the substrate that is bound to the enzyme.

We, therefore, calculated the K_{MA} values according to Equation (2):

$$v = \frac{k_{cat}}{2} \cdot ((K_M + [E] + [A]) - \sqrt{(K_M + [E] + [A])^2 - 4 \cdot [A] \cdot [E]}) \quad (2)$$

Unless otherwise stated, estimates of kinetic parameters had standard errors of <25%.

Acknowledgements

This work was supported by the Federal Ministry of Economy, Family and Youth (BMWFJ), the Federal Ministry of Traffic, Innovation and Technology (BMVIT), the Styrian Business Promotion Agency, SFG, the Standortagentur Tirol and ZIT-Technology Agency of the City of Vienna through the COMET-Funding Programme managed by the Austrian Research Promotion Agency FFG. The authors gratefully acknowledge Gerlinde Offenmüller, Margaretha Schiller, Hannelore Mandl and Thorsten Bachler for excellent technical support.

[1] S. G. Van Lanen, J. S. Reader, M. A. Swairjo, V. de Crecy-Lagard, B. Lee, D. Iwata-Reuyl, *Proc. Natl. Acad. Sci. USA* **2005**, *102*, 4264–4269.

[2] Y. Kim, M. Zhou, S. Moy, J. Morales, M. A. Cunningham, A. Joachimiak, *J. Mol. Biol.* **2010**, *404*, 127–137.

[3] M. A. Swairjo, R. R. Redy, B. Lee, S. G. Van Lanen, S. Brown, V. de Crecy-Lagard, D. Iwata-Reuyl, P. Schimmel, *Acta Crystallogr. Sect. F* **2005**, *61*, 945–948.

[4] V. M. Chikwana, B. Stec, B. W. K. Lee, V. de Crecy-Lagard, D. Iwata-Reuyl, A. Swairjo, *J. Biol. Chem.* **2012**, *287*, 30560–30570.

[5] B. W. K. Lee, S. G. Van Lanen, D. Iwata-Reuyl, *Biochemistry* **2007**, *46*, 12844–12854.

[6] a) B. M. Trost, I. Fleming, in *Comprehensive Organic Synthesis Vol. 8*, Pergamon, Oxford, **1991**, pp. 251–254; b) P. N. Rylander, in *Hydrogenation Methods*, Chapter 7, Academic Press, New York, **1985**; c) G. Cimino, M. Gavagnin, G. Sodano, A. Spinella, G. Strazzullo, F. J. Schmitz, G. Yalamanchili, *J. Org. Chem.* **1987**, *52*, 2301–2303; d) E. H. R. Walker, *Chem. Soc. Rev.* **1976**, *5*, 23–50; e) W. Huber, *J. Am. Chem. Soc.* **1944**, *66*, 876–879; f) A. Homer, H. R. Billica, *J. Am. Chem. Soc.* **1948**, *70*, 695–698; g) M. Somei, K. Kobayashi, K. Shimizu, T. Kawasaki, *Heterocycles* **1992**, *33*, 77–80; h) S. E. Klohr, J. M. Cassady, *Synth. Commun.* **1988**, *18*, 671–674; i) N. Yamazaki, W. Dokoshi, C. Kibayashi, *Org. Lett.* **2001**, *3*, 193–196; j) H. C. Brown, J. V. B. Kanth, P. V. Dalvi, M. Zaidlewicz, *J. Org. Chem.* **1999**, *64*, 6263–6274.

[7] Reviews: a) V. Mylerová, L. Martínkova, *Curr. Org. Chem.* **2003**, *7*, 1–17; b) L. Martínková, V. Kren, *Biocatal. Biotransform.* **2002**, *20*, 73–93; c) A. Banerjee, R. Sharma, U. C. Banerjee, *Appl. Microbiol. Biotechnol.* **2002**, *60*, 33–44; d) M. Kobayashi, S. Shimidzu, *Nat. Biotechnol.* **1998**, *16*, 733–736; e) L. Martínková, V. Kren, *Curr. Opin. Chem. Biol.* **2010**, *14*, 130–137; f) S. Prasad, T. C. Bhalla, *Biotechnol. Adv.* **2010**, *28*, 725–741; g) A. Yanenko, S. Osswald, in *Enzyme Catalysis in Organic Synthesis Vol. 2* (Eds.: K. Drautz, H. Gröger, O. May), Wiley-VCH, Weinheim **2012**, pp. 533–544; h) S. Osswald, A. Yanenko, in *Enzyme Catalysis in Organic Synthesis Vol. 2* (Eds.: K. Drautz, H. Gröger, O. May), Wiley-VCH, Weinheim **2012**, pp. 544–559; selected references: i) C. D. Mathew, T. Nagasawa, M. Kobayashi, H. Yamada, *Appl. Environ. Microbiol.* **1988**, *54*, 1030–1032; j) M. Winkler, A. C. Knall, M. R. Kulterer, N. Klempier, *J. Org. Chem.* **2007**, *72*, 7423–7426; k) M. Winkler, D. Meischler, N. Klempier, *Adv. Synth. Catal.* **2007**, *349*, 1475–1480; l) B. C. M. Fernandez, C. Mateo, C. Kiziak, A. Chmura, J. Wacker, F. van Rantwijk, A. Stolz, R. A. Sheldon, *Adv. Synth. Catal.* **2006**, *348*, 2597–2603; m) M. Winkler, L. Martínková, A. C. Knall, S. Krahulec, N. Klempier, *Tetrahedron* **2005**, *61*, 4249–4260; n) L. Martínková, N. Klempier, M. Preiml, M. Ovesná, M. Kuzma, V. Mylerová, V. Kren, *Can. J. Chem.* **2002**, *80*, 724–727.

[8] Reviews: a) M. Dadashipour, Y. Asano, *ACS Catalysis* **2011**, *1*, 1121–1149; b) M. Avi, H. Griengl, in *Organic Synthesis with Enzymes in Non-aqueous Media* (Eds.: G. Carrea, S. Riva), Wiley-VCH, Weinheim, **2008**, pp. 211–226; c) F. Effenberger, *Angew. Chem.* **1994**, *106*, 1609–1619; *Angew. Chem. Int. Ed. Engl.* **1994**, *33*, 1555–1564; d) J. Holt, U. Hanefeld, *Curr. Org. Synth.* **2009**, *6*, 15–37; e) V. Gotor, *Org. Process Res. Dev.* **2002**, *6*, 420–426; f) M. Gruber-Khadjawi, M. H. Fechter, H. Griengl, in *Enzyme Catalysis in Organic Synthesis Vol.2* (Eds.: K. Drautz, H. Gröger, O. May), Wiley-VCH, Weinheim **2012**, pp. 947–990; g) F. L. Cabirol, A. E. C. Lim, U. Hanefeld, R. A. Sheldon, *Org. Process Res. Dev.* **2010**, *14*, 114–118; selected references: h) O. Sosedov, K. Matzer, S. Buerger, C. Kiziak, S. Baum, J. Altenbuchner, A. Chmura, F. van Rantwijk, A. Stolz, *Adv. Synth. Catal.* **2009**, *351*, 1531–1538; i) J. von Langermann, A. Mell, E. Paetzold, T. Draußmann, U. Kragl, *Adv. Synth. Catal.* **2007**, *349*, 1418–1424; j) S. Rustler, H. Motejadded, J. Altenbuchner, A. Stolz, *Appl. Genet. Mol. Biotech.* **2008**, *80*, 87–97; k) S. Nanda, Y. Kato, Y. Asano, *Tetrahedron* **2005**, *61*, 10908–10919; l) H. Griengl, N. Klempier, P. Pöchlauer, M. Schmidt, N. Shi, A. Zabelinskaja-Mackova, *Tetrahedron* **1998**, *54*, 14477–14486; m) N. Klempier, U. Pichler, H. Griengl, *Tetrahedron: Asymmetry* **1995**, *6*, 845–848; n) F. Effenberger, S. Heid, *Tetrahedron: Asymmetry* **1995**, *6*, 2945–2952.

[9] B. Wilding, M. Winkler, B. Petschacher, R. Kratzer, A. Glieder, N. Klempier, *Adv. Synth. Catal.* **2012**, *354*, 2191–2198.

[10] Pyrrolopyrimidine numbering, as depicted in Figure 2, is used throughout this study; in this case this corresponds to positions 9 and 3 in (7-deaza)purine numbering.

[11] a) E. Krieger, T. Darden, S. B. Nabuurs, A. Finkelstein, G. Vriend, *Proteins* **2004**, *57*, 678–683; b) E. Krieger, G. Koraimann, G. Vriend, *Proteins* **2002**, *47*, 393–402.

[12] Y. Duan, C. Wu, S. Chowdhury, M. C. Lee, G. Xiong, W. Zhang, R. Yang, P. Cieplak, R. Luo, T. Lee, J. Caldwell, J. Wang, P. Kollman, *J. Comput. Chem.* **2003**, *24*, 1999–2012.

[13] a) R. A. Friesner, R. B. Murphy, M. P. Repasky, L. L. Frye, J. R. Greenwood, T. A. Halgren, P. C. Sanschagrin, D. T. Mainz, *J. Med. Chem.* **2006**, *49*, 6177–6196; b) L. L. C. Schrödinger, Glide version 5.8, New York, **2012**.

[14] L. L. C. Schrödinger, Maestro version 9.3, New York, **2012**.

[15] L. L. C. Schrödinger, Jaguar version 7.9, New York, **2012**.

[16] L. L. C. Schrödinger, The PyMOL Molecular Graphics System, version 1.41, New York, **2012**.

[17] G. Steinkellner, R. Rader, G. G. Thallinger, C. Kratzky, K. Gruber, *BMC Biochem.* **2009**, *10*, 32.

[18] H. Liu, J. H. Naismith, *Protein Expr. Purif.* **2009**, *63*, 102–111.

Received: January 16, 2013
Published online: April 17, 2013

 © 2013 Wiley-VCH Verlag GmbH & Co. KGaA, Weinheim

DOI: 10.1002/adsc.201200109

Nitrile Reductase from *Geobacillus kaustophilus*: A Potential Catalyst for a New Nitrile Biotransformation Reaction

Birgit Wilding,[a] Margit Winkler,[b] Barbara Petschacher,[b] Regina Kratzer,[c] Anton Glieder,[b] and Norbert Klempier[a,*]

[a] ACIB GmbH, c/o Institute of Organic Chemistry, Graz University of Technology, Stremayrgasse 9, 8010 Graz, Austria
Fax: (+43)-316-873-32402; e-mail: klempier@tugraz.at
[b] ACIB GmbH, c/o Institute of Molecular Biotechnology, Graz University of Technology, Petersgasse 14, 8010 Graz, Austria
[c] Institute of Biotechnology and Biochemical Engineering, Graz University of Technology, Petersgasse 12, 8010 Graz, Austria

Received: February 9, 2012; Revised: May 7, 2012; Published online: July 29, 2012

Supporting information for this article is available on the WWW under http://dx.doi.org/10.1002/adsc.201200109.

Abstract: The cloning, expression and characterization of a nitrile reductase (NRed) from the thermophile *Geobacillus kaustophilus* is reported. The enzyme shows a 12-fold increase in activity in response to a temperature change from 25 °C to 65 °C. The substrate scope regarding its biocatalytic applicability was investigated by testing a range of common nitriles. The narrow substrate range observed for the wild-type enzyme prompted the rational design of *Gk*NRed active site mutants based on a previously published homology model from *Bacillus subtilis*. The activities of the mutants and the wild-type enzyme were investigated in their structure-function relationship regarding the natural substrate 7-cyano-7-deazaguanine ($preQ_0$) as well as a range of synthesized $preQ_0$-like substrate structures. A distinct dependence of the wild-type enzyme activity on specific structural modifications of the natural substrate was observed. Two non-natural nitriles derived from $preQ_0$ could be reduced to their corresponding amino compounds.

Keywords: active site mutants; amines; 7-cyano-7-deazaguanine reductase; enzyme catalysis; *Geobacillus kaustophilus*; nitrile reductase; nitriles; thermostability

Introduction

Recently, a novel enzymatic activity has been reported as part of the biosynthetic pathway to the modified nucleosides queuosine Q and archaeosine G^+. The nucleosides share an unusual 7-deazaguanine core structure and are among the most complex modified nucleosides in tRNA. They are ubiquitous in prokaryotes and eukaryotes (Q) and archaea (G^+). The new protein 7-cyano-7-deazaguanine reductase QueF involved in the nitrile metabolism catalyzes the NADPH-dependent reduction of the nitrile group to its corresponding amine and is so far the only enzyme known to be capable of reducing a nitrile group to the primary amine (Scheme 1). The genes from *B. subtilis* (*Bacillus subtilis*) and *E. coli* (*Escherichia coli*) were recently cloned and the recombinant enzymes were characterized.[1]

There are two related sequence subfamilies of QueF enzymes known: type I single domain enzymes (YkvM subfamily) found in *B. subtilis* and type II two domain proteins (YqcD subfamily) found in *E. coli*. Both proteins show sequence similarity to the family of GTP cyclohydrolases I.[1] Recently, a high resolution crystal structure together with molecular simulation studies of the NRed from *Vibrio cholerae* (a type II subfamily enzyme) was published providing further insight into the catalytic mechanism.[2]

Chemical nitrile reduction generally involves expensive or dangerous chemicals, such as $LiAlH_4$,

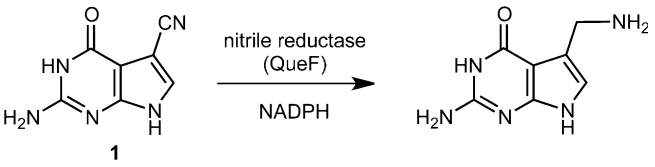

Scheme 1. Reduction of 7-cyano-7-deazaguanine ($preQ_0$) to 7-aminomethyl-7-deazaguanine ($preQ_1$) depicted as substep from the biosynthetic pathway of queuosine.

 © 2012 Wiley-VCH Verlag GmbH & Co. KGaA, Weinheim

borane or molecular hydrogen under high pressure in presence of Pt, Pd, Ru or Raney-Ni catalysts.[3]

Hence, a nitrile reductase would be a valuable contribution to the currently available biocatalytic tools of nitrile transforming enzymes (i.e., oxynitrilases,[4] nitrilases and nitrile hydratases[5]).

Recently, the isolation of an old yellow enzyme (OYE) from the thermophile *G. kaustophilus* (*Geobacillus kaustophilus*) has been reported.[6] This prompted us to search for nitrile reductase activity in this organism with all the benefits in enzyme isolation and purification of a thermostable enzyme.

Here we wish to report the cloning, expression and characterization of the first nitrile reductase from thermophilic origin. The enzyme from *G. kaustophilus* belongs to the type I enzyme subfamily and showed an 82% sequence homology with *Bs*NRed (*B. subtilis* nitrile reductase). The substrate scope of *Gk*NRed (*Geobacillus kaustophilus* nitrile reductase) was investigated regarding its biocatalytic applicability by testing a range of common nitriles. These investigations were supported by the rational design of *Gk*NRed active site mutants based on a previously published homology model from *B. subtilis*. Compounds structurally derived from the natural substrate $preQ_o$ were synthesized and tested with wild-type enzyme and mutants.

Results and Discussion

Cloning and Expression

The WTNRed (wild-type) and six NRed mutants from *G. kaustophilus* were cloned, heterologously expressed in *E. coli* and purified to homogeneity as described in the Experimental Section. The thus prepared protein was used throughout the characterization studies, whereas for bioreduction reactions, a less tedious purification by thermoprecipitation was found to be sufficient.

Enzyme Characterization

Specific reductase activities of *Gk*NRedWT and mutants were assayed spectrophotometrically by monitoring the depletion of NADPH and by an HPLC-based activity measurement method using the natural substrate $preQ_0$. The same methods were applied for all screenings with non-natural substrates (see Experimental Section).

The overall behaviour of the new *Gk*NRed in terms of optimum pH and pH stability does not differ significantly from that of *B. subtilis* NRed, thus exhibiting a bell-shaped pH profile within a range of pH 5.5 to 10 with maximal activity at 7.5 (see the Supporting Information, Figure S4). The enzymatic activity increased 12-fold in response to a change in temperature from 25 to 65 °C. Half life times of 43 h and 15 h were determined at 55 °C, the latter with tris(2-carboxyethyl)phosphine hydrochloride (TCEP) (Supporting Information, Figure S5).

The apparent kinetic parameters of *Gk*NRedWT of $preQ_0$ reduction are given in Table S1 (Supporting Information). Thus the K_m values of *Gk*NRed for $preQ_0$ and NADPH are 11 μM and 34 μM, respectively. The K_{mNADPH} is comparable to a value of 19 μM found in the literature for *Bs*NRed. The corresponding *Bs*NRed K_{mpreQ_0} value is 0.24 μM and therefore 46-fold smaller as that determined for *Gk*NRed. For *Gk*NRred a turnover number of 3.9 min^{-1} was obtained, a 5.5-fold increase as compared to published data for *Bs*NRed.[1b] The increased k_{cat} and higher K_{mpreQ_0} values of *Gk*NRred are ascribed to the 25 °C higher temperature in initial rate measurements. *Gk*NRed activities were determined spectrophotometrically by monitoring NADPH depletion at 55 °C (a 2:1 stoichiometry of NADPH:$preQ_0$ is required in a 4-electron reduction). The k_{cat} was calculated according to the previous assumption that the minimal biological unit is a dimer of 38.8 kDa.[1a,8]

Screening of *Gk*NRedWT

An initial substrate screening of different aliphatic, aromatic and heterocyclic nitriles (for structures see Figure S1 in the Supporting Information) with wild-type QueF from *Geobacillus kaustophilus* as well as the previously reported *Escherichia coli* and *Bacillus subtilis* QueF has revealed that these enzymes are highly specific for their natural substrate 7-cyano-7-deazaguanosine (**1**, Scheme 1).[7]

In a recent publication a three-dimensional homology model of the *B. subtilis* QueF active site has been presented based on sequence alignment with the structure of GTP cyclohydrolase I from *E. coli*,[8] however, a crystal structure is not yet available. The active site model shows a conserved Glu and an invariant Cys residue shared between QueF and GTP-CH I. The Cys residue is considered as relevant for the covalent catalytic mechanism postulated. Other residues presumably important for binding were identified as Glu97 and His96, both involved in hydrogen bonding to the 6-oxo and 2-amino substituents of 7-cyano-7-deazaguanine ($preQ_0$).[8]

With this model at hand, we made a sequence comparison of *B. subtilis* and *G. kaustophilus* QueF, (both type I enzymes) by using ClustalW2 multiple sequence alignment, which revealed an 82% sequence identity between the enzymes. These facts have suggested the design and expression of several active site mutants of *G. kaustophilus* QueF (Table 1).

 © 2012 Wiley-VCH Verlag GmbH & Co. KGaA, Weinheim

Table 1. Screening results of wild-type and mutant QueF from *Geobacillus kaustophilus*.

G. kaustophilus	**1**	**2**[a]	**3**[b]	**4–9**
wild-type	+++	++	+	–
His96Ala	++	++	+	–
His96Phe	++	++	+	–
Glu97Ala	++	++	+	–
Glu97Ser	++	++	+	–
Phe95Ala	++	++	+	–
Cys55Ala	–			

[a] Activities observed were in an equal range of magnitude to those of the natural substrate **1**.
[b] Activities observed were significantly lower compared to substrates **1** and **2**.

We chose the initial replacement of Phe95, His96 and Glu97 by Ala with the intention to broaden the enzyme's substrate specificity by reducing strong polar residues in the putative binding site. The Cys55Ala mutation was intended to verify the Cys55 residue to be essential for covalent catalysis as described for *B. subtilis* QueF.[1b]

The subsequent screening of all nitriles depicted in Figure S1 (Supporting Information) has revealed that all QueF mutants tested were active with respect to the natural substrate **1**. To our disappointment, however, no reaction could be detected with any of the remaining non-natural substrates.

This prompted us to address the problem from a substrate-based approach as well. Thus, we synthesized compounds structurally closely related to the parent natural substrate preQ$_0$ (**1**) to systematically study the impact of these structural changes on binding and catalytic activity. The analogues are depicted in Figure 1.

The structural changes in analogues **2** and **3** were made regarding their purine ring substituents, in particular the the 2-amino (**2**) and 6-oxo (**3**) functionality,[9] both substituents assumedly essential for binding to the Glu97 and His96 residues. The 6-oxo group in compound **4** was replaced by an amino group and the pyrimidine ring in compound **5** was replaced by benzene. Compound **6**, devoid of the pyrimidine ring, is supposed to represent the pyrrole part of the bicyclic structure. Nitriles **7** and **8** are analogues bearing the presumably essential substituents of the pyrimidine ring in identical positions in a phenyl ring, but carry the nitrile group in an open chain fragment of comparable distance to the parent structure **1**. Analogue **9** is identically substituted to the natural substrate but has no pyrrole ring.

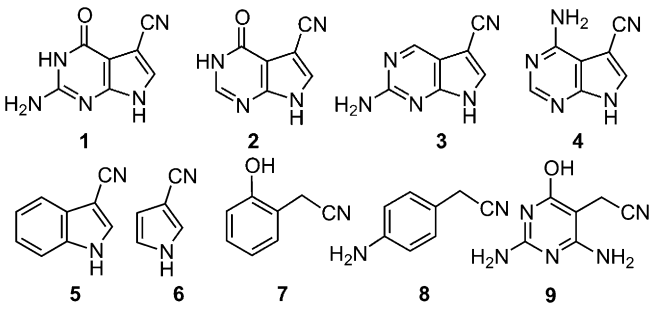

Figure 1. Substrate analogues for wild-type and mutant *Gk*NRed characterization studies.

The syntheses of compounds **1**, **2**, **4**, **6, 7** and **9** have been described, modifications made by us to previously published procedures are given in the Experimental Section. Compound **3** has not yet been reported in the literature. All experimental and spectroscopic data are given in the Experimental Section. The ^{13}C NMR data for some of the literature known compounds have not been published so far; these data are therefore included in the Experimental Section together with their corresponding spectra in the Supporting Information.

Investigation of the Substrate Scope

The results given in Table 1 suggest the indispensable presence of an appropriately substituted pyrimidine ring for binding. An estimate of the activities of compounds **2** and **3**, differing from the natural substrate only in one functional group suggests that the impact of the 6-oxo functionality seems to be more important than that of the 2-amino group (Table 1) since the conversion of nitrile **3** was significantly lower. This can also be deduced from comparison of the respective K_m and k_{cat} values. While k_{cat} (for compound **2**) is in an equal range of magnitude compared to the natural substrate **1**, the active site binding is diminished, as indicated by the K_m value (Table S1 in the Supporting Information). Interestingly, replacement of the 6-oxo functionality by an amino group (nitrile **4**) resulted in a complete loss of activity. In addition to that, the reduction of preQ$_0$ by *Gk*NRed was not inhibited by **4** (Table S2 in the Supporting Information) further suggesting the 6-oxo group as essential anchor for substrate binding. The phenyl-replaced nitriles **7** and **8** – both have the oxo or amino group placed in equivalent ring positions compared to the pyrimidine ring in the natural substrate **1** – are not accepted as substrates, neither is analogue **9**, though this compound has exactly the substitution pattern of the natural substrate. These facts indicate that the ring nitrogen atoms of the pyrimidine and pyrrole rings are probably necessary for active site binding. Interestingly, compound **8** showed strong inhibition on preQ$_0$ reduction, while compound **7** did not inhibit it (Supporting Information, Table S2). Nitrile **6** representing the pyrrole ring fragment of the parent deazapurine as

 © 2012 Wiley-VCH Verlag GmbH & Co. KGaA, Weinheim

well as indole-3-carbonitrile **5** with the complete bicyclic system but devoid of both substituents and pyrimidine ring nitrogens are neither accepted as substrates nor do they act as inhibitors. A range of additional nitriles (see Figure S2 in the Supporting Information) was screened with the mutants but they were not accepted as substrates.

Conclusions

The cloning, expression and characterization of an NRed from *G. kaustophilus* – the first nitrile reductase from a thermophile – was accomplished. The substrate scope regarding its biocatalytic applicability was investigated by testing a range of common nitriles. The narrow substrate tolerance observed for the wild-type enzyme prompted the rational design of active site mutants based on a previously published homology model from *B. subtilis*.

The activities of the mutants and the wild-type enzyme were investigated in their structure-function relationship regarding a range of synthesized substrates, which were structurally closely related to $preQ_0$. A distinct dependence of specific structural elements on catalytic activity of *Gk*NRedWT and mutants could be observed, in particular the presence of the 6-oxo group in the pyrimidine ring was recognized to be essential for a reduction reaction just as any fragmentation of the parent deazapurine ring resulted in complete loss of catalytic activity (compounds **6** and **9**). Two non-natural nitriles (**2** and **3**) differing in their substitution pattern of the pyrimidine ring could be reduced to the corresponding amino compounds.

Studies are in progress to elucidate the role of the individual ring nitrogen atoms, in particular of position N-9 (purine numbering), since the homology model is suggesting a possible binding interaction. However, to draw a clear picture of the *Gk*Nred active site an exact crystal structure of the enzyme is needed. Consequently, work is in progress in this direction.

Given the generally low (water) solubility of all substrates with the 7-deazapurine core structure, an enhanced thermostabilty of the enzyme can be very useful. Apart from this specific solubility behaviour of this compound class, the possibility of running a biocatalytic reaction at elevated temperature is often beneficial in terms of higher k_{cat} values.[10]

The present work has demonstrated a straightforward preparation of a nitrile reductase capable of reducing nitriles closely related to the natural substrate as well as first insights into the demands regarding the structural properties of possible substrates. Nevertheless, further investigations including different approaches in catalyst design will be necessary to generate a more broadly applicable biocatalyst.

Experimental Section

Chemicals, Strains and General Procedures

NADPH (sodium salt; $\geq$ 97% pure) was obtained from Roth (Karlsruhe, Germany). All other chemicals were purchased from Sigma–Aldrich/Fluka (Gillingham, Dorset, U.K.) or Roth (Karlsruhe, Germany), and were of the highest purity available. The microorganism used was *E. coli* BL21 (DE3).

Reagents and starting materials used for substrate synthesis were obtained from commercial suppliers, and used without further purification. Substrates **5** and **8** were obtained from Sigma–Aldrich in the highest purity available. Syntheses of substrates **6**[11] and **7**,[12] as well as other substrates screened, and their precursors,[13] were done according to literature procedures and can be found in the Supporting Information. Thin layer chromatography was carried out with precoated aluminium silica gel 60 F_{254} plates, column chromatography with Merck Silica Gel 60 (0.040–0.063 mm). ^{1}H NMR and ^{13}C NMR spectra were recorded on a Bruker AVANCE III with autosampler (^{1}H NMR 300.36 MHz, ^{13}C NMR 75.53 MHz). Chemical shifts for ^{1}H NMR are reported in ppm relative to Me_4Si as internal standard. Screening reactions were run on an Eppendorf comfort thermomixer. Absorption measurements were done on a Fluostar plate reader from BMG lab tech at 340 nm and HPLC-MS analysis on an Agilent 1200 series using a phenomenex Gemini-NX 3 C18 110 A (150 × 2.0 mm) column and 20 mM ammonium acetate in water and acetonitrile as eluents.

Preparation of Wild-Type and Mutant NRed for Screening Reactions

Strains, vectors and growth conditions: *Geobacillus kaustophilus* HTA426 was grown on LB agar medium. The pEamTA vector[14] was used for recombinant expression. *E. coli* K12 Top10F' (Invitrogen, Carlsbad, CA, USA) was used to amplify and maintain engineered constructs and *E. coli* BL21 (DE3) (Invitrogen, Carlsbad, CA, USA) for protein expression. LB medium and LB agar supplemented with ampicillin when appropriate (100 mg L^{-1}) was used for cell cultivation.

Vector construction and preparation of mutants: The *Geobacillus kaustophilus* nitrile reductase (*Gk*NRed) was amplified from genomic *G. kaustophilus* DNA employing the primers *Gk*Nred TA f: 5′-*atg g*ca gga aga aaa g-3′; *Gk*Nred TA r: 5′-*gaa ttc cta* gcg gtt gtc gac-3′ and Phusion DNA polymerase (Finnzymes, Espoo, Finland) according to the manufacturer's protocol. All oligonucleotides used were manufactured by Integrated DNA Technologies, San Jose, CA, USA. The amplified PCR product was purified using a preparative gel. The DNA fragment was recovered from the gel using the QIAquick® Gel Extraction Kit (Qiagen, Hilden, Germany). The fragment (31 μL) was A-tailed by incubation with 5 μL of dNTPs (2 mM, each), 8 μL of magnesium chloride (25 mM), 5 μL of *Taq* buffer and 1 μL *of Taq* Polymerase (5 U μL^{-1}, Fermentas, Burlington, Canada) at 72 °C for 30 min. Subsequent purification with the QIAquick® PCR Purification Kit (Qiagen, Hilden, Germany) yielded the A-tailed insert in approx. 5 ng mL^{-1} concentration. The linear pEamTA vector was prepared by digestion

 © 2012 Wiley-VCH Verlag GmbH & Co. KGaA, Weinheim

of 44 μL of plasmid DNA (isolated with the http://www.fermentas.com/en/products/all/nucleic-acid-purification/kits/k050-genejet-plasmid-miniprep from Fermentas, Burlington, Canada) supplemented with 5 μL Eam1105I buffer (10X) and 1 μL of Eam1105I (Fermentas) at 37 °C for 4 h. The DNA fragment was recovered from the gel using the QIAquick® Gel Extraction Kit (Qiagen) yielded the linear vector in approx. 40 ng mL^{-1} concentration. The insert (110 ng, 22 μL) was ligated with the vector (80 ng, 2 μL) in an overnight reaction at 16 °C using 3 μL T4 DNA ligase buffer and 3 μL T4 ligase (Promega, Madison, WI, USA). After heat inactivation (65 °C, 20 min) and desalting on ultradialysis membranes (Millipore, 0.025 μm), the entire ligation mixtures were transformed into 180 μL of electrocompetent *E. coli* K12 Top10F' cells (Invitrogen) and selected on LB-ampicillin agar plates. Colonies with correctly integrated inserts were confirmed by digestions of plasmid DNA (isolated with the http://www.fermentas.com/en/products/all/nucleic-acid-purification/kits/k050-genejet-plasmid-miniprep from Fermentas) with *Nde*I and *Hind*III fast digest restriction enzymes (Fermentas) and verified by sequencing (LCG Genomics, Berlin, Germany) using the primers pEam f1 (5′-ttgtgagcggataacaatttc-3′) or pEam r1 (5′-tactgccgccaggcaaattct-3′). Retransformation of 1 μL of plasmid into chemically competent *E. coli* BL21 (DE3) (Invitrogen) resulted in the *Gk*NRedWT expression strain.

Site specific mutagenesis: pEamTA *Gk*NRedWT, was employed as the template for a two stage mutagenesis reaction protocol. Briefly, 5 μL of *PfuUltra* HF reaction buffer (10X), the template (1 μL, 10 ng), 1 μL dNTP mix (10 mM), 1 μL of forward OR reverse primer (5 mM) and 1 μL of *PfuUltra* High Fidelity DNA polymerase (2.5 U μL^{-1} from Stratagene (La Jolla, CA, USA) were added to 41 μL of doubly distilled water (Fresenius, Graz, Austria). The two-stage PCR was conducted on a Gene Amp System 2400 thermo cycler (Applied Biosystems, Foster City, CA) under the following conditions: 95 °C for 1 min, 4 cycles of 50 s at 95 °C, 50 s at 60 °C and 5 min at 68 °C and then 7 min at 68 °C for the final elongation step. After these initial 4 cycles of primer extension, 25 μL of the reaction containing the forward primer were combined with 25 μL of the reaction containing the reverse primer. Additional 18 cycles were run under the above conditions. Subsequently, dpnI (1 μL, Fermentas) was added to digest the template at 37 °C for 1 h. 2 μL of the mixture were transformed into 60 μL of electrocompetent *E. coli* K12 Top10F' cells (Invitrogen) and selected on LB-ampicillin agar plates. The mutations were confirmed by sequencing (LCG Genomics). Plasmids from mutants having the correct sequence were replicated and transformed into *E. coli* BL21 (DE3). PAGE purified primers used for site specific mutagenesis: *Gk*NRedC55Af 5′-c cgg agt tta cga cgt tgg **cgc** caa aaa ccg gac aac cg-3′; *Gk*NRedC55Ar 5′-cgg ttg tcc ggt ttt tgg **cgc** caa cgt cgt aaa ctc cgg-3' *Gk*NRedF95Af 5′-c ttc cgc aat cat ggc gac **gcg** cac gaa gac tgc gtc aac a-3′; *Gk*NRedF95Ar 5′-t gtt gac gca gtc ttc gtg **cgc** gtc gcc atg att gcg gaa g-3′; *Gk*NRedH96Af 5′-gc ttc cgc aat cat ggc gac ttt **gc**c gaa gac tgc gt-3′; *Gk*NRedH96Ar 5′-ac gca gtc ttc g**gc** aaa gtc gcc atg att gcg gaa gc-3′; *Gk*NRedH96Ff 5′-gc ttc cgc aat cat ggc gac ttt **tt**c gaa gac tgc gt-3′; *Gk*NRedH96Fr 5′-ac gca gtc ttc g**aa** aaa gtc gcc atg att gcg gaa gc-3′; *Gk*NRedE97Af 5′-cat ggc gac ttt cac g**c**a gac tgc gtc aac atc-3′; *Gk*NRedE97Ar 5′-gat gtt gac gca gtc t**g**c gtg aaa gtc gcc atg-3′; *Gk*NRedE97Sf 5′-gc aat cat ggc gac ttt cac **tc**a gac tgc gtc aac atc att a-3′; *Gk*NRedE97Sr 5′-t aat gat gtt gac gca gtc t**ga** gtg aaa gtc gcc atg att gc-3′.

Protein expression and purification: The wild-type *Gk*NRedWT and the mutants were cultivated as follows: overnight cultures (20 mL LB/Amp, inoculated with a single colony and grown at 37 °C in an orbital shaker) were used to inoculate 500 mL LB/Amp medium in 2-L baffled Erlenmayer flasks. These main cultures were grown at 37 °C and 130 rpm to an OD of 0.7, induced with 0.5 mL of IPTG (1 M) and incubated for 24 h at 16 °C and 130 rpm. The cells were harvested by centrifugation (4,000 rpm, 4 °C, 10 min). The pellet was resuspended in reaction buffer [12.1 $g L^{-1}$ Tris, 3.73 $g L^{-1}$ KCl, 287 $mg L^{-1}$ tris(2-carboxyethyl)phosphine hydrochloride (TCEP); pH 7.5 adjusted with HCl 37%] and disrupted by ultrasonication. The cell debris was removed by ultracentrifugation at 40,000 rpm for 45 min at 4 °C. The supernatant (crude lysate) was purified by heat precipitation of host proteins at 70 °C for 10 min and then applied to a centrifugation step (4,000 rpm, 4 °C, 10 min). The supernatant contained fairly pure nitrile reductases and was stored at −20 °C.

Enzyme Characterization and Determination of Kinetic Parameters

Cultivation: *E. coli* BL21 *Gk*NR was grown in 1000-mL baffled shaken flasks containing 200 mL of LB media supplemented with 115 mg/L ampicillin. Flasks were shaken at 120 rpm and 37 °C in a Certomat® BS-1 incubator from Sartorius. Recombinant protein production used a standard procedure in which cultures were cooled to 25 °C when an optical density of 0.6 (±10%) was reached. Isopropylthio-β-D-galactoside (IPTG) was added in a concentration of 1.0 mM, and the cultivation time after induction was 18 h. Cells were harvested by centrifugation, washed with physiological NaCl solution, re-centrifuged and diluted into 100 mM Tris buffer, pH 7.5, supplemented with 50 mM KCl and 1 mM TCEP. Cells were disrupted by two passages through a French press (American Instrument Company, Silver Springs, Maryland, USA) operated at an internal cell pressure of 25,000 psi. The crude cell extract obtained was clarified by centrifugation (16,000 *g*, 45 min, 4 °C) prior to enzyme purification.

Enzyme purification: *E. coli* protein was separated from the cell-free extract by incubation at 75 °C for 10 min, thermo-precipitated protein was centrifuged (16,000 *g*, 10 min).

Recombinant enzyme was further purified by ion exchange chromatography using a QFF from GE Healthcare (bed volume 55 mL). The column was equilibrated with 100 mM Tris buffer, 50 mM KCl, pH 7.5. Adsorbed protein was eluted at a flow rate of 4 $mL min^{-1}$ with a step gradient of 0.1 M and 1 M KCl. Fractions of 5 mL were collected and the 0.1 M KCl peak containing most of the *Gk*NR, as judged by activity measurements and SDS-PAGE, was pooled. The pooled fractions were concentrated in Vivaspin 20-mL Concentrator tubes with 10,000 molecular weight cut off to a volume of less than 0.5 mL and re-diluted into 100 mM Tris, 50 mM KCl and 1 mM TCEP.

Reductase activity measurement: Specific reductase activity was assayed spectrophotometrically by monitoring the

 © 2012 Wiley-VCH Verlag GmbH & Co. KGaA, Weinheim

reduction of NADPH at 340 nm. Typically, rates of 0.05–0.10 ΔA/min were measured over a time period of 5 min. One unit of enzyme activity refers to 1 μmol of NADPH consumed per minute. All measurements were performed with a Beckman DU-800 spectrophotometer thermostated at 55 °C. The assay contained 100 μM $preQ_0$ and 250 μM NADPH. $preQ_0$ was dissolved in DMSO prior to dilution into buffer to give a final DMSO concentration of 1% (v/v). Unless otherwise stated, Tris/HCl buffer, pH 7.5 supplemented with 50 mM KCl was used. Reactions were always started by the addition of coenzyme. Activity measurements for pH studies were performed in either 100 mM Tris buffer (pH values 5.5; 6,0; 6.5; 7.0) or Bis-Tris buffer (pH values 7.0; 7.5; 8.0; 8.5; 9.0; 10.0) supplemented with 100 mM KCl. Measured rates were corrected for appropriate blank readings accounting for non-specific decomposition of NADPH.

Enzyme stability: Purified enzyme was diluted to 11 mg mL^{-1} in 100 mM Tris buffer, pH 7.5, containing 100 mM KCl with or without 1 mM TCEP [tris(2-carboxyethyl)phosphine]. Experiments were carried out in Eppendorf tubes incubated at 55 °C and 500 rpm in a Thermomixer comfort from Eppendorf. Samples were withdrawn every hour and specific activities were determined as described above.

Steady-state enzyme kinetics: All experiments were carried out in 100 mM Tris buffer, pH 7.5, supplemented with 50 mM KCl, and, unless otherwise stated, at 55 °C. Measurements of the initial rates of substrate reduction were performed with a Beckman DU-800 monitoring the consumption of NADPH over a time period of 5 min. Initial rate data were measured under conditions where substrate (or coenzyme) was held at a constant saturating concentration and the coenzyme (or substrate) was varied in the range $0.4 < K_m < 4$- to 10-fold. Typical reaction mixtures contained 80 μM *Gk*NRed wild-type. Kinetic parameters were obtained from unweighted non-linear least-square fits of experimental data to Eq. (1) using the program Sigmaplot 2004 (for Windows, version 9.0). In Eq. (1),
v is the initial rate, [E] is the molar concentration of the enzyme subunit (38.8 kDa), [A] is the substrate or coenzyme concentration, k_{cat} is the turnover number (min^{-1}) and $K_{m\,A}$ is an apparent Michaelis–Menten constant. Two NADPH

$$v = k_{cat}[E][A]/(K_{m\,A} + [A]) \quad (1)$$

consumed account for one turnover. All rates were corrected for the appropriate blank readings accounting for the non-specific decomposition of NADPH. Unless otherwise stated, estimates of kinetic parameters had standard errors of $< 20\%$.

Substrate Screening

Photometric assays for substrate screening were carried out as described for $preQ_0$. Activities were normalized to $preQ_0$ reductase activity. Assays for inhibitor screening contained 10 μM $preQ_0$ and the compounds listed in the Supporting Information, Table S2. Residual activities refer to reductase activities obtained with 10 μM $preQ_0$. Measured rates were corrected for appropriate blank readings accounting for non-specific decomposition of NADPH.

Substrate Synthesis

2-Chloro-3-oxopropanenitrile: NaH (1.0 g, 50% in mineral oil) was washed twice with cyclohexane and once with THF and was then suspended in 20 mL THF. The suspension was cooled to 0 °C and methyl formate (0.90 mL, 14 mmol) was added. Chloroacetonitrile (0.83 mL, 13 mmol) was added dropwise to the stirred solution and the solution was stirred for additional 3.5 h. Afterwards, 20 mL deionized water were added and the mixture was extracted twice with ethyl acetate. The layers were separated and the pH value of the aqueous layer was adjusted to pH 4 with 5 M HCl. The aqueous layer was then extracted three times with diethyl ether. The combined organic phases from the second extraction were dried over Na_2SO_4 and concentrated under reduced pressure to afford a brown oil which was used for the next synthetic step without further purification; yield: 1.142 g (85%).

2-Amino-5-cyano-7H-pyrrolo[2,3-d]pyrimidin-4-one (preQ$_0$, 1):[15] Sodium acetate trihydrate (2.693 g, 19.79 mmol) was dissolved in 40 mL deionized water and 4-diamino-6-hydroxypyrimidine (1.225 g, 9.32 mmol) was added. The suspension was heated to reflux. 2-Chloro-3-oxopropanenitrile (1.142 g, 11.03 mmol) was dissolved in 20 mL deionized water and added dropwise to the reaction mixture. The reaction mixture was stirred at reflux overnight. On cooling to room temperature the beige product precipitated from the solution. The product was filtered off, washed with copious amounts of water and acetone. After drying, the product was obtained; yield: 840 mg (51%). ^{1}H NMR (DMSO-d_6): $\delta = 6.39$ (s, 2H, NH_2), 7.62 (s, 1H, H-6), 10.72 (s, 1H, NH-7), 11.99 (s, 1H, H-3); ^{13}C NMR (DMSO-d_6): $\delta = 85.53$ (C-5), 98.73 (C-4a), 115.87 (CN), 127.77 (C-6), 151.66 (C-7a), 153.72 (C-2), 157.56 (C-4).

4-Amino-5-cyano-7H-pyrrolo[2,3-d]pyrimidine (4): 4-Amino-5-cyano-7*H*-pyrrolo[2,3-*d*]pyrimidine was prepared analogous to a literature procedure.[16] 4-Amino-6-bromo-5-cyano-7*H*-pyrrolo[2,3-*d*]pyrimidine (1.60 g, 6.72 mmol) was dissolved in 300 mL ethanol and 300 mL 33% aqueous ammonium hydroxide solution. 10% palladium on charcoal catalyst was added and the reaction mixture was stirred in a hydrogen atmosphere (hydrogen balloon) for 12 h. The catalyst was removed by filtration over celite, and washed with hot ethanol/ammonium hydroxide solution. The filtrate was concentrated under vacuum to about one half of the original volume. On cooling a white solid precipitated from the solution. The product was isolated by filtration. After drying the product was obtained; yield: 686.5 mg (64%). ^{1}H NMR (DMSO-d_6) δ 6.75 (bs, 2H, NH_2), 8.16 (s, 1H, H-6), 8.20 (s, 1H, H-2), 12.60 (bs, 1H, NH); ^{13}C NMR (DMSO-d_6): $\delta =$ 82.02 (C-5), 100.89 (C-4a), 115.96 (CN), 132.33 (C-6), 150.88 (C-7a), 153.52 (C-2), 156.89 (C-4).

5-Cyano-7H-pyrrolo[2,3-d]pyrimidin-4-one (2):[17] Starting from 6-bromo-5-cyano-7*H*-pyrrolo[2,3-*d*] pyrimidin-4-one (836 mg, 3.50 mmol), the product was obtained; yield: 200 mg (36%). Anal. calcd. for $C_7H_4N_4O$: C 58.33, H 2.80, N 38.87; found: C 58.23, H 2.88, N 38.90; ^{1}H NMR (DMSO-d_6): $\delta = 12.14$ (bs, 1H, NH-7), 8.02 (s, 1H, H-2), 8.01 (s, 1H, H-6); ^{13}C NMR (DMSO-d_6): $\delta = 85.98$ (C-5), 107.13 (C-4a),

 © 2012 Wiley-VCH Verlag GmbH & Co. KGaA, Weinheim

115.24 (-CN), 130.82 (C-6), 145.85 (C-2), 148.56 (C-7a), 157.07 (C-4).

2-Amino-4-chloro-5-cyano-7H-pyrrolo[2,3-d]pyrimidine: 2-Amino-4-chloro-5-cyano-7*H*-pyrrolo[2,3-*d*]pyrimidine was prepared according to a modified literature procedure.[18] $PreQ_0$, **1**, (2.00 g, 11.42 mmol) was suspended in 12 mL acetonitrile. Triethylamine (3.2 mL, 23 mmol) was added and the suspension was heated to 95 °C. Phosphoryl chloride (2.2 mL, 24 mmol) was slowly added to the warm reaction mixture. The reaction mixture was allowed to stir at 95 °C overnight. The reaction mixture was then allowed to cool to 65 °C and an additional 10 mL acetonitrile, phosphoryl chloride (2.2 mL, 24 mmol), and triethylamine (3.2 mL, 23 mmol) were added. The reaction was allowed to stir at 65 °C for additional 48 h at which time HPLC-MS analysis showed full conversion. The reaction mixture was cooled to room temperature and ice was slowly added. The mixture was then heated to 75 °C for 15 min and subsequently the precipitate was filtered off. The pH value of the filtrate was adjusted to pH 2 using aqueous ammonia solution. The filtrate was then cooled to 0 °C. The product precipitated from the solution and was isolated by vacuum filtration. After washing with water and drying the product was isolated as a brown solid; yield: 807.7 mg (37%). ^{1}H NMR (DMSO-d_6): $\delta = 6.96$ (s, 2H, NH_2), 8.12 (s, 1H, H-6); ^{13}C NMR (DMSO-d_6): $\delta = 83.05$ (C-5), 106.10 (C-4a), 115.05 (CN), 134.16 (C-6), 151.09 (C-7a), 154.49 (C-4), 160.38 (C-2).

2-Amino-5-cyano-7*H*-pyrrolo[2,3-*d*]pyrimidine (3): 2-Amino-4-chloro-5-cyano-7*H*-pyrrolo[2,3-*d*]pyrimidine (650 mg, 3.36 mmol) was suspended in 80 mL ethanol. 10% palladium on charcoal catalyst (65 mg) and sodium bicarbonate (33.8 mg, 4.02 mmol) were added. The suspension was stirred at 500 rpm at 90 °C and 80 bar of hydrogen pressure in a steel autoclave for 40 h. The catalyst was removed by filtration over celite and washed with ethanol. The filtrate ws concentrated under vacuum until dryness. 2-Amino-5-cyano-7*H*-pyrrolo[2,3-*d*]pyrimidine was obtained as brown solid; yield: 440 mg (82%). Anal. calcd. for $C_7H_5N_5$ C 52.83, H 3.17, N 44.01: found: C 54.30, H 4.23, N 41.47; ^{1}H NMR (DMSO-d_6): $\delta = 6.55$ (s, 2H, NH_2), 8.02 (s, 1H, H-6), 8.63 (s, 1H, H-4); ^{13}C NMR (DMSO-d_6): $\delta = 82.83$ (C-5), 108.96 (C-4a), 115.45 (CN), 133.01 (C-6), 149.93 (C-4), 153.55 (C-7a), 161.13 (C-2).

Screening Reactions

Screening reactions were run in 96-deep well plates using the following conditions and concentrations: nitrile reductase (55 μM, purified by heat precipitation, purity between 60% and 85%) in buffer (100 mM Tris, 50 mM KCl, 1.15 mM TCEP, pH 7.5 adjusted with conc. HCl), substrate in DMSO (2 mM, 10% v/v DMSO), NADPH (0.25 mM in buffer), total volume 200 μL. Blank reactions contained buffer, substrate in DMSO (2 mM, 10% v/v DMSO), and NADPH (0.25 mM in buffer). Reactions were started by addition of NADPH, and NADPH depletion was monitored at 30 °C on a plate reader for 14 h. Subsequently, additional 4 mM of NADPH were added to each well and the screening reactions were placed on a thermomixer at 30 °C and 500 rpm for 24 h to allow full conversion. Samples were then analyzed with HPLC-MS to observe possible product formation. In the case of the natural substrate $preQ_0$, additionally, a synthetic reference material was used to verify the HPLC-MS results. For all screening reactions, including blank reactions, multiple parallel determinations were run.

Acknowledgements

This study was performed within the Austrian Centre of Industrial Biotechnology (ACIB GmbH). This work has been supported by the Federal Ministry of Economy, Family and Youth (BMWFJ), the Federal Ministry of Traffic, Innovation and Technology (bmvit), the Styrian Business Promotion Agency SFG, the Standortagentur Tirol and ZIT-Technology Agency of the City of Vienna through the COMET-Funding Program managed by the Austrian Research Promotion Agency FFG. We gratefully acknowledge Christoph Reisinger, Margaretha Schiller, Elena Loncar, Torsten Bachler and Hannelore Mandl for technical support and Prof. Bernd Nidetzky and Sigrid Egger for helpful advice.

References

[1] a) S. G. Van Lanen, J. S. Reader, M. A. Swairjo, V. de Crecy-Lagard, B. Lee, D. Iwata-Reuyl, *Proc. Natl. Acad. Sci. USA* **2005**, *102*, 4264–4269; b) B. Lee, S. G. Van Lanen, D. Iwata-Reuyl, *Biochemistry* **2007**, *46*, 12844–12854.

[2] Y. Kim, M. Zhou, S. Moy, J. Morales, M. A. Cunningham, A. Joachimiak, *J. Mol. Biol.* **2010**, *404*, 127–137.

[3] a) B. M. Trost, I. Fleming, in: *Comprehensive Organic Synthesis* Pergamon Press, Oxford, Vol 8, **1991**, pp 251–254; b) P. N. Rylander, in: *Hydrogenation Methods*, Academic Press, New York, **1985**, Chapt.7; c) G. Cimino, M. Gavagnin, G. Sodano, A. Spinella, G. Strazzullo, F. J. Schmitz, G. Yalamanchili, *J. Org. Chem.* **1987**, *52*, 2301–2303; d) E. H. R. Walker, *Chem. Soc. Rev.* **1976**, *5*, 23–50; e) W. Huber, *J. Am. Chem. Soc.* **1944**, *66*, 876–879; f) A. Homer, H. R. Billica, *J. Am. Chem. Soc.* **1948**, *70*, 695–698; g) M. Somei, K. Kobayashi, K. Shimizu, T. Kawasaki, *Heterocycles* **1992**, *33*, 77–80; h) S. E. Klohr, J. M. Cassady, *Synth. Commun.* **1988**, *18*, 671–674; i) N. Yamazaki, W. Dokoshi, C. Kibayashi, *Org. Lett.* **2001**, *3*, 193–196; j) H. C. Brown, J. V. B. Kanth, P. V. Dalvi, M. Zaidlewicz, *J. Org. Chem.* **1999**, *64*, 6263–6274.

[4] a) Reviews: M. Dadashipour, Y. Asano, *ACS Catal.* **2011**, *1*, 1121–1149; b) M. Avi, H. Griengl, in: *Organic Synthesis with Enzymes in Non-Aqueous Media*, (Eds.: G. Carrea, S. Riva), Wiley-VCH, Weinheim, **2008**, pp 211–226; c) F. Effenberger, *Angew. Chem.* **1994**, *106*, 1609–1619; *Angew. Chem. Int. Ed. Engl.* **1994**, *33*, 1555–1564; d) J. Holt, U. Hanefeld, *Curr. Org. Synth.* **2009**, *6*, 15–37; e) V. Gotor, *Org. Process Res. Dev.* **2002**, *6*, 420–426; some selected references: f) O. Sosedov, K. Matzer, S. Buerger, C. Kiziak, S. Baum, J. Altenbuchner, A. Chmura, F. van Rantwijk; A. Stolz, *Adv. Synth. Catal.* **2009**, *351*, 1531–1538; g) H. Griengl, N. Klempier, P. Pöchlauer, M. Schmidt, N. Shi, A. Za-

 © 2012 Wiley-VCH Verlag GmbH & Co. KGaA, Weinheim

belinskaja-Mackova, *Tetrahedron* **1998**, *54*, 14477–14486.
[5] Reviews: a) V. Mylerová, L. Martínkova, *Curr. Org. Chem.* **2003**, *7*, 1–17; b) L. Martínkova, V. Kren, *Biocatal. Biotransform.* **2002**, *20*, 73–93; c) A. Banerjee, R. Sharma, U. C. Banerjee, *Appl. Microbiol. Biotechnol.* **2002**, *60*, 33–44; d) M. Kobayashi, S. Shimidzu, *Nature: Biotechnology* **1998**, *16*, 733–736; some selected references: e) C. D. Mathew, T. Nagasawa, M. Kobayashi, H. Yamada, *Appl. Environ. Microbiol.* **1988**, *54*, 1030–1032; f) M. Winkler, A. C. Knall, M. R. Kulterer, N. Klempier, *J. Org. Chem.* **2007**, *72*, 7423–7426.
[6] M. Schittmayer, A. Glieder, M. K. Uhl, A. Winkler, S. Zach, J. H. Schrittwieser, W. Kroutil, P. Macheroux, K. Gruber, S. Kambourakis, J. D. Rozzell, M. Winkler, *Adv. Synth. Catal.* **2011**, *353*, 268–274.
[7] Several non-natural substrates are claimed to be reduced by QueF: *US Patent* 7,364,882 (B1); 20080429 CAN 148:511878; AN 2008:522455 CAPLUS.
[8] M. A. Swairjo, R. R. Reddy, B. Lee, S. G. Van Lanen, S. Brown, V. de Crecy-Lagard, D. Iwata-Reuyl, P. Schimmel, *Acta Crystallogr. Sect. F:* **2005**, *61*, 945–948.
[9] Here, the 6-oxo position refers to the purine numbering; throughout the experimental part the pyrrolopyrimidine nomenclature/numbering is applied; in the above case this would refer to the 4-oxo position.
[10] G. Feller, C. Gerday, *Cell. Mol. Life Sci.* **1997**, *53*, 830–841.
[11] C. E. Loader, H. J. Anderson, *Can. J. Chem.* **1981**, *59*, 2673–2676.
[12] C.-Z. Dong, A. Ahamada-Himidi, S. Plocki, D. Aoun, M. Touaiba, N. Habich, J. Huet, C. Redeuilh, J.-E. Ombetta, J.-J. Godfroid, F. Massicot, F. Heymans, *Bioorg. Med. Chem.* **2005**, *13*, 1989–2007.
[13] a) E. E. Swayze, J. M. Hinkley, L. B. Townsend, *Nucleic Acid Chemistry, Improved and New Synthetic Procedures, Methods and Techniques*, Part 4. (Eds.: L. B. Townsend, R. S. Tipson), Wiley-Interscience, New York, **1991**, pp 16–18; b) A. R. Porcari, L. B Townsend, *Nucleosides Nucleotides Nucleic Acids* **2004**, *23*, 31–39.
[14] C. Reisinger, A. Kern, K. Fesko, H. Schwab, *Appl. Microbiol. Biotechnol.* **2007**, *77*, 241–244.
[15] A. Gangjee, A. Vidwans, E. Elzein, J. J. MacGuire, S. F. Queener, R. L. Kisliuk, *J. Med. Chem.* **2001**, *44*, 1993–2003.
[16] P. Leonard, S. A. Ingale, P. Ding, X. Ming, F. Seela, *Nucleosides Nucleotides Nucleic Acids* **2009**, *28*, 678–694.
[17] R. L. Tolman, R. K. Robins, L. B. Townsend, *J. Am. Chem. Soc.* **1969**, *91*, 2102–2108.
[18] C. L. Gibson, S. LaRosa, K. Ohta, P. H. Boyle, F. Leurquin, A. Lemacon, C. J. Suckling, *Tetrahedron* **2004**, *60*, 943–959.

 © 2012 Wiley-VCH Verlag GmbH & Co. KGaA, Weinheim

8.2 Oral presentations

presenting author underlined

15. Österreichische Chemietage 2013, Graz, Austria, 23-26 September 2013.
Birgit Wilding, Barbara Petschacher, Margit Winkler, Regina Kratzer, Georg Steinkellner, Andrzej Lyskowski, Karl Gruber, Bernd Nidetzky, Norbert Klempier: *Biological nitrile reduction - exploring a remarkable reaction.*

acib Science Days 2013, Graz, Austria, 10-12 September 2013.
Birgit Wilding, Barbara Petschacher, Margit Winkler, Regina Kratzer, Gerlinde Offenmüller, Georg Steinkellner, Andrzej Lyskowski, Karl Gruber, Bernd Nidetzky, Norbert Klempier: *Exploring the active binding site of nitrile reductase queF.*

NAWI Graz DocDays 2011, Graz, Austria, 7-9 June 2011.
Birgit Wilding, Norbert Klempier: *Enzymatic nitrile reduction*.

CMST COST Action CM0701, Cascade Chemoenzymatic Processes - New Synergies Between Chemistry and Biochemistry , Vilnius, Lithuania, 8-10 September 2010.
Norbert Klempier, **Birgit Wilding**, Margit Winkler: *Biotransformation of purine and pyrimidine carbonitriles.*

8.3 Poster presentations

presenting author underlined

15. Österreichische Chemietage 2013, Graz, Austria, 23-26 September 2013.
Birgit Wilding, Alicja Veselá, Jasmin Resch, Ludmila Martínková, Norbert Klempier: *Biocatalytic synthesis of taxol sidechain precursors.*

15. Österreichische Chemietage 2013, Graz, Austria, 23-26 September 2013.
Stefan Faschauner, Wilfried Sailer-Kronlachner, Melanie Zechner, **Birgit Wilding**, Norbert Klempier: *Synthesis of substituted cyclopenta-, thieno-, and pyrazolopyrimidines.*

acib Science Days 2013, Graz, Austria, 10-12 September 2013.
Jihye Jung, Tibor Czabany, Regina Kratzer, **Birgit Wilding**, Norbert Klempier, Bernd Nidetzky: *The mechanism of Escherichia coli nitrile reductase.*

Biotrans 2013, Manchester, United Kingdom, 21-25 July 2013.
Birgit Wilding, Barbara Petschacher, Regina Kratzer, Georg Steinkellner, Andrzej Lyskowski, Norbert Klempier: *Exploring the active binding site of nitrile reductase queF.*

Biotrans 2013, Manchester, United Kingdom, 21-25 July 2013.
Birgit Wilding, Alicja Veselá, Jasmin Resch, Justin Perry, Gary Black, Meng Zhang, Ludmila Martínková, Norbert Klempier: *Synthesis of a taxol sidechain precursor with bacterial and fungal nitrilases.*

Gordon Research Conference Biocatalysis 2012, Smithfield, RI, U.S.A., 8-13 July 2012.
Norbert Klempier, **Birgit Wilding**, Margit Winkler, Regina Kratzer, Bernd Nidetzky, Sigrid Egger, Andrzej Lyskowski, Georg Steinkellner, Karl Gruber: *Investigations of the substrate scope of nitrile reductase queF*

Challenges in Organic Chemistry and Chemical Biology (ISACS 7), Edinburgh, United Kingdom, 12-15 June 2012.
Birgit Wilding, Cornelia Hojnik, Margit Winkler, Norbert Klempier: *Synthesis of 7-deazaguanine analogues including a novel biotransformation step.*

Multistep Enzyme-Catalyzed Processes 2012 (MECP 2012), Graz, Austria, 10-13 April 2012.
Birgit Wilding, Maria Koshanskaya, Margit Winkler, Justin Perry, Gary Black, Norbert Klempier: *A two enzyme approach to a Taxol sidechain precursor.*

Biotrans 2011, Giardini Naxos, Sicily, Italy, 2-6 October 2011.
Birgit Wilding, Carina Hasenoehrl, Gary Black, Justin Perry, Margit Winkler, Norbert Klempier: *Preparation of an enantioenriched taxol sidechain precursor by nitrilase and nitrile hydratase.*

Biotrans 2011, Giardini Naxos, Sicily, Italy, 2-6 October 2011.
Birgit Wilding, Barbara Petschacher, Margit Winkler, Sigrid Egger, Regina Kratzer, Bernd Nidetzky, Georg Steinkellner, Andrzej Lyskowski, Karl Gruber, Norbert Klempier: *Enzymatic Nitrile Reduction using wild type and mutant nitrile reductase queF.*

European Symposium on Organic Chemistry 2011 (ESOC 2011), Hersonissos, Crete, Greece, 10-15 July 2011.
Carina Hasenoehrl, **Birgit Wilding**, Gary Black, Justin Perry, Margit Winkler, Norbert Klempier: *Biocatalytic synthesis of an enantioenriched taxol sidechain precursor.*

5th International Congress on Biocatalysis (BIOCAT 2010), Hamburg, Germany, 29 August - 2 September 2010.
Birgit Wilding, Norbert Klempier: *Biotransformation of purine, pyrimidine and pyrrole carbonitriles.*

Bibliography

(1) Sheldon, R. A. *Green Chemistry* **2008**, *10*, 359–360.

(2) Ran, N.; Zhao, L.; Chen, Z.; Tao, J. *Green Chemistry* **2008**, *10*, 361–372.

(3) Constable, D. J. C.; Dunn, P. J.; Hayler, J. D.; Humphrey, G. R.; Leazer, Jr., J. L.; Linderman, R. J.; Lorenz, K.; Manley, J.; Pearlman, B. A.; Wells, A.; Zaks, A.; Zhang, T. Y. *Green Chemistry* **2007**, *9*, 411–420.

(4) Strohmeier, G. A.; Pichler, H.; May, O.; Gruber-Khadjawi, M. *Chemical Reviews* **2011**, *111*, 4141–4164.

(5) Koeller, K. M.; Wong, C.-H. *Nature* **2001**, *409*, 232–240.

(6) Schmid, A.; Dordick, J.; Hauer, B.; Kiener, A.; Wubbolts, M.; Witholt, B. *Nature* **2001**, *409*, 258–268.

(7) Burton, S. G.; Cowan, D. A.; Woodley, J. M. *Nature Biotechnology* **2002**, *20*, 37–45.

(8) Wildeman, S. M. A. D.; Sonke, T.; Schoemaker, H. E.; May, O. *Accounts of Chemical Research* **2007**, *40*, 1260–1266.

(9) Van Lanen, S. G.; Reader, J. S.; Swairjo, M. A.; de Crécy-Lagard, V.; Lee, B.; Iwata-Reuyl, D. *Proceedings of the National Academy of Sciences of the United States of America* **2005**, *102*, 4264–4269.

(10) Banerjee, A.; Sharma, R.; Banerjee, U. *Applied Microbiology and Biotechnology* **2002**, *60*, 33–44.

(11) Nagasawa, T.; Yamada, H. *Trends in Biotechnology* **1989**, *7*, 153 –158.

(12) Mathew, C. D.; Nagasawa, T.; Kobayashi, M.; Yamada, H. *Applied and Environmental Microbiology* **1988**, *54*, 1030–1032.

(13) Lee, B. W. K.; Van Lanen, S. G.; Iwata-Reuyl, D. *Biochemistry* **2007**, *46*, 12844–12854.

(14) Hwang, J.; Burris, R. *Biochimica et Biophysica Acta - Bioenergetics* **1972**, *283*, 339 –350.

(15) Fisher, K.; Dilworth, M. J.; Newton, W. E. *Biochemistry* **2006**, *45*, 4190–4198.

(16) Dadashipour, M.; Asano, Y. *ACS Catalysis* **2011**, *1*, 1121–1149.

(17) Johnson, D. V.; Zabelinskaja-Mackova, A. A.; Griengl, H. *Current Opinion in Chemical Biology* **2000**, *4*, 103 –109.

(18) Zuegg, J.; Gruber, K.; Gugganig, M.; Wagner, U. G.; Kratky, C. *Protein Science* **1999**, *8*, 1990–2000.

(19) Klempier, N.; Pichler, U.; Griengl, H. *Tetrahedron: Asymmetry* **1995**, *6*, 845 –848.

(20) O'Reilly, C.; Turner, P. *Journal of Applied Microbiology* **2003**, *95*, 1161–1174.

(21) Thuku, R.; Brady, D.; Benedik, M.; Sewell, B. *Journal of Applied Microbiology* **2009**, *106*, 703–727.

(22) Williamson, D.; Dent, K.; Weber, B.; Varsani, A.; Frederick, J.; Thuku, R.; Cameron, R.; Heerden, J.; Cowan, D.; Sewell, B. *Applied Microbiology and Biotechnology* **2010**, *88*, 143–153.

(23) Fernandes, B. C.; Mateo, C.; Kiziak, C.; Chmura, A.; Wacker, J.; van Rantwijk, F.; Stolz, A.; Sheldon, R. *Advanced Synthesis & Catalysis* **2006**, *348*, 2597–2603.

(24) Brenner, C. *Current Opinion in Structural Biology* **2002**, *12*, 775 –782.

(25) Martínková, L.; Křen, V. *Current Opinion in Chemical Biology* **2010**, *14*, 130 –137.

(26) Thimann, K. V.; Mahadevan, S. *Archives of Biochemistry and Biophysics* **1964**, *105*, 133 –141.

(27) Ehmann, A. *Journal of Chromatography A* **1977**, *132*, 267 –276.

(28) Hook, R. H.; Robinson, W. G. *Journal of Biological Chemistry* **1964**, *239*, 4263–4267.

(29) Nakai, T.; Hasegawa, T.; Yamashita, E.; Yamamoto, M.; Kumasaka, T.; Ueki, T.; Nanba, H.; Ikenaka, Y.; Takahashi, S.; Sato, M.; Tsukihara, T. *Structure* **2000**, *8*, 729 –738.

(30) Pace, H.; Hodawadekar, S.; Draganescu, A.; Huang, J.; Bieganowski, P.; Pekarsky, Y.; Croce, C.; Brenner, C. *Current Biology* **2000**, *10*, 907 –917.

(31) Raczynska, J. E.; Vorgias, C. E.; Antranikian, G.; Rypniewski, W. *Journal of Structural Biology* **2011**, *173*, 294 –302.

(32) Mueller, P.; Egorova, K.; Vorgias, C. E.; Boutou, E.; Trauthwein, H.; Verseck, S.; Antranikian, G. *Protein Expression and Purification* **2006**, *47*, 672 –681.

(33) Stevenson, D. E.; Feng, R.; Storer, A. C. *FEBS Letters* **1990**, *277*, 112 –114.

(34) Banerjee, A.; Kaul, P.; Banerjee, U. *Archives of Microbiology* **2006**, *184*, 407–418.

(35) Winkler, M.; Kaplan, O.; Vejvoda, V.; Klempier, N.; Martínková, L. *Journal of Molecular Catalysis B: Enzymatic* **2009**, *59*, 243 –247.

(36) Preiml, M.; Hillmayer, K.; Klempier, N. *Tetrahedron Letters* **2003**, *44*, 5057 –5059.

(37) Winkler, M.; Knall, A. C.; Kulterer, M. R.; Klempier, N. *The Journal of Organic Chemistry* **2007**, *72*, 7423–7426.

(38) Winkler, M.; Meischler, D.; Klempier, N. *Advanced Synthesis & Catalysis* **2007**, *349*, 1475–1480.

(39) Winkler, M.; Glieder, A.; Klempier, N. *Chemical Communications* **2006**, 1298–1300.

(40) Brady, D.; Beeton, A.; Zeevaart, J.; Kgaje, C.; Rantwijk, F.; Sheldon, R. *Applied Microbiology and Biotechnology* **2004**, *64*, 76–85.

(41) Gong, J.-S.; Lu, Z.-M.; Li, H.; Shi, J.-S.; Zhou, Z.-M.; Xu, Z.-H. *Microbial Cell Factories* **2012**, *11*, 142 –160.

(42) Klempier, N.; de Raadt, A.; Faber, K.; Griengl, H. *Tetrahedron Letters* **1991**, *32*, 341 –344.

(43) Stalker, D.; McBride, K. *Science* **1988**, *242*, 419.

(44) Bergeron, S.; Chaplin, D. A.; Edwards, J. H.; Ellis, B. S. W.; Hill, C. L.; Holt-Tiffin, K.; Knight, J. R.; Mahoney, T.; Osborne, A. P.; Ruecroft, G. *Organic Process Research & Development* **2006**, *10*, 661–665.

(45) Wilding, B. Functionalized Silicon Particles for the Preparation of Pharmaceutical Products., MA thesis, Graz, Austria: Graz University of Technology, 2008.

(46) McMorn, P.; Hutchings, G. J. *Chemical Society Reviews* **2004**, *33*, 108–122.

(47) Cao, L.; van Langen, L.; Sheldon, R. A. *Current Opinion in Biotechnology* **2003**, *14*, 387 –394.

(48) Kabaivanova, L.; Dobreva, E.; Dimitrov, P.; Emanuilova, E. *Journal of Industrial Microbiology & Biotechnology* **2005**, *32*, 7 –11.

(49) Banerjee, A.; Kaul, P.; Banerjee, U. *Applied Microbiology and Biotechnology* **2006**, *72*, 77–87.

(50) Vejvoda, V.; Kaplan, O.; Kubáč, D.; Křen, V.; Martínková, L. *Biocatalysis & Biotransformation* **2006**, *24*, 414 –418.

(51) Sheldon, R. A.; Schoevaart, R.; Van Langen, L. M. *Biocatalysis & Biotransformation* **2005**, *23*, 141 –147.

(52) Sheldon, R. A. *Biochemical Society Transactions* **2007**, *35*, 1583 –1587.

(53) Kumar, S.; Mohan, U.; Kamble, A. L.; Pawar, S.; Banerjee, U. C. *Bioresource Technology* **2010**, *101*, 6856 –6858.

(54) Prasad, S.; Bhalla, T. C. *Biotechnology Advances* **2010**, *28*, 725 –741.

(55) Huang, W.; Jia, J.; Cummings, J.; Nelson, M.; Schneider, G.; Lindqvist, Y. *Structure* **1997**, *5*, 691 –699.

(56) Kobayashi, M.; Shimizu, S. *Nature: Biotechnology* **1998**, *16*, 733 –736.

(57) Nojiri, M.; Nakayama, H.; Odaka, M.; Yohda, M.; Takio, K.; Endo, I. *FEBS Letters* **2000**, *465*, 173 –177.

(58) Hashimoto, Y.; Sasaki, S.; Herai, S.; Oinuma, K.-I.; Shimizu, S.; Kobayashi, M. *Journal of Inorganic Biochemistry* **2002**, *91*, 70–77.

(59) Miyanaga, A.; Fushinobu, S.; Ito, K.; Shoun, H.; Wakagi, T. *European Journal of Biochemistry* **2004**, *271*, 429–438.

(60) Sugiura, Y.; Kuwahara, J.; Nagasawa, T.; Yamada, H. *Journal of the American Chemical Society* **1987**, *109*, 5848–5850.

(61) Miyanaga, A.; Fushinobu, S.; Ito, K.; Wakagi, T. *Biochemical and Biophysical Research Communications* **2001**, *288*, 1169 –1174.

(62) Kubiak, K.; Nowak, W. *Biophysical Journal* **2008**, *94*, 3824 –3838.

(63) Payne, M. S.; Wu, S.; Fallon, R. D.; Tudor, G.; Stieglitz, B.; Turner, I. M.; Nelson, M. J. *Biochemistry* **1997**, *36*, 5447–5454.

(64) Martínková, L.; Křen, V. *Biocatalysis & Biotransformation* **2002**, *20*, 73–93.

(65) Klempier, N.; Harter, G.; De Raadt, A.; Griengl, H.; Braunegg, G. *Food Technology and Biotechnology* **1996**, *34*, 67–70.

(66) Martínková, L.; Klempier, N.; Bardakji, J.; Kandelbauer, A.; Ovesná, M.; Podařilová, T.; Kuzma, M.; Přepechalová, I.; Griengl, H.; Kren, V. *Journal of Molecular Catalysis B: Enzymatic* **2001**, *14*, 95 –99.

(67) Bauer, R.; Knackmuss, H.-J.; Stolz, A. *Applied Microbiology and Biotechnology* **1998**, *49*, 89–95.

(68) Přepechalová, I.; Martínková, L.; Stolz, A.; Ovesná, M.; Bezouška, K.; Kopecký, J.; Křen, V. *Applied Microbiology and Biotechnology* **2001**, *55*, 150–156.

(69) Liese, A.; Seelbach, K.; Buchholz, A.; Haberland, J., *Industrial Biotransformations*; Liese, A., Seelbach, K., Wandrey, C., Eds.; Wiley-VCH: 2006; Chapter 6: Processes.

(70) Fournand, D.; Arnaud, A. *Journal of Applied Microbiology* **2001**, *91*, 381–393.

(71) Sonke, T.; Kaptein, B., *Enzyme Catalysis in Organic Synthesis*; Drauz, K., Gröger, H., May, O., Eds.; Wiley-VCH: 2012; Chapter 15: Hydrolysis of Amides.

(72) Reader, J. S.; Metzgar, D.; Schimmel, P.; de Crécy-Lagard, V. *Journal of Biological Chemistry* **2004**, *279*, 6280–6285.

(73) Swairjo, M. A.; Reddy, R. R.; Lee, B.; Van Lanen, S. G.; Brown, S.; de Crécy-Lagard, V.; Iwata-Reuyl, D.; Schimmel, P. *Acta Crystallographica Section F* **2005**, *61*, 945–948.

(74) Ge, X.; Campbell, R. E.; van de Rijn, I.; Tanner, M. E. *Journal of the American Chemical Society* **1998**, *120*, 6613–6614.

(75) Campbell, R. E.; Sala, R. F.; van de Rijn, I.; Tanner, M. E. *Journal of Biological Chemistry* **1997**, *272*, 3416–3422.

(76) Egger, S.; Chaikuad, A.; Kavanagh, K. L.; Oppermann, U.; Nidetzky, B. *Biochemical Society Transactions* **2010**, *38*, 1378–1385.

(77) Rajakannan, V.; Lee, H.-S.; Chong, S.-H.; Ryu, H.-B.; Bae, J.-Y.; Whang, E.-Y.; Huh, J.-W.; Cho, S.-W.; Kang, L.-W.; Choe, H.; Robinson, R. C. *PLoS ONE* **2011**, *6*, e25226.

(78) Rocha, J.; Popescu, A. O.; Borges, P.; Mil-Homens, D.; Moreira, L. M.; Sá-Correia, I.; Fialho, A. M.; Frazão, C. *Journal of Bacteriology* **2011**, *193*, 3978–3987.

(79) Görisch, H *Biochem. J.* **1979**, *181*, 153–157.

(80) Grubmeyer, C. T.; Chu, K. W.; Insinga, S. *Biochemistry* **1987**, *26*, 3369–3373.

(81) Lang, B. S.; Gorren, A. C. F.; Oberdorfer, G.; Wenzl, M. V.; Furdui, C. M.; Poole, L. B.; Mayer, B.; Gruber, K. *Journal of Biological Chemistry* **2012**, *287*, 38124–38134.

(82) Wenzl, M. V.; Beretta, M.; Gorren, A. C. F.; Zeller, A.; Baral, P. K.; Gruber, K.; Russwurm, M.; Koesling, D.; Schmidt, K.; Mayer, B. *Journal of Biological Chemistry* **2009**, *284*, 19878–19886.

(83) Wenzl, M. V.; Beretta, M.; Griesberger, M.; Russwurm, M.; Koesling, D.; Schmidt, K.; Mayer, B.; Gorren, A. C. F. *Molecular Pharmacology* **2011**, *80*, 258–266.

(84) Watanabe, S.; Kodaki, T.; Makino, K. *Journal of Biological Chemistry* **2006**, *281*, 28876–28888.

(85) Jo, J.-E.; Mohan Raj, S.; Rathnasingh, C.; Selvakumar, E.; Jung, W.-C.; Park, S. *Applied Microbiology and Biotechnology* **2008**, *81*, 51–60.

(86) Iwata-Reuyl, D. *Current Opinion in Chemical Biology* **2008**, *12*, 126 –133.

(87) Bürger, E.; Görisch, H. *European Journal of Biochemistry* **1981**, *116*, 137–142.

(88) Auerbach, G.; Herrmann, A.; Bracher, A.; Bader, G.; Gütlich, M.; Fischer, M.; Neukamm, M.; Garrido-Franco, M.; Richardson, J.; Nar, H.; Huber, R.; Bacher, A. *Proceedings of the National Academy of Sciences* **2000**, *97*, 13567–13572.

(89) Chikwana, V. M.; Stec, B.; Lee, B. W. K.; de Crécy-Lagard, V.; Iwata-Reuyl, D.; Swairjo, M. A. *Journal of Biological Chemistry* **2012**, *287*, 30560–30570.

(90) Iwata-Reuyl, D.; Swairjo, M. A. Crystal Structure of Queuosine Biosynthesis Enzyme QueF Bound to Substrate PreQ0. Patent, US2011295582 (A1) (US), Dec. 2011.

(91) Kim, Y.; Zhou, M.; Moy, S.; Morales, J.; Cunningham, M. A.; Joachimiak, A. *Journal of Molecular Biology* **2010**, *404*, 127 –137.

(92) Moeller, K.; Nguyen, G.-S.; Hollmann, F.; Hanefeld, U. *Enzyme and Microbial Technology* **2013**, *52*, 129 –133.

(93) Iwata-Reuyl, D.; De Crécy-Lagard, V.; Van Lanen, S. G. Enzymatic reduction of a nitrile containing compound to the corresponding amine. Patent, US7364882 (B1) (US), Apr. 2008.

(94) Jordan, F.; Niv, H. *Nucleic Acids Research* **1977**, *4*, 697–709.

(95) McCarty, R. M.; Bandarian, V. *Bioorganic Chemistry* **2012**, *43*, 15 –25.

(96) Phillips, G.; El Yacoubi, B.; Lyons, B.; Alvarez, S.; Iwata-Reuyl, D.; de Crécy-Lagard, V. *Journal of Bacteriology* **2008**, *190*, 7876–7884.

(97) Smulson, M. E.; Suhadolnik, R. J. *Journal of Biological Chemistry* **1967**, *242*, 2872–2876.

(98) Suhadolnik, R. J.; Uematsu, T. *Journal of Biological Chemistry* **1970**, *245*, 4365–4371.

(99) Kuchino, Y.; Kasai, H.; Nihei, K.; Nishimura, S. *Nucleic Acids Research* **1976**, *3*, 393–398.

(100) Iwata-Reuyl, D. *Bioorganic Chemistry* **2003**, *31*, 24 –43.

(101) McCarty, R. M.; Somogyi, Á.; Bandarian, V. *Biochemistry* **2009**, *48*, 2301–2303.

(102) McCarty, R. M.; Somogyi, Á.; Lin, G.; Jacobsen, N. E.; Bandarian, V. *Biochemistry* **2009**, *48*, 3847–3852.

(103) Frey, P. A. *Annual Review of Biochemistry* **2001**, *70*, 121–146.

(104) McCarty, R. M.; Krebs, C.; Bandarian, V. *Biochemistry* **2013**, *52*, 188–198.

(105) Cicmil, N.; Huang, R. H. *Proteins: Structure, Function, and Bioinformatics* **2008**, *72*, 1084–1088.

(106) Roth, A.; Winkler, W. C.; Regulski, E. E.; Lee, B. W. K.; Lim, J.; Jona, I.; Barrick, J. E.; Ritwik, A.; Kim, J. N.; Welz, R.; Iwata-Reuyl, D.; Breaker, R. R. *Nature Structural & Molecular Biology* **2007**, *14*, 308 –317.

(107) Frey, B; McCloskey, J; Kersten, W; Kersten, H *Journal of Bacteriology* **1988**, *170*, 2078–2082.

(108) Slany, R. K.; Boesl, M.; Crain, P. F.; Kersten, H. *Biochemistry* **1993**, *32*, 7811–7817.

(109) Okada, N.; Noguchi, S.; Nishimura, S.; Ohgi, T.; Goto, T.; Crain, P.; McCloskey, J. A. *Nucleic Acids Research* **1978**, *5*, 2289–2296.

(110) Noguchi, S.; Nishimura, Y.; Hirota, Y.; Nishimura, S. *Journal of Biological Chemistry* **1982**, *257*, 6544–50.

(111) Roth, A.; Winkler, W. C.; Regulski, E. E.; Lee, B. W. K.; Lim, J.; Jona, I.; Barrick, J. E.; Ritwik, A.; Kim, J. N.; Welz, R.; Iwata-Reuyl, D.; Breaker, R. R. *Nature Structural & Molecular Biology* **2007**, *14*, 308 –317.

(112) Klein, D. J.; Edwards, T. E.; Ferré-D'Amaré, A. R. *Nature Structural & Molecular Biology* **2009**, *16*, 343 –344.

(113) Santner, T.; Rieder, U.; Kreutz, C.; Micura, R. *Journal of the American Chemical Society* **2012**, *134*, 11928–11931.

(114) Hoops, G. C.; Townsend, L. B.; Garcia, G. A. *Biochemistry* **1995**, *34*, 15381–15387.

(115) Slany, R.; Bösl, M.; Kersten, H. *Biochimie* **1994**, *76*, 389 –393.

(116) Kinzie, S. D.; Thern, B.; Iwata-Reuyl, D. *Organic Letters* **2000**, *2*, 1307–1310.

(117) Miles, Z. D.; McCarty, R. M.; Molnar, G.; Bandarian, V. *Proceedings of the National Academy of Sciences* **2011**, *108*, 7368–7372.

(118) Sabina, J.; Söll, D. *Journal of Biological Chemistry* **2006**, *281*, 6993–7001.

(119) Phillips, G.; Chikwana, V. M.; Maxwell, A.; El-Yacoubi, B.; Swairjo, M. A.; Iwata-Reuyl, D.; de Crécy-Lagard, V. *Journal of Biological Chemistry* **2010**, *285*, 12706–12713.

(120) Phillips, G.; Swairjo, M. A.; Gaston, K. W.; Bailly, M.; Limbach, P. A.; Iwata-Reuyl, D.; de Crécy-Lagard, V. *ACS Chemical Biology* **2012**, *7*, 300–305.

(121) McCarty, R. M.; Bandarian, V. *Chemistry & Biology* **2008**, *15*, 790 –798.

(122) Tumkevicius, S.; Dodonova, J. *Chemistry of Heterocyclic Compounds* **2012**, *48*, 258 –279.

(123) Cohen, M. H.; Justice, R.; Pazdur, R. *The Oncologist* **2009**, *14*, 930–935.

(124) Wang, L.; Desmoulin, S. K.; Cherian, C.; Polin, L.; White, K.; Kushner, J.; Fulterer, A.; Chang, M.-H.; Mitchell-Ryan, S.; Stout, M.; Romero, M. F.; Hou, Z.; Matherly, L. H.; Gangjee, A. *Journal of Medicinal Chemistry* **2011**, *54*, 7150–7164.

(125) Desmoulin, S. K.; Wang, L.; Polin, L.; White, K.; Kushner, J.; Stout, M.; Hou, Z.; Cherian, C.; Gangjee, A.; Matherly, L. H. *Molecular Pharmacology* **2012**, *82*, 591–600.

(126) Wang, L.; Cherian, C.; Kugel Desmoulin, S.; Mitchell-Ryan, S.; Hou, Z.; Matherly, L. H.; Gangjee, A. *Journal of Medicinal Chemistry* **2012**, *55*, 1758–1770.

(127) Gangjee, A.; Zeng, Y.; McGuire, J. J.; Mehraein, F.; Kisliuk, R. L. *Journal of Medicinal Chemistry* **2004**, *47*, 6893–6901.

(128) Gangjee, A.; Lin, X.; Kisliuk, R. L.; McGuire, J. J. *Journal of Medicinal Chemistry* **2005**, *48*, 7215–7222.

(129) Gangjee, A.; Zeng, Y.; McGuire, J. J.; Kisliuk, R. L. *Journal of Medicinal Chemistry* **2005**, *48*, 5329–5336.

(130) Gangjee, A.; Jain, H. D.; Phan, J.; Lin, X.; Song, X.; McGuire, J. J.; Kisliuk, R. L. *Journal of Medicinal Chemistry* **2006**, *49*, 1055–1065.

(131) Gangjee, A.; Jain, H. D.; Queener, S. F.; Kisliuk, R. L. *Journal of Medicinal Chemistry* **2008**, *51*, 4589–4600.

(132) Mesa, R. A.; Yasothan, U.; Kirkpatrick, P. *Nature Reviews Drug Discovery* **2012**, *11*, 103–104.

(133) Garber, K. *Nature Biotechnology* **2011**, *29*, 467–468.

(134) Garber, K. *Nature Biotechnology* **2013**, *31*, 3–4.

(135) Frank, K. E.; Burchat, A.; Cox, P.; Ihle, D. C.; Mullen, K. D.; Somal, G.; Vasudevan, A.; Wang, L.; Wilson, N. S. Novel tricyclic compounds. Patent, WO2012149280 (A2) (WO), Nov. 2012.

(136) Bentires-Alj, M.; Britschgi, A. Combination of a phsphoinosite 3-kinase inhibitor and a modulator of the janus kinase 2-signal transducer and activator of transcription 5 pathway. Patent, WO2013072392 (WO), May 2013.

(137) Kim, J. K.; Diehl, J. A. *Journal of Cellular Physiology* **2009**, *220*, 292–296.

(138) Koziczak, M.; Holbro, T.; Hynes, N. E. *Oncogene* **2004**, *23*, 3501–3508.

(139) Kim, S.; Doshi, S.; Haas, K.; Kovats, S. Combination therapy. Patent, WO2013006368 (A1) (WO), Jan. 2013.

(140) Kim, S.; Doshi, S.; Haas, K.; Kovats, S.; Huang, A. X.; Chen, Y. Combination therapy comprising a CDK4/6 inhibitor and a PI3K inhibitor for use in the treatment of cancer. Patent, WO2013006532 (A1) (WO), Jan. 2013.

(141) Gangjee, A.; Namjoshi, O. A.; Yu, J.; Ihnat, M. A.; Thorpe, J. E.; Bailey-Downs, L. C. *Bioorganic & Medicinal Chemistry* **2013**, *21*, 1312 –1323.

(142) Goldstein, D. M.; Brameld, K. A.; Verner, E. Azaindole derivatives as tyrosine kinase inhibitors. Patent, WO2012158785 (A1) (WO), Nov. 2012.

(143) Brugge, J. S.; Muranen, T.; Mills, G.; Selfors, L. Methods and compositions for the treatment of cancer. Patent, WO2011133668 (A2) (WO), Oct. 2011.

(144) Gangjee, A.; Zhao, Y.; Lin, L.; Raghavan, S.; Roberts, E. G.; Risinger, A. L.; Hamel, E.; Mooberry, S. L. *Journal of Medicinal Chemistry* **2010**, *53*, 8116–8128.

(145) Gangjee, A.; Pavana, R.; Li, W.; Hamel, E.; Westbrook, C.; Mooberry, S. *Pharmaceutical Research* **2012**, *29*, 3033–3039.

(146) Arnold, L. D.; Calderwood, D. J.; Dixon, R. W.; Johnston, D. N.; Kamens, J. S.; Munschauer, R.; Rafferty, P.; Ratnofsky, S. E. *Bioorganic & Medicinal Chemistry Letters* **2000**, *10*, 2167 –2170.

(147) Calderwood, D. J.; Johnston, D. N.; Munschauer, R.; Rafferty, P. *Bioorganic & Medicinal Chemistry Letters* **2002**, *12*, 1683 –1686.

(148) Atapour-Mashhad, H.; Tayarani-Najaran, Z.; Davoodnia, A.; Moloudi, R.; Mousavi, S. H. *Drug & Chemical Toxicology* **2011**, *34*, 271 –276.

(149) Mohamed, M. S.; Kamel, R.; Fatahala, S. S. *European Journal of Medicinal Chemistry* **2011**, *46*, 3022 –3029.

(150) Raghavan, S.; Stelmach, J. E.; Smith, C. J.; Li, H.; Whitehead, A.; Waddell, S. T.; Chen, Y.-H.; Miao, S.; Ornoski, O. A.; Garfunkle, J.; Liao, X.; Chang, J.; Han, X.; Go, J.; Groeper, J. A.; Brockunier, L. L.; Rosauer, K.; Parmee, E. Soluble guanylate cyclase activators. Patent, WO2011149921 (A1) (WO), Dec. 2011.

(151) Popowycz, F.; Routier, S.; Joseph, B.; Mérour, J.-Y. *Tetrahedron* **2007**, *63*, 1031 –1064.

(152) Popowycz, F.; Mérour, J.-Y.; Joseph, B. *Tetrahedron* **2007**, *63*, 8689 –8707.

(153) Song, J. J.; Reeves, J. T.; Gallou, F.; Tan, Z.; Yee, N. K.; Senanayake, C. H. *Chemical Society Reviews* **2007**, *36*, 1120–1132.

(154) Walker, S. R.; Carter, E. J.; Huff, B. C.; Morris, J. C. *Chemical Reviews* **2009**, *109*, 3080–3098.

(155) Gompel, M.; Leost, M.; Joffe, E. B. D. K.; Puricelli, L.; Franco, L. H.; Palermo, J.; Meijer, L. *Bioorganic & Medicinal Chemistry Letters* **2004**, *14*, 1703 –1707.

(156) Arendt, C.; Barberis, C.; Levit, M.; Majid, T. N. Azaindole derivatives, their preparation and their therapeutic application. Patent, WO2011075613 (A1) (WO), June 2011.

(157) Nemecek, C.; Metz, W. A.; Wentzler, S.; Lesuisse, D.; El-Ahmad, Y. Novel bis-azaindole derivatives, preparation and pharmaceutical use thereof as kinase inhibitors. Patent, US2010256141 (A1) (US), Oct. 2010.

(158) Salituro, F.; Farmer, L.; Bethiel, R.; Harrington, E.; Green, J.; John, C.; Come, J.; Lauffer, D.; Aronov, A.; Binch, H.; Boyall, D.; Charrier, J.-D.; Everitt, S.; Fraysse, D.; Mortimore, M.; Perard, F.; Robinson, D. Azaindoles useful as inhibitors of JAK and other protein kinases. Patent, WO2005095400 (A1) (WO), Oct. 2005.

(159) Berthel, S. J.; Chen, L.; Corbett, W. L.; Feng, L.; Haynes, N.-E.; Kester, R. F.; So, S.-S.; Tilley, J. W. Azaindole glucokinase activators. Patent, WO2011073117 (A1) (WO), June 2011.

(160) Farmer, L.; Martinez-Botella, G.; Albert, P.; Salituro, F.; Wang, J.; Wannamker, M.; Wang, T. Azaindoles useful as inhibitors of Janus kinase. Patent, WO2007084557 (A2) (WO), July 2007.

(161) Allegretti, M.; Anacardio, R.; Cesta, M. C.; Curti, R.; Mantovanini, M.; Nano, G.; Topai, A.; Zampella, G. *Organic Process Research & Development* **2003**, *7*, 209–213.

(162) Takeuchi, K.; Bastian, J. A.; Gifford-Moore, D. S.; Harper, R. W.; Miller, S. C.; Mullaney, J. T.; Sall, D. J.; Smith, G. F.; Zhang, M.; Fisher, M. J. *Bioorganic & Medicinal Chemistry Letters* **2000**, *10*, 2347 –2351.

(163) Carniato, D.; Schultz, M.; Roche, D.; Hallakou-Bozec, S. 7-Azaindole derivatives as selective 11-beta-hydroxysteroid dehydrogenase type I inhibitors. Patent, WO2009059666 (A1) (WO), May 2009.

(164) Heinrich, T.; Wucherer-Plietker, M.; Buchstaller, H.-P. 7-Azaindole derivatives suitable for treatment of cancers. Patent, WO2012175168 (A1) (WO), Dec. 2012.

(165) Dorsch, D.; Sirrenberg, C.; Mueller, T.; Merkul, E.; Karapetyan, G. 7-Azaindole derivatives. Patent, WO2012104007 (A2) (WO), Aug. 2012.

(166) Heinrich, T.; Katzer, M. Azaindole compounds for treatment of central nervous system disorders. Patent, WO2009112139 (A1) (WO), Sept. 2009.

(167) De la Rosa, M. A.; Johns, B. A.; Samano, V.; Velthuisen, E. J.; Weatherhead, J. Azaindole compounds and methods for treating HIV. Patent, WO2013012649 (A1) (WO), Jan. 2013.

(168) Steinhagen, H.; Scheiper, B.; Matter, H.; Maccort, G. Cyclic azaindole-3-carboxamides, their preparation and their use as pharmaceuticals. Patent, WO2009095162 (A1) (WO), Aug. 2009.

(169) Anilkumar, G.; Rosenblum, S. B.; Venkatraman, S.; Njoroge, F. G.; Kozlowski, J. A. 2,3-substituted azaindole derivatives for treating viral infections. Patent, WO2009032125 (A1) (WO), Mar. 2009.

(170) Nettekoven, M.; Plancher, J.-M.; Richter, H.; Roche, O.; Taylor, S. Azaindole-2-carboxamide derivatives. Patent, WO2007057329 (A1) (WO), May 2007.

(171) Stoit, A.; Coolen, H. K. A. C.; Van der Neut, M.; Kruse, C. G. Azaindole derivatives with a combination of partial nicotinic acetylcholine receptor agonism and dopamine reuptake inhibition. Patent, WO2008003736 (A1) (WO), Jan. 2008.

(172) Aly, A. A.; Ishak, E. A.; Ramadan, M.; Germoush, M. O.; El-Emary, T. I.; Al-Muaikel, N. S. *Journal of Heterocyclic Chemistry* **2013**, *50*, 451–472.

(173) Litvinov, V. In, Katritzky, A. R., Ed.; Advances in Heterocyclic Chemistry, Vol. 92; Academic Press: 2006, pp 83 –143.

(174) Herdewijn, P.; De Jonghe, S.; Gao, L.-J.; JAng, M.-Y.; Vanderhoydonck, B.; Waer, M. J. A.; Lin, Y.; Herman, J. F.; Louat, T. A. M. Novel bicyclic heterocycles. Patent, WO2010103130 (A2) (WO), Sept. 2010.

(175) Aponte, J. C.; Vaisberg, A. J.; Castillo, D.; Gonzalez, G.; Estevez, Y.; Arevalo, J.; Quiliano, M.; Zimic, M.; Verástegui, M.; Málaga, E.; Gilman, R. H.; Bustamante, J. M.; Tarleton, R. L.; Wang, Y.; Franzblau, S. G.; Pauli, G. F.; Sauvain, M.; Hammond, G. B. *Bioorganic & Medicinal Chemistry* **2010**, *18*, 2880 –2886.

(176) Kjær, S.; Linch, M.; Purkiss, A.; Kostelecky, B.; Knowles, P. P.; Rosse, C.; Riou, P.; Soudy, C.; Kaye, S.; Patel, B.; Soriano, E.; Murray-Rust, J.; Barton, C.; Dillon, C.; Roffey, J.; Parker, P. J.; McDonald, N. Q. *Biochemical Journal* **2013**, *451*, 329–342.

(177) Horiuchi, T.; Takeda, Y.; Haginoya, N.; Miyazaki, M.; Nagata, M.; Kitagawa, M.; Akahane, K.; Uoto, K. *Chemical and Pharmaceutical Bulletin* **2011**, *59*, 991–1002.

(178) Horiuchi, T.; Nagata, M.; Kitagawa, M.; Akahane, K.; Uoto, K. *Bioorganic & Medicinal Chemistry* **2009**, *17*, 7850 –7860.

(179) Heckel, A.; Himmelsbach, F.; Lehmann-Lintz, T.; Redemann, N.; Sauer, A.; Thomas, L.; Black, P.; Blackby, W.; Danilewicz, J.; Linney, I.; Austen, M.; Schneider, M.; Schreiter, K. Halogen or cyano substituted thieno[2,3-d]pyrimidines having Mnk1/Mnk2 inhibiting activity for pharmaceutical compositions. Patent, WO2011104338 (A1) (WO), Sept. 2011.

(180) Roth, B. *Journal of Medicinal Chemistry* **1969**, *12*, 227–232.

(181) Rosowsky, A.; Papoulis, A. T.; Queener, S. F. *Journal of Medicinal Chemistry* **1997**, *40*, 3694–3699.

(182) Deng, Y.; Zhou, X.; Kugel Desmoulin, S.; Wu, J.; Cherian, C.; Hou, Z.; Matherly, L. H.; Gangjee, A. *Journal of Medicinal Chemistry* **2009**, *52*, 2940–2951.

(183) Gangjee, A.; Li, W.; Kisliuk, R. L.; Cody, V.; Pace, J.; Piraino, J.; Makin, J. *Journal of Medicinal Chemistry* **2009**, *52*, 4892–4902.

(184) Gangjee, A.; Qiu, Y.; Li, W.; Kisliuk, R. L. *Journal of Medicinal Chemistry* **2008**, *51*, 5789–5797.

(185) Link, H. *Helvetica Chimica Acta* **1990**, *73*, 797–803.

(186) Gangjee, A.; Qiu, Y.; Kisliuk, R. L. *Journal of Heterocyclic Chemistry* **2004**, *41*, 941–946.

(187) Ashour, H. M.; Shaaban, O. G.; Rizk, O. H.; El-Ashmawy, I. M. *European Journal of Medicinal Chemistry* **2013**, *62*, 341 –351.

(188) Nunokawa, Y.; Nakatsuka, T.; Saitoh, M.; Abe, K. NF-κB-Inhibitors containing indan derivatives as the active ingredient. Patent, EP1018514 A1 (EP), July 2000.

(189) Shook, B. C.; Chakravarty, D.; Barbay, J. K.; Wang, A.; Leonard, K.; Alford, V.; Powell, M. T.; Rassnick, S.; Scannevin, R. H.; Carroll, K.; Wallace, N.; Crooke, J.; Ault, M.; Lampron, L.; Westover, L.; Rhodes, K.; Jackson, P. F. *Bioorganic & Medicinal Chemistry Letters* **2013**, *23*, 2688 –2691.

(190) El-Kerdawy, M. M.; El-Bendary, E. R.; Abdel-Aziz, A. A.-M.; El-wasseef, D. R.; El-Aziz, N. I. A. *European Journal of Medicinal Chemistry* **2010**, *45*, 1805 –1820.

(191) Kung, P.-P.; Meng, J. J. 2-Amino pyridine compounds. Patent, WO2008059368 (A2) (WO), May 2008.

(192) Ross, L. O.; Goodman, L.; Baker, B. R. *Journal of the American Chemical Society* **1959**, *81*, 3108–3114.

(193) Curd, F. H. S.; Rose, F. L. *Journal of the Chemical Society* **1946**, 362–366.

(194) Hull, R.; Lovell, B. J.; Openshaw, H. T.; Payman, L. C.; Todd, A. R. *Journal of the Chemical Society* **1946**, 357–362.

(195) Rosowsky, A.; Papoulis, A. T.; Queener, S. F. *Journal of Medicinal Chemistry* **1998**, *41*, 913–918.

(196) Rosowsky, A.; Papoulis, A.; Queener, S. F. *Journal of Medicinal Chemistry* **2002**, *45*, 1957–1957.

(197) Gangjee, A.; Zhao, Y.; Hamel, E.; Westbrook, C.; Mooberry, S. L. *Journal of Medicinal Chemistry* **2011**, *54*, 6151–6155.

(198) Blake, J. F.; Xu, R.; Bencsik, J. R.; Xiao, D.; Kallan, N. C.; Schlachter, S.; Mitchell, I. S.; Spencer, K. L.; Banka, A. L.; Wallace, E. M.; Gloor, S. L.; Martinson, M.; Woessner, R. D.; Vigers, G. P.; Brandhuber, B. J.; Liang, J.; Safina, B. S.; Li, J.; Zhang, B.; Chabot, C.; Do, S.; Lee, L.; Oeh, J.; Sampath, D.; Lee, B. B.; Lin, K.; Liederer, B. M.; Skelton, N. J. *Journal of Medicinal Chemistry* **2012**, *55*, 8110–8127.

(199) Lin, J.; Sampath, D.; Nannini, M. A.; Lee, B. B.; Degtyarev, M.; Oeh, J.; Savage, H.; Guan, Z.; Hong, R.; Kassees, R.; Lee, L. B.; Risom, T.; Gross, S.; Liederer, B. M.; Koeppen, H.; Skelton, N. J.; Wallin, J. J.; Belvin, M.; Punnoose, E.; Friedman, L. S.; Lin, K. *Clinical Cancer Research* **2013**, *19*, 1760–1772.

(200) Bencsik, J. R.; Blake, J. F.; Chabot, C.; Do, S.; Kallan, N. C.; Liang, J.; Mitchell, I. S.; Safina, B.; Spencer, K. L.; Xiao, D.; Xu, R.; Zhang, B. Hydroxylated and methoxylated cyclopenta[*d*]pyrimidines as AKT protein kinase inhibitors. Patent, WO2008006040 (A1) (WO), Jan. 2008.

(201) Bencsik, J. R.; Blake, J. F.; Kallan, N.; Mitchell, I. S.; Spencer, K. L.; Xiao, D.; Xu, R.; Chabot, C.; Do, S.; Liang, J.; Safina, B.; Zhang, B. Hydroxylated pyrimidyl cyclopentane as AKT protein kinase inhibitor. Patent, WO2009089453 (A1) (WO), July 2009.

(202) Matasi, J. J.; Caldwell, J. P.; Hao, J.; Neustadt, B.; Arik, L.; Foster, C. J.; Lachowicz, J.; Tulshian, D. B. *Bioorganic & Medicinal Chemistry Letters* **2005**, *15*, 1333 –1336.

(203) Shook, B. C.; Rassnick, S.; Osborne, M. C.; Davis, S.; Westover, L.; Boulet, J.; Hall, D.; Rupert, K. C.; Heintzelman, G. R.; Hansen, K.; Chakravarty, D.; Bullington, J. L.; Russell, R.; Branum, S.; Wells, K. M.; Damon, S.; Youells, S.; Li, X.; Beauchamp, D. A.; Palmer, D.; Reyes, M.; Demarest, K.; Tang, Y.; Rhodes, K.; Jackson, P. F. *Journal of Medicinal Chemistry* **2010**, *53*, 8104–8115.

(204) Lozano, A. M.; Lang, A. E.; Hutchison, W. D.; Dostrovsky, J. O. *Current Opinion in Neurobiology* **1998**, *8*, 783 –790.

(205) Richardson, P. J.; Kase, H.; Jenner, P. G. *Trends in Pharmacological Sciences* **1997**, *18*, 338 –344.

(206) Shook, B. C.; Rassnick, S.; Hall, D.; Rupert, K. C.; Heintzelman, G. R.; Hansen, K.; Chakravarty, D.; Bullington, J. L.; Scannevin, R. H.; Magliaro, B.; Westover, L.; Carroll, K.; Lampron, L.; Russell, R.; Branum, S.; Wells, K.; Damon, S.; Youells, S.; Li, X.; Osbourne, M.; Demarest, K.; Tang, Y.; Rhodes, K.; Jackson, P. F. *Bioorganic & Medicinal Chemistry Letters* **2010**, *20*, 2864 –2867.

(207) Shook, B. C.; Rassnick, S.; Wallace, N.; Crooke, J.; Ault, M.; Chakravarty, D.; Barbay, J. K.; Wang, A.; Powell, M. T.; Leonard, K.; Alford, V.; Scannevin, R. H.; Carroll, K.; Lampron, L.; Westover, L.; Lim, H.-K.; Russell, R.; Branum, S.; Wells, K. M.; Damon, S.; Youells, S.; Li, X.; Beauchamp, D. A.; Rhodes, K.; Jackson, P. F. *Journal of Medicinal Chemistry* **2012**, *55*, 1402–1417.

(208) Takasaki, W.; Yamamura, M.; Shigehara, E.; Suzuki, Y.; Tonohiro, T.; Hara, T.; Tanaka, Y. *Biological & Pharmaceutical Bulletin* **1999**, *22*, 498–503.

(209) Itoh, K.; Nishiya, Y.; Takasaki, W.; Adachi, M.; Tanaka, Y. *Chirality* **2006**, *18*, 592–598.

(210) Itoh, K.; Yamamura, M.; Muramatsu, S.; Hoshino, K.; Masubuchi, A.; Sasaki, T.; Tanaka, Y. *Xenobiotica* **2005**, *35*, 561 –573.

(211) Boy, K. M.; Guernon, J. M.; Macor, J. E.; A, T. I. L.; Wu, Y.-J.; Zhang, Y. Compounds for the reduction of beta-amyloid production. Patent, WO2012009309 (A1) (WO), Jan. 2012.

(212) Elion, G. B. *Nobel Lectures, Physiology or Medicine* **1981-1990**.

(213) Pacher, P.; Nivorozhkin, A.; Szabó, C. *Pharmacological Reviews* **2006**, *58*, 87–114.

(214) Bacon, E. R.; Singh, B.; Lesher, G. Y. 6-heterocyclyl pyrazolo [3,4-d]pyrimidin-4-ones and compositions and method of use thereof. Patent, US5294612 (A) (US), Mar. 1994.

(215) Kobayashi, S. *Chemical & Pharmaceutical Bulletin* **1973**, *21*, 941–951.

(216) Ovcharova, I.; Zasosova, I.; Gerchikov, L.; Shuvalova, M.; Golovchinskaya, E.; Liberman, S. *Pharmaceutical Chemistry Journal* **1973**, *7*, 735–737.

(217) Hanke, J. H.; Gardner, J. P.; Dow, R. L.; Changelian, P. S.; Brissette, W. H.; Weringer, E. J.; Pollok, B. A.; Connelly, P. A. *Journal of Biological Chemistry* **1996**, *271*, 695–701.

(218) Dinér, P.; Alao, J. P.; Söderlund, J.; Sunnerhagen, P.; Grøtli, M. *Journal of Medicinal Chemistry* **2012**, *55*, 4872–4876.

(219) Corbett, M. S.; Kauffman, G. S.; Freeman-Cook, K. D.; Lippa, B. S.; Luzzio, M. J.; Morris, J. Amine derivatives useful as anticancer agents. Patent, WO2008012635 (A2) (WO), Jan. 2008.

(220) Woller, K.; Curtin, M. L.; Frank, K. E.; Josephson, N. S.; Li, B. C.; Wishart, N. Novel pyrazolo[3,4-d]pyrimidine compounds. Patent, WO2011156698 (A2) (WO), Dec. 2011.

(221) Liu, M.; Fung, S.-Y.; Keshavjee, S. Compositions comprising self-assembling peptide and amino acid vehicles and active agents PP1 or PP2 and uses therof. Patent, WO2012109732 (A1) (WO), Aug. 2012.

(222) Burchat, A. F.; Calderwood, D. J.; Friedman, M. M.; Hirst, G. C.; Li, B.; Rafferty, P.; Ritter, K.; Skinner, B. S. *Bioorganic & Medicinal Chemistry Letters* **2002**, *12*, 1687 –1690.

(223) Carraro, F.; Naldini, A.; Pucci, A.; Locatelli, G. A.; Maga, G.; Schenone, S.; Bruno, O.; Ranise, A.; Bondavalli, F.; Brullo, C.; Fossa, P.; Menozzi, G.; Mosti, L.; Modugno, M.; Tintori, C.; Manetti, F.; Botta, M. *Journal of Medicinal Chemistry* **2006**, *49*, 1549–1561.

(224) Radi, M.; Dreassi, E.; Brullo, C.; Crespan, E.; Tintori, C.; Bernardo, V.; Valoti, M.; Zamperini, C.; Daigl, H.; Musumeci, F.; Carraro, F.; Naldini, A.; Filippi, I.; Maga, G.; Schenone, S.; Botta, M. *Journal of Medicinal Chemistry* **2011**, *54*, 2610–2626.

(225) Radi, M.; Tintori, C.; Musumeci, F.; Brullo, C.; Zamperini, C.; Dreassi, E.; Fallacara, A. L.; Vignaroli, G.; Crespan, E.; Zanoli, S.; Laurenzana, I.; Filippi, I.; Maga, G.; Schenone, S.; Angelucci, A.; Botta, M. *Journal of Medicinal Chemistry* **2013**, *56*, 5382–5394.

(226) Kaplan, J.; Verheijen, J. C.; Brooijmans, N.; Toral-Barza, L.; Hollander, I.; Yu, K.; Zask, A. *Bioorganic & Medicinal Chemistry Letters* **2010**, *20*, 640 –643.

(227) Congxin, L. mTOR selective kinase inhibitors. Patent, WO2011146594 (A2) (WO), Nov. 2011.

(228) Ali, A.; Taylor, G. E.; Ellsworth, K.; Harris, G.; Painter, R.; Silver, L. L.; Young, K. *Journal of Medicinal Chemistry* **2003**, *46*, 1824–1830.

(229) Eweas, A.; Swelam, S.; Fathalla, O.; Fawzy, N.; Abdel-Moez, S. *Medicinal Chemistry Research* **2012**, *21*, 3848–3857.

(230) Quintela, J. M.; Peinador, C.; González, L.; Devesa, I.; Ferrándiz, M. L.; Alcaraz, M. J.; Riguera, R. *Bioorganic & Medicinal Chemistry* **2003**, *11*, 863 –868.

(231) Devesa, I.; Alcaraz, M. J.; Riguera, R.; Ferrándiz, M. L. *European Journal of Pharmacology* **2004**, *488*, 225 –230.

(232) Azam, M. A.; Dharanya, L.; Mehta, C. C.; Sachdeva, S. *Acta Pharmaceutica* **2013**, *63*, 19–30.

(233) Ballell, L.; Field, R. A.; Chung, G. A.; Young, R. J. *Bioorganic & Medicinal Chemistry Letters* **2007**, *17*, 1736 –1740.

(234) Chern, J.-H.; Shia, K.-S.; Hsu, T.-A.; Tai, C.-L.; Lee, C.-C.; Lee, Y.-C.; Chang, C.-S.; Tseng, S.-N.; Shih, S.-R. *Bioorganic & Medicinal Chemistry Letters* **2004**, *14*, 2519 –2525.

(235) *Amino Group Chemistry: From Synthesis to the Life Sciences*; Ricci, A., Ed.; Wiley-VCH: 2008.

(236) Faber, K., *Biotransformations in Organic Chemistry*; Springer-Verlag: 2011; Chapter 2: Biocatalytic Applications.

(237) Höhne, M.; Bornscheuer, U. *ChemCatChem* **2009**, *1*, 42–51.

(238) Koszelewski, D.; Tauber, K.; Faber, K.; Kroutil, W. *Trends in Biotechnology* **2010**, *28*, 324 –332.

(239) Miriyala, B.; Bhattacharyya, S.; Williamson, J. S. *Tetrahedron* **2004**, *60*, 1463 –1471.

(240) Kroutil, W.; Fischereder, E.-M.; Fuchs, C. S.; Lechner, H.; Mutti, F. G.; Pressnitz, D.; Rajagopalan, A.; Sattler, J. H.; Simon, R. C.; Siirola, E. *Organic Process Research & Development* **2013**, *17*, 751–759.

(241) Mitsukura, K.; Suzuki, M.; Tada, K.; Yoshida, T.; Nagasawa, T. *Organic & Biomolecular Chemistry* **2011**, *8*, 4533–4535.

(242) Rodríguez-Mata, M.; Frank, A.; Wells, E.; Leipold, F.; Turner, N. J.; Hart, S.; Turkenburg, J. P.; Grogan, G. *ChemBioChem* **2013**, *14*, 1372–1379.

(243) Das, S.; Zhou, S.; Addis, D.; Enthaler, S.; Junge, K.; Beller, M. *Topics in Catalysis* **2010**, *53*, 979–984.

(244) Gomez, S.; Peters, J.; Maschmeyer, T. *Advanced Synthesis & Catalysis* **2002**, *344*, 1037–1057.

(245) Klenke, B.; Gilbert, I. H. *The Journal of Organic Chemistry* **2001**, *66*, 2480–2483.

(246) Kukula, P.; Studer, M.; Blaser, H.-U. *Advanced Synthesis & Catalysis* **2004**, *346*, 1487–1493.

(247) Wu, B.; Zhang, J.; Yang, M.; Yue, Y.; Ma, L.-J.; Yu, X.-Q. *ARKIVOC* **2008**, *xii*, 95–102.

(248) Keay, J. G. In, Katritzky, A. R., Ed.; Advances in Heterocyclic Chemistry, Vol. 39; Academic Press: 1986, pp 1 –77.

(249) Winans, C. F.; Adkins, H. *Journal of the American Chemical Society* **1932**, *54*, 306–312.

(250) Juday, R.; Adkins, H. *Journal of the American Chemical Society* **1955**, *77*, 4559–4564.

(251) Adkins, H.; Billica, H. R. *Journal of the American Chemical Society* **1948**, *70*, 695–698.

(252) Gowda, S.; Gowda, D. *Tetrahedron* **2002**, *58*, 2211 –2213.

(253) Enthaler, S.; Junge, K.; Addis, D.; Erre, G.; Beller, M. *ChemSusChem* **2008**, *1*, 1006–1010.

(254) Walker, E. R. H. *Chemical Society Reviews* **1976**, *5*, 23–50.

(255) Brown, H. C.; Kanth, J. V. B.; Dalvi, P. V.; Zaidlewicz, M. *The Journal of Organic Chemistry* **1999**, *64*, 6263–6274.

(256) Faber, K., *Biotransformations in Organic Chemistry*; Springer-Verlag: 2011; Chapter 1: Introduction and Background Information.

(257) Kondo, T.; Nakatsuka, S.; Goto, T. *Chemistry Letters* **1980**, *9*, 559–562.

(258) Migawa, M. T.; Hinkley, J. M.; Hoops, G. C.; Townsend, L. B. *Synthetic Communications* **1996**, *26*, 3317–3322.

(259) Gangjee, A.; Vidwans, A.; Elzein, E.; McGuire, J. J.; Queener, S. F.; Kisliuk, R. L. *Journal of Medicinal Chemistry* **2001**, *44*, 1993–2003.

(260) Klepper, F.; Polborn, K.; Carell, T. *Helvetica Chimica Acta* **2005**, *88*, 2610–2616.

(261) Ohno, H.; Terui, T.; Kitawaki, T.; Chida, N. *Tetrahedron Letters* **2006**, *47*, 5747 –5750.

(262) Brückl, T.; Klepper, F.; Gutsmiedl, K.; Carell, T. *Organic & Biomolecular Chemistry* **2007**, *5*, 3821–3825.

(263) Ölgen, S.; Isgör, Y. G.; Çoban, T. *Archiv der Pharmazie* **2008**, *341*, 113–120.

(264) Wilding, B.; Winkler, M.; Petschacher, B.; Kratzer, R.; Glieder, A.; Klempier, N. *Advanced Synthesis & Catalysis* **2012**, *354*, 2191–2198.

(265) Ohgi, T.; Kondo, T.; Goto, T. *Chemistry Letters* **1979**, *8*, 1283–1286.

(266) Akimoto, H.; Imamiya, E.; Hitaka, T.; Nomura, H.; Nishimura, S. *Journal of the Chemical Society, Perkin Transactions 1* **1988**, 1637–1644.

(267) Gerber, H.-D.; Klebe, G. *Organic & Biomolecular Chemistry* **2012**, *10*, 8660–8668.

(268) Chen, Y.-C.; Brooks, A. F.; Goodenough-Lashua, D. M.; Kittendorf, J. D.; Showalter, H. D.; Garcia, G. A. *Nucleic Acids Research* **2011**, *39*, 2834–2844.

(269) West, R. A. *The Journal of Organic Chemistry* **1961**, *26*, 4959–4961.

(270) Seela, F.; Richter, R. *Chemische Berichte* **1978**, *111*, 2925–2930.

(271) Ing, H. R.; Manske, R. H. F. *Journal of the Chemical Society* **1926**, *129*, 2348–2351.

(272) Huber, W. *Journal of the American Chemical Society* **1944**, *66*, 876–879.

(273) Gangjee, A.; Mavandadi, F.; Queener, S. F.; McGuire, J. J. *Journal of Medicinal Chemistry* **1995**, *38*, 2158–2165.

(274) Balow, G.; Brugger, J.; Lesnik, E.; Acevedo, O. L. *Nucleosides and Nucleotides* **1997**, *16*, 941–944.

(275) Gibson, C. L.; Rosa, S. L.; Ohta, K.; Boyle, P. H.; Leurquin, F.; Lemaçon, A.; Suckling, C. J. *Tetrahedron* **2004**, *60*, 943 –959.

(276) Ramasamy, K.; Joshi, R. V.; Robins, R. K.; Revankar, G. R. *Journal of the Chemical Society, Perkin Transactions 1* **1989**, 2375–2384.

(277) Ramasamy, K.; Robins, R. K.; Revankar, G. R. *Journal of the Chemical Society, Chemical Communications* **1989**, 560–562.

(278) Davoll, J. *Journal of the Chemical Society* **1960**, 131–138.

(279) Salituro, F.; Wang, T.; Wang, J.; Bethiel, R.; Wannamaker, M.; Martinez-Botella, G.; Duffy, J.; Aronov, A.; Lauffer, D.; Pierce, A. Deazapurines useful as inhibitors of Janus kinases. Patent, WO2007041130 (A2) (WO), Apr. 2007.

(280) Funakoshi, Y.; Tanaka, C.; Park, C. H.; Ro, S. G. Azaindole derivative. Patent, WO2012002568 (A1) (WO), Jan. 2012.

(281) Renau, T. E.; Kennedy, C.; Ptak, R. G.; Breitenbach, J. M.; Drach, J. C.; Townsend, L. B. *Journal of Medicinal Chemistry* **1996**, *39*, 3470–3476.

(282) Reigan, P.; Gbaj, A.; Stratford, I. J.; Bryce, R. A.; Freeman, S. *European Journal of Medicinal Chemistry* **2008**, *43*, 1248 –1260.

(283) Stoit, A.; Coolen, H. K. A. C.; Van der Neut, M. A. W.; Kruse Cornelis, G. Azaindole derivatives with a combination of partial nicotinic acetyl-choline receptor agonism and dopamine reuptake inhibition. Patent, US2008009514 (A1) (US), Jan. 2008.

(284) Shi, J.; Van de Water, R.; Hong, K.; Lamer, R. B.; Weichert, K. W.; Sandoval, C. M.; Kasibhatla, S. R.; Boehm, M. F.; Chao, J.; Lundgren, K.; Timple, N.; Lough, R.; Ibanez, G.; Boykin, C.; Burrows, F. J.; Kehry, M. R.; Yun, T. J.; Harning, E. K.; Ambrose, C.; Thompson, J.; Bixler, S. A.; Dunah, A.; Snodgrass-Belt, P.; Arndt, J.; Enyedy, I. J.; Li, P.; Hong, V. S.; McKenzie, A.; Biamonte, M. A. *Journal of Medicinal Chemistry* **2012**, *55*, 7786–7795.

(285) Kasibhatla, S. R.; Biamonte, M. A.; Shi, J.; Boehm, M. F. Alkynyl pyrrolopyrimidines and related analogs as HSP-90 inhibitors. Patent, US2006/0223797 A1 (US), Oct. 2006.

(286) Taylor, E. C.; Kuhnt, D.; Shih, C.; Rinzel, S. M.; Grindey, G. B.; Barredo, J.; Jannatipour, M.; Moran, R. G. *Journal of Medicinal Chemistry* **1992**, *35*, 4450–4454.

(287) Wilding, B.; Winkler, M.; Petschacher, B.; Kratzer, R.; Egger, S.; Steinkellner, G.; Lyskowski, A.; Nidetzky, B.; Gruber, K.; Klempier, N. *Chemistry - A European Journal* **2013**, *19*, 7007–7012.

(288) Hoops, G. C.; Park, J.; Garcia, G. A.; Townsend, L. B. *Journal of Heterocyclic Chemistry* **1996**, *33*, 767–781.

(289) Seela, F.; Kehne, A.; Winkeler, H.-D. *Liebigs Annalen der Chemie* **1983**, *1983*, 137–146.

(290) Middleton, W. J.; Engelhardt, V. A.; Fisher, B. S. *Journal of the American Chemical Society* **1958**, *80*, 2822–2829.

(291) Swayze, E. E.; Hinkley, J.; Townsend, L., *Nucleic Acid Chemistry*; Townsend, L., Tipson, R., Eds.; Wiley-Interscience New York: 1991; Vol. 4; Chapter The improved preparation of a versatile synthon for the synthesis of pyrrolo[2,3-*d*]primidines, pp 16–17.

(292) Tolman, R. L.; Robins, R. K.; Townsend, L. B. *Journal of the American Chemical Society* **1969**, *91*, 2102–2108.

(293) Tolman, R. L.; Robins, R. K.; Townsend, L. B. *Journal of the American Chemical Society* **1968**, *90*, 524–526.

(294) Porcari, A. R.; Townsend, L. B. *Nucleosides and Nucleotides* **1999**, *18*, 153–159.

(295) Xiao, C.; Sun, C.; Han, W.; Pan, F.; Dan, Z.; Li, Y.; Song, Z.-G.; Jin, Y.-H. *Bioorganic & Medicinal Chemistry* **2011**, *19*, 7100 –7110.

(296) Porcari, A. R.; Townsend, L. B. *Synthetic Communications* **1998**, *28*, 3835–3843.

(297) Townsend, L. B.; Drach, J. C. Pyrrolo[2,3-d]pyrimidines as antiviral agents. Patent, US6342501 (B1) (US), Jan. 2002.

(298) Uematsu, T.; Suhadolnik, R. J. *The Journal of Organic Chemistry* **1968**, *33*, 726–728.

(299) Porcari, A. R.; Townsend, L. B. *Nucleosides, Nucleotides and Nucleic Acids* **2004**, *23*, 31–39.

(300) Taylor, E. C.; Hendess, R. W. *Journal of the American Chemical Society* **1964**, *86*, 951–952.

(301) Taylor, E. C.; Hendess, R. W. *Journal of the American Chemical Society* **1965**, *87*, 1995–2003.

(302) Mahadevan, I.; Rasmussen, M. *Journal of Heterocyclic Chemistry* **1992**, *29*, 359–367.

(303) Ducrocq, C.; Bisagni, E.; Lhoste, J.-M.; Mispelter, J.; Defaye, J. *Tetrahedron* **1976**, *32*, 773 –780.

(304) Clark, B. A. J.; El-Bakoush, M. M. S.; Parrick, J. *Journal of the Chemical Society, Perkin Transactions 1* **1974**, 1531–1536.

(305) Hojnik, C. Synthesis of substituted 1*H*-pyrrolo[3,2-*c*]pyridines and 1*H*-pyrrolo[2,3-*b*]pyridines., MA thesis, Graz, Austria: Graz University of Technology, 2012.

(306) Zelikin, A.; Shastri, V. R.; Langer, R. *The Journal of Organic Chemistry* **1999**, *64*, 3379–3380.

(307) Schneller, S. W.; Luo, J. K.; Hosmane, R. S.; De Clercq, E.; Stoeckler, J. D.; Agarwal, K. C.; Parks, R. E.; Saunders, P. P. *Journal of Medicinal Chemistry* **1984**, *27*, 1737–1739.

(308) Brodrick, A.; Wibberley, D. G. *Journal of the Chemical Society, Perkin Transactions 1* **1975**, 1910–1913.

(309) Schneller, S. W.; Luo, J.-K. *The Journal of Organic Chemistry* **1980**, *45*, 4045–4048.

(310) Arita, M.; Saito, T.; Okuda, H.; Sato, H.; Uehata, M. 4-Amino(alkyl)cyclohexane-1-carboxamid compound and use of therof. Patent, 5,478,838 (US), Dec. 1995.

(311) Goodcare, S. C.; Lai, Y.; Liang, J.; Magnuson, S. R.; Robarge, K. D.; Stanley, M. S.; Hsiao-Wei Tsui, V.; Williams, K.; Zhang, B.; Zhou, A. Janus kinase inhibitor compounds and methods. Patent, US2010/0317643 (A1) (US), Dec. 2010.

(312) Xu, S.; Huang, X.; Hong, X.; Xu, B. *Organic Letters* **2012**, *14*, 4614–4617.

(313) Vorbrüggen, H.; Krolikiewicz, K. *Tetrahedron* **1994**, *50*, 6549 –6558.

(314) Reddy, B. S.; Begum, Z.; Reddy, Y. J.; Yadav, J. *Tetrahedron Letters* **2010**, *51*, 3334 –3336.

(315) Leysen, D. C. M.; Defert, O. R.; De Kerpel, J. O. A.; Fourmaintraux, E. P. P.; Arzel, P.; De Wilde, G. J. H. Kinase inhibitors. Patent, WO2005082367 (A1) (WO), Sept. 2005.

(316) VanRheenen, V.; Kelly, R.; Cha, D. *Tetrahedron Letters* **1976**, *17*, 1973 –1976.

(317) Pappo, R.; Allen Jr., D. S.; Lemieux, R. U.; Johnson, W. S. *The Journal of Organic Chemistry* **1956**, *21*, 478–479.

(318) Kitov, P. I.; Bundle, D. R. *Organic Letters* **2001**, *3*, 2835–2838.

(319) Bergstad, K.; Piet, J. J. N.; Bäckvall, J.-E. *The Journal of Organic Chemistry* **1999**, *64*, 2545–2548.

(320) Kim, S.; Chung, J.; Kim, B. M. *Tetrahedron Letters* **2011**, *52*, 1363 –1367.

(321) Verbiscar, A. J. *Journal of Medicinal Chemistry* **1972**, *15*, 149–152.

(322) Chatterjee, A.; Biswas, K. M. *The Journal of Organic Chemistry* **1973**, *38*, 4002–4004.

(323) Masurier, N.; Moreau, E.; Lartigue, C.; Gaumet, V.; Chezal, J.-M.; Heitz, A.; Teulade, J.-C.; Chavignon, O. *The Journal of Organic Chemistry* **2008**, *73*, 5989–5992.

(324) Casuscelli, F.; Casale, E.; Faiardi, D.; Mongelli, N.; Piutti, C.; Traquandi, G. Cyclocondensed azaindoles active as kinase inhibitors. Patent, EP2002836 (A1) (EP), Dec. 2008.

(325) Leroy, V.; Bacque, E.; Conseiller, E.; Steinmetz, A.; Ronan, B.; Letallec, J.-P. New imidazolone derivatives, preparation thereof as drugs, pharmaceutical compositions, and use therof as protein kinase inhibitors, in particular CDC7. Patent, US2009253679 (A1) (US), Oct. 2009.

(326) Duff, J. C.; Bills, E. J. *Journal of the Chemical Society* **1932**, 1987–1988.

(327) Duff, J. C.; Bills, E. J. *Journal of the Chemical Society* **1934**, 1305–1308.

(328) Duff, J. C. *Journal of the Chemical Society* **1941**, 547–550.

(329) Duff, J. C. *Journal of the Chemical Society* **1945**, 276–277.

(330) Ferguson, L. N. *Chemical Reviews* **1946**, *38*, 227–254.

(331) Duff, J. C.; Furness, V. I. *Journal of the Chemical Society* **1951**, 1512–1515.

(332) Blažzević, N.; Kolbah, D.; Belin, B.; Šunjić, V.; Kajfež, F. *Synthesis* **1979**, 161–176.

(333) Li, X.; Wells, K. M.; Branum, S.; Damon, S.; Youells, S.; Beauchamp, D. A.; Palmer, D.; Stefanick, S.; Russell, R. K.; Murray, W. *Organic Process Research & Development* **2012**, *16*, 1727–1732.

(334) Kauffmann, G. S.; Li, C.; Lippa, B. S.; Morris, J.; Pan, G. Bicyclic heteroaromatic derivatives useful as anticancer agent. Patent, WO2006090261 (A1) (WO), Aug. 2006.

(335) Isbecque, D.; Promel, R.; Quinaux, R. C.; Martin, R. H. *Helvetica Chimica Acta* **1959**, *42*, 1317–1323.

(336) Koppel, H. C.; Springer, R. H.; Robins, R. K.; Cheng, C. *The Journal of Organic Chemistry* **1961**, *26*, 792–803.

(337) Hevener, K. E.; Yun, M.-K.; Qi, J.; Kerr, I. D.; Babaoglu, K.; Hurdle, J. G.; Balakrishna, K.; White, S. W.; Lee, R. E. *Journal of Medicinal Chemistry* **2010**, *53*, 166–177.

(338) Elion, G. B.; Lange, W. H.; Hitchings, G. H. *Journal of the American Chemical Society* **1956**, *78*, 2858–2863.

(339) Klepper, F.; Jahn, E.-M.; Hickmann, V.; Carell, T. *Angewandte Chemie International Edition* **2007**, *46*, 2325–2327.

(340) Miller, D. J.; Ravikumar, K.; Shen, H.; Suh, J.-K.; Kerwin, S. M.; Robertus, J. D. *Journal of Medicinal Chemistry* **2002**, *45*, 90–98.

(341) Rosowsky, A.; Papoulis, A. T.; Queener, S. F. *Journal of Medicinal Chemistry* **2002**, *45*, 1957–1957.

(342) Roth, B.; Laube, R.; Tidwell, M. Y.; Rauckman, B. S. *The Journal of Organic Chemistry* **1980**, *45*, 3651–3657.

(343) Banno, H.; Tanaka, T.; Sasaki, S. Fused heterocyclic ring derivative and use thereof. Patent, EP2471793 (A1) (EP), July 2012.

(344) Sabnis, R. W.; Rangnekar, D. W.; Sonawane, N. D. *Journal of Heterocyclic Chemistry* **1999**, *36*, 333–345.

(345) Gewald, K. *Chemische Berichte* **1965**, *98*, 3571–3577.

(346) Herdewijn, P.; De Jonghe, S.; Gao, L.-J.; Jang, M.-Y.; Vanderhoydonck, B.; Waer, M. J. A.; Lin, Y.; Herman, J. F.; Louat, T. A. M. Thiazolopyrimidine modulators as immunosuppressive agents. Patent, US2012046278 (A1) (US), Feb. 2012.

(347) De Jonghe, S.; Gao, L.-J.; Herdewijn, P.; Herman, J.; Jang, M.; Leyssen, P.; Louat, T.; Neyts, J.; Pannecouque, C.; Vanderhoydonck, B. Antiviral activity of novel bicyclic heterocycles. Patent, US2013190297 (A1) (US), July 2013.

(348) Taylor, E. C.; Young, W. C.; Chaudhari, R.; Patel, H. H. *Heterocycles* **1993**, *36*, 1897–1908.

(349) Schoenberg, A.; Heck, R. F. *Journal of the American Chemical Society* **1974**, *96*, 7761–7764.

(350) Brennführer, A.; Neumann, H.; Beller, M. *Angewandte Chemie International Edition* **2009**, *48*, 4114–4133.

(351) Brückl, T.; Thoma, I.; Wagner, A. J.; Knochel, P.; Carell, T. *European Journal of Organic Chemistry* **2010**, *2010*, 6517–6519.

(352) Klepper, F. Synthese der natürlichen tRNA Nukleosidmodifikationen Queuosin und Archaeosin., Ph.D. Thesis, Munich, Germany: Ludwig-Maximilians-Universität München, 2007.

(353) Sundermeier, M.; Zapf, A.; Beller, M. *European Journal of Inorganic Chemistry* **2003**, *2003*, 3513–3526.

(354) Krasovskiy, A.; Knochel, P. *Angewandte Chemie International Edition* **2004**, *43*, 3333–3336.

(355) Krasovskiy, A.; Straub, B. F.; Knochel, P. *Angewandte Chemie International Edition* **2006**, *45*, 159–162.

(356) Hevia, E.; Mulvey, R. E. *Angewandte Chemie International Edition* **2011**, *50*, 6448–6450.

(357) Peters, M. A Flexible and Modular Approach for the Synthesis of Teraryls: α-Helical Peptidomimetics as Potential Inhibitors in Protein-Protein-Interactions., Ph.D. Thesis, Graz, Austria: Graz University of Technology, 2012.

(358) Hess, K.; Fink, H. *Berichte der deutschen chemischen Gesellschaft* **1915**, *48*, 1986–2005.

(359) VanBrunt, M. P.; Ambenge, R. O.; Weinreb, S. M. *The Journal of Organic Chemistry* **2003**, *68*, 3323–3326.

(360) Pratt, J. K.; Betebenner, D. A.; Donner, P. L.; Green, B. E.; Kempf, D. J.; McDaniel, K. F.; Maring, C. J.; Stoll, V. S.; Zhang, R. Anti-infective agents. Patent, US2004087577 (A1) (US), May 2004.

(361) Pratt, J. K.; Betebenner, D. A.; Donner, P. L.; Green, B. E.; Kempf, D. J.; McDaniel, K. F.; Maring, C. J.; Stoll, V. S.; Zhang, R. Anti-infective agents. Patent, US2004162285 (A1) (US), Aug. 2004.

(362) Rong, L.; Han, H.; Wang, H.; Jiang, H.; Tu, S.; Shi, D. *Journal of Heterocyclic Chemistry* **2009**, *46*, 152–157.

(363) Shaabani, A.; Mirzaei, P.; Naderi, S.; Lee, D. G. *Tetrahedron* **2004**, *60*, 11415 –11420.

(364) Henderson, E. A.; Bavetsias, V.; Theti, D. S.; Wilson, S. C.; Clauss, R.; Jackman, A. L. *Bioorganic & Medicinal Chemistry* **2006**, *14*, 5020 –5042.

(365) Salmond, W. G.; Barta, M. A.; Havens, J. L. *The Journal of Organic Chemistry* **1978**, *43*, 2057–2059.

(366) Allen, S. E.; Walvoord, R. R.; Padilla-Salinas, R.; Kozlowski, M. C. *Chemical Reviews* **2013**, *113*, 6234–6458.

(367) Barton, D. H. R.; Doller, D. *Accounts of Chemical Research* **1992**, *25*, 504–512.

(368) DeBernardis, J. F.; Kyncl, J. J.; Basha, F. Z.; Arendsen, D. L.; Martin, Y. C.; Winn, M.; Kerkman, D. J. *Journal of Medicinal Chemistry* **1986**, *29*, 463–467.

(369) Fukatsu, K.; Uchikawa, O.; Kawada, M.; Yamano, T.; Yamashita, M.; Kato, K.; Hirai, K.; Hinuma, S.; Miyamoto, M.; Ohkawa, S. *Journal of Medicinal Chemistry* **2002**, *45*, 4212–4221.

(370) McLean, T. H.; Parrish, J. C.; Braden, M. R.; Marona-Lewicka, D.; Gallardo-Godoy, A.; Nichols, D. E. *Journal of Medicinal Chemistry* **2006**, *49*, 5794–5803.

(371) Harusawa, S.; Yoneda, R.; Kurihara, T.; Hamada, Y.; Shioiri, T. *Tetrahedron Letters* **1984**, *25*, 427 –428.

(372) Smith, A. B.; Fukui, M.; Vaccaro, H. A.; Empfield, J. R. *Journal of the American Chemical Society* **1991**, *113*, 2071–2092.

(373) Cason, J. *Organic Syntheses* **1955**, *Collective Volume 3*, 169.

(374) Tao, C.; Wang, Q.; NAllan, L.; Polat, T.; Koroniak, L.; Desai, N. Triazine derivatives and their therapeutical applications. Patent, WO2010144338 (A1) (WO), Dec. 2010.

(375) Siegel, A.; Wessely, F.; Stockhammer, P.; Antony, F.; Klezl, P. *Tetrahedron* **1958**, *4*, 49 –67.

(376) Buechi, G.; Roberts, E. C. *The Journal of Organic Chemistry* **1968**, *33*, 460–462.

(377) Crabtree, S. R.; Chu, W. L. A.; Mander, L. N. *Synlett* **1990**, *3*, 169–170.

(378) Faschauner, S. Synthesis of 5,6-functionalized thieno- and cyclopentapyrimidines., MA thesis, Graz, Austria: Graz University of Technology, in progress.

(379) Dickinson, C. L.; Williams, J. K.; McKusick, B. C. *The Journal of Organic Chemistry* **1964**, *29*, 1915–1919.

(380) Dickinson, C. L. J.; Middleton, W. J. Improvements relating to substituted pyrazoles. Patent, GB923734 (GB), June 1959.

(381) Dickinson, C. L. J.; Middleton, W. J. Certain amino, dicyano pyrazoles and process. Patent, US2998419 (A) (US), Aug. 1961.

(382) Bulychev, Y.; Korbukh, I.; Preobrazhenskaya, M.; Chernyshov, A.; Esipov, S. *Chemistry of Heterocyclic Compounds* **1984**, *20*, 215–221.

(383) Taylor, E. C.; Abul-Husn, A. *The Journal of Organic Chemistry* **1966**, *31*, 342–343.

(384) Earl, R. A.; Pugmire, R. J.; Revankar, G. R.; Townsend, L. B. *The Journal of Organic Chemistry* **1975**, *40*, 1822–1828.

(385) Robins, R. K. *Journal of the American Chemical Society* **1956**, *78*, 784–790.

(386) Taylor, E. C.; Hartke, K. S. *Journal of the American Chemical Society* **1959**, *81*, 2456–2464.

(387) Xu, J.; Liu, H.; Li, G.; He, Y.; Ding, R.; Wang, X.; Feng, M.; Zhang, S.; Chen, Y.; Li, S.; Zhao, M.; Qi, C.; Dang, Y. *Bioorganic & Medicinal Chemistry Letters* **2011**, *21*, 4736 –4741.

(388) Shaikh, A. C.; Chen, C. *Journal of Labelled Compounds and Radiopharmaceuticals* **2008**, *51*, 72–76.

(389) Tominaga, Y.; Luo, J.-K.; Castle, L. W.; Castle, R. N. *Journal of Heterocyclic Chemistry* **1993**, *30*, 267–273.

(390) Smith, C. J.; Iglesias-Siguenza, F. J.; Baxendale, I. R.; Ley, S. V. *Organic & Biomolecular Chemistry* **2007**, *5*, 2758–2761.

(391) Peet, N. P. *Journal of Heterocyclic Chemistry* **1986**, *23*, 193–197.

(392) Kreutzberger, A.; Burgwitz, K. *Journal of Heterocyclic Chemistry* **1980**, *17*, 265–266.

(393) Todorovic, N.; Awuah, E.; Shakya, T.; Wright, G. D.; Capretta, A. *Tetrahedron Letters* **2011**, *52*, 5761 –5763.

(394) Cottam, H. B.; Wasson, D. B.; Shih, H. C.; Raychaudhuri, A.; Di Pasquale, G.; Carson, D. A. *Journal of Medicinal Chemistry* **1993**, *36*, 3424–3430.

(395) Bui, M.; Chen, Y.; Cushing, T.; Duquette, J. A.; Fisher, B.; Gonzalez Lopez de Turiso, F.; Hao, X.; Xiao, H.; Johnson, M.; Lucas, B. Heterocyclic compounds and their uses. Patent, US2010331306 (A1) (US), Dec. 2010.

(396) Tominaga, Y.; Honkawa, Y.; Hara, M.; Hosomi, A. *Journal of Heterocyclic Chemistry* **1990**, *27*, 775–783.

(397) Takahashi, Y.; Hibi, S.; Hoshino, Y.; Kikuchi, K.; Shin, K.; Murata-Tai, K.; Fujisawa, M.; Ino, M.; Shibata, H.; Yonaga, M. *Journal of Medicinal Chemistry* **2012**, *55*, 5255–5269.

(398) Sailer-Kronlachner, W. Synthesis of pyrazolo[3,4-*d*]pyrimidines as substrates for xanthine oxidase transformations., MA thesis, Graz, Austria: Graz University of Technology, in progress.

(399) Hocková, D.; Holý, A.; Masojídková, M.; Andrei, G.; Snoeck, R.; De Clercq, E.; Balzarini, J. *Journal of Medicinal Chemistry* **2003**, *46*, 5064–5073.

(400) Punna, S.; Meunier, S.; Finn, M. G. *Organic Letters* **2004**, *6*, 2777–2779.

(401) Dong, C.-Z.; Ahamada-Himidi, A.; Plocki, S.; Aoun, D.; Touaibia, M.; Habich, N. M.-B.; Huet, J.; Redeuilh, C.; Ombetta, J.-E.; Godfroid, J.-J.; Massicot, F.; Heymans, F. *Bioorganic & Medicinal Chemistry* **2005**, *13*, 1989 –2007.

(402) Schwartz, M. A.; Zoda, M.; Vishnuvajjala, B.; Mami, I. *The Journal of Organic Chemistry* **1976**, *41*, 2502–2503.

(403) Kim, H. J.; Seo, J. W.; Lee, M. H.; Shin, D. S.; Kim, H. B.; Cho, H.; Lee, B. S.; Chi, D. Y. *Tetrahedron* **2012**, *68*, 3942 –3947.

(404) Loader, C. E.; Anderson, H. J. *Canadian Journal of Chemistry* **1981**, *59*, 2673–2683.

(405) Anderson, H. J.; Clase, J. A.; Loader, C. E. *Synthetic Communications* **1987**, *17*, 401–407.

(406) Giradet, J. L.; Koh, Y.-H.; Shaw, S.; Kin, H. W. Diaryl-purine, azapurines and -deazapurines as non-nucleoside reverse transcriptase inhibitors for treatment of HIV. Patent, WO2006122003 (A2) (WO), Nov. 2006.

(407) Van Camp, J.; Xu, X.; Osuma, A. T.; Gregg, R.; Longenecker, K. L. Pyrrolopyrimidines as FAK and ALK inhibitors for treatment of cancers and other diseases. Patent, WO2012045195 (A1) (WO), Apr. 2012.

(408) Dax, S.; Woodward, R.; Peng, S. Novel compounds as respiratory stimulants for treatment of breathing control disorders and diseases. Patent, WO2012074999 (A1) (WO), June 2012.

(409) Blagg, J. Heterocyclic GTP cyclohydrolase 1 inhibitors for the treatment of pain. Patent, WO2011035009 (A1) (WO), Mar. 2011.

(410) Vilsmeier, A.; Haack, A. *Berichte der deutschen chemischen Gesellschaft (A and B Series)* **1927**, *60*, 119–122.

(411) Becker Heinz, G.; Beckert, R.; Domschke, G.; Fanghänel, E.; Habicher, W.; Metz, P.; Pavel, D.; Schwetlick, K., *Organikum*, 21st ed.; Wiley-VCH: 2001.

(412) Barnett, C. J.; Kobierski, M. E. *Journal of Heterocyclic Chemistry* **1994**, *31*, 1181–1183.

(413) Gangjee, A.; Yu, J.; Kisliuk, R. L.; Haile, W. H.; Sobrero, G.; McGuire, J. J. *Journal of Medicinal Chemistry* **2003**, *46*, 591–600.

(414) Seela, F.; Peng, X. *Synthesis* **2004**, 1203–1210.

(415) Balow, G. B.; Acevedo, O. L.; Cook, P. D. Sugar-modified 7-deaza-7-substituted oligonucleotides. Patent, 6,093,807 (US), July 2000.

(416) Benner, S. A.; Hutter, D.; Leal, N. A.; Karalkar, N. B. Reagents for reversibly terminating primer extension. Patent, WO2012110775 (A1) (WO), Sept. 2010.

(417) Baillargeon, V. P.; Stille, J. K. *Journal of the American Chemical Society* **1983**, *105*, 7175–7176.

(418) Scott, W. J.; Crisp, G. T.; Stille, J. K. *Journal of the American Chemical Society* **1984**, *106*, 4630–4632.

(419) Baillargeon, V. P.; Stille, J. K. *Journal of the American Chemical Society* **1986**, *108*, 452–461.

(420) Pri-Bar, I.; Buchman, O. *The Journal of Organic Chemistry* **1984**, *49*, 4009–4011.

(421) Misumi, Y.; Ishii, Y.; Hidai, M. *Organometallics* **1995**, *14*, 1770–1775.

(422) Ashfield, L.; Barnard, C. F. J. *Organic Process Research & Development* **2007**, *11*, 39–43.

(423) Hartwig, J. F. *Angewandte Chemie International Edition* **1998**, *37*, 2046–2067.

(424) Zapf, A.; Beller, M. *Chemical Communications* **2005**, 431–440.

(425) Barnett, C. J.; Grubb, L. M. *Tetrahedron Letters* **2000**, *41*, 9741 –9745.

(426) Wang, R.-W.; Gold, B. *Organic Letters* **2009**, *11*, 2465–2468.

(427) Angelin, M.; Hermansson, M.; Dong, H.; Ramström, O. *European Journal of Organic Chemistry* **2006**, *2006*, 4323–4326.

(428) Fürstner, A.; Kattnig, E.; Lepage, O. *Journal of the American Chemical Society* **2006**, *128*, 9194–9204.

(429) Druais, V.; Hall, M. J.; Corsi, C.; Wendeborn, S. V.; Meyer, C.; Cossy, J. *Organic Letters* **2009**, *11*, 935–938.

(430) Nacro, K.; Baltas, M.; Gorrichon, L. *Tetrahedron* **1999**, *55*, 14013 –14030.

(431) Hiroi, K.; Watanabe, T.; Tsukui, A. *Chemical & Pharmaceutical Bulletin* **2000**, *48*, 405–409.

(432) Ferrie, L.; Boulard, L.; Pradaux, F.; Bouzbouz, S.; Reymond, S.; Capdevielle, P.; Cossy, J. *The Journal of Organic Chemistry* **2008**, *73*, 1864–1880.

(433) Reddy Chada, R.; Dharmapuri, G. *Synthesis* **2013**, *45*, 673–677.

(434) Barry, C. S.; Bushby, N.; Harding, J. R.; Willis, C. L. *Organic Letters* **2005**, *7*, 2683–2686.

(435) Brooks, A. F.; Garcia, G. A.; Showalter, H. H. *Tetrahedron Letters* **2010**, *51*, 4163 –4165.

(436) Gangjee, A.; Shi, J.; Queener, S. F.; Barrows, L. R.; Kisliuk, R. L. *Journal of Medicinal Chemistry* **1993**, *36*, 3437–3443.

(437) Gangjee, A.; Mavandadi, F.; Queener, S. F. *Journal of Medicinal Chemistry* **1997**, *40*, 1173–1177.

(438) Backeberg, O. G.; Staskun, B. *Journal of the Chemical Society* **1962**, 3961–3963.

(439) Stirling, C. J. M.; Gosselin, C. C.; Holt, A.; Lowe, P. A.; Staskun, B.; Backeberg, O. G.; Thynne, J. C. J.; Charton, M.; Willner, D.; Gestetner, B.; Lavie, D.; Birk, Y.; Bondi, A.; Gold, V.; Socrates, G.; Crampton, M. R.; Birch, A. J.; Hughes, G. A.; Kruger, G.; Rao, G. S. R. S.; Bell, F.; Buck, K. R.; Emeleus, H. J.; Tattershall, B. W.; Dobbie, R. C.; Cavell, R. G.; Gee, N.; Nicholls, D.; Vincent, V.; Bruce, J. M.; Knowles, P.; Coffin, B.; Robbins, R. F.; Davidson, J. S.; Gill, J. B.; Taylor, R. M. *Journal of the Chemical Society* **1964**, 5875–5906.

(440) Flanagan, D. M.; Joullié, M. M. *Synthetic Communications* **1990**, *20*, 459–467.

(441) Rockhill, J. K.; Wilson, S. R.; Gumport, R. I. *Journal of the American Chemical Society* **1996**, *118*, 10065–10068.

(442) Plieninger, H.; Werst, G. *Angewandte Chemie* **1955**, *67*, 156–157.

(443) Tinapp, P. *Chemische Berichte* **1969**, *102*, 2770–2776.

(444) Rupe, H.; Hodel, E. *Helvetica Chimica Acta* **1923**, *6*, 865–880.

(445) Rupe, H.; Brentano, W. *Helvetica Chimica Acta* **1936**, *19*, 588–596.

(446) Cossrow, J.; Guan, B.; Ishchenko, A.; Jones, J. H.; Kumaravel, G.; Lugovsky, A.; Peng, H.; Powell, N.; Raimundo, B. C.; Tanaka, H.; Vessels, J.; Wynn, T.; Xin, Z. Heterocyclic Compounds Useful as RAF Kinase Inhibitors. Patent, US2009005359 (A1) (US), Jan. 2009.

(447) carried out by Dipl.-Ing. Dr.techn. Margit Winkler.

(448) carried out by Dipl.-Ing. Dr.techn. Barbara Petschacher.

(449) carried out by Dipl.-Ing. Dr.techn. Regina Kratzer.

(450) Liu, H.; Naismith, J. H. *Protein Expression and Purification* **2009**, *63*, 102 –111.

(451) carried out by Dipl.-Ing. Dr.techn. Sigrid Egger.

(452) core facility structural biology (Mag. Dr.rer.nat. Georg Steinkellner, Dr. Andrzej Lyskowski, Univ.-Prof. Mag. Dr.rer.nat. Karl Gruber).

(453) Feller, G.; Gerday, C. *Cellular and Molecular Life Sciences* **1997**, *53*, 830–841.

(454) Smith, D. R.; Calvo, J. M. *Nucleic Acids Research* **1980**, *8*, 2255–2274.

(455) Reimmann, C.; Patel, H. M.; Serino, L.; Barone, M.; Walsh, C. T.; Haas, D. *Journal of Bacteriology* **2001**, *183*, 813–820.

(456) Meneely, K. M.; Lamb, A. L. *Biochemistry* **2012**, *51*, 9002–9013.

(457) Espinoza-Moraga, M.; Petta, T.; Vasquez-Vasquez, M.; Laurie, V. F.; Moraes, L. A.; Santos, L. S. *Tetrahedron: Asymmetry* **2010**, *21*, 1988 –1992.

(458) Vaijayanthi, T.; Chadha, A. *Tetrahedron: Asymmetry* **2008**, *19*, 93 –96.

(459) Li, H.; Williams, P.; Micklefield, J.; Gardiner, J. M.; Stephens, G. *Tetrahedron* **2004**, *60*, 753 –758.

(460) Li, W.; Khullar, A.; Chou, S.; Sacramo, A.; Gerratana, B. *Applied and Environmental Microbiology* **2009**, *75*, 2869–2878.

(461) Li, W.; Chou, S.; Khullar, A.; Gerratana, B. *Applied and Environmental Microbiology* **2009**, *75*, 2958–2963.

(462) Mitsukura, K.; Suzuki, M.; Shinoda, S.; Kuramoto, T.; Yoshida, T.; Nagasawa, T. *Bioscience, Biotechnology, and Biochemistry* **2011**, *75*, 1778–1782.

(463) Godoy-Alcántar, C.; Yatsimirsky, A. K.; Lehn, J.-M. *Journal of Physical Organic Chemistry* **2005**, *18*, 979–985.

(464) Layer, R. W. *Chemical Reviews* **1963**, *63*, 489–510.

(465) Layer, R. *Chemical Reviews* **1964**, *64*, 703–703.

(466) script by Dipl.-Ing. Andreas Feuersinger.

(467) Reisinger, C.; Kern, A.; Fesko, K.; Schwab, H. *Applied Microbiology and Biotechnology* **2007**, *77*, 241–244.

(468) Krieger, E.; Darden, T.; Nabuurs, S. B.; Finkelstein, A.; Vriend, G. *Proteins: Structure, Function, and Bioinformatics* **2004**, *57*, 678–683.

(469) Krieger, E.; Koraimann, G.; Vriend, G. *Proteins: Structure, Function, and Bioinformatics* **2002**, *47*, 393–402.

(470) Duan, Y.; Wu, C.; Chowdhury, S.; Lee, M. C.; Xiong, G.; Zhang, W.; Yang, R.; Cieplak, P.; Luo, R.; Lee, T.; Caldwell, J.; Wang, J.; Kollman, P. *Journal of Computational Chemistry* **2003**, *24*, 1999–2012.

(471) Friesner, R. A.; Murphy, R. B.; Repasky, M. P.; Frye, L. L.; Greenwood, J. R.; Halgren, T. A.; Sanschagrin, P. C.; Mainz, D. T. *Journal of Medicinal Chemistry* **2006**, *49*, 6177–6196.

(472) Steinkellner, G.; Rader, R.; Thallinger, G.; Kratky, C.; Gruber, K. *BMC Bioinformatics* **2009**, *10*, 32.

(473) Yui, K.; Aso, Y.; Otsubo, T.; Ogura, F. *Bulletin of the Chemical Society of Japan* **1988**, *61*, 953–959.

(474) Snegaroff, K.; Lassagne, F.; Bentabed-Ababsa, G.; Nassar, E.; Ely, S. C. S.; Hesse, S.; Perspicace, E.; Derdour, A.; Mongin, F. *Organic & Biomolecular Chemistry* **2009**, *7*, 4782–4788.